

Université de Montréal

Oscillations cérébrales et performances cognitives : Études à l'état de repos en MEG chez des  
sujets contrôles et des survivants de cancer pédiatrique

*Par*

Oswald Victor

Département de Neurosciences, Faculté de médecine

Thèse présentée en vue de l'obtention du grade de doctorat  
en neuroscience option neuropsychologie

Avril 2021

© Oswald, 2021



Université de Montréal

Département Neurosciences, Faculté de médecine

---

*Cette thèse intitulée*

**Oscillations cérébrales et performances cognitives : Études à l'état de repos en MEG chez des sujets contrôles et des survivants de cancer pédiatrique**

*Présentée par*

**Victor Oswald**

*A été évaluée par un jury composé des personnes suivantes*

**Yvan Samson**

Président-rapporteur

**Philippe Robaey**

Directeur de recherche

**Karim Jerbi**

Codirecteur

**Christophe Grova**

Membre du jury

**Véronique Boulenger**

Examineur externe



## Résumé

Cette étude s'intéresse au lien entre les dynamiques cérébrales et les capacités cognitives, cette problématique a déjà été explorée auparavant en imagerie cérébrale, notamment à l'aide de tâches effectuées pendant l'imagerie. Cependant la caractérisation de l'activité spontanée a principalement été faite soit avec une faible précision spatiale (capteur EEG/MEG), soit en IRMf qui a une faible résolution temporelle. L'objectif de cette thèse est de caractériser l'activité spontanée au repos au niveau cortical associée à différents processus cognitifs et leur performance.

Le second chapitre cherche à établir les corrélats neuronaux de la performance de la mémoire au repos à l'aide des puissances spectrales localisées au niveau des sources corticales. Le troisième chapitre cherche à répliquer les méthodes utilisées dans l'article 1 avec les mêmes participants, mais dans un autre domaine cognitif afin d'établir les corrélats neuronaux de la fluence verbale ainsi que de discriminer une composante verbale et exécutive. Ces deux composantes ont été mises en évidence en utilisant une factorisation avec un test purement exécutif (*Trail making test-condition 4*) et un autre purement verbal (richesse du vocabulaire). Dans le quatrième chapitre, nous répliquons encore la méthode de l'article 1 avec les mêmes sujets, mais sur un test d'apprentissage verbal. Lors de l'apprentissage verbal, deux stratégies d'apprentissage (sériel et sémantique) possibles sont utilisées de manière concurrente, nous avons cherché à établir si des différences comportementales se traduisaient par des patrons d'activation différents. Dans le cinquième chapitre, nous avons cherché à établir des différences fonctionnelles entre les survivants de la leucémie et des sujets contrôles, puis à établir un lien entre la neurotoxicité et le déficit cognitif rencontré chez cette population, finalement nous avons établi un modèle intégrant neurotoxicité, performance cognitive et marqueur neurophysiologique fonctionnel cérébral.

Cette recherche aura approfondi les connaissances sur l'état de repos et principalement fourni les premiers travaux qui mettent en lien l'activité cérébrale spontanée au repos au niveau des sources corticales avec plusieurs tests neuropsychologiques comportementaux. Les résultats ont

amené des patrons d'activation spatio-fréquentielle différents, démontrant des spécificités reliées à certains tests comportementaux ou des traitements de l'information (sériel ou sémantique). Finalement les travaux sur les survivants de la leucémie ont montré que l'état de repos pouvait caractériser le fonctionnement des déficits cognitifs à long terme et être un marqueur de remédiation pour de futurs traitements.

**Mots-clés :** performance cognitive, états de repos, électrophysiologie, MEG, leucémie lymphoblastique aiguë

## **Abstract**

This study is interested in the link between brain dynamics and cognitive abilities. This problem has already been explored before in brain imaging, notably with the help of task performed during imaging. However, the characterization of spontaneous activity has mainly been done either with weak spatial resolution (EEG/MEG sensor) or in fMRI which has a low temporal resolution. The objective of this thesis is to characterize the spontaneous activity at rest at the cortical level associated with different cognitive processes and their performance.

The second chapter seeks to establish the neural correlates of resting memory performance using spectral powers localized at cortical sources. The third chapter seeks to replicate the methods used in article 1 with the same participants but in another cognitive domain in order to establish the neural correlates of verbal fluency as well as to discriminate a verbal and an executive component. These two components were highlighted using a factorization with a purely executive test (Trail making test-condition 4) and another purely verbal one (vocabulary richness). In the fourth chapter, we replicate the method of article 1 with the same subjects, but on a verbal learning test. During verbal learning, two possible learning strategies (serial and semantic) are used concurrently, we sought to establish whether behavioural differences translate into different activation patterns. In the fifth chapter, we sought to establish functional differences between leukemia survivors and control subjects, then to search for a link between neurotoxicity and the cognitive deficit encountered in this population; finally we established a model integrating neurotoxicity, cognitive performance and functional neurophysiological brain markers.

This research will have deepened the knowledge on the resting state and mainly provided the first works that link the spontaneous brain activity at rest at the level of cortical sources with several behavioural neuropsychological tests. The results led to different spatio-frequential activation patterns, showing specificities related to certain behavioural tests or information processing (serial or semantic). Finally, work on leukemia survivors has shown that resting states

could characterize the functioning of long-term cognitive deficits and be a remediation marker for future treatments.

**Keywords** cognitive performance, resting states, electrophysiology, MEG, acute lymphoblastic leukemia



# Table des matières

<b>Résumé.....</b>	<b>5</b>
<b>Abstract.....</b>	<b>7</b>
<b>Table des matières.....</b>	<b>9</b>
<b>Liste des tableaux.....</b>	<b>17</b>
<b>Liste des figures.....</b>	<b>19</b>
<b>Liste des sigles et abréviations.....</b>	<b>27</b>
<b>Remerciements.....</b>	<b>29</b>
<b>Chapitre 1 – Introduction.....</b>	<b>31</b>
<b>État de repos en imagerie cérébrale.....</b>	<b>31</b>
Mise en contexte.....	31
Fluctuations spontanées cérébrales.....	32
L'état de repos en MEG.....	33
Bases physiologiques de l'état de repos.....	34
La Magnétoencéphalographie (MEG).....	36
Les oscillations cérébrales.....	38
Activité non oscillatoire à large bande (1/f).....	39
Les sources corticales une analyse récente.....	40
<b>Modèle des processus cognitifs.....</b>	<b>40</b>
Modèle modal de la mémoire.....	40
Les niveaux de traitement : Un cadre pour la mémoire.....	41
Modèle de la mémoire de travail.....	42
Boucle phonologique.....	43
Mémoire sémantique et épisodique.....	43
Fonctions exécutives.....	44
<b>Tests neuropsychologiques.....</b>	<b>45</b>
Wechsler Adult Intelligence Scale (WAIS–IV).....	46
Trail Making Test.....	46

La fluence verbale ( <i>verbal fluency</i> ) .....	47
Apprentissage verbal ( <i>California Verbal Learning Test 2</i> ).....	47
<b>Lien entre imagerie de repos et processus cognitifs.....</b>	<b>48</b>
Fonction exécutive.....	48
Mémoire de travail verbale.....	48
Fluence verbale .....	49
Flexibilité cognitive .....	50
Traitement du langage.....	50
<b>Leucémie lymphoblastique aiguë et atteintes cognitives .....</b>	<b>52</b>
Leucémie lymphoblastique aiguë .....	52
Atteinte cognitive .....	52
Corrélat fonctionnels des atteintes cognitives.....	53
Paradigme de tâche en IRMf.....	53
État de repos et connectivité en IRMf .....	53
Oscillations cérébrales .....	54
<b>Mise en évidence de la problématique .....</b>	<b>54</b>
<b>Approche méthodologique générale .....</b>	<b>55</b>
Source corticale MEG/IRM.....	55
Fréquence au repos au niveau des sources corticales.....	57
Interprétation fonctionnelle (approche par clusters).....	57
Test neuropsychologique standardisé .....	57
Réplication et domaines cognitifs.....	58
Connectivité spectrale .....	58
Application clinique .....	59
<b>Plan de la thèse.....</b>	<b>60</b>
Objectifs et hypothèses .....	60
<b><i>Chapitre 2 — Spontaneous brain oscillations as neural fingerprints of working memory capacities: A resting-state MEG study .....</i></b>	<b><i>63</i></b>
<b>Abstract .....</b>	<b>64</b>
<b>Introduction .....</b>	<b>65</b>
<b>Methods and materials .....</b>	<b>68</b>

Participants .....	68
Neuropsychological Assessment.....	68
MEG and Anatomical MRI Data Acquisition .....	69
Data Pre-Processing .....	70
MEG Sources Estimation .....	70
Spectral Power Analysis .....	71
Correlation Analyses and Cluster-Level Statistics .....	71
<b>Results .....</b>	<b>73</b>
Neuropsychological assessment .....	73
Normalized Resting-State MEG Power .....	73
Correlation results .....	74
Visuo-spatial working memory (SA) .....	77
Working memory residual (WMIr).....	78
<b>Discussion .....</b>	<b>83</b>
Passive Brain Recordings Correlation Pattern and Working Memory Capacities .....	84
Relationship with previous task-based WM studies: the anatomical substrates .....	86
Relationship with previous task-based WM studies: the frequency patterns .....	87
Links to findings from lesion studies.....	89
<b>Conclusions .....</b>	<b>90</b>
Acknowledgements .....	91
<b>References .....</b>	<b>92</b>
<b><i>Chapitre 3 — Resting-state cortical activity in MEG reveals the neural correlate of executive and phonological complexity of verbal fluency.....</i></b>	<b><i>100</i></b>
<b>Abstract .....</b>	<b>101</b>
<b>Introduction .....</b>	<b>102</b>
<b>Method .....</b>	<b>106</b>
Participants .....	106
Neuropsychological Assessment.....	106
MEG and Anatomical MRI Data Acquisition .....	107
<b>Data Pre-Processing .....</b>	<b>107</b>
<b>MEG Sources Estimation.....</b>	<b>108</b>

Spectral Power Analysis .....	108
Correlation Analyses and Cluster-Level Statistics .....	109
Steps for conjunction analysis .....	110
Step 1: Cluster analyses with individual scaled tests scores .....	110
Step 2: Cluster analyses with factor loadings combining test scores.....	110
Step 3: Conjunction analysis .....	112
<b>Results .....</b>	<b>113</b>
Verbal Fluency Letter (initial brain behaviour pattern) .....	113
Conjunction 1.....	113
Conjunction 2.....	114
Conjunction 3.....	114
<b>Discussion .....</b>	<b>115</b>
<b>Figures .....</b>	<b>122</b>
<b>References .....</b>	<b>127</b>
<b>Supplementary material.....</b>	<b>132</b>
<b><i>Chapitre 4 — Resting state MEG power correlates of semantic and serial strategy in learning a list of words .....</i></b>	<b><i>135</i></b>
<b>Abstract .....</b>	<b>136</b>
<b>Introduction .....</b>	<b>137</b>
<b>Method .....</b>	<b>140</b>
Participants.....	140
Neuropsychological Assessment.....	140
MEG and Anatomical MRI Data Acquisition .....	141
Data Pre-Processing.....	141
MEG Sources Estimation.....	142
Spectral Power Analysis .....	142
Correlation Analyses and Cluster-Level Statistics .....	143
Comparison Between Brain-Behaviour Pattern.....	144
<b>Results .....</b>	<b>145</b>
Behavioural performance .....	145
Brain Behaviour Correlation for Mean Performance Across Trials 1 to 5.....	145

Correlation Pattern .....	145
Anticorrelation Pattern .....	145
Brain Behaviour Correlation for Semantic Strategy Across Trials 1 to 5.....	146
Correlation Pattern .....	146
Anticorrelation pattern .....	146
Brain Behaviour Correlation for Serial Backward Strategy Across Trials 1 to 5 .....	146
Correlation Pattern .....	146
Anticorrelation Pattern .....	147
Brain Behaviour Correlation for Serial Forward Strategy Across Trials 1 to 5 .....	147
Correlation Pattern .....	147
Anticorrelation Pattern .....	147
Difference of brain-behaviour pattern between both strategies (semantic versus serial).....	148
<b>Discussion .....</b>	<b>149</b>
Behavioural Result .....	149
Semantic Strategies Neural Correlate.....	149
Neural Correlates of Serial Clustering.....	150
Verbal Performance Memory and Semantic Verbal Memory Sharing Common Neural Substrate .....	151
Language network as key component for learning performance, through the semantic strategies.....	153
<b>Conclusion.....</b>	<b>155</b>
<b>References .....</b>	<b>156</b>
<b>Table and Figures .....</b>	<b>164</b>
<b>Supplementary figures .....</b>	<b>168</b>
<b><i>Chapitre 5 — Enhanced alpha long-range brain synchrony mediates the long-term effects of intrathecal methotrexate on executive deficits in ALL survivors.....</i></b>	<b>170</b>
<b>Abstract .....</b>	<b>171</b>
<b>Introduction .....</b>	<b>172</b>
Population.....	173
Neuropsychological Assessment.....	174
MEG & MRI Acquisition and Pre-Processing.....	174
Cortical Sources Estimation and Spectral Connectivity Analysis .....	174
Statistical Analyses.....	175

<b>Results .....</b>	<b>176</b>
Neuropsychological results (Table 2) .....	176
Spectral connectivity .....	176
Neuropsychological Scores and Spectral Connectivity .....	176
Chemotherapy and Spectral Connectivity.....	177
Mediation models (Table 3).....	177
<b>Discussion .....</b>	<b>179</b>
<b>References .....</b>	<b>187</b>
<b>Appendix.....</b>	<b>192</b>
<b><i>Chapitre 6 : Synthèse des résultats et discussion .....</i></b>	<b><i>195</i></b>
<b>Résumé des résultats .....</b>	<b>195</b>
<b>Synthèse des résultats.....</b>	<b>197</b>
Discussion générale .....	197
Contribution.....	206
<b>Limites .....</b>	<b>208</b>
Participants et populations.....	208
Composante oscillatoire ou effet de large bande.....	208
Corrélation et Variabilité Inter-individuelle .....	209
Bases d'interprétations psychologiques du comportement.....	210
<b>Conclusions .....</b>	<b>213</b>
<b><i>Annexes .....</i></b>	<b><i>214</i></b>
<b><i>Annexe 1 — chapitre 2 .....</i></b>	<b><i>215</i></b>
<b>Methods .....</b>	<b>215</b>
Population.....	215
Neuropsychological Assessment.....	215
MEG & MRI Acquisition and Pre-Processing.....	216
Cortical Sources Estimation and Spectral Connectivity Analysis .....	216
Statistical Analyses.....	217
<b>Results .....</b>	<b>217</b>
Neuropsychological assessment .....	217

Neuropsychological scores and spectral connectivity .....	218
<b>Annexe 2 — chapitre 3 .....</b>	<b>221</b>
<b>Additional results .....</b>	<b>221</b>
Vocabulary .....	221
Trail Making Test (Condition 4).....	222
F2_VOC (second factors between verbal fluency and vocabulary) .....	222
Similar clusters between F2_VOC and VF initial pattern .....	223
Disappearing clutters between F2_VOC and VF initial pattern.....	223
Added clusters between F2_VOC and VF initial pattern .....	223
F1_TMT (first factor between verbal fluency and TMT4) .....	223
Similar clusters between F1_TMT and VF initial pattern .....	223
Disappearing clutters between F1_TMT and VF initial pattern .....	224
Added clusters between F1_TMT and VF initial pattern.....	224
<b>Annexe 3 — chapitre 4 .....</b>	<b>227</b>
<b>Additional results .....</b>	<b>227</b>
Neuropsychological performance.....	227
Trial by trial correlation for learning performance .....	228
Two distinct learning slope correlation pattern .....	229
<b>Références bibliographiques .....</b>	<b>237</b>





## Liste des tableaux

Tableau 1. – Scaled score, mean, standard deviation, minimum and maximum value of neuropsychological assessments for 26 subjects. The WAIS-IV battery includes subtest DS and LNS form WMI. SA is a simple subtest from the WMS Test. Note that all standardized indices (i.e. WMI and FSIQ) are designed such that $m=100$ & $SD=15$ , while the subtests have $m=10$ and $SD=3$ . .....	73
Tableau 2. – Table 1: Learning performance and strategy correlation trial by trial in CVLT-2 (n=28).....	164
Tableau 3. – Table 2: Correlation between mean performance and strategy used across the fifth trial correlation trial (n=28).....	164
Tableau 4. – Survivor Demographic and Treatment Characteristics .....	183
Tableau 5. – Neurocognitive performance data .....	184
Tableau 6. – Mediation analysis .....	186
Tableau 7. – Tableau récapitulatif des résultats puissance des clusters à travers tous les tests comportementaux .....	199
Tableau 8. – Table 1: Scaled score, mean, standard deviation, minimum and maximum value of neuropsychological assessments for 34 subjects. The WAIS-IV battery includes subtest DS and LNS form WMI. Note that all standardized indices (i.e. WMI and FSIQ) are designed such that $m=100$ & $SD=15$ , while the subtests have $m=10$ and $SD=3$ . .....	218
Tableau 9. – Table 2: Correlation between mean spectral connectivity (wPLI)and working memory index performance across the 7 resting state network pour Working memory index (n=34;p-value uncorrected).....	218
Tableau 10. –Summarizes the mean and standard deviation, and min/ max values for the scores on the neuropsychological tests from CVLT-2 .....	227



## Liste des figures

Figure 1. –	(A) Exemple d’une forme possible de boucle de contrôle d’inférence générale illustrée dans un modèle bayésien hiérarchique. (B) Exemple très schématique illustrant que les informations intéroceptives et extéroceptives sont intégrées simultanément pour informer les représentations perceptives et la sélection d’actions dirigées vers l’intérieur et vers l’extérieur. Tiré de Khalsa et al. (2018)..	32
Figure 2. –	Les principaux rythmes cérébraux sont classés selon leur plage de fréquence tiré de (Buzsaki & Draguhn, 2004).	38
Figure 3. –	Exemple, C) spectre de puissance D) spectre de puissance (échelle log-log) (tirée de (Ouyang et al., 2020).	39
Figure 4. –	Modèle modal de la mémoire, issu de Atkinson et Shiffrin (1968)	41
Figure 5. –	Modèle des niveaux de traitement de la mémoire issue de Craik et Lockhart (1972).	42
Figure 6. –	Les composantes du modèle de la mémoire de travail (A. Baddeley, 2000)	42
Figure 7. –	Boucle phonologique (A. Baddeley, 2000)	43
Figure 8. –	Modèle Unité/diversité des fonctions exécutives (Miyake et al., 2000)	45
Figure 9. –	Sous test et indexes du WAIS-IV (Welscher et al., 2000).	46
Figure 10. –	Modèle du langage et ses corrélats neuronaux d’après Hickok et Poeppel tiré de (Hickok & Poeppel, 2007)	51
Figure 11. –	Le modèle inverse et direct permettant de passer de décours temporel des capteurs à celui des sources corticales	57
Figure 12. –	Parcellisations des 7 réseaux au repos d’après (Schaefer et al., 2018)	59
Figure 13. –	(A) Topographical plots of relative mean power across all subjects (n=26) for each frequency band. The top row shows sensor-level topographies while the bottom row shows normalized power at the cortical source level. Power values were normalized by the maximum across sensors or vertices in each band and then averaged across participants. (B) Grand average power spectrum with its standard deviation across all subjects for the 12 brain regions.	76
Figure 14. –	Brain-Behavior correlations based on resting spectral power and DS test scores (n=26). Spatial distribution of clusters with statistically significant correlations (p<.001) between resting MEG source-space power (z-scores across vertices) and neuropsychological performance on the Digit Span (DS, WAIS-IV) subtest. Each column shows the significant correlations for a given range of frequencies, in both hemispheres (right lateral and media view, followed by left-lateral and	

medial views). The results are corrected across space using cluster-level corrections. All results remain significant at  $p < .05$ , with Bonferroni correction for multiple comparisons across space, frequency bands, and WM tests. No significant clusters were observed in the Theta and Gamma 1 ranges. .... 77

- Figure 15. – Brain-Behavior correlations based on resting spectral power and LNS test scores ( $n=26$ ). Spatial distribution of clusters with statistically significant correlations ( $p < .001$ ) between resting MEG source-space power (z-scores across vertices) and neuropsychological performance on the Letter-Number Sequencing (LNS, WAIS-IV) subtest. The formatting of the figure and statistical significance of the results are identical to those in Fig. 14. .... 79
- Figure 16. – Brain-Behavior correlations based on resting spectral power and WMI ( $n=26$ ). Spatial distribution of clusters with statistically significant correlations ( $p < .001$ ) between resting MEG source-space power (z-scores across vertices) and neuropsychological performance on the Working Memory Index (WMI, WAIS-IV). The formatting of the figure and statistical significance of the results are identical to those in Fig. 14. .... 80
- Figure 17. – Brain-Behavior correlations based on resting spectral power and SA ( $n=26$ ). Spatial distribution of clusters with statistically significant correlations ( $p < .001$ ) between resting MEG source-space power (z-scores across vertices) and neuropsychological performance on the Spatial Addition (SA, WMS-IV) subtest. The formatting of the figure and statistical significance of the results are identical to those in Fig. 14. .... 81
- Figure 18. – Brain-Behavior correlations based on resting spectral power and WMlr ( $n=26$ ). Spatial distribution of clusters with statistically significant correlations ( $p < .001$ ) between resting MEG source-space power (z-scores across vertices) and neuropsychological performance on the Working Memory Index residual (WMlr). WMlr is a measure of working memory, where all correlations with other intelligence indices (PRI then PSI then VCI) were removed. WMlr is the residual component of the WMI score, after all correlations with the other three indices of the WAIS-IV (PRI, PSI, VCI) were successively removed. Clusters observed with the WMlr correlations should not be observed with any one of these three indices, and are thus specific to WMI. The formatting of the figure and statistical significance of the results are identical to those in Fig. 14. .... 81
- Figure 19. – Scatter plots of the main six significant clusters, using standard linear regression with standardized working memory test scores (WMI) on the x-axis and normalized resting-state alpha-band oscillatory power on the y-axis. (a) right intra-parietal sulcus, (b) right dorso-lateral prefrontal cortex, (c) left paracentral gyrus (paracentral lobule), (d,e) left and right dorsomedial prefrontal cortex

(dmPFC), respectively, and (f) right paracentral gyrus (paracentral lobule). The cortical representations in the middle indicate the location of the clusters associated with each scatter plot panel. Clusters g and h also showed statistically significant but weaker correlation coefficients..... 82

- Figure 20. – Figure 1: Schema showing the 3 steps methods used to explore relative specificity and different neural correlates of verbal fluency. The first step is to perform brain-behavior correlation/anticorrelation pattern between rsMEG power and each neuropsychological test independently (VOC, VF, TMT4). The second step consists of factorizing Voc and VF and TMT4 and VF, from this factorization brain-behavior correlation/anticorrelation pattern was performed with residual regression from F2\_VOC and F1\_TMT. The third step was to make conjunction maps between F2\_VOC & VF (conjunction 1) and F1\_TMT & VF (conjunction 2). Conjunction 3 is the overlapping cluster between conjunction 1 & conjunction 2..... 122
- Figure 21. – Figure 2: Spatial distribution of clusters with statistically significant correlations ( $p < .001$ ) between resting MEG source-space power (z-scores across vertices) and neuropsychological performance on the **Verbal Fluency** test. Each column shows the significant correlations for a given range of frequencies, in both hemispheres (right lateral and medial view, followed by left lateral and medial views). The results are corrected across space using cluster-level corrections. All results remain significant at  $p < .05$ , correction for multiple comparisons across space and frequency bands. .... 123
- Figure 22. – Figure 3: Spatial distribution of clusters with statistically significant correlations ( $p < .001$ ) in resting MEG source-space power (z-scores across vertices) on the **Conjunction 1**. Each column shows the significant correlations for a given range of frequencies, in both hemispheres (right lateral and medial view, followed by left lateral and medial views). The results are corrected across space using cluster-level corrections. All results remain significant at  $p < .05$ , correction for multiple comparisons across space and frequency bands..... 124
- Figure 23. – Figure 4: Spatial distribution of clusters with statistically significant correlations ( $p < .001$ ) in resting MEG source-space power (z-scores across vertices) on the **Conjunction 2**. Each column shows the significant correlations for a given range of frequencies, in both hemispheres (right lateral and medial view, followed by left lateral and medial views). The results are corrected across space using cluster-level corrections. All results remain significant at  $p < .05$ , correction for multiple comparisons across space and frequency bands..... 125
- Figure 24. – Figure 5: Spatial distribution of clusters with statistically significant correlations ( $p < .001$ ) in resting MEG source-space power (z-scores across vertices) on the

**Conjunction 3.** Spatial frequencies are described as following: delta band (1–4 Hz) in blue, alpha band (8–13 Hz) in yellow, clusters found in both (alpha (8–13 Hz) band and beta (13–30 Hz) band) are in red..... 126

- Figure 25. – Figure S1: Spatial distribution of clusters with statistically significant correlations ( $p < .001$ ) between resting MEG source-space power (z-scores across vertices) and neuropsychological performance on the **Vocabulary** test. The formatting of the figure and statistical significance of the results are identical to those in Fig. 1..... 132
- Figure 26. – Figure S2: Spatial distribution of clusters with statistically significant correlations ( $p < .001$ ) between resting MEG source-space power (z-scores across vertices) and neuropsychological performance on the **Trail Making Test (Condition 4)** test. The formatting of the figure and statistical significance of the results are identical to those in Fig. 1..... 133
- Figure 27. – Figure S3: Spatial distribution of clusters with statistically significant correlations ( $p < .001$ ) between resting MEG source-space power (z-scores across vertices) and individual regression of **F2\_VOC**. The formatting of the figure and statistical significance of the results are identical to those in Fig. 1. .. 133
- Figure 28. – Figure S4: Spatial distribution of clusters with statistically significant correlations ( $p < .001$ ) between resting MEG source-space power (z-scores across vertices) and individual regression of **F1\_TMT**. The formatting of the figure and statistical significance of the results are identical to those in Fig. 1. .. 134
- Figure 29. – Bain-behaviour correlation/anticorrelation pattern (corrected:  $p > 0,001$ ) with mean raw performance between trial 1 to 5 in CVLT-2..... 165
- Figure 30. – Bain-behaviour correlation/anticorrelation pattern (corrected:  $p > 0,001$ ) with Semantic strategy indices grouping related to performance in trial 1 to 5 in CVLT-2..... 165
- Figure 31. – Bain-behaviour correlation/anticorrelation pattern (corrected:  $p > 0,001$ ) with Serial Backward strategy indices grouping related to performance in trial 1 to 5 in CVLT-2..... 166
- Figure 32. – Bain-behaviour correlation/anticorrelation pattern (corrected:  $p > 0,001$ ) with Serial Forward strategy indices grouping related to performance in trial 1 to 5 in CVLT-2..... 166
- Figure 33. – Comparison between Correlation/Anticorrelation pattern in strategy: Significant difference (FDR  $p > 0,05$ ) between correlation pattern between strategies across all frequencies, upper line show difference between semantic strategies minus serial backward strategies, lower line show difference between semantic strategies minus serial forward strategies. .... 167

Figure 34. – Scatter plot between normalized power and strategies scores: mean across clusters and frequencies show correlation relationship with semantic scores (left), Serial backward scores (middle) and serial forward scores (right).The spatial mask is spatial .....	167
Figure 35. – Figure Supplementary 1: Comparison between Correlation/Anticorrelation pattern in strategy in all frequency: Significant difference (FDR $p > 0,05$ ) between correlation pattern in semantic strategies minus serial backward strategies .....	168
Figure 36. – Figure Supplementary 2: Comparison between Correlation/Anticorrelation pattern in strategy in all frequency: Significant difference (FDR $p > 0,05$ ) between correlation pattern in semantic strategies minus serial forward strategies.....	169
Figure 37. – CONSORT diagram for PETALE study .....	182
Figure 38. – Mean weighted phase lag index (Wpli) in ALL non-overlapping, overlapping and healthy control groups in 7 resting state networks and across the whole brain. A: Theta band, B: Alpha band. The horizontal grey bars indicate significant difference between groups ( $p < .01$ after FDR) (Ncog: Normal cognitive performance; Lcog: Low cognitive performance).....	185
Figure 39. – Mediation models between cumulative doses of IT:MTX and cognitive performance (DIV). After introducing whole brain connectivity in alpha band (8–13 Hz) as mediator direct pathways found nonsignificant (effect=-0.0115, $p=0.12$ ) while total effect found to be significant (-0.0045, $p=0,04$ ), the total accounted variance in indirect pathways is 28,12%. .....	185
<i>Figure 40.</i> – Supplementary figure 1 (SF1): mean wPLI in healthy controls (N=39) and ALL survivors (N=36) for each resting state network and whole brain level. * indicates significant difference ( $p=0.05$ FDR corrected. Cont: control (frontoparietal), Def: default, Dat: dorsal attention, Lim: limbic, Sal: Saliency (ventral attention), Som: somato-motor, Vis: visual. ....	192
Figure 41. – Supplementary figure 2 (SF2): Scatter plot of correlation between Cumulative IT:MTX and Alpha band spectral connectivity (8–13 Hz) at Whole brain (upper left). Scatter plot of correlation between performance in digit span (DS) and trail Making test condition 4 (TMT-4) and Alpha band spectral connectivity (8–13 Hz) at Whole brain (upper right). Scatter plot of correlation between Cumulative IT:MTX and Theta band spectral connectivity (4–8 Hz) at Whole brain (middle left). Scatter plot of correlation between performance in digit span (DS) and trail Making test condition 4 (TMT-4) and Alpha band spectral connectivity (4–8 Hz) at Whole brain (middle right). Scatter plot of correlation between Cumulative Corticosteroids and Gamma band spectral connectivity (90–120 Hz) at Whole brain (lower left). Scatter plot of correlation between	

	performance in digit span (DS) and trail Making test condition 4 (TMT-4) and Gamma band spectral connectivity (90–120 Hz) at Whole brain (lower right). ...	193
Figure 42. –	Esquisse partielle d’une taxonomie conceptuelle implicite dans les sciences cognitives et les neurosciences courantes extraites. Tiré de (Cisek, 2019) .....	211
Figure 43. –	Parcellations used from Schaffer et al. (2018) 7 networks .....	217
Figure 44. –	Figure 1: Scatter plot with significant network (Cont, Def, Lim, Vis) between mean spectral connectivity (wPLI) and working memory index performance .....	219
Figure 45. –	Figure 2. — Spatial distribution of clusters with statistically significant correlations ( $p < .001$ ) between resting MEG source-space power (z-scores across vertices) and neuropsychological performance on the <b>Vocabulary</b> test. The formatting of the figure and statistical significance of the results are identical to those in Fig. 1.....	224
Figure 46. –	Figure 3. — Spatial distribution of clusters with statistically significant correlations ( $p < .001$ ) between resting MEG source-space power (z-scores across vertices) and neuropsychological performance on the <b>Trail Making Test (Condition 4)</b> test. The formatting of the figure and statistical significance of the results are identical to those in Fig. 1.....	225
Figure 47. –	Figure 4: Spatial distribution of clusters with statistically significant correlations ( $p < .001$ ) between resting MEG source-space power (z-scores across vertices) and neuropsychological performance on the Contrast factor (F2_VOC) between <b>Verbal Fluency</b> and <b>Vocabulary</b> . The formatting of the figure and statistical significance of the results are identical to those in Fig. 1.....	225
Figure 48. –	Figure 5: Spatial distribution of clusters with statistically significant correlations ( $p < .001$ ) between resting MEG source-space power (z-scores across vertices) and neuropsychological performance on the Contrast factor (F1_TMT) between <b>Verbal Fluency</b> and <b>Trail Making Test (Condition 4)</b> . The formatting of the figure and statistical significance of the results are identical to those in Fig. 1. ..	226
Figure 49. –	Correlation Pattern with learning slope trial 1 to 3 .....	231
Figure 50. –	Correlation Pattern with learning slope trial 3 to 5 .....	231
Figure 51. –	Strategy uses and correlation with performance trial by trial. Left panel shows the mean performance across trials and evaluates short- and long-term recall. The score presented here are the raw (ie the number of word memorized), Participants performance improved consistently trial after trial. Up until trial 3, the sequence was encoded, while between trials 3 to 5, a memory consolidation process occurs that is reflect by a plateau in performance in between trial 3 and 4. Across participants the learning occurs in a similar and constantly manner, trial after trial showing a progressive learning process. This	



is confirmed by the performance during recall (short and long delay). Right panel show correlation between raw score and strategy used trial by trial. Semantic strategy show and increase in performance until the fifth trial and for the recall. .... 232

Figure 52. – Correlation Pattern with performance trial by trial and recall of CVLT-2, for the Left hemisphere ..... 234

Figure 53. – Correlation Pattern with performance trial by trial and recall of CVLT-2 for the right hemisphere ..... 236



## Liste des sigles et abréviations

ACC: anterior cingulate cortex	MTX: methotrexate
ALE: activation likelihood estimation	NMDA: N-méthyl-D-aspartate
CA: Cornu Ammonis	PET : Tomographie par émission de positons
CRT: cranial radiation therapy	PETALE : prévention des effets tardifs à long terme des survivants de leucémie
CVLT: California Verbal Learning Test	PFC : cortex préfrontal
dIPFC: dorsolateral prefrontal cortex	PLI: Phase locking Index
DMN : réseau du mode par défaut	PLV: Phase locking Value
dmPFC: dorsomedial prefrontal cortex	PRI: Perceptual Reasoning Index
DS: digit Span	PSD: power spectral density
ECOG: Electrocorticography	PSI: Phase slope index
EEG: Electroencephalographie	PSI: Processing Speed Index
FA: fractional anisotropy	QI : quotient intellectuel
fMRI: functional Magnetic Resonance Imaging	RD: radial diffusivity
GC: glucocorticoids	SA: Spatial Addition
GE: General Electric	SEEG: stéréoélectroencéphalographie
iEEG: intra-Electroencephalographie	SQUID: Superconducting Quantum Interference Device
ITC: Intensive intrathecal chemotherapy	SSP: Signal-Space-Projection method
IT-MTX: intrathecal MTX	tDCS: direct current stimulation
IV-MTX: intravenous MTX	<i>TMT: Trail Making Test</i>
LAL : leucémie aiguë lymphoblastique	VCI: Verbal Comprehension Index
LCR : Liquide Céphalorachidien	VF: verbal fluency
LNS: Letter Number Sequencing	vmPFC: ventromedial prefrontal cortex
LRS: long-range brain synchrony	WM: white matter
MCT : mémoire à court terme	WM: Working Memory
MEG : Magnetoencephalographie	WMI: Working Memory Index
MLT : mémoire à long terme	WMIr: residual score of WMI
MNI Montreal Neurological Institute	wPLI: Weighed Phase locking Index
MPSI: Multivariate phase slope index	

*Toujours cette peur...peur qu'il y ait quelque chose à rater, peur qu'il y ait quelque chose à réussir, qui nous fend le cœur et les membres.*

- P.Y. Cataphard

*Success is the ability to go from one failure to another with no loss of enthusiasm*

- Winston Churchill

## Remerciements

On ne fait rien tout seul, alors c'est avec et grâce à vous tous que cela a été possible.

Je tiens à remercier, Philippe Robaey, mon directeur avec qui cette aventure a duré 8 ans (incluant la maîtrise). Merci pour votre présence, votre confiance, votre écoute, l'énergie que vous avez mise pour m'aider à évoluer, vos conseils, votre humilité, votre humanité, votre sincérité, et vos partages.

Merci à Karim Jerbi pour ton professionnalisme, ton éthique, ton soutien, ton expertise, ton ouverture, ton accueil et ta confiance au Coco-lab, laboratoire d'adoption.

Merci à mes amis et collègues du Coco-lab plus particulièrement ceux avec qui j'ai eu la chance de travailler; Tarek, Golnoush, Thomas, Anne Lise, Vanessa, David, Anna Lisa, Yann et Gabrielle.

Merci au soutien et au travail de toute l'équipe PETALE de Sainte Justine, notamment Sarah Lippé et Aubrée Craig-Boulet pour votre travail.

Merci à Ping de la MEG de l'UdeM pour ta gentillesse ainsi que Pierre Jolicoeur et Jean-Pierre Grossard pour mon comité de parrainage.

Merci à ma famille, mes parents et mon frère pour leur soutien et présence inébranlable.

Merci à mes amis et collègues du CEO de Montréal plus particulièrement, Virginie Saumade, Sandra O'connor, Joseph Gill Lussier, Julien Fatisson.

Merci à Pierre Yves Cataphard pour ce voyage au cœur de la pensée ensemble.

Merci à Vincent Verfaille pour tes conseils et ton travail.

Merci à toi belle Lila, qui ne comprends toujours pas en quoi consiste mon travail !

Merci aux organismes de subventions, fondation Cole, CHIR et l'université de Montréal.

Merci à tous mes amis et membres de la famille élargie pour leur soutien, leur bienveillance et présence dans ce long parcours.



# Chapitre 1 – Introduction

## État de repos en imagerie cérébrale

### Mise en contexte

L'état de repos en imagerie se définit par rapport à l'opposition d'une activité cérébrale en réponse à un stimulus en fonction d'instructions. L'intérêt pour l'activité cérébrale à l'état de repos à plusieurs origines qui se sont rejointes entre elles avec le temps, mais ont émergé chacune de leur côté. L'une d'entre elles est issue de l'épistémologie philosophique qui repose sur l'idée du cerveau comme « page blanche ». Cette idée prend sa source bien antérieurement chez Aristote qui présente l'esprit comme une « tabula rasa » sur laquelle les expériences s'écrivent au cours du temps. Cette idée a longtemps dominé les paradigmes expérimentaux en psychologie cognitive (Buzsáki, 2019). On considère en psychologie expérimentale que le cerveau était le reflet de stimuli extérieurs et donc que les réponses physiologiques étaient uniquement évoquées par les stimuli extérieurs ou induites, par exemple dans un cadre expérimental. Cependant avec le temps cette théorie a perdu de plus en plus en faveur, du moins pour une théorie généralisée. En effet si certaines fonctions physiologiques, comme les stimulations sensorielles dans le système somato-sensoriel, peuvent démontrer des fonctions linéaires d'intensité stimulus/activation, ce modèle ne suffit pas à expliquer les variabilités comportementales dès que l'on inclut des fonctions cognitives plus complexes. Le système nerveux central et plus particulièrement le cerveau possède sa propre activité interne qui est auto-organisée au lieu d'être déterminée par les stimuli extérieurs. L'exploration de cette activité inhérente au cerveau et plus précisément ses corrélations avec le comportement fait l'objet de recherche depuis deux décennies. L'imagerie au repos permet l'exploration des caractéristiques de cette auto-organisation physiologique dite « spontanée » (van Diessen et al., 2015). L'étude de l'activité spontanée a donné lieu à des modèles computationnels caractérisant l'activité spontanée. Un modèle propose que l'activité spontanée serait soutenue par un modèle cérébral prédictif, qui combine l'information extéroceptive et intéroceptive, et permette d'agir sur le monde extérieur

ou intérieur, de prédire les effets de ces actions (figure 1), et d'en minimiser l'erreur de prédiction (Friston et al., 2016 ; Friston et al., 2010 ; Khalsa et al., 2018).

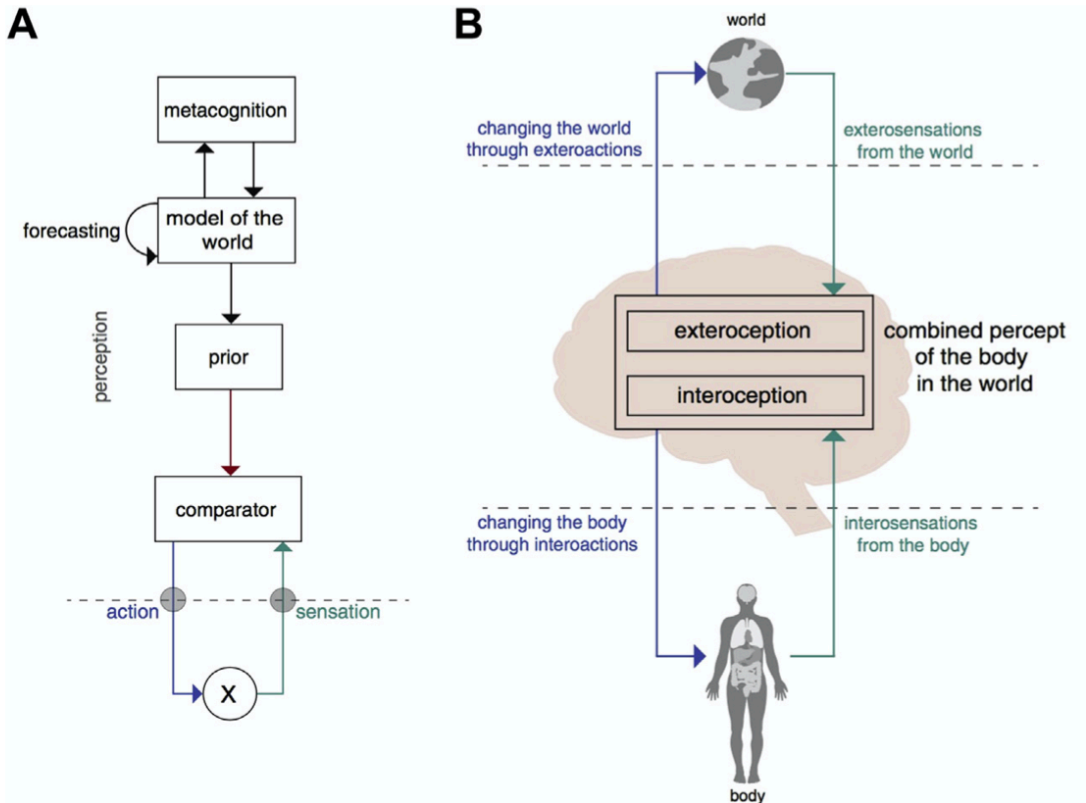


Figure 1. – (A) Exemple d'une forme possible de boucle de contrôle d'inférence générale illustrée dans un modèle bayésien hiérarchique. (B) Exemple très schématique illustrant que les informations intéroceptives et extéroceptives sont intégrées simultanément pour informer les représentations perceptives et la sélection d'actions dirigées vers l'intérieur et vers l'extérieur. Tiré de Khalsa et al. (2018)

## Fluctuations spontanées cérébrales

Cette auto-organisation est supportée par les rythmes neuronaux locaux et à travers le cerveau. Ces rythmes sont caractérisés par les oscillations cérébrales qui sont mesurées directement en électrophysiologie. L'étude des corrélats neuronaux en électrophysiologie a une longue tradition. L'utilisation de paradigme expérimental utilisant les tâches implique un sujet dans une activité, sollicite son engagement et permet donc d'examiner ses fonctions cognitives. Le reste de l'activité cérébrale a longtemps été considéré comme du bruit (physiologique et environnemental). L'état



de repos est enregistré chez le patient éveillé, autant que possible au repos, détendu. Il se définit surtout comme l'opposé de l'état actif où un sujet fait une tâche en fonction d'instructions qui lui sont données. L'existence d'un « état de repos » fut découverte fortuitement en imagerie par résonance magnétique fonctionnelle (IRMf) par Bharat Biswal (1995) (Biswal et al., 1995). Alors qu'il cherchait à réduire les bruits de fond générés en IRMf, il trouve une corrélation d'activation entre le cortex moteur droit et gauche tandis que le sujet était parfaitement immobile (Biswal et al., 1995). Ses résultats ont été reproduits, ce qui a donné lieu aux premières études sur l'état de repos. Puis des synchronies entre des régions cérébrales ont été trouvées et le réseau du mode par défaut a été le premier réseau identifié lorsqu'un sujet n'est pas engagé dans une tâche, d'où son nom « mode par défaut ». Par la suite d'autres réseaux fonctionnels de l'état de repos ont été caractérisés par la présence de fluctuations synchrones de basses fréquences en IRMf, et attribués à des fonctions connues spécifiques (Buckner et al., 2008 ; Fox & Raichle, 2007 ; Raichle et al., 2001). Les fluctuations cérébrales au repos dites « spontanées » semblent donc le reflet de schémas d'activités spatiotemporelles coordonnées et très structurées plutôt que le résultat du bruit. De manière plus élargie, les différentes régions cérébrales présentent des fluctuations cohérentes de leur activité spontanée, formant des réseaux fonctionnellement couplés qui changent de composition en fonction de leur état (Fox & Greicius, 2010). Ainsi, le cortex et, dans un sens plus large le cerveau apparaît comme un système continuellement très actif avec un fonctionnement interne qui a une organisation propre, plutôt que comme un système passif qui est organisé seulement par des stimuli externes. Cette approche a donné lieu à une littérature abondante dans le champ de la neuro-imagerie.

### **L'état de repos en MEG**

Si l'état de repos a d'abord été exploré via l'IRM fonctionnelle qui utilise un signal métabolique lié à la réponse vasculaire qui fait suite au couplage neurovasculaire, il a été pertinent de reproduire ces résultats en électrophysiologie qui fournit un corrélat fonctionnel beaucoup plus direct de l'activité neuronale précédant la réponse vasculaire. Grâce à la localisation de sources corticales, les études de l'activité de repos en électrophysiologie se sont notamment centrées sur la connectivité fonctionnelle. Les méthodes d'étude de la connectivité fonctionnelle utilisaient la corrélation d'amplitude (couplage d'amplitude, corrélation d'enveloppe) (Brookes et al., 2011 ;

Hipp et al., 2012), les couplages de phase (PLV, PLI, wPLI, PSI, MPSI) (Basti et al., 2018; Canolty et al., 2006; Ewald et al., 2012; Lachaux et al., 1999; Lobier et al., 2014; Nolte et al., 2004, 2008; J. M. Palva & Palva, 2012; Stam et al., 2007; Vinck et al., 2011), ou une combinaison des deux (couplage de phase et d'amplitude) (Canolty et al., 2006; Florin & Baillet, 2015; Özkurt & Schnitzler, 2011; Tort et al., 2010). La première étude démontrant des corrélats neuronaux de l'état de repos similaires à l'IRMf, en utilisant le signal MEG, est celle de (Nikouline et al., 2001). Il s'agit des premières démonstrations de corrélations entre une puissance de bande de fréquence au repos entre deux hémisphères ayant fait émerger un réseau. Dix années plus tard, (Liu et al., 2010) démontrent une cohérence dans les très basses fréquences (<0,1 Hz) à travers des régions opposées homologues dans chaque hémisphère. (De Pasquale et al., 2010) ont utilisé une méthode de connectivité avec un nœud de référence pour reproduire le réseau pariétal dorsal lié à l'attention et le réseau par défaut bien connu en IRMf. Prenant en compte l'instabilité (fluctuation dans le temps) du signal, ils trouvent des réseaux observables de façon transitoire. Finalement, la première étude démontrant des réseaux spatialement indépendants et très similaires à ceux démontrés en IRMf, est celle de (Brookes et al., 2011) qui montre 8 réseaux différents, pour la plupart reliés à la bande de fréquence bêta comme la majorité des études précédentes. Globalement, ces études démontrent que les corrélations à travers les régions cérébrales sont les plus fortes dans les bandes alpha et bêta (8-32 Hz). De plus, une affinité particulière a été observée entre régions cérébrales et bandes de fréquence, notamment entre le lobe temporal médial et la bande thêta (4-6 Hz), les régions pariétales latérales et la bande alpha-beta (8-23 Hz), ainsi que les régions sensorimotrices et les plus hautes fréquences (32-45 Hz). Les résultats de ces études démontrent de forts liens entre les réseaux basés sur les réponses hémodynamiques et les oscillations électromagnétiques cérébrales et mettent en avant l'intérêt de la MEG et la richesse de son signal pour étudier les réseaux neuronaux fonctionnels (Cabral et al., 2014).

### **Bases physiologiques de l'état de repos**

L'électrophysiologie est l'étude des phénomènes électriques chez les êtres vivants. En neurosciences, cette branche de la physiologie se consacre à l'étude de l'activité électrique des cellules du système nerveux. Le signal mesuré en électro-encéphalographie est un champ de

potentiel électrique, et dans le cas de la magnétoencéphalographie (MEG), un champ électromagnétique. Ce champ de potentiel électrique local extracellulaire est le résultat d'une différence de potentiel électrique entre une région d'intérêt et une référence préalablement déterminée. Il est constitué de la superposition de toutes les activités ioniques membranaires dans une région mesurée, des activités neuronales plus rapides aux activités gliales généralement plus lentes. Cependant, le principal acteur de ce champ électrique local est l'activité synaptique des neurones pyramidaux. L'activité synaptique représente l'effet des neurotransmetteurs activant les récepteurs AMPA et NMDA. Ces derniers créent un courant excitateur qui est le produit de l'activité ionique  $\text{Na}^+$  et  $\text{Ca}^{2+}$  extracellulaire autour de la synapse (Riedner et al., 2011). Pour garder un système électriquement homéostatique, un courant opposé intracellulaire parcourt le neurone, ce qui crée un dipôle électrique ou N-pole suivant le nombre de synapses actives en même temps (Buzsáki et al., 2012).

Malgré le très grand nombre de synapses et donc une grande contribution électrique au champ extracellulaire, d'autres phénomènes électriques participent à former le champ de potentiel électrique. Les potentiels d'actions rapides, identifiés comme des pointes ou « spikes » (Koch, 1999), participent au champ électrique extracellulaire en générant le courant le plus fort le long de la membrane du neurone. Ces pointes ont une forte amplitude, sont relativement courtes (environ 2 ms) et joueraient un rôle dans les hautes fréquences au-dessus de 100 Hz, et nécessitent une méthode d'analyse adaptée pour les étudier (Andersen et al., 1971). Les pointes  $\text{Ca}^{2+}$  constituent un autre phénomène qui participe au champ électrique extracellulaire mesuré, mais ces pointes ne sont pas en lien avec l'activité de la synapse. L'activité calcique des dendrites dure entre 10 à 50 ms alors que celle de l'axone dure entre 10 à 100 ms. La différence temporelle est ce qui permet de différencier les deux mécanismes, mais ce phénomène est encore peu connu (Wong et al., 1979). Les courants intrinsèques et le phénomène de résonance électrique contribuent aussi au champ électrique extracellulaire. Ces effets électriques ont été observés indépendamment de l'activité synaptique (Llinas, 1988). Par exemple, le voltage ainsi que la fréquence sont des caractéristiques de résonance. En effet, certains neurones résonnent en fréquence thêta basée sur le voltage alors que d'autres neurones inhibitoires résonnent davantage sur la fréquence gamma (Cardin et al., 2010; Freund & Buzsáki, 1996). Un autre

évènement contribue au champ électrique, ce sont les périodes réfractaires après l'hyperpolarisation, encore appelées « down states ». Ces états sont observés par une oscillation delta des couches corticales 2 et 3 lors du sommeil non-REM (Hotson & Prince, 1980). Les jonctions lacunaires peuvent augmenter la synchronie neuronale et contribuent au champ extracellulaire par leurs échanges ioniques (Bennett & Zukin, 2004). Les activités entre neurones et cellules gliales ainsi que l'activité vasculaire contribuent aussi au potentiel de champ électrique cérébral (Poskanzer & Yuste, 2011). Finalement, l'effet « ephaptic » est un phénomène de conduction électrique au sein même du milieu extracellulaire (Chan & Nicholson, 1986). Cette conduction participerait au phénomène de résonance et serait un moyen de communication parallèle entre les neurones hors synapses. Ce phénomène participe aussi au champ électrique extracellulaire enregistré (Anastassiou et al., 2010). Les variations recueillies par le champ potentiel électrique cérébral sont probablement la mesure la plus directe de l'activité des neurones et sont considérées comme le « gold standard » pour investiguer la dynamique neuronale. Cependant, il ne faut pas perdre de vue qu'elle est aussi constituée de plusieurs autres sources contribuant au champ de potentiel électrique que l'activité synaptique (Buzsáki et al., 2012; Scanziani & Häusser, 2009).

### **La Magnétoencéphalographie (MEG)**

L'apparition de la MEG est plus tardive que l'EEG, car c'est seulement en 1972, que David Cohen procède à des enregistrements de champs magnétiques cérébraux donnant ainsi naissance à la magnétoencéphalographie. Ce délai d'apparition est dû à la difficulté d'enregistrer les très faibles champs magnétiques cérébraux, puisque ceux-ci sont de l'ordre de la centaine de femtoeslas ( $10^{-13}\text{T}$ ), c'est-à-dire dix milliards de fois plus faibles que le champ magnétique terrestre. La MEG est donc basée exactement sur le même fonctionnement que l'EEG à la différence qu'elle ne recueille pas des variations de courant électrique sur le scalp, mais des variations de champ électromagnétique au pourtour du crâne. La MEG utilise des magnétomètres basés sur l'effet Josephson appelés « Superconducting Quantum Interference Device » (SQUID) qui sont actuellement les instruments les plus sensibles disponibles pour mesurer l'intensité du champ magnétique. Les magnétomètres SQUID mesurent la variation du champ magnétique d'un certain degré de champ arbitraire ; ils ne mesurent pas la valeur absolue du champ. Le rôle des

magnétomètres est de transformer le flux magnétique en tension électrique et pour ce faire ils doivent être gardés dans de l'hélium liquide à une température de  $-269\text{ }^{\circ}\text{C}$ . Les systèmes de MEG comptent typiquement entre 100 et 300 capteurs par casque. Comme les champs magnétiques cérébraux sont extrêmement faibles, toute source de contamination électromagnétique doit être éliminée. Il est donc nécessaire d'adopter des techniques d'atténuation du bruit. Pour cela, les moyens généralement mis en œuvre sont tout d'abord l'utilisation d'un gradiomètre axial où les deux bobines des capteurs s'enroulent en directions opposées pour annuler l'effet des champs éloignés et garder seulement les champs venant du cortex. Ensuite, le système est installé dans une cabine blindée pour le protéger des bruits ambiants. Le revêtement est fait de métal isolant qui est mis à la terre ; cela élimine le bruit électromagnétique des appareils électriques et des autres sources. La présence d'une chambre blindée permet d'atténuer les champs magnétiques extérieurs d'un facteur d'environ  $10^3$ . Et finalement, l'utilisation de capteurs de référence a pour effet de bloquer des sources de bruits lointains (Garnero et al., 1998; Gosseries et al., 2008). Les dipôles électriques orientés parallèlement à la surface du crâne sont les seuls capables de donner naissance à un champ magnétique mesurable à l'extérieur du scalp et la MEG est particulièrement sensible à ce type de dipôle. Ces dipôles se retrouvent principalement dans les sillons et scissures corticales, qui constituent environ  $2/3$  de la surface corticale. Le signal enregistré en MEG est donc le résultat de l'activité simultanée de millions de neurones (Garnero et al., 1998; Gavaret et al., 2008; Gosseries et al., 2008; Vrba & Robinson, 2001). L'utilisation de la MEG comporte plusieurs avantages. Dans un premier temps, la MEG se caractérise par une excellente résolution temporelle, de l'ordre de la milliseconde. Lorsqu'elle est combinée avec l'imagerie par résonance magnétique (IRM), la MEG permet aussi la localisation des sources électriques d'où proviennent les champs magnétiques en utilisant un modèle inverse. La MEG possède également un grand nombre de capteurs et n'est pas sensible aux variations de conductivité et à l'anisotropie, c'est-à-dire que son signal n'est pas altéré par les structures qu'elle traverse à savoir les méninges, le liquide céphalo-rachidien et la boîte crânienne (Garnero et al., 1998; Gavaret et al., 2008; Gosseries et al., 2008; Vrba & Robinson, 2001).

## Les oscillations cérébrales

Le signal collecté en électrophysiologie correspond à une variation d'énergie contenant une résolution temporelle assez élevée de l'ordre de la milliseconde, de sorte qu'il est possible d'en étudier les caractéristiques fréquentielles, notamment en calculant la décomposition spectrale du signal. La méthode la plus classique et la plus utilisée est la transformation de Fourier qui permet d'étudier la partie oscillatoire du signal, classiquement regroupée en bandes de fréquences. L'oscillation possède deux caractéristiques, une d'amplitude (absolue ou relative) souvent reliée à l'amplitude du signal même et une d'information de phase. Ces paramètres du signal permettent d'observer comment des groupes de neurones déchargent de façon synchrone ou asynchrone et à différents rythmes. L'amplitude est modulée par la synchronie ou l'asynchronie et reflète de manière indirecte le nombre de neurones impliqués alors que la fréquence dépend du rythme de décharge des différents groupes de neurones (Niedermayer, E. & Lopes da Silva, 2005). L'activité des groupes neuronaux se caractérise par plusieurs bandes oscillatoires dont les fréquences vont d'environ 0,05 Hz à 500 Hz (Buzsaki & Draguhn, 2004). Ces fréquences sont classées en plusieurs bandes de fréquences. La figure 2 ci-dessous montre un schéma de classification typique, bien que d'autres classifications soient également possibles.

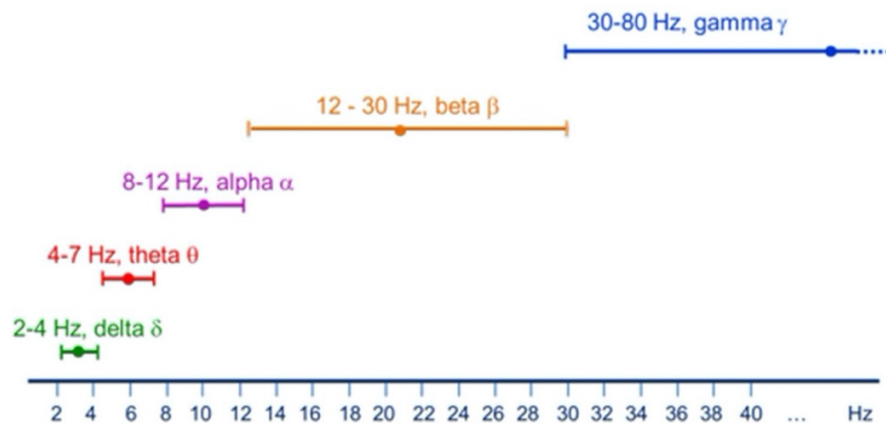


Figure 2. – Les principaux rythmes cérébraux sont classés selon leur plage de fréquence tiré de (Buzsaki & Draguhn, 2004).

## Activité non oscillatoire à large bande (1/f)

On trouve dans l'activité cérébrale une composante à large bande (ou arythmique) qui représente une part importante du signal électrique cérébral (B. J. He, 2014). En effet, sur un spectre de décomposition spectrale cela correspond à la partie dite de « fond », davantage observable comme la partie linéaire représentée avec une échelle logarithmique (figure 3). Longtemps considéré comme un bruit physiologique, il a récemment été exploré pour avoir un lien avec la performance cognitive, notamment le coefficient de la pente 1/f (Ouyang et al., 2020). Les hypothèses physiologiques quant au processus sous-jacent ne font pas consensus. Il a été démontré que l'équilibre excitation-inhibition des circuits neuronaux modifie la pente du spectre de la loi de puissance. Des modèles computationnels ont été développés pour simuler ce processus, permettant ainsi l'inférence de l'équilibre excitation-inhibition à partir de signaux neurophysiologiques (Gao et al., 2017). Une autre théorie bien connue destinée à expliquer la genèse des phénomènes de loi de puissance est la théorie dite de la criticalité auto-organisée (Beggs, 2008; Beggs & Plenz, 2003; Hesse & Gross, 2014; Per Bak, Chao Tang, 1987). Cette théorie postule que la loi de puissance est un phénomène émergent qui provient de systèmes dynamiques en interaction qui fonctionnent dans des états critiques, ce qui est optimal pour le traitement de l'information (Beggs, 2008).

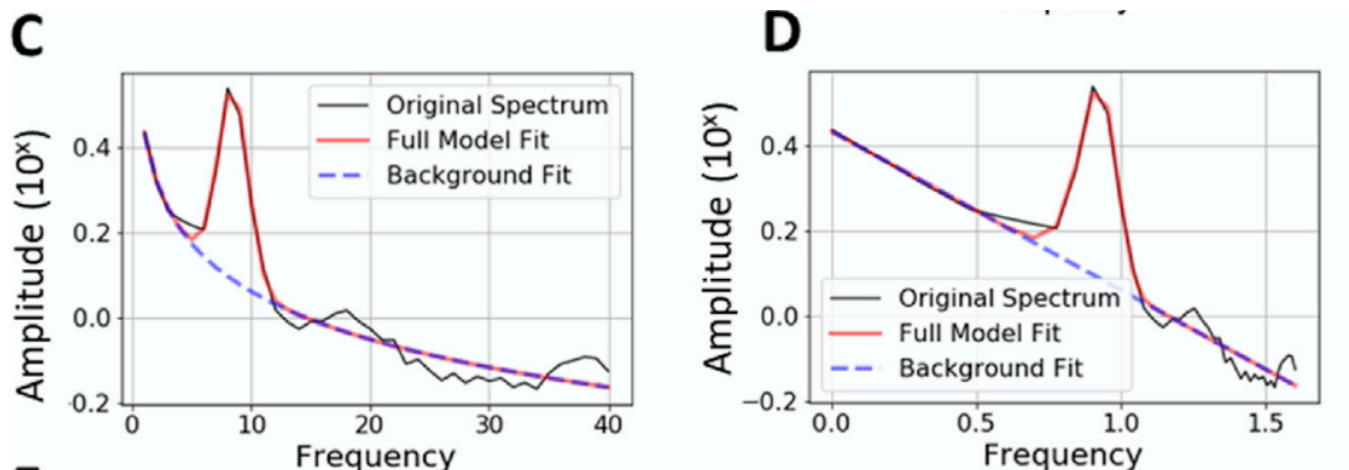


Figure 3. – Exemple, C) spectre de puissance D) spectre de puissance (échelle log-log) (tirée de (Ouyang et al., 2020)

## **Les sources corticales une analyse récente**

Une fois établi que l'activité spontanée en électrophysiologie à l'état de repos possède des caractéristiques autoémergentes, il est pertinent de voir comment elle permet d'aider la compréhension des processus cognitifs. Étonnamment, les études en électrophysiologie se sont souvent partagées entre deux types d'analyses quant aux processus cognitifs à l'état de repos (donc en excluant les paradigmes en tâche). Elles ont utilisé soit des analyses spectrales quantitatives au niveau des capteurs (EEG ou MEG), soit la connectivité spectrale (connectivité, réseaux et dynamique des réseaux ou topologie des réseaux). Les premières analyses renseignent sur les variations de puissances sans préciser spatialement les régions cérébrales impliquées, et les analyses de connectivité renseignent sur l'interaction des régions cérébrales entre elles, mais ne fournissent pas de renseignement sur l'activité neuronale et ses caractéristiques. Finalement les seules études qui mesurent l'activité spectrale au niveau local dans le cortex sont les techniques invasives d'enregistrement intracrânien (iEEG, SEEG). Mais comme dans ces enregistrements l'activité n'est pas enregistrée dans tout le cerveau, il n'est donc pas possible d'avoir une comparaison spatiale de l'activité cérébrale à travers tout le cerveau et entre des participants. De plus les participants qui participent à ces enregistrements sont toujours des patients qui ont des pathologies cérébrales (épilepsie réfractaire, chirurgie en lien avec des processus tumoraux, etc.). Il est donc difficile d'affirmer qu'ils représentent une population dite neurotypique fonctionnellement, principalement dans l'auto-organisation spontanée cérébrale.

## **Modèle des processus cognitifs**

### **Modèle modal de la mémoire**

Le modèle modal de la mémoire a été proposé par (Atkinson & Shiffrin, 1968) et constitue un modèle structurel. Ils ont proposé que la mémoire soit constituée de trois magasins : un registre sensoriel, la mémoire à court terme (MCT) et la mémoire à long terme (MLT). L'information passe d'une étape à l'autre de manière linéaire, et a été décrite comme un modèle de traitement de l'information de manière linéaire avec une entrée, un traitement et une sortie (figure 4). Les informations sont détectées par les organes des sens et entrent dans la mémoire sensorielle. Si l'on y prête attention, cette information entre dans la mémoire à court terme. Les informations



de la mémoire à court terme ne sont transférées à la mémoire à long terme que si elles sont répétées. S'il n'y a pas de répétition, l'information est oubliée et disparaît de la mémoire à court terme par les processus de déplacement ou de dégradation.

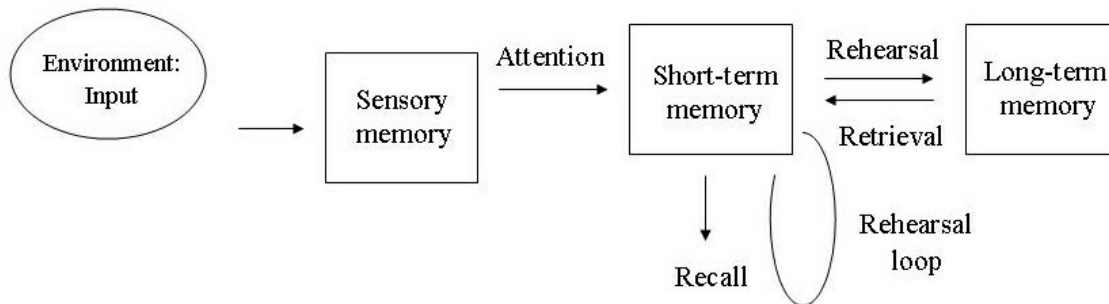


Figure 4. – Modèle modal de la mémoire, issu de Atkinson et Shiffrin (1968)

### **Les niveaux de traitement : Un cadre pour la mémoire**

Le modèle des niveaux de traitement ( Craik & Lockhart, 1972) se concentre sur la profondeur du traitement impliqué dans la mémoire, et prédit que plus l'information est traitée en profondeur, plus la trace mnésique sera longue. Cela est divisé en deux types de traitement superficiel et profond. Dans le traitement superficiel, on trouve le traitement structurel qui consiste à coder uniquement les qualités physiques de quelque chose. Par exemple, la police de caractères d'un mot ou l'apparence des lettres et le traitement phonémique c'est-à-dire lorsque nous encodons le son. Le traitement superficiel n'implique qu'une répétition dite « d'entretien » pour garder l'information en mémoire à court terme. Le traitement profond implique le traitement sémantique, qui se produit lorsque nous encodons la signification d'un mot et que nous le mettons en relation avec des mots similaires ayant une signification similaire.

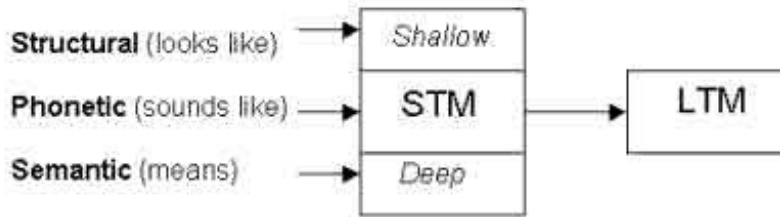


Figure 5. – Modèle des niveaux de traitement de la mémoire issue de Craik et Lockhart (1972).

### Modèle de la mémoire de travail

(A. D. Baddeley & Hitch, 1974) proposent d’ajouter au modèle modal de la mémoire de Atkinson & Shiffrin des sous-systèmes, notamment le calepin visuospatial qui permet le maintien des informations visuelles ainsi que phonologiques permettant de retenir et de manipuler des informations sous forme verbale (A. D. Baddeley, 1978). Plus récemment, l’ajout d’un tampon épisodique permet aux informations contenues en mémoire de travail d’accéder à la mémoire à long terme épisodique. La dernière composante de son modèle est l’administrateur central qui agit comme mécanisme attentionnel de coordination et de contrôle (A. Baddeley, 2000).

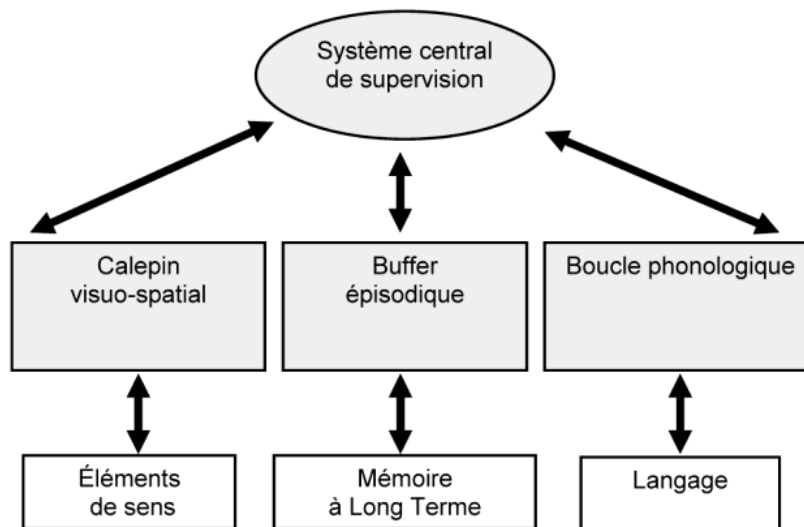


Figure 6. – Les composantes du modèle de la mémoire de travail (A. Baddeley, 2000)

## Boucle phonologique

La boucle phonologique est une composante du modèle de mémoire de travail qui traite du matériel parlé et écrit. Elle se subdivise en deux parties : le magasin phonologique (qui conserve l'information sous forme de discours) et le processus articulatoire (qui nous permet de répéter l'information verbale en boucle). Le magasin phonologique (lié à la perception de la parole) agit comme une oreille interne et retient les informations sous une forme basée sur la parole (c'est-à-dire les mots prononcés) pendant 1 à 2 secondes. Les mots parlés entrent directement dans la mémoire. Les mots écrits doivent d'abord être convertis en un code articulatoire (parlé) avant de pouvoir entrer dans la mémoire phonologique. Le processus de contrôle articulatoire (lié à la production de la parole) agit comme une voix intérieure qui répète les informations provenant de la mémoire phonologique. Il fait circuler l'information en boucle comme une boucle de bande magnétique. C'est ainsi que nous nous souvenons d'un numéro de téléphone que nous venons d'entendre. Tant que nous le répétons, nous pouvons conserver l'information dans la mémoire de travail. Le processus de contrôle articulatoire convertit également le matériel écrit en un code articulatoire et le transfère dans la mémoire phonologique.

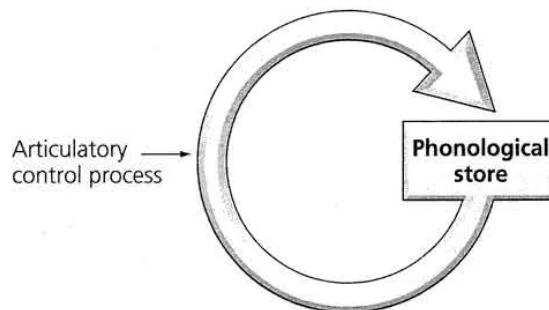


Figure 7. – Boucle phonologique (A. Baddeley, 2000)

## Mémoire sémantique et épisodique

La mémoire sémantique est une partie de la mémoire explicite à long terme chargée de stocker des informations sur le monde. Cela inclut les connaissances sur la signification des mots, ainsi

que les connaissances générales. La mémoire épisodique est une partie de la mémoire explicite à long terme chargée de stocker des informations sur des événements (c'est-à-dire des épisodes) que nous avons vécus dans notre vie (Tulving, 1972).

### **Fonctions exécutives**

En psychologie, les fonctions exécutives désignent un ensemble assez hétérogène de processus cognitifs de haut niveau. Elles permettent aux individus de réguler leurs pensées et leurs actions lors d'un comportement orienté vers un objectif. Dans le développement, leur mise en place est cruciale pour prédire la réussite de tout apprentissage futur, réussite scolaire ou même professionnelle. D'un point de vue cognitif ou neuropsychologique traditionnel, on pense que les fonctions exécutives comprennent un ensemble de domaines cognitifs distincts qui comprennent la vigilance ou l'attention soutenue (Pennington & Ozonoff, 1996; Smith & Jonides, 1999); l'initiation de comportements complexes orientés vers un but (Muriel Deutsch Lezak, 1995); l'inhibition de réponses prépotentes, mais incorrectes (Luna et al., 2010; Smith & Jonides, 1999); la flexibilité pour passer facilement d'un état à l'autre (Ravizza & Carter, 2008); la planification des étapes nécessaires pour atteindre un objectif (Smith & Jonides, 1999); et la mémoire de travail, la capacité à garder des informations à l'esprit et à les manipuler pour guider la sélection des réponses (Goldman-Rakic, 1996). La théorie Unité/diversité (Friedman & Miyake, 2017; Miyake et al., 2000; Miyake & Friedman, 2012) est une théorie très dominante dans la littérature sur les fonctions exécutives. Grâce à une analyse de régression basée sur une série de tests comportementaux neuropsychologiques, ils ont pu mettre à jour trois fonctions exécutives spécifiques indépendantes, la première est une dimension commune partagée par tous les tests exécutifs, c'est la composante d'inhibition, la seconde est spécifique aux capacités de mise à jour et la troisième est spécifique aux capacités de flexibilité cognitive (figure 8).

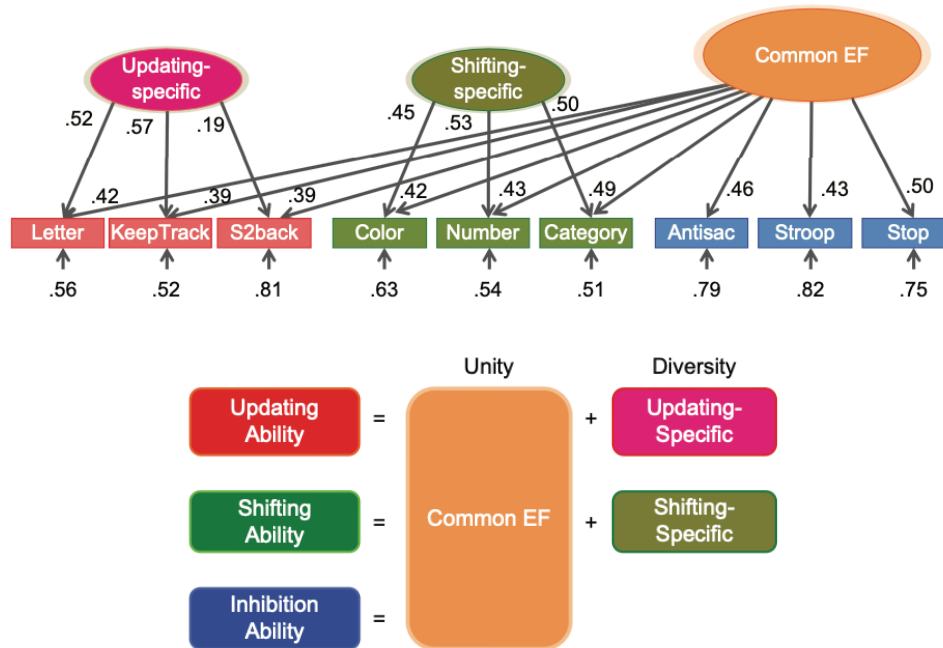


Figure 8. – Modèle Unité/diversité des fonctions exécutives (Miyake et al., 2000)

## Tests neuropsychologiques

Un test neuropsychologique est un questionnaire, une échelle ou un paradigme permettant d'évaluer le bon fonctionnement des fonctions ou processus cognitifs. Les tests utilisés pour l'évaluation neuropsychologique prennent souvent la forme de tâches papier/crayon, de questions orales ou parfois de tâches sur l'ordinateur. Il permet une mesure objective et standardisée d'un échantillon du comportement et permettent de comparer un sujet à un échantillon de sujets représentatif de sa population d'origine. Les tests sont indépendants de la plainte du sujet/patient, c'est-à-dire qu'ils évaluent directement le processus ou la fonction cognitive impliquée dans le comportement. Les tests sont standards, car reproductibles selon l'évaluateur (si le test nécessite un évaluateur), ils sont aussi reproductibles et fiables le temps. Enfin, le test est validé et offre la possibilité d'obtenir une standardisation des scores suivant l'âge, la langue et les facteurs culturels et le niveau d'éducation cela est possible grâce à de grands échantillons effectués au préalable.

## Wechsler Adult Intelligence Scale (WAIS-IV)

La Wechsler Adult Intelligence Scale (WAIS) est un test conçu pour mesurer l'intelligence des adultes. L'échelle WAIS est composée de plusieurs tests brefs, les sous-tests. Chaque sous-test commence par un problème simple, puis se poursuit avec des problèmes de plus en plus difficiles à résoudre. L'échelle se compose de tests impliquant une modalité verbale et de tests non verbaux moteurs ou visuospatiaux. Chaque sous-test donne un nombre de points au participant. Ces scores sont normalisés et correspondent à la performance du participant par rapport à une population générale. Le score global donne un quotient intellectuel (QI) (*Full-Scale Intellectual Quotient*). La quatrième version du WAIS permet aussi de calculer des index (mémoire de travail, vitesse de traitement, compréhension verbale, raisonnement perceptuel (figure 9), ces index peuvent être regroupés en facteur verbal ou non verbal ou intelligence fluide ou cristallisée (GAI, CPI).

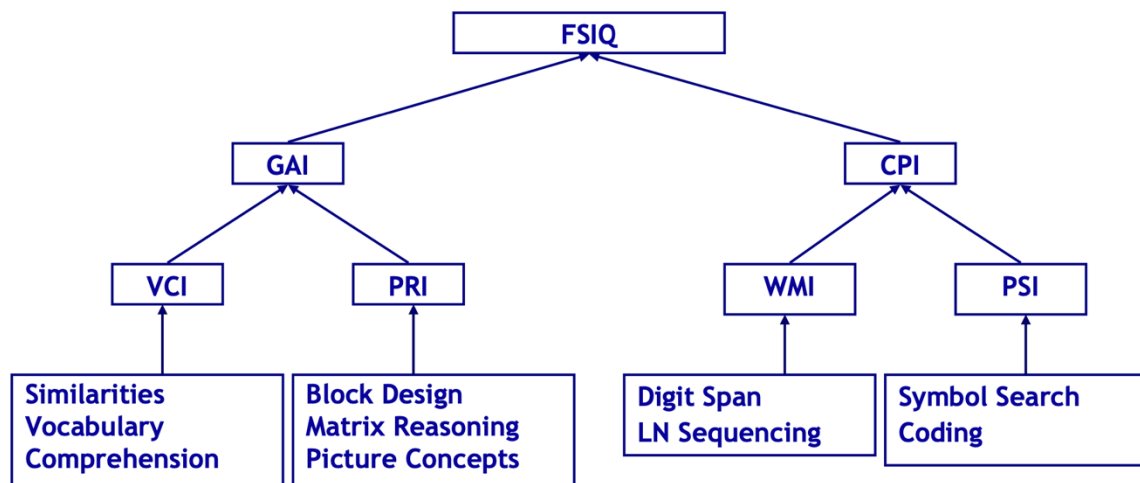


Figure 9. – Sous test et indexes du WAIS-IV (Welscher et al., 2000)

## Trail Making Test

Le *Trail Making Test* (TMT) est un test neuropsychologique d'attention visuelle et de rapidité motrice, il implique une flexibilité cognitive et ainsi qu'une capacité de rétention et de manipulation de l'information. Il se compose de deux parties dans lesquelles le sujet doit relier

un ensemble de 25 points aussi rapidement que possible tout en restant précis. Plus globalement ce test peut fournir des informations sur les fonctions exécutives (Arnett & Labovitz, 1995; Tombaugh, 2004). La première version consistait en deux tests (conditions A et B), la version contemporaine comprend 4 tests (condition 1 à 4). Dans la condition A, le participant doit tracer des lignes pour relier des chiffres encerclés dans une séquence numérique (par exemple 1-2-3, etc.) aussi rapidement que possible. Dans la condition B, le participant doit tracer des lignes pour relier des chiffres et des lettres encerclés dans une séquence numérique et alphabétique alternée (par exemple, 1-A-2-B, etc.) aussi rapidement que possible (Butler et al., 1991; Rabin et al., 2005; Salthouse, 2011; Sellers & Nadler, 1993).

### **La fluence verbale (*verbal fluency*)**

Le test de fluidité (ou fluence) verbale est un test court du fonctionnement verbal. Il se compose généralement de deux tâches : la fluidité des catégories (parfois appelée fluidité sémantique) et la fluidité des lettres (parfois appelée fluidité phonémique). Dans les versions standard des tâches, les participants disposent d'une minute pour produire autant de mots uniques que possible dans une catégorie sémantique (fluence de catégorie) ou commençant par une lettre donnée (fluence de lettre). Le score du participant dans chaque tâche correspond au nombre de mots uniques corrects (Shao et al., 2014). La fluence verbale est une fonction cognitive qui facilite la récupération des informations en mémoire. Une récupération réussie exige un contrôle exécutif des processus cognitifs tels que l'attention sélective, l'inhibition sélective, le changement d'ensemble mental et la génération de réponses internes (Muriel D Lezak et al., 2004).

### **Apprentissage verbal (*California Verbal Learning Test 2*)**

Le *California Verbal Learning Test* - deuxième édition (D.C. Delis, J.H. Kramer, E. Kaplan, 2000) est un outil clinique très largement utilisé, principalement pour évaluer l'apprentissage verbal, la mémoire épisodique ou la mémoire verbale (Rabin et al., 2005). Une liste de 16 items (Liste A) organisée en quatre catégories sémantiques (meubles, légumes, moyens de transport et animaux), sans mots consécutifs de la même catégorie, est répétée au sujet au cours de cinq essais de rappel immédiat. Une liste d'interférence (liste B) est présentée, qui partage deux catégories de la liste A et possède deux catégories non partagées. Le rappel libre et le rappel par

catégorie sont testés immédiatement après (délai court) et après 20 minutes (délai long). Enfin, un test de reconnaissance « oui/non », composé de 16 items de la liste A, de huit (8) de la liste B et de 20 distracteurs aléatoires, est présenté. Le CVLT-2 fait partie des cinq instruments d'évaluation les plus couramment utilisés par les neuropsychologues cliniques en Amérique du Nord (Rabin et al., 2005) et la validité de construction du CVLT a reçu un soutien considérable dans la littérature neuropsychologique (M. P. Alexander et al., 2003; Baldo et al., 2020; Crosson, 2008; Kibby et al., 1998; Schear & Craft, 1989). La mesure principale de l'apprentissage sur le CVLT est le rappel total des réponses correctes sur les cinq essais d'apprentissage de la liste A. En outre, le CVLT a également permis de mesurer la stratégie d'apprentissage préférée en comptant le nombre de groupes de mots par association sémantique, ou par l'ordre dans lequel ils ont été présentés et leur association en série tout en corrigeant pour le hasard.

## **Lien entre imagerie de repos et processus cognitifs**

### **Fonction exécutive**

#### Mémoire de travail verbale

Au cours des dernières années, plusieurs études d'IRMf et en PET ont spécifiquement étudié les zones cérébrales impliquées dans la mémoire de travail verbale (Honey et al., 2000; Narayanan et al., 2005; Veltman et al., 2003). En effet une variété de réseaux cérébraux sont activés pendant une tâche de mémoire de travail verbale, notamment des zones du cortex préfrontal (PFC) et du cortex pariétal, ainsi que des régions du cervelet et des ganglions de la base (Buchsbaum et al., 2011; Chai et al., 2018; Chang et al., 2007; Crosson et al., 1999; Desmond et al., 1997; Lewis et al., 2004; Paulesu et al., 1993; Petrides et al., 1993; Thürling et al., 2012). Un effet de latéralisation dû à la modalité a été rapporté dans plusieurs méta-analyses, le PFC gauche pourrait être impliqué de manière prédominante dans les processus de la mémoire de travail verbale alors que le PFC droit semble être plus fortement impliqué dans la mémoire de travail spatiale (Owen et al., 2005). La boucle articulatoire est associée au cortex frontal inférieur gauche (l'aire de Broca), ainsi qu'à l'aire motrice supplémentaire gauche, au cortex prémoteur gauche et à l'insula gauche. Il a été démontré que le stockage phonologique est associé au gyrus supramarginal gauche situé dans



le lobule pariétal inférieur gauche. Ainsi, ces régions sont essentielles pour tout type de tâche de mémoire de travail verbale (Buchsbaum & D'Esposito, 2008; Paulesu et al., 1993; Smith & Jonides, 1999). L'activation pariétale a été interprétée comme un tampon relatif à la modalité utilisée pendant une tâche de mémoire. Enfin, on sait que les zones limbiques, comme le cortex cingulaire, sont impliquées dans la mémoire de travail en lien avec l'effort demandé pendant une tâche.

Des preuves d'une relation entre les oscillations neuronales et l'activité de la mémoire de travail chez l'homme ont été rapportées lors de tâches par des études en EEG, MEG et ECOG. Ces études montrent une augmentation de l'amplitude et de la synchronisation de l'activité oscillatoire en fonction de la charge cognitive pendant une tâche mémoire de travail, ces effets ont été trouvés dans différentes bandes de fréquences, en particulier dans la bande thêta (4–7 Hz), alpha (8–13 Hz) et gamma (30–200 Hz), ces activations ont été localisées principalement dans les régions fronto-pariétales et le cortex cingulaire antérieure (Bonfond & Jensen, 2012; Jensen et al., 2002; Jensen & Mazaheri, 2010; W. Klimesch et al., 1993; Wolfgang Klimesch, 1999, 2012; Wolfgang Klimesch et al., 2007; S. Palva & Palva, 2007; Scheeringa et al., 2009; Tuladhar et al., 2007).

### Fluence verbale

Les corrélats neuronaux de la fluence verbale indiquent que la génération de verbes implique les zones frontales-striatales, notamment les ganglions de la base, le cortex préfrontal dorsolatéral et le gyrus frontal inférieur gauche (Sanjuán et al., 2010). Une méta-analyse d'IRM fonctionnelle a montré une activation significative dans le cortex préfrontal médian gauche et droit pendant les tâches de fluence verbale phonémique (Wagner et al., 2014). L'implication des régions frontales semble cruciale pour la fluence verbale, en effet les déficiences en performance de fluence verbale sont associées à des lésions du lobe frontal (Beber & Chaves, 2014; Davis et al., 2010; Piatt et al., 1999). De plus, des différences d'activations ont été trouvées entre les tâches de fluence verbale, sémantique et phonémique (Clark et al., 2014; Faroqi-Shah & Milman, 2018; Gordon et al., 2018; Henry et al., 2004; Östberg et al., 2007; Stokholm et al., 2013). Néanmoins, peu de recherches en IRMf ont été menées sur les mécanismes neuronaux soutenant la performance de la tâche de fluence verbale (Kochhann et al., 2018). En électrophysiologie, il a été montré que la récupération phonologique était associée à une diminution du bêta et à une

augmentation du thêta dans le lobe frontal gauche en revanche ces changements ne sont pas observés lors d'une récupération sémantique des mots (Mousavi et al., 2020). En utilisant la stimulation transcrânienne magnétique pour moduler la phase de l'oscillation thêta dans le cortex gauche péri-sylvien et frontal gauche inférieur, ils montrent que la phase de cette oscillation est cruciale pour les associations sémantiques et leur récupération (Marko et al., 2019).

### Flexibilité cognitive

Dans une revue systématique qui compare plusieurs résultats en neuro-imagerie sur les corrélats neuronales du TMT (Varjadic et al., 2018), trois études ont été retenues pour montrer des activations pour la différence entre les conditions (TMTA et TMTB). Deux entre elles (Jacobson et al., 2011; Zakzanis et al., 2005) démontrent des activations frontales (du cortex moteur au cortex préfrontal) ainsi que des activations dans la voie ventrale à gauche (insula/gyrus médian temporal/gyrus supérieur temporal), alors que la troisième étude (Moll et al., 2002), qui a adapté le TMT pour les besoins expérimentaux, a modifié la tâche sous forme verbale ; elle ne démontre aucune activité dans la voie ventrale et seulement des activations dans la voie dorsale complète (lobe pariétal au lobe pré-frontale). Une étude a été faite à l'état de repos en MEG au niveau des capteurs ; ils ont constaté que, chez les adultes plus âgés (>54 ans), une puissance delta et thêta plus élevée était associée à une meilleure performance (temps de réalisation) dans le TMT. Aucune corrélation de ce type n'a été observée chez les participants plus jeunes (18–54 ans). La performance sur le TMT était positivement corrélée avec la puissance de la bande delta (0,5–4 Hz) dans les régions temporales et centrales droites, et avec la puissance de la bande thêta (4,5–7,5 Hz) dans les régions temporales gauches.

### Traitement du langage

Au cours des dernières décennies, des avancées majeures dans la compréhension de la neurobiologie du langage verbal humain ont conduit au développement d'alternatives au modèle classique de Wernicke-Lichtheim-Geschwind (par exemple, Hagoort & Indefrey, 2014; Hickok & Poeppel, 2004; Tremblay & Dick, 2016). La théorie la plus influente (c'est-à-dire le modèle à double voie) considère deux voies chevauchant partiellement et remplissant des fonctions différentes : (i) une voie ventral impliquant les aires temporales bilatérales pour les processus de

la parole au sens ; et (ii) une voie dorsal dominant gauche impliquant les aires fronto-insulo-Wernicke pour la cartographie de la parole à l'articulation (Hickok & Poeppel, 2004, 2007).

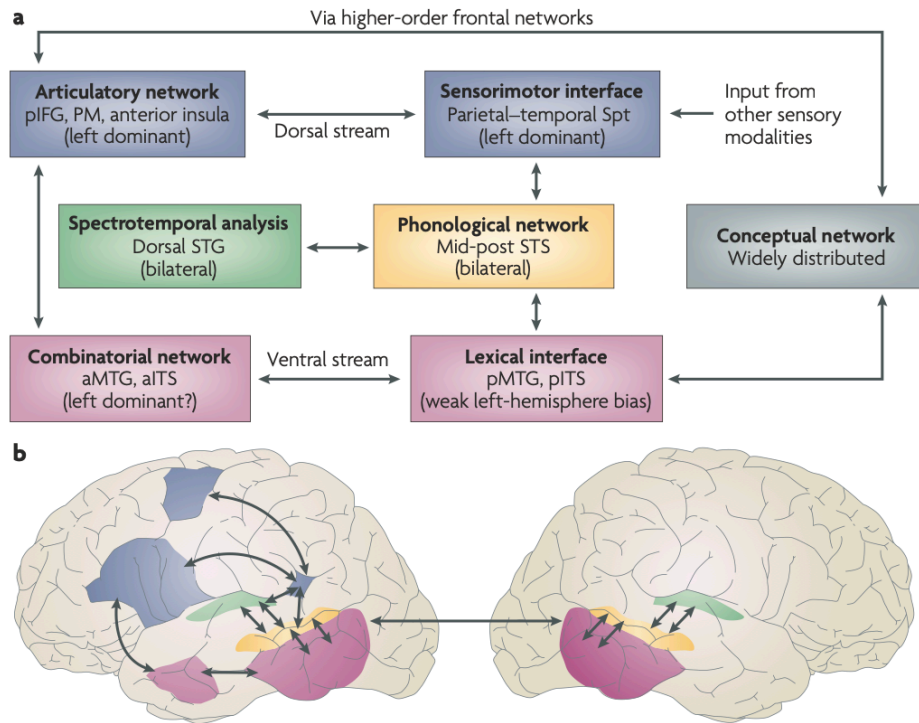


Figure 10. – Modèle du langage et ses corrélats neuronaux d'après Hickok et Poeppel tiré de (Hickok & Poeppel, 2007)

Les corrélats neuronaux du langage ont été étudiés par PET ou IRMf depuis plus de 20 ans, deux principales méta-analyses établissent bien les régions majoritairement latéralisées à gauche et impliquées dans l'articulation, la phonation ou la représentation sémantique (Price, 2012; Vigneau et al., 2006). En électrophysiologie en tâche, les bandes thêta et alpha sont liées aux fonctions réceptives du langage (Bastiaansen et al., 2005; Obleser & Weisz, 2012; Rommers et al., 2017; Scheeringa et al., 2009), telles que la récupération lexico-sémantique au sein des aires temporelles gauches (Bastiaansen et al., 2005) et la prédiction du langage dans les régions fronto-temporelles gauches (T. C. Alexander et al., 2018). En revanche, la production de la parole et les processus syntaxiques sont reflétés par des changements impliquant les bandes  $\beta$  et  $\gamma$  dans les aires frontales gauches (Liljeström et al., 2015).

## **Leucémie lymphoblastique aiguë et atteintes cognitives**

### **Leucémie lymphoblastique aiguë**

La leucémie aiguë lymphoblastique (LAL) représente 25 % des cancers pédiatriques. Grâce au progrès médical des dernières décennies le taux de guérison chez les enfants atteint aujourd'hui près de 80 %. Par conséquent, aujourd'hui un jeune adulte sur 450 est un survivant d'un cancer pédiatrique. Ces progrès sont en partie expliqués par la reconnaissance de la rechute méningée (définie par la présence de blastes dans les méninges) et le traitement prophylactique du cerveau par radiothérapie crânienne et chimiothérapie intrathécale (par ponction lombaire). Le taux de rechute est tombé de 60 % dans les années 50 à moins de 10 % aujourd'hui. Toutefois, la majorité des survivants présentent des effets secondaires chroniques et sérieux causés par les traitements, en particulier neurocognitifs. Les déficits d'attention, de mémoire de travail et de vitesse de traitement de l'information ont été le plus documentés à ce jour (Boulet-Craig et al., 2018; Cheung et al., 2016; Fella et al., 2019; Krull et al., 2016). Ces atteintes neurocognitives sont principalement en lien avec des atteintes diffuses de la substance blanche (Billiet et al., 2018; Cheung et al., 2016; Pääkkö et al., 2000) et des altérations de la connectivité fonctionnelle cérébrale à la suite des traitements par chimiothérapie intrathécale ou par irradiation crânienne (Kesler et al., 2018; Krull et al., 2016).

### **Atteinte cognitive**

Une abondante littérature documente les effets cognitifs tardifs décelés chez cette population. De nombreux domaines de fonctionnement cognitif peuvent être affectés, globalement une moins bonne performance intellectuelle générale (IQ) est rapportée (Cheung et al., 2016). Des difficultés scolaires liées à des troubles d'apprentissage notamment grâce à une moins bonne habileté en mathématiques et des difficultés de compréhension en lecture ont été rapportées (Campbell et al., 2007; Cheung & Krull, 2015; Conklin et al., 2012; Iyer et al., 2015). Mais aussi des troubles de la dextérité fine et de la coordination visuo-motrice. Mais les séquelles neurocognitives les plus courantes sont les troubles du fonctionnement exécutif et de l'attention, les survivants présentent des capacités attentionnelles réduites, une mémoire de travail et une vitesse de traitement réduites, ainsi que des performances inférieures dans différents domaines

de fonctionnement exécutif comme la flexibilité cognitive, la fluidité verbale et l'inhibition (T. C. Alexander et al., 2018; Boulet-Craig et al., 2018; Vijayanathan et al., 2011).

## **Corrélat fonctionnels des atteintes cognitives**

### Paradigme de tâche en IRMf

Des résultats ont été trouvés dans des régions cérébrales au cours d'une tâche chez les survivants de leucémie Lymphoblastique Aigue. Le volume d'activation des survivants de la LAL lors de stimuli visuels était significativement plus faible que celui des sujets sains dans le cortex visuel (P. Zou et al., 2005). Dans une autre étude utilisant un paradigme de tâche, les survivants ont montré une activation significativement plus importante dans les zones sous-jacentes à la mémoire de travail (cortex préfrontal dorso-latéral et ventro-latéral) et au contrôle des erreurs (cortex cingulaire antérieur dorsal et ventral) pendant une tâche de n-back (Robinson et al., 2010). Enfin, l'activation cérébrale pendant les tâches d'attention et de fonction exécutive était associée à l'exposition au méthotrexate et à l'âge du diagnostic (Fellah et al., 2019).

### État de repos et connectivité en IRMf

Une étude a trouvé une différence dans l'activité cérébrale avant la chimiothérapie, les valeurs de connectivité des survivants ont diminué globalement, en particulier dans le réseau du mode par défaut (DMN), le lobe frontal gauche, le lobe occipital gauche et les gyri postcentraux bilatéraux, par rapport aux sujets sains. Après la chimiothérapie, les valeurs étaient presque similaires à celles des sujets sains (D. Zou et al., 2019). Les patients atteints de dysfonctionnement exécutif ont également montré une hyperconnectivité dans les régions de traitement sensori-moteur, visuel et auditif et une mauvaise séparation entre les réseaux sensorimoteurs, exécutifs/attentionnels, de saillance et de mode par défaut (Kesler et al., 2018). En utilisant la cartographie de la densité de connectivité fonctionnelle mesurée par fMRI au repos, on a constaté que les survivants comparés aux témoins sains présentaient une diminution de la connectivité distale incluant les régions du gyrus lingual bilatéral, le cortex cingulaire, le gyrus hippocampique et la fissure calcarine droite. Ils ont également constaté une augmentation de la connectivité fonctionnelle entre la région présentant une diminution de la connectivité distale et le lobe cérébelleux postérieur, et une diminution entre le gyrus occipital moyen, le cunéus et le gyrus

lingual (Chen et al., 2020). Dans une autre étude, il a été démontré une connectivité significativement réduite entre l'hippocampe bilatéral, l'occipital inférieur gauche, le gyrus lingual gauche, le sillon calcarin bilatéral et l'amygdale droite dans le groupe LAL par rapport à des sujets contrôle. Le groupe de survivants a également montré des régions d'hyperconnectivité fonctionnelle, notamment le gyrus lingual droit, le précuneus, le lobe occipital supérieur bilatéral et le lobe occipital inférieur droit (Kesler et al., 2014).

### Oscillations cérébrales

La seule étude comparant des sujets contrôle aux survivants en MEG a trouvé que la puissance thêta relative (4–8 Hz) était légèrement augmentée et que la puissance alpha (10–12 Hz) était significativement diminuée par rapport aux sujets contrôle (Daams et al., 2012). Plusieurs études ont montré des tracés EEG anormaux chez les patients atteints de LAL, avant le traitement et diminuant pendant le traitement (Goldberg-Stern et al., 2011). Les patients atteints de LAL présentent un ralentissement léger à modéré dès le diagnostic. De plus, la puissance spectrale de l'EEG a diminué, et l'abondance relative des ondes lentes a augmenté, avec la récupération après traitement. D'autres études EEG confirment le ralentissement focal relié parfois avec des crises sporadiques suite aux traitements (Lichter-Konecki et al., 1987; Nigro et al., 2000; Ueberall et al., 1997). Les patients présentaient des perturbations de l'activité de fond significativement plus fréquentes et plus sévères que les témoins, une augmentation des ondes lentes dans les régions occipitales et temporales (L. VAINIONPAA, 1991). Le ralentissement de la fréquence dominante a été observé chez les patients atteints de leucémie plus grave et chez ceux dont l'EEG était nettement anormal au moment du diagnostic (Korinthenberg & Igel, 1990). Enfin, une réduction de l'amplitude du spectre de puissance dans l'occipital, et une augmentation des ondes lentes thêta, ont été trouvées et le spectre de puissance est largement diffus de thêta à alpha chez les patients comparés au contrôle (Tucker et al., 1989).

## **Mise en évidence de la problématique**

Cette étude s'intéresse au lien entre les dynamiques cérébrales et les capacités cognitives, cette problématique a déjà été explorée auparavant en imagerie cérébrale, notamment à l'aide de

tâches effectuées pendant l'imagerie. Cette littérature exhaustive a constitué une connaissance des processus cognitifs discutés brièvement dans les parties précédentes.

Cependant depuis un petit nombre d'années il est reconnu que quand le cerveau n'est pas engagé dans une telle tâche, une activité spontanée en émerge. Il a été démontré que cette activité n'est pas du bruit, mais qu'elle est structurée, temporellement et spatialement. L'étude de cette activité spontanée a été faite en IRM fonctionnelle, en MEG et en EEG, tous s'accordent à décrire une organisation fonctionnelle comme par exemple les bien connus réseaux de l'état de repos. Le lien entre cette activité spontanée et les performances cognitives a aussi été exploré, cependant deux limites sont apparues, la première est celle reliée à l'IRM fonctionnelle et sa résolution temporelle qui ne permet pas de caractériser la cognition à l'échelle temporelle à laquelle elle se passe, de plus les études en IRMf ont principalement utilisé l'état de repos avec la connectivité et non l'activité locale, la deuxième est reliée aux études en EEG ou MEG qui ont limité leurs analyses au niveau des capteurs, dans ce cas la résolution spatiale ne permet pas de savoir quelles régions cérébrales est impliquées. Dans cette étude, nous proposons d'investiguer les corrélats neuronaux au niveau local, donc au niveau des sources corticales, ainsi qu'avec une haute résolution temporelle. Pour cela, nous avons utilisé l'activité localisée au repos en MEG, puis établi des patrons de corrélation et d'anti-corrélation spatio-fréquentiels avec la performance comportementale. De plus, nous avons ciblé et reproduit cette méthode sur différentes fonctions cognitives afin de tester la spécificité de ces patrons d'activations. Finalement nous avons cherché à savoir si cette approche pourrait aussi caractériser des troubles fonctionnels cognitifs comme dans le cas des survivants de la leucémie qui ont subi des traitements neurotoxiques importants qui ont perturbé leur développement cérébral.

## **Approche méthodologique générale**

### **Source corticale MEG/IRM**

Des problèmes de distorsion dans la propagation du signal électrique ont limité la localisation des sources corticales provenant des tracés EEG. En effet, le courant électrique ne suit pas une trajectoire linéaire, mais suit la densité des milieux qu'il traverse entre le cortex cérébral et

l'électrode (c.-à-d. liquide LCR, méninges, densité osseuse, vaisseaux sanguins). L'apparition de la MEG dans les années 1960, et aujourd'hui de premiers systèmes MEG portatifs, a permis d'étudier les champs électromagnétiques. Les propriétés des champs électromagnétiques sont telles qu'il n'y a pas de distorsion causée par le milieu qu'il traverse. La MEG enregistre les champs électromagnétiques générés par le cerveau dans une pièce isolée magnétiquement afin de réduire la contamination des influences externes sur les enregistrements cérébraux. Les signaux peuvent être utilisés au niveau de capteurs, mais cela donne très peu de résolution spatiale puisqu'elle est limitée par le nombre de capteurs. La localisation des décours temporels au niveau de sources corticales a permis d'étudier l'électrophysiologie au niveau cortical dans des volumes relativement précis ( $3 \text{ mm}^3$ ). Pour obtenir l'estimation des décours temporels de l'activité cérébrale au niveau des sources corticales, il faut calculer la relation mathématique entre les courants cérébraux (sources) et le champ magnétique mesuré (le modèle direct). Le modèle direct comprend des modèles pour les sources, la géométrie du milieu conducteur (c'est-à-dire la tête) et les capteurs MEG (figure 11). Le modèle de tête dans ces opérations joue un rôle important, la meilleure estimation étant d'utiliser les modèles de tête issus de la segmentation d'une imagerie par résonance magnétique (IRM) anatomique (T1) (Stenroos & Nummenmaa, 2016; Vorwerk et al., 2014). L'approche de localisation de source vise à estimer la distribution globale de l'activité neuronale à travers tout le cerveau. En général, on utilise une grille de sources élémentaires (dipôles), fixées en emplacement et, éventuellement, en orientation, dans le volume du cerveau ou limitées à la surface corticale. La solution du problème inverse (le calcul des courants cérébraux [sources] à partir du champ magnétique mesuré) aboutit à l'estimation de l'amplitude de toutes ces sources élémentaires. Parmi ces approches d'imagerie, plusieurs stratégies ont été développées, notamment les méthodes d'imagerie à source distribuée (par exemple, les techniques des moindres carrés telles que les approches d'estimation de la norme minimale), les méthodes de balayage et les méthodes de filtrage spatial (Baillet et al., 2001; B. He et al., 2019).



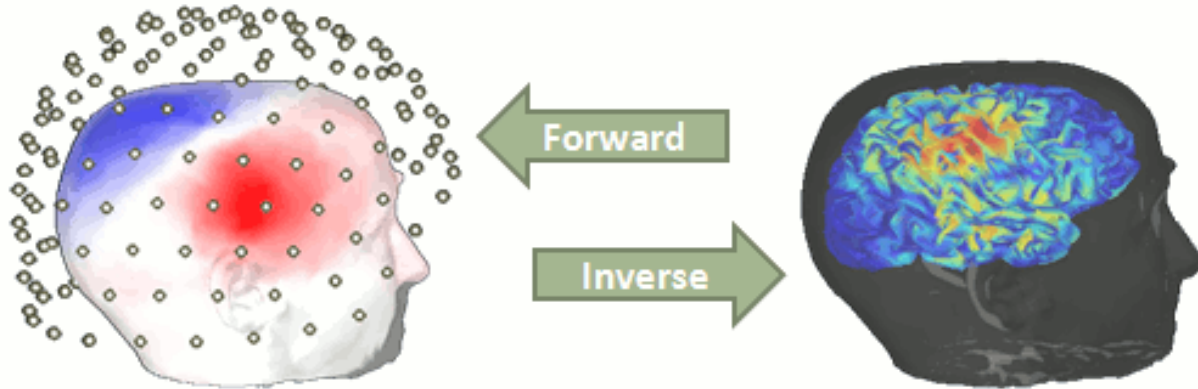


Figure 11. – Le modèle inverse et direct permettant de passer de décours temporel des capteurs à celui des sources corticales

### **Fréquence au repos au niveau des sources corticales**

Nous avons élaboré une méthode spécifique pour explorer les corrélats cognitifs de fonctions cognitives précises à partir de l'activité spontanée électrophysiologique au niveau des sources corticales. Cette méthode combine plusieurs outils déjà décrits dans la littérature. La localisation de source au niveau cortical est basée sur une méthode de localisation de type estimation du minimum norme. Cette activité est projetée sur la segmentation anatomique de chaque sujet individuellement. Ensuite la puissance moyenne à travers le temps d'enregistrement (environ 5 minutes) est calculée sur un maillage distribué sur tout le cerveau qui comporte une résolution d'environ 10 000 points.

### **Interprétation fonctionnelle (approche par clusters)**

Ensuite des patrons de corrélation sont calculés pour chaque point pour tous les sujets, et finalement une approche par cluster statistique déjà décrite par (Maris & Oostenveld, 2007) est utilisée pour établir des clusters d'intérêt significatif. Cette méthode est décrite plus en détail dans le deuxième chapitre puis reprise à l'identique dans le chapitre trois et quatre.

### **Test neuropsychologique standardisé**

Les mesures comportementales utilisées pour calculer ces corrélations avec les puissances spectrales ont été des tests neuropsychologiques standardisés issus de différentes batteries bien connues et couramment utilisés en clinique pour des évaluations cognitives, ou pour l'estimation

du Quotient Intellectuel (QI). Ces mesures comportent plusieurs avantages. Elles sont très reproductibles, stables dans le temps, standardisées pour l'âge, la langue et les aspects culturels. Une littérature abondante en neuropsychologie démontre la standardisation de ces tests. De plus ils permettent aussi d'évaluer certaines dimensions du comportement dans un paradigme psychométrique et de discriminer certaines fonctions cognitives spécifiques entre elles.

### **Réplication et domaines cognitifs**

Dans un but de caractériser l'activité spontanée au repos avec différents processus cognitifs, nous avons ensuite reproduit cette méthode sur un même échantillon, mais pour différentes fonctions cognitives. La première fonction cognitive explorée a été la mémoire de travail (chapitre 2), puis les fonctions exécutives et verbales (chapitre 3), et l'apprentissage verbal ainsi que les stratégies utilisées lors de cet apprentissage (chapitre 4).

### **Connectivité spectrale**

Dans une autre phase nous avons développé une approche similaire, mais cette fois, à l'aide d'une mesure de connectivité fonctionnelle caractérisant le couplage entre les régions cérébrales. La connectivité fonctionnelle a été calculée avec une mesure de couplage de phase (wPLI), une métrique qui tient compte du problème de conduction volumique. Ce calcul a été également été fait à partir du décours temporel des sources corticales. Deux types d'analyses ont ensuite été réalisées. Nous avons calculé les corrélations entre des mesures neuropsychologiques et chacun des liens de connectivité suivis d'une correction par maximum statistique. Deuxièmement, nous avons calculé les corrélations entre des mesures neuropsychologiques et une moyenne de la connectivité calculée pour les 7 réseaux de repos établis d'après les parcellisations de (Schaefer et al., 2018) illustré à la figure 12. Ces résultats sont soit intégrés aux articles ou décrits dans les résultats en annexe. La connectivité spectrale au repos a été explorée pour la mémoire de travail (résultat en annexe chapitre 1), pour la fluence verbale et la richesse de vocabulaire (annexe chapitre 2), ainsi que dans l'application clinique de cette thèse (chapitre 5).

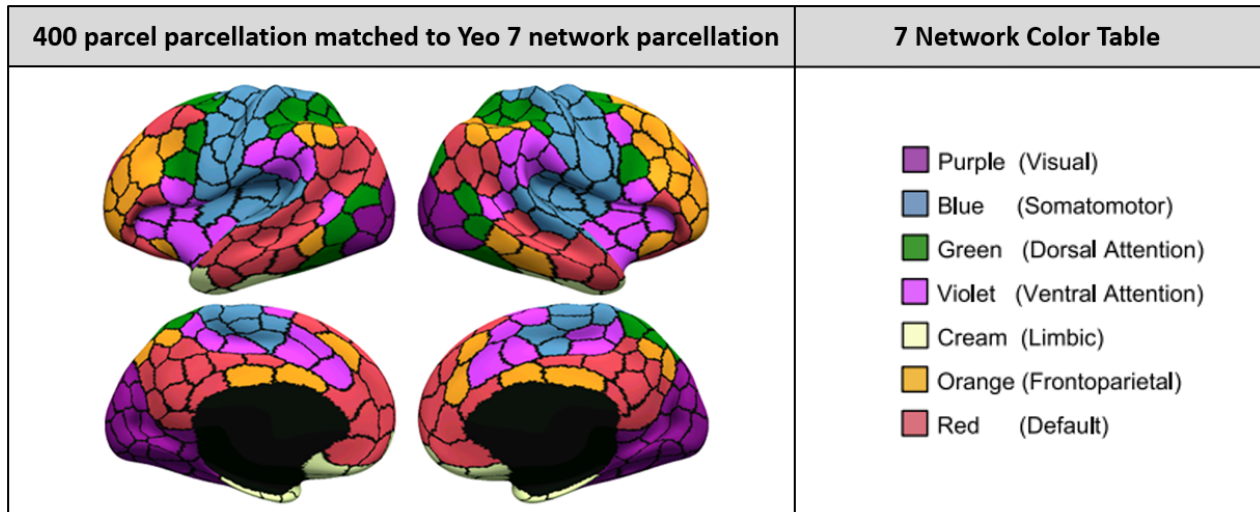


Figure 12. – Parcellisations des 7 réseaux au repos d’après (Schaefer et al., 2018)

### Application clinique

La dernière partie de cette thèse (chapitre 5) est un travail qui inclut une cohorte de patients survivants à long terme de la leucémie lymphoblastique aiguë (LLA). Dans le cadre d’une recherche multidisciplinaire sur la prévention des effets tardifs à long terme des survivants de leucémie (PETALE), une cohorte de patients a participé à une série d’évaluations neuropsychologiques ainsi qu’à plusieurs protocoles d’imagerie cérébrale (MEG, IRM). La leucémie lymphoblastique aiguë est un cancer principalement pédiatrique. Il a été établi qu’une proportion significative des survivants à long terme ont des déficits cognitifs à long terme accompagnés de plusieurs comorbidités psychiatriques (trouble attentionnel, anxiété, dépression) principalement dus à la toxicité pour le développement cérébral des traitements anticancéreux. La littérature rapporte chez cette population une grande prévalence d’atteinte de la substance blanche en général, ce qui a dirigé notre approche à caractériser la connectivité fonctionnelle chez cette population et de comparer les survivants avec des sujets contrôles. Nous avons testé l’impact des doses cumulatives des substances utilisées pendant les traitements et de la radiothérapie. Finalement, nous avons testé l’hypothèse que la connectivité cérébrale soit un médiateur de l’effet des doses cumulatives des substances reçues au cours du traitement les capacités cognitives dans un suivi à long terme.

## Plan de la thèse

### Objectifs et hypothèses

L'objectif de cette thèse est de caractériser l'activité spontanée au repos au niveau cortical associé à différents processus cognitifs, incluant des sujets contrôle et des patients en déficit cognitif.

#### **Article 1 – Spontaneous brain oscillations as neural fingerprints of working memory capacities: A resting-state MEG study**

Les corrélats neuronaux de la mémoire de travail ont été caractérisés lors de tâches. Au repos, les précédents travaux montrent seulement des résultats soit au niveau des capteurs en électrophysiologie, soit au niveau des interactions interrégionales corticales. Ce travail explore les corrélats neuronaux au repos en lien avec la performance cognitive en mémoire de travail.

**Objectif 1 :** Établir les corrélats neuronaux de la performance de la mémoire au repos à l'aide des puissances spectrales localisées au niveau des sources corticales.

**Hypothèse 1 :** L'augmentation de la performance de la mémoire de travail devrait être associée à des modulations de puissance dans les régions établies dans d'autres modalités (c.-à-d. fronto-pariétal).

#### **Article 2 – Resting-state cortical activity in MEG reveals the neural correlate of executive and phonological complexity of verbal fluency**

**Objectif 1:** Répliquer les méthodes utilisées dans l'article 1 avec les mêmes participants, mais dans un autre domaine cognitif. Établir les corrélats neuronaux de la fluence verbale ainsi que de discriminer un composant verbal et exécutif. Ces deux composantes ont été mises en évidence en utilisant une factorisation avec un test purement exécutif (Trail making test-condition 4) et un autre purement verbal (richesse du vocabulaire).

**Hypothèse 1 :** Les fonctions exécutives verbales devraient montrer des corrélats neuronaux en lien avec les régions frontales déjà établies en tâche et les régions verbales associées au test exécutif devraient montrer des régions verbales impliquées dans les processus verbaux en tâche.

### **Article 3 – Resting state MEG power correlates of semantic and serial strategy in learning a list of words**

**Objectif 1 :** Répliquer encore la méthode de l'article 1 avec les mêmes sujets, mais sur un test d'apprentissage verbal.

**Hypothèse 1 :** Les corrélats neuronaux du test d'apprentissage verbal trouvés au repos pourraient engager les régions impliquées dans l'apprentissage verbal lors d'une tâche

**Objectif 2 :** Lors de l'apprentissage verbal, comme deux stratégies d'apprentissage (sériel et sémantique) possibles peuvent être utilisées, est-il possible de mettre en évidence des patrons de corrélation basés sur l'état de repos basé sur ces stratégies d'apprentissage ?

**Hypothèse 2 :** Les corrélats neuronaux reliés aux stratégies d'apprentissage montrent des patrons de corrélation qui divergent.

### **Article 4 – Enhanced alpha long-range brain synchrony mediates the long-term effects of intrathecal methotrexate on executive deficits in ALL survivors**

**Objectif 1 :** Établir des différences fonctionnelles entre survivants de leucémie et des sujets contrôles

**Hypothèse 1 :** La synchronie entre les régions cérébrales dans les réseaux exécutifs est augmentée chez les survivants de la leucémie

**Objectif 2 :** Établir un lien entre neurotoxicité et déficit cognitif ainsi qu'entre neurotoxicité et un marqueur physiologique cérébral

**Hypothèse 2 :** La synchronie cérébrale augmente en fonction de la dose cumulative de chimiothérapie, et plus la synchronie augmente plus le déficit des fonctions cognitives s'accroît chez les survivants de la leucémie.

**Objectif 3 :** Établir un modèle intégrant neurotoxicité, performance cognitive et marqueur neurophysiologique fonctionnel cérébral.

**Hypothèse 3 :** La synchronie cérébrale est un médiateur de l'effet de la neurotoxicité sur les performances cognitives chez les survivants de la leucémie.

# Chapitre 2 — Spontaneous brain oscillations as neural fingerprints of working memory capacities: A resting-state MEG study

Victor Oswald<sup>a,b</sup>, Younes Zerouali<sup>c,d</sup>, Aubrée Boulet-Craig<sup>e</sup>, Maja Krajcinovic<sup>a,g</sup>, Caroline Laverdière<sup>a,g</sup>, Daniel Sinnott<sup>a,g</sup>, Pierre Jolicoeur<sup>e,f</sup>, Sarah Lippé<sup>e,g</sup>, Karim Jerbi<sup>e,f</sup> and Philippe Robaey<sup>a,h,i,j</sup>

<sup>a</sup> Service Hématologie Oncologie, Charles-Bruneau Cancer Center, Sainte-Justine Hospital, Montreal, QC, Canada

<sup>b</sup> Department of Neurosciences, Faculty of Medicine, University of Montreal, Montreal, QC, Canada

<sup>c</sup> Department of Biomedical Engineering, école Polytechnique de Montréal, Montreal, QC, Canada

<sup>d</sup> Department of Neurology, CHU Notre-Dame Research Center, University of Montreal, Montreal QC, Canada

<sup>e</sup> Department of Psychology, University of Montreal, Montreal, QC, Canada

<sup>f</sup> MEG Core Facility, University of Montreal, Montreal, QC, Canada

<sup>g</sup> Department of Pediatric, CHU Sainte-Justine Research Center, Montreal, QC, Canada

<sup>h</sup> Department de Psychiatrie, University of Montreal, Montreal, QC, Canada

<sup>i</sup> Children's Hospital of Eastern Ontario, Ottawa, ON, Canada

<sup>j</sup> Department de Psychiatrie, University of Ottawa, Ottawa, ON, Canada

*Article Publié dans le Journal Cortex*

## Abstract

Short-term storage and mental information manipulation capacities in the human brain are key to healthy cognition. These brain processes collectively known as working memory (WM) are associated with modulations of rhythmic brain activity across multiple brain areas and frequencies. Yet, it is not clear whether — and, if so, how intrinsic — resting-state neuronal oscillations are related to individual WM capacities, as measured by standard neuropsychological tests. We addressed this question by probing the correlation between resting-state brain activity, recorded with magnetoencephalography (MEG), and verbal and visuo-spatial WM indices obtained from the standardized Wechsler Adult Intelligence Scale (WAIS-IV) and the Wechsler Memory Scale (WMS-IV). To this end, 5-min eyes-open resting-state MEG data were acquired in 28 healthy participants. Source-reconstructed spectral power estimates were then computed in standard frequency bands and their correlation with neuropsychological indices across individuals was assessed using Pearson's correlation and cluster-level statistics. We found statistically significant positive correlations between spectral amplitudes measured at rest and standardized scores on both verbal and visuo-spatial WM performance. The correlation clusters primarily involved key medial and dorsolateral components within the parietal and prefrontal regions. In addition, while the correlation in some clusters was frequency selective (e.g. alpha-band oscillations), other areas showed correlations with WM across a wide range of frequencies reflecting a broadband effect. These results provide the first evidence for a positive correlation between neuromagnetic signals measured at rest and WM performance separately assessed by standardized neuropsychological tests. Our results advance our understanding of the link between WM capacities and intrinsic oscillatory dynamic networks. They also suggest that individual differences in baseline spectral power might need to be taken into account when probing differences in brain responses during the execution of WM tasks.



## Introduction

Rhythmic neuronal activity is a hallmark of brain function that is prominent during rest. It is dynamically modulated in a wide range of perceptual and goal-directed tasks (Buzsaki & Silva, 2012; Dalal et al., 2011; Guntekin & Basar, 2014; Jensen, Gips, Bergmann & Bonnefond, 2014; Jerbi et al., 2009; Klimesch, 2012; Palva & Palva, 2007; Ruhnau, Hauswald & Weisz, 2014). Cognitive tasks that require short-term storage and manipulation of information — i.e. processes collectively referred to as working memory (WM) (e.g. Wager & Smith, 2003) — are associated with modulations in oscillatory brain dynamics across multiple brain areas and frequency bands, including delta (1–4 Hz) (Harmony et al., 1996), theta (4–8 Hz) (Gevins, Smith, McEvoy & Yu, 1997), and alpha (9–12 Hz) (Jensen, Gelfand, Kounios & Lisman, 2002). Oscillations at higher frequencies, in particular in the gamma band (>30 Hz) (Morgan et al., 2011; Meeuwissen, Takashima, Fernandez, & Jensen, 2011; Bonnefond & Jensen, 2013; Lozano-Soldevilla, ter Huurne, Cools, & Jensen, 2014; Honkanen, Rouhinen, Wang, Palva, & Palva, 2015; Lundqvist et al., 2016) and cross-frequency coupling mechanisms (Axmacher, Henseler, Jensen, Weinreich & Elger, 2010; Park et al., 2011; Roux & Uhlhaas, 2014; Leszczynski, Fell & Axmacher, 2015) have also been found to play a role in the neuronal processes involved in WM.

Most of the above EEG and MEG studies that have probed the neuronal underpinnings of WM employ a task-based approach where brain signals are recorded while subjects perform a WM task. However, task-based investigations are not the only way to tap into the basic mechanisms underlying brain function. Indeed, mounting evidence from a parallel stream of research indicates that task-free investigations of ongoing brain signals can also reveal activity patterns that are tightly linked to basic structural and functional properties of the brain (Bullmore & Sporns, 2009; Foster et al., 2016). Converging evidence for the functional relevance of spontaneous brain activity has come from multiple modalities, including neuroimaging (Biswal, Zerrin Yetkin, Haughton, & Hyde, 1995; Buckner, Andrews-Hanna, & Schacter, 2008; Fox & Raichle, 2007; Raichle et al., 2001), invasive (Foster et al., 2016; Jerbi et al., 2010; Ossandon et al., 2011), and non-invasive electrophysiological measurements (e.g. Brookes, Woolrich et al., 2011a; Liuzzi et al., 2016; de Pasquale, Della Penna, Sporns, Romani, & Corbetta, 2016, de Pasquale et al., 2010). Remarkably, beyond refuting the view that spontaneous brain activity consists of irrelevant noise,

resting-state studies have revealed prominent differences between healthy controls and patients with brain disorders (e.g., Greicius, 2008; Broyd et al., 2009; Fox & Greicius, 2010; Hinkley et al., 2011). Interestingly, reports that altered resting-state network properties are associated with cognitive impairments (e.g. in Schizophrenia or Alzheimer's) indirectly suggest that resting-state brain dynamics may also reflect the variability of cognitive abilities among healthy individuals. This led us to ask whether variable WM memory performance across individuals can be traced back to distinct properties of the brain's resting-state activity. And, more specifically, if this were indeed the case, one may ask whether the WM-related spontaneous brain patterns overlap with those detected during the execution of WM tasks? Some studies using resting state fMRI explored the correlation between intrinsic networks and WM (e.g. Liang, Zou, He & Yang, 2013), showing decoupling between nodes of the default mode and the fronto-parietal networks (Keller et al., 2015), or increased coupling within the fronto-parietal network (Yamashita, Kawato & Imamizu, 2015). However, only a handful of studies have sought to correlate resting state oscillatory activity with WM. Frontal EEG alpha peak frequency has been shown to be a significant predictor of performance on the reverse digit span (DS) test (Richard et al., 2004). Changes in low frequency power between eyes open and eyes closed have been linked to subject performance on a verbal n-back WM task (Heister et al., 2013). In older adults (>54 yrs), higher delta and theta power have been associated with improved performance on the Trail Making Test (TMT) (Vlahou, Thurm, Kolassa & Schlee, 2014), but not for younger participants. Because most of these studies derived WM performance measures from a single task, it is still unclear how task-specific versus WM-specific the reported findings are. More importantly, to the best of our knowledge, no study to date has reported significant correlations between neuro-magnetic oscillation amplitudes measured at rest and standardized WM scores in healthy adults. Thus, taken together, although MEG/EEG resting-state studies have achieved important progress in unravelling fundamental patterns of oscillatory network dynamics at rest, little is known about whether and how the properties of these spontaneous brain oscillations are related to cognitive abilities, and in particular to WM capacities. Therefore, in the present study, we set-out to test the hypothesis that distinct neuronal oscillatory patterns observed in spontaneous (rather than task-based) brain activity may relate to an individual's WM capacities, as assessed with standardized

neuropsychological testing. In other words, rather than using MEG or EEG to monitor changes in brain activity during the performance of a specific WM, we aimed to test whether the amplitudes of ongoing brain oscillations across different frequencies and brain regions may correlate with an individual's WM score obtained on standardized neuropsychological tests. More specifically, we hypothesized that such links between WM behavior and ongoing neuronal oscillations might occur in key WM brain areas (including the fronto-parietal network), and in key WM frequency bands (including the alpha band). We further hypothesized that MEG would be a particularly fitting tool to investigate this question, given its established ability to monitor the spectral and spatial organization of resting-state neuronal oscillations in source- space (Brookes, Woolrich et al., 2011a; de Pasquale et al., 2010, 2016). Based on the working hypotheses described above, the goal of this study was to test whether spatial and spectral patterns of brain oscillations measured at rest show a correlation pattern with global standardized indices of WM abilities. In particular, we set out to probe the link between source-reconstructed MEG resting-state oscillations and the Working Memory Index (WMI) from the widely used Wechsler Adult Intelligence Scale (WAIS) (4th edition). As the subtests that constitute the WMI are essentially verbal, we also administered a test of visuo-spatial WM the Spatial Addition (SA) subtest from the Wechsler Memory Scale (WMS) (4th edition) to verify whether any correlation patterns (if any are found) depend on the nature of the encoded material. Finally, we also sought to isolate behavior brain correlation patterns that are unique to WMI, and which are not correlated with the other main indices that make up the WAIS-V IQ test. Across individuals, we found WM indexes to be positively correlated with resting-state oscillation amplitudes. The correlation was predominant in the alpha band, but was also found in lower (theta/delta) and higher (beta/gamma) frequency ranges. Interestingly, the correlation patterns involved key medial and dorsolateral areas within the parietal and prefrontal regions, medially. Interestingly, while verbal WM capacities appeared to be correlated with bilateral patterns of spontaneous oscillations, visuo-spatial WM abilities were correlated with left lateralized oscillatory pattern. Taken together, our data provides the first evidence for a direct relationship between neuromagnetic signals measured at rest and WM performance assessed by standardized neuropsychological tests in healthy young adults.

## **Methods and materials**

### **Participants**

Twenty-eight healthy subjects (13 males and 15 females, mean = 25.76 yrs, Std = 4.84 yrs) with no reported history of neurological or psychiatric disorders took part in this study. The project was reviewed and approved by the University of Montreal and the CHU Sainte-Justine Research Ethics Board. Informed consent was obtained prior to the experiment and financial compensation was given upon completion of the experiment.

### **Neuropsychological Assessment**

A neuropsychological evaluation was carried out on the same day as the MEG recordings. The battery of neuropsychological tests consisted of subtests from the WAIS e 4th edition (Wechsler, 2008a, 2008b): Letter-Number Sequencing (LNS) and DS, as well as the subtest of SA from the WMS Test, 4th edition (Wechsler, 2008a, 2008b). In the DS subtest, the participants must recall a series of numbers in order. This subtest involves WM, attention, encoding, and auditory processing. LNS requires the participants to recall a series of numbers in increasing order, and letters in alphabetical order. This subtest assesses WM, attention, and mental control. The SA subtest is based on a modified n-back paradigm and assesses visual-spatial storage and manipulation in WM. Since the participants were all francophone, the French Canadian versions of the tests were used, and all the subtests from the neuropsychological evaluation were compiled and transformed to normative scale scores using Canadian norms (Wechsler, 2008a, 2008b). We calculated different indices: WMI with its LNS and DS components, and the Full-Scale IQ Index with all its subtests. We used scaled scores of the different subtests and indices to compute the correlations with MEG data. The WAIS-IV was standardized on a sample of 2200 people in the United States, ranging in age from 16 to 90. The derived scaled scores (z-scores) allow a direct numerical comparison between individuals (Wechsler, 2008a, 2008b). In order to obtain a measure that probes the specificity of

WM, we used the residuals (the differences between the observed value and the predicted value) of the linear regression between the WMI and the other indices of the WAIS, entered in a

sequentially forward regression: first Perceptual Reasoning Index (PRI), then Processing Speed Index (PSI), followed by Verbal Comprehension Index (VCI). We refer to the resulting metric as a residual score of WMI (WMIr). As a result, the correlations between WMIr and the different WAIS-IV indices were null. To avoid any bias caused by the presence of outliers, only participants with scaled scores on all tests that were fewer than three standard deviations from the mean were included in the correlation analyses. This only led us to exclude 2 participants out of the 28 for the correlation computations.

### **MEG and Anatomical MRI Data Acquisition**

All 28 subjects were comfortably seated with eyes open, fixating a back-illuminated screen located 75 cm in front of them. Two 5-min periods of resting-state data were recorded at a sampling rate of 4000 Hz, using a CTF-VSM whole head 275-sensor MEG system (MEG core facility, Psychology Department, University of Montreal, QC, Canada). Following standard procedures, third-order gradiometer noise reduction was computed based on twenty-nine reference channels. Bipolar EOG (Vertical EOG and Horizontal EOG) was recorded in order to monitor eye blinks and ocular movements. ECG was also recorded to monitor heartbeats. Three head coils fixed at the nasion and the bilateral preauricular points were used for head localization and were monitored at the beginning and the end of each session. Particular care was taken to ensure that head displacement across sessions remained below 5 mm. The neuropsychological assessments were done in the morning at the Ste-Justine Hospital (Montreal, QC, Canada). Later in the afternoon, the participants went to the MEG facility, located in the Psychology Department of the University of Montreal, for the MEG recordings. Structural MRI images were obtained for each subject with a 3-T General Electric (GE) scanner (Saint-Justine Hospital, Montreal, QC, Canada). The individual surfaces were used to carry out the co-registration between the MEG fiducial markers (LAP, NAS, RAP) and the MRI structural image. In addition, the exact position of the head was refined based on head shape position files obtained using a 3D-localization Polhemus system.

### Data Pre-Processing

MEG data pre-processing was performed using the Matlab based Brainstorm open-source software (Tadel, Baillet, Mosher, Pantazis & Leahy, 2011). The data was first notch filtered at 60 Hz, and then between 0.5 Hz and 120 Hz. Cardiac artefacts, eye blinks, and eye movements were corrected using the Signal-Space-Projection method (SSP) (Uusitalo & Ilmoniemi, 1997). Fifty signal epochs, centered on each artefact, were selected, and a singular value decomposition was applied to each artefact using built-in Matlab functions. Eigenvectors explaining at least 10% of the variance of the artefacts were discarded and the remaining eigenvectors were used to define the SSP. The SSP method relies on a signal space decomposition procedure, where the statistical characteristics of the measured signals are used to determine the two subspaces spanned by the MEG brain signals and the unwanted artifacts, respectively. Projecting the continuous MEG data onto the signal subspace effectively removes the components belonging to the artifact subspace.

### MEG Sources Estimation

MEG source reconstruction was performed using a standard weighted minimum-norm approach, with the Brainstorm software (Tadel et al., 2011). T1-weighted brain volumes were acquired in all participants and were used to generate a cortical surface model, using the FreeSurfer software package (Fischl et al., 2002). Forward modelling of the magnetic field was defined based on an overlapping-sphere method (Huang, Mosher & Leahy, 1999). The weighted minimum norm solution was computed using a loose dipolar orientation constraint (set at .5), signal-to-noise ratio of 3, whitening PCA and a depth weighting of .5 (Baillet, Mosher & Leahy, 2001). The noise covariance matrix for each participant was estimated from a 2-min empty room recording performed earlier the same day (same acquisition parameters but with no subject in the shielded room) (e.g. Ghuman, McDaniel & Martin, 2011). The source time series were initially reconstructed on a 15,000-vertex individual brain tessellation, and then spatially interpolated to the MNI ICBM152 brain template and down-sampled to a 10,000-vertices template.

### Spectral Power Analysis

Resting-state power spectral density was measured using the modified Welch periodogram technique (1-sec Hamming window and 50% time-window overlap). The mean PSD for each frequency band of interest was obtained for each subject by averaging the PSD values across the frequency bins of each band. Power estimates were computed for all elemental cortical sources and all participants in the following frequency bands: Delta (1–4 Hz), theta (4–8 Hz), alpha (8–13 Hz), beta (13–30 Hz), gamma 1 (30–60 Hz), gamma 2 (60–90 Hz) and gamma 3 (90–120 Hz). Next, for each participant, the PSD values (i.e. oscillatory power) were standardized using a z-score transformation (computed at each vertex using the mean and standard deviation of the power values across all vertices within the same frequency band).

### Correlation Analyses and Cluster-Level Statistics

A correlation analysis was carried out to probe the putative relationship across individuals between spontaneous brain oscillation amplitudes (separately for each frequency band) and neuropsychological capacities (on various subtests and indices). The computation and assessment of correlation was achieved via a two-step procedure. First, the Pearson correlation coefficients were computed between resting-state power (z-scores) at each cortical vertex and scaled scores from the neuropsychological tests. Next, the statistical significance of the correlation results was evaluated using t- statistics and nonparametric cluster-wise correction for multiple testing (Maris & Oostenveld, 2007). More specifically, the correlation was computed using MATLAB's built-in `corrcoef` function at each cortical node (vertex), for each frequency band and each subject (n=26). In addition to computing the Pearson correlation coefficient, the correlation function also returns p-values obtained by transforming the correlation to create a t-statistic with n-2 degrees of freedom. Setting the threshold for the first-level statistical significance to  $p < .05$  (uncorrected) provides a spatial mask in source space. Next, within this mask (i.e. significant correlation coefficients, uncorrected), we determined clusters of spatially contiguous (neighboring) vertices, which were identified based on the FreeSurfer adjacency matrix. The correlation coefficients within each cluster were then added up to obtain a cluster mass (cluster mass statistics). In order to assess the statistical significance of the obtained clusters, we used nonparametric permutation testing. We randomly shuffled the subjects' neuropsychological scores, while keeping the MEG

source power data across subjects intact. This essentially creates random associations that destroy any putative correlation between the two types of observations. Using 1000 permutations of the data (and replicating the cluster mass computation described above for each set of permuted data) provides an estimate for the null distribution against which we can then test the significance of the truly observed clusters in the original data. Statistically significant correlation clusters at  $p < .001$  were then defined as those with a cluster mass larger than the correlation value ranked 999 on the null distribution. By choosing such a restrictive significance threshold (i.e.  $p < .001$ ), not only do we minimize the type I errors, but we also ensure that the reported results would remain significant e for instance, at a level of  $p < .05$ , accounting for up to 50 multiple tests e based on a regular Bonferroni correction. In other words, all our results remain significant at  $p < .05$  if we correct for tests across all frequency bands, and all the WAIS-V subtests and indices used (as the number of comparisons does not exceed 50). The results reported here are therefore statistically significant at  $p < .001$  levels, corrected across space, for each frequency band and neuropsychological test, but they are all also significant at  $p < .05$  when corrected for comparisons across space, frequency bands, and subtests.



## Results

### Neuropsychological assessment

Table 1 summarizes the mean and standard deviation, and min/max values for the scaled scores on the neuropsychological tests. The participants' IQs were in the average range ( $106.25 \pm 11.91$ ) and all subtest scores fell within normal limits. The participants' scores were normally distributed, and no clinically meaningful cognitive deficits were found in any of the participants.

Neuropsychological tests N=26	Results scaled score mean (SD) [min-max]
Digit Span subtest (DS)	8.69 (2.09) [4–13]
Letter-Number sequencing (LNS)	9.11 (1.63) [6–12]
Working Memory Index (WMI)	93.19 (8.64) [76–108]
Spatial Addition (SA)	12.38 (2.40) [6–17]
Full Scaled Intelligence Quotient (FSIQ)	104.38 (10.08) [74–120]

Tableau 1. – Scaled score, mean, standard deviation, minimum and maximum value of neuropsychological assessments for 26 subjects. The WAIS-IV battery includes subtest DS and LNS form WMI. SA is a simple subtest from the WMS Test. Note that all standardized indices (i.e. WMI and FSIQ) are designed such that  $m=100$  &  $SD=15$ , while the subtests have  $m=10$  and  $SD=3$ .

### Normalized Resting-State MEG Power

Fig. 1 shows 2-D topographical representations of band- specific normalized spectral power over the MEG sensor array and in cortical source space. For each subject, the mean resting-state power at each sensor (or vertex) was normalized by the maximum value over the sensor array. The group-level plots in Fig. 13 represent standardized spectral power (z-scores) across all participants ( $n=26$ ). The results indicate that the spatial pattern of resting-state spectral power has relative peaks over posterior, parietal, and central brain regions, with similar patterns across frequency bands. Because of the band-specific normalization (z-scores across sensors or vertices), the amplitudes of patterns are similar, yet the raw power amplitudes per se decreased with increasing

frequencies, following a typical 1/f-like power law, with a few bumps at frequencies where intrinsic oscillations were present. The use of the z-score normalization led to a comparable range of power features with unit variance across all bands, which was convenient for the subsequent correlation analyses.

## Correlation results

The cortical topographies in Figs. 14–18 depict the spatial distribution of areas where resting levels of neural oscillations<sup>1</sup> are significantly correlated with individual scores extracted from standard WM subtests and indices ( $p < .001$ , cluster-level correction).

Fig. 14 depicts brain areas where oscillatory power is significantly correlated with individual scores on the DS subtest. The most prominent correlations were found in the alpha (8–13 Hz) band and arose primarily in prefrontal cortex. In particular, the significant clusters were located in the bilateral superior frontal gyrus, the dorsomedial prefrontal cortex (dmPFC), the ventromedial prefrontal cortex (vmPFC), and the dorsolateral prefrontal cortex (dlPFC). Although weaker in amplitude and size, the right dmPFC cluster also reached statistical significance in the delta (1–4 Hz) and beta (13–30 Hz) bands. Correlations between DS and resting-state beta oscillations were also significant in the posterior cingulate cortex (PCC), and within a left dmPFC. Interestingly, significant correlations were also observed in the higher gamma frequency range (above 60 Hz), with clusters in left dlPFC and dmPFC. The significant correlations between resting oscillations and scores on the LNS subtest were also dominant in the alpha range, but their spatial distribution was different (Fig. 15). Prominent positive alpha-range correlation clusters were found in the bilateral paracentral gyrus, the superior parietal lobule, and dlPFC. Moreover, significant clusters in the band were found in right dmPFC and PCC. The delta (1–4 Hz) and theta (4–8 Hz) frequency ranges revealed statistically significant correlation patterns in smaller clusters. These included dmPFC and left dlPFC for delta, and bilateral paracentral gyrus and left dlPFC for theta. In the beta band, positive correlations with LNS were found in the left dmPFC, while a very focal correlation in left dlPFC cluster emerged in the gamma 3 band (90–120 Hz). The results obtained when using the WMI are shown in Fig. 16. Arithmetically speaking, the score on the WMI

---

<sup>1</sup> Digit span, number letter sequencing and working memory index

is a combination of DS and LNS scores. We would therefore expect WMI to yield correlation patterns that represent, to a certain extent, a summation of the patterns observed with DS and LNS. The patterns shown in Fig. 16 largely confirm this expectation. In the delta band, we found clusters in the bilateral dmPFC. Theta band clusters were found in the bilateral paracentral lobule and right dmPFC. The main alpha-band correlation clusters were located in bilateral dmPFC, the paracentral lobule, and the superior parietal lobule. A very focal alpha cluster was also detected in left dlPFC. In the beta band, two significant clusters were found in the right PCC and left dmPFC. Left lateralized correlations were also visible in the higher (>60 Hz) frequencies (gamma 2 and 3) in dmPFC, and between the inferior parietal lobule and the post central gyrus. Interestingly, some clusters consistently appear across a broad range of the frequency spectrum (e.g. dmPFC) while others appear to be more specific to oscillations within defined frequency bands (see Discussion).

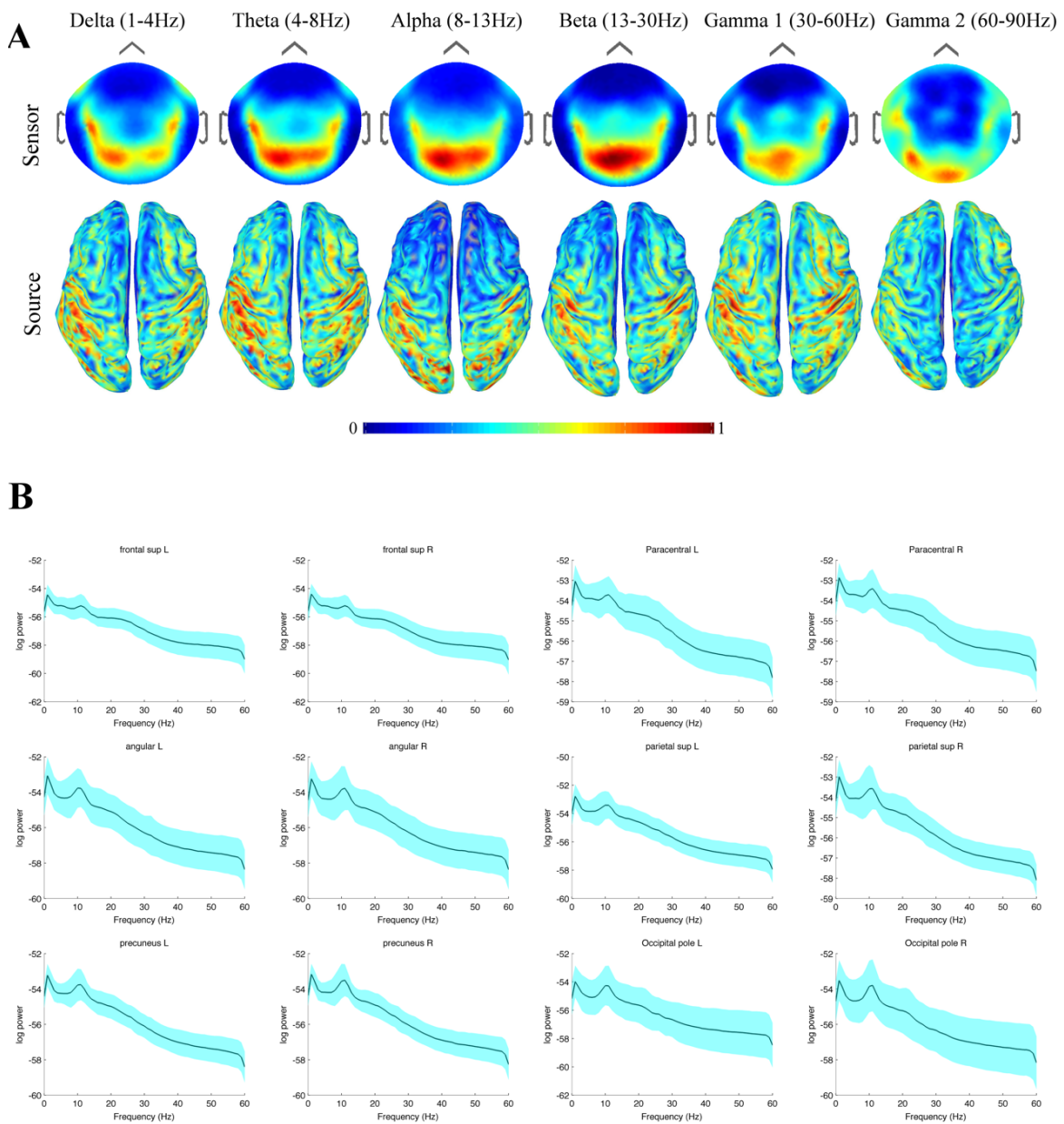


Figure 13. – (A) Topographical plots of relative mean power across all subjects ( $n=26$ ) for each frequency band. The top row shows sensor-level topographies while the bottom row shows normalized power at the cortical source level. Power values were normalized by the maximum across sensors or vertices in each band and then averaged across participants. (B) Grand average power spectrum with its standard deviation across all subjects for the 12 brain regions.

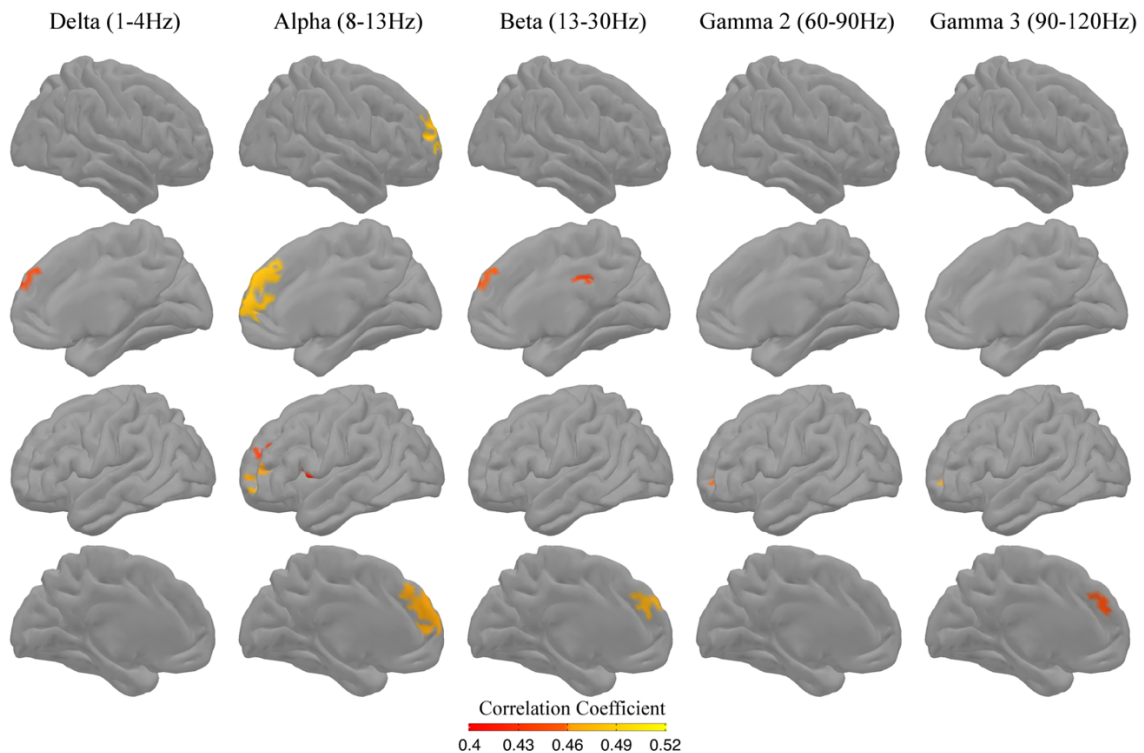


Figure 14. – Brain-Behavior correlations based on resting spectral power and DS test scores (n=26). Spatial distribution of clusters with statistically significant correlations ( $p < .001$ ) between resting MEG source-space power (z-scores across vertices) and neuropsychological performance on the Digit Span (DS, WAIS-IV) subtest. Each column shows the significant correlations for a given range of frequencies, in both hemispheres (right lateral and medial view, followed by left-lateral and medial views). The results are corrected across space using cluster-level corrections. All results remain significant at  $p < .05$ , with Bonferroni correction for multiple comparisons across space, frequency bands, and WM tests. No significant clusters were observed in the Theta and Gamma 1 ranges.

#### Visuo-spatial working memory (SA)

While DS and LNS (and the combined WMI) primarily involve auditory-verbal WM, the SA test mainly relies on another form of WM, which is visuo-spatial WM. We thus hypothesized that SA would yield a different correlation pattern, potentially involving areas and frequencies that mediate cognitive processes relevant to visual and spatial manipulations. The correlations pattern we found using SA scores (Fig. 16) did indeed differ from those reported when using WMI. A strong left hemisphere dominance was found across most frequency bands, with the exception of the beta band, which also yielded correlation clusters in the right paracentral gyrus and right

dmPFC. Delta and theta-band correlation clusters showed similar distributions in the left hemisphere, including the dlPFC, the post central sulcus, the superior and middle temporal gyri, the superior temporal sulcus, and the intra-parietal sulcus. Correlations between SA and alpha power were significant in multiple areas in the left hemisphere, in the post-central sulcus, the superior and middle temporal gyri, the superior temporal sulcus, as well as in the inferior parietal lobule, the intraparietal sulcus, and the superior parietal gyrus. It is noteworthy that a small cluster at the junction between the precuneus and superior occipital gyrus was detected in the right hemisphere. In the beta band, correlation clusters were found in bilateral dmPFC, the right paracentral gyrus, left dlPFC, pre- and post-central gyri, post central sulcus, superior and middle temporal gyri, superior temporal sulcus, angular gyrus, intraparietal sulcus, and superior parietal gyrus. In the gamma 1 band, we found significant clusters of correlation in the left dlPFC, central sulcus, post central gyrus and sulcus, superior temporal sulcus, intraparietal sulcus, and superior parietal gyrus (superior parietal lobule). Finally, a significant left dmPFC cluster was found in the higher gamma 3 band.

#### Working memory residual (WMIr)

To probe the WM-specificity of the observed correlation clusters, we also ran the correlation replacing WMI with a standardized residual score (WMIr) e.i. the degree to which the observed scores of WMI deviate from those predicted by other indices of IQ. The results shown in Fig. 18 indicate prominent correlations in a medial prefrontal cluster, encompassing portions of anterior cingulate cortex (ACC) and vmPFC (bilaterally). Significant clusters were also found at the junction between left PCC, precuneus, and occipito-parietal sulcus, in frequencies extending from theta to gamma 1. A left dmPFC cluster was also present across frequencies ranging from alpha to high gamma. Interestingly, most of these clusters were present for several frequency bands, indicating that it may represent a broadband phenomenon. By contrast, a small occipital pole cluster with high correlation values was observed specifically in the delta/theta range. Moreover, a cluster in the fusiform gyrus/sulcus was found across theta, alpha and beta bands. These correlations between band-limited power and WMIr reflect correlation patterns that are correlated only with the component of the WM index and uncorrelated with the other WAIS-IV indices (PRI, PSI and VCI). In addition to dmPFC and fusiform gyrus, the main nodes we found include ACC/vmPFC and

PCC/precuneus, both of which one could be tempted to relate to key components of the default mode network (DMN).

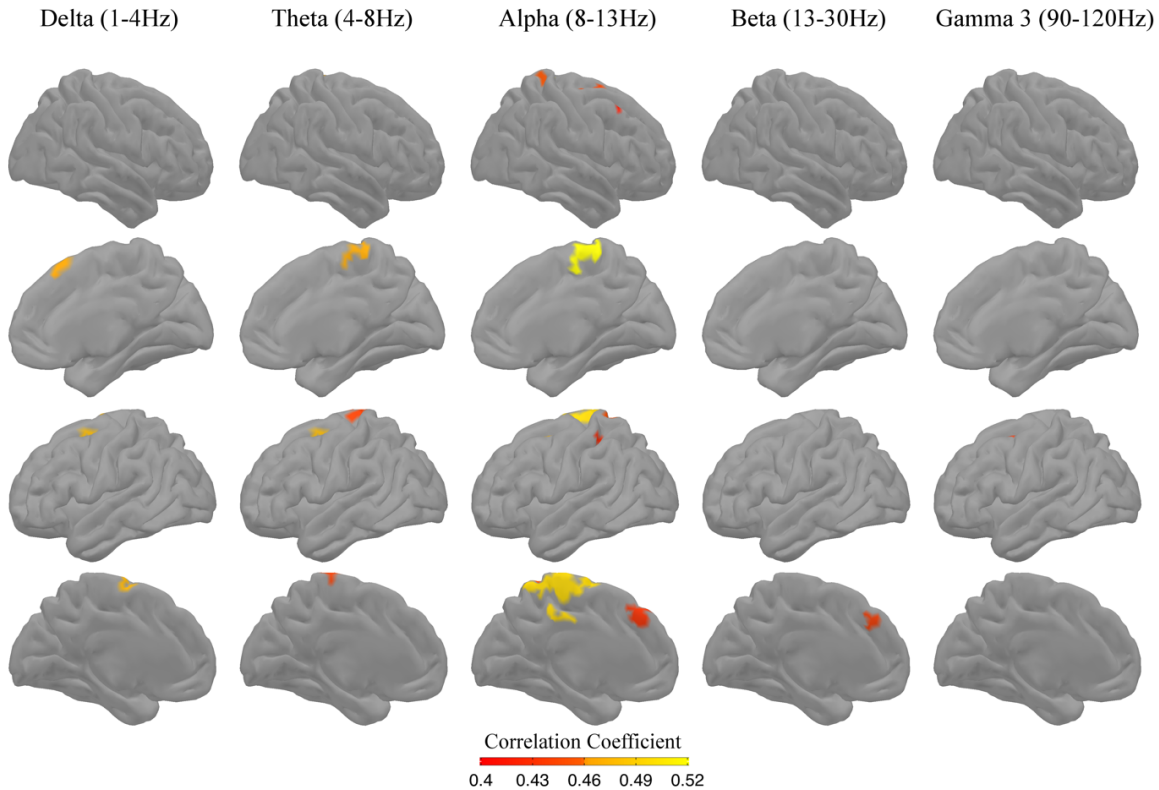


Figure 15. – Brain-Behavior correlations based on resting spectral power and LNS test scores (n=26). Spatial distribution of clusters with statistically significant correlations ( $p < .001$ ) between resting MEG source-space power (z-scores across vertices) and neuropsychological performance on the Letter-Number Sequencing (LNS, WAIS-IV) subtest. The formatting of the figure and statistical significance of the results are identical to those in Fig. 14.

Scatter diagrams and illustrative regression analyses with WMI. To visualize the correlation phenomenon identified in this study we also computed linear regression and scatter plots for the statistically significant clusters. Fig. 19 shows six illustrative scatter plots and linear regression analyses obtained for the source-space resting-state alpha power and the WMI, across the 26 participants. The results are shown for the six most prominent correlation clusters that arise within the alpha band. The represented correlations were computed using the mean power feature across the vertices of each cluster in each individual. Note that this differs slightly from the

correlation analyses and related statistical evaluations that led to the identification of the clusters per se (Section 3.3.1). Here, we focus on these significant clusters and run a linear regression between mean alpha power features per cluster and per subject, with respect to individual WMI scores, to illustrate the observed correlations.

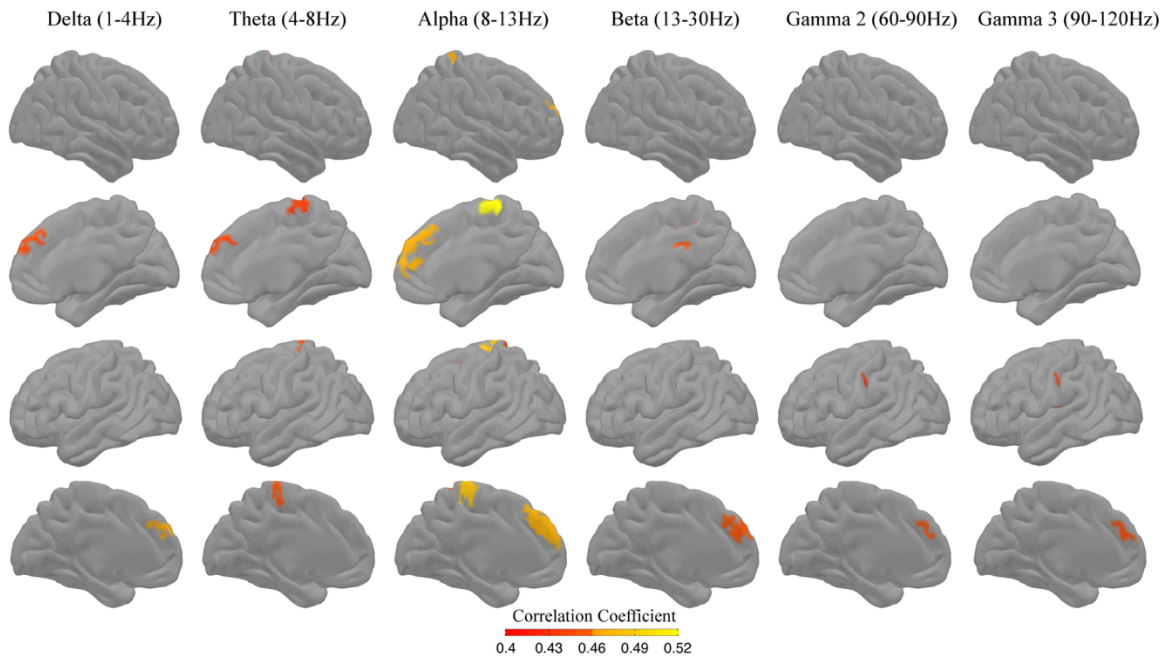


Figure 16. – Brain-Behavior correlations based on resting spectral power and WMI (n=26). Spatial distribution of clusters with statistically significant correlations ( $p < .001$ ) between resting MEG source-space power (z-scores across vertices) and neuropsychological performance on the Working Memory Index (WMI, WAIS-IV). The formatting of the figure and statistical significance of the results are identical to those in Fig. 14.



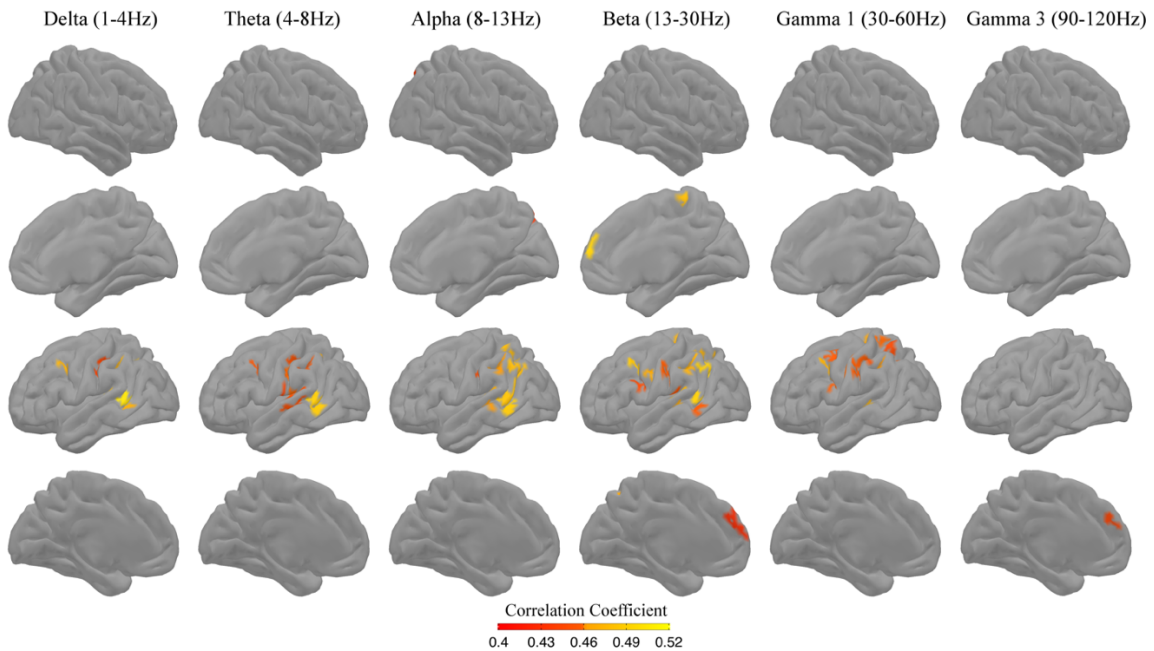


Figure 17. – Brain-Behavior correlations based on resting spectral power and SA (n=26). Spatial distribution of clusters with statistically significant correlations ( $p < .001$ ) between resting MEG source-space power (z-scores across vertices) and neuropsychological performance on the Spatial Addition (SA, WMS-IV) subtest. The formatting of the figure and statistical significance of the results are identical to those in Fig. 14.

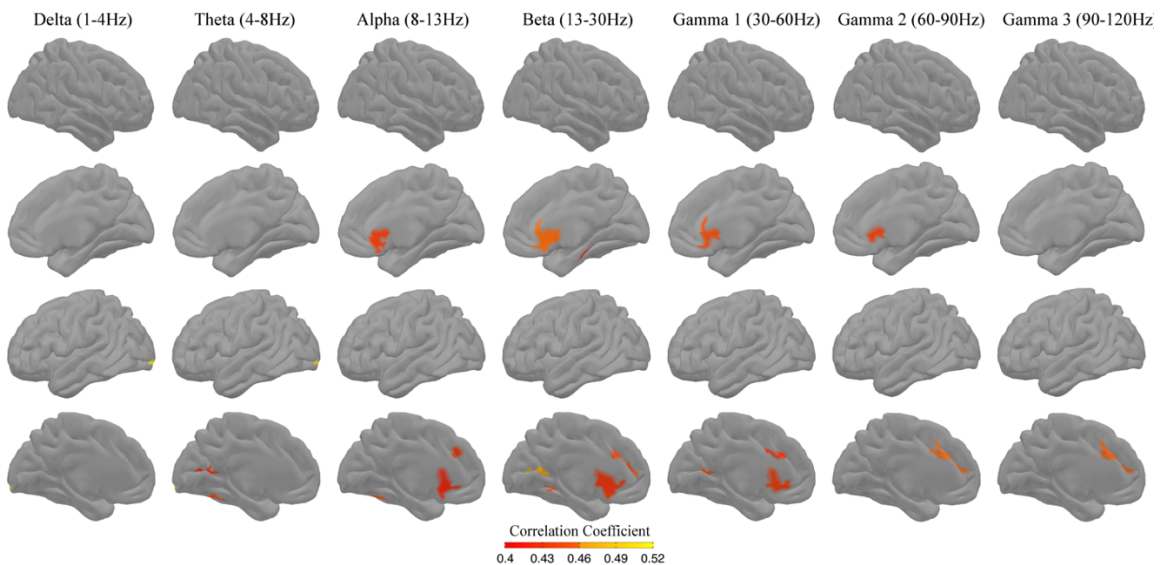


Figure 18. – Brain-Behavior correlations based on resting spectral power and WMIr (n=26). Spatial distribution of clusters with statistically significant correlations ( $p < .001$ ) between resting MEG source-space power (z-scores across vertices) and neuropsychological performance on the Working Memory Index residual (WMIr). WMIr is a measure of working memory, where all correlations with other intelligence indices (PRI then PSI

then VCI) were removed. WMIr is the residual component of the WMI score, after all correlations with the other three indices of the WAIS-IV (PRI, PSI, VCI) were successively removed. Clusters observed with the WMIr correlations should not be observed with any one of these three indices, and are thus specific to WMI. The formatting of the figure and statistical significance of the results are identical to those in Fig. 14.

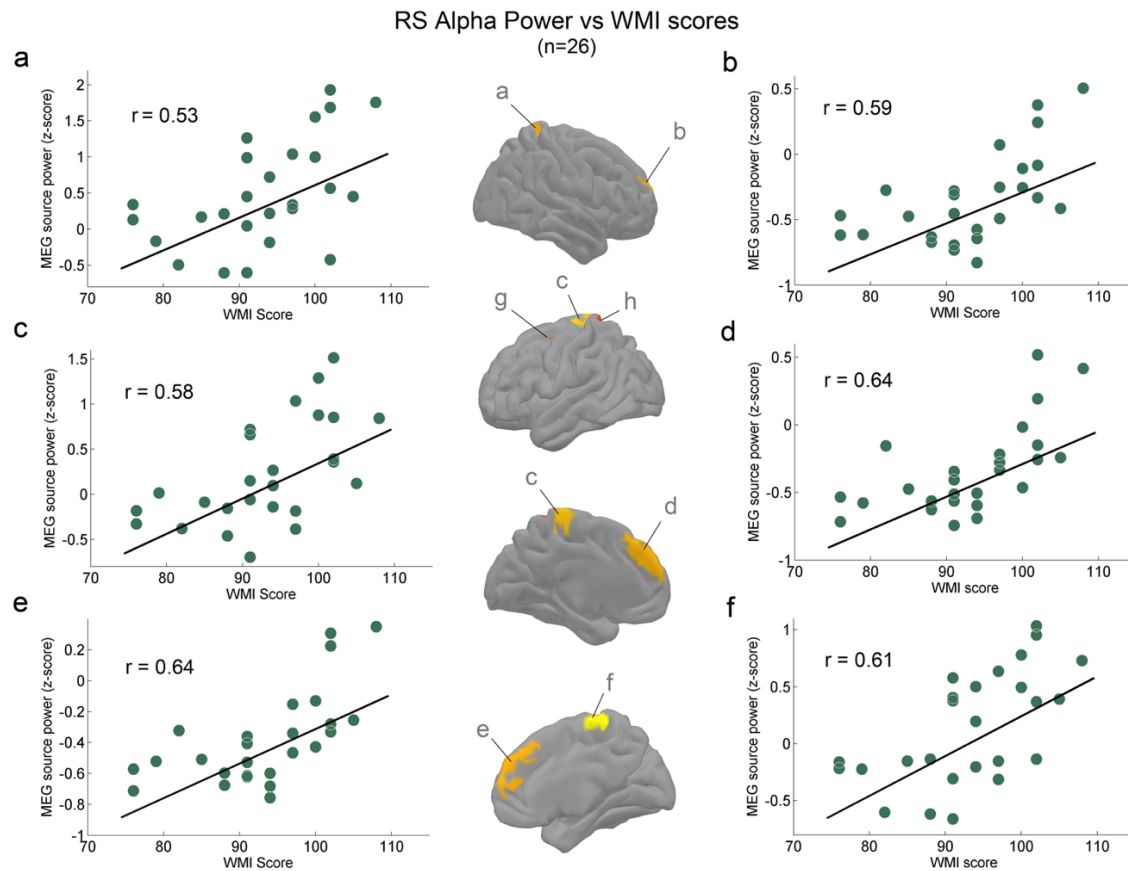


Figure 19. – Scatter plots of the main six significant clusters, using standard linear regression with standardized working memory test scores (WMI) on the x-axis and normalized resting-state alpha-band oscillatory power on the y-axis. (a) right intra-parietal sulcus, (b) right dorso-lateral prefrontal cortex, (c) left paracentral gyrus (paracentral lobule), (d,e) left and right dorsomedial prefrontal cortex (dmPFC), respectively, and (f) right paracentral gyrus (paracentral lobule). The cortical representations in the middle indicate the location of the clusters associated with each scatter plot panel. Clusters g and h also showed statistically significant but weaker correlation coefficients.

## Discussion

In this study we investigated whether standard measures of individual WM capacities are correlated with neuronal oscillation amplitudes, measured at rest with MEG. Our results confirm our working hypothesis that resting-state spectral power levels in distinct brain areas and frequency bands are significantly correlated with WM scores. Our findings also support our hypothesis that the resting-state correlates of WM abilities overlap with (but are not identical to) prominent brain areas and frequency bands previously reported in various task-based WM studies. Beyond suggesting that spectral properties of spontaneous brain activity are indicative of WM capacities in healthy individuals, our results also provide novel insights into the role of brain oscillations and WM processes. The significant correlation between resting-state power and standard neuropsychological scores revealed distinct patterns across space and frequency for DS, LNS and SA. While correlations with DS were mainly found in lateral and medial PFC, correlations with LNS were detected in clusters in left dlPFC, dmPFC and bilateral paracentral gyri. In contrast to the bilateral patterns observed with DS and LNS (verbal/auditory WM), correlations with SA (visual/spatial WM) arose predominantly in the left hemisphere, and included parietal, temporal, and dlPFC areas. Of note, the spatial pattern of significant correlation obtained for WMI broadly consists of a combination of the same clusters that were correlated with LNS or DS. This nicely reflects the fact that WMI is, by construction, comprised of the DS subtest and the LNS subtest. In terms of frequency bands, our results suggest the coexistence of band-specific (narrow-band) and band-unspecific (broadband) effects. The frequency band with the highest degree of specificity was the alpha band, which is in line with the presence of intrinsic alpha-band generators at rest, and with the established involvement of the alpha band in WM processes (Jensen et al., 2002). Brain regions that consistently showed significant correlations across several frequency bands (i.e. frequency-unspecific) include, for instance, the dmPFC. The findings reported here indicate that the resting-state neuronal features that correlate with WM capacities only partly overlap (across space and frequency) with the established parieto-frontal oscillatory networks that are generally detected when using task-based MEG/EEG investigations of WM. Although alpha-band oscillations in parietal and frontal areas were consistently identified in our correlation analyses, a fair amount of variability in brain regions and frequencies was observed

when probing correlations with different WM subtests. One could thus argue that resting-state activity might provide a window into multiple dimensions and types of WM (e.g. modality and content) beyond what is possible with a specific WM paradigm, as probed in some task-based studies. Our results show a left lateralization for SA that assessed visuo/spatial WM, whereas DS and LNS using verbal/auditory modalities show a bilateral pattern. It is noteworthy that the substantial overlap in the spatial patterns of resting-state MEG spectral power across frequency bands (seen both at sensors and source level) may be taken as an indication that power at harmonics (e.g. of alpha spectral peaks) arising from the same generators could in theory be driving the effects observed in other frequency bands. Inspection of the grand average and individual spectra across multiple brain regions, and cross-frequency power correlations argue against the hypothesis that our results can be systematically and entirely related to harmonics. In particular, harmonics were only visible in a few regions and not in all individuals, and most importantly, there was no obvious match between these observations and the main correlations reported with the neuropsychological test scores. Taken together, these results provide the first evidence for a correlation between the amplitude of spontaneous brain activity measured with MEG (no task) and individual WM indices obtained from standard neuropsychological evaluation tests performed outside the scanner (WAIS and the WMS). In the following, we discuss the link, relevance, and novelty of our results in the context of previous research, along four specific angles: (i) previous work that has sought to link resting-state brain activity and WM performance, (ii) the overlap and discrepancies between the correlation networks revealed here and those reported using active WM tasks, (iii) the relationship between our frequency domain results and those typically reported in task-based MEG/EEG studies of WM, and (iv) the link between our resting-state MEG findings and relevant lesion studies.

### **Passive Brain Recordings Correlation Pattern and Working Memory Capacities**

Only very few MEG studies have sought to examine the link between spontaneous oscillations and WM performance. A study by Heister et al. (2013) explored the link between resting-state oscillation amplitude and performance on a subsequent verbal n-back WM task. Interestingly, the authors reported that the normalized difference in low frequency (delta and theta) power

between eyes closed and eyes open was negatively correlated with three-back performance in sensors located over the right posterior frontal and right parietal regions. However, no statistically significant correlations with verbal n-back WM performance were found when using ongoing normalized spectral power, with eyes open or closed. Our source-space results also include delta/theta range correlations that may be related to those reported by Heister et al. (2013). However, our results also differ in significant ways. Most importantly, we found statistically significant correlations between WM performance and eyes-open resting state. In the study by Heister et al. (2013), only power changes between eyes open and closed showed statistically significant correlations with WM. As we did not use an eyes-closed condition, we were not able to confirm this finding in our data. Moreover, we found the most prominent effects in the alpha and beta band, and even observed correlations in higher broadband gamma portions of the spectrum. Several methodological differences between the two studies could partly explain the discrepancies. First, Heister et al. (2013) used a verbal n-back task, whereas we used standardized indices of WM performances (DS, LNS and SA subtests). Second, a major methodological difference lies in the fact that we performed correlation analyses in MEG source-space (with source reconstructions based on individual anatomical MRIs of all participants), while Heister et al. (2013) analyzed MEG sensor signals. Furthermore, we used scaled scores while Heister et al. (2013) used the d prime measure. Additionally, the two studies differ in the way spectral power was normalized, as well as in terms of statistical evaluation. In another MEG study, Vlahou et al. (2014) investigated the effects of healthy aging on spontaneous spectral power and explored the relationship between age-dependent power changes and behavioral performance in the TMT. They found that, in older adults (>54 yrs), higher delta and theta power were associated with improved performance (completion time) in the TMT. No such correlation was observed for younger participants (18-54 yrs). Performance on the TMT was positively correlated with delta band (.5-4 Hz) power in the right temporal and central regions, and with theta band (4.5-7.5 Hz) power in the left temporal regions. Thus, the spectral and spatial patterns of the correlations reported by Vlahou et al., 2014 bear a few interesting similarities with our findings. However, while the correlations between oscillations and cognitive performance they reported were only found in the older adults group, our results indicate significant correlations in young adults (mean

26 yrs) and in a wider range of frequencies. A further important difference is that they used the TMT test, which globally assesses perceptual speed, WM, and executive function, whereas we used more specific WM indices that assess specific neuropsychological abilities. It would be of high interest in future studies to see whether our findings also hold with healthy aging. In EEG, spontaneous alpha peak frequency was found to be a significant predictor of reverse DS (Richard et al., 2004). Each 1 Hz increase in frequency was found to be associated with a .21 increase in reverse DS score, and this was independent of age, indicating a positive relationship between alpha peak frequency and WM performance (Richard et al., 2004). Specifically exploring the peak alpha frequency across cortical source-space in all participants was beyond the scope of the current study, but attempting to replicate EEG results by Richard et al. (2004) observations with our MEG data could be an interesting venue for future work. Similarly, further work should be pursued to relate our alpha-band results to previous reports of distinct links between lower and upper alpha frequencies with WM (Klimesch, Doppelmayr, Schwaiger, Auinger & Winkler, 1999).

### **Relationship with previous task-based WM studies: the anatomical substrates**

Our results show spatial patterns that are fairly consistent with the large body of literature linking fronto-parietal circuits to working memory using various methods. A fronto-parieto-cerebellar network has repeatedly been identified with fMRI, with various types of WM tasks using letter or number stimuli (e.g. Chen & Desmond, 2005; Linden et al., 2003; Majerus et al., 2006, 2007, 2008, 2010, 2012; Majerus, Salmon & Attout, 2013). Generally speaking, the brain areas identified in our correlation analyses (during rest) appear to include areas that have been found to be part of activation or deactivation networks in previous task-based fMRI studies. Our results in the superior and inferior parietal lobule, dmPFC, and dlPFC are in line with fMRI activation during WM tasks reported in previous studies (cf. Owen, McMillan, Laird, and Bullmore (2005); Rottschy et al., 2012, Chang et al., 2001; Tomasi, Ernst, Caparelli & Chang, 2006, Kirschen, Chen, Schraedley-Desmond & Desmond, 2005). Whereas other areas we found here (including the bilateral para central lobule, superior frontal gyrus, left central gyrus, and right PCC) were previously found to be deactivated during WM tasks (Tomasi et al., 2006; Zou et al., 2013). The frontal regions present in our results (across all subtests DS, LNS and SA) show spatial clusters in the bilateral vmPFC,

dmPFC and dlPFC (in particular BA 6, 8, 9, 10, 32). Interestingly, in the literature, these areas are alternately found to be part of a task-negative or task-positive network (Owen et al., 2005; Rottschy et al., 2012; Tomasi et al., 2006). It is noteworthy that an fMRI study by Zou et al. (2013) found that resting-state activity and task-based activation in the superior parietal lobule/precuneus were both significantly correlated with behavioral performance on a WM task, explaining similar portions of inter-subject performance variance. Zou et al. (2013) interpret their findings as suggesting that intrinsic resting-state activity facilitates specific brain circuit engagement to perform a cognitive task, and that resting activity can predict subsequent task-based brain responses and behavioral performance. Interestingly, PET data acquired during performance of the LNS WM subtest has revealed activation within the orbital frontal lobe, dlPFC, and posterior parietal cortex (Haut, Kuwabara, Leach & Arias, 2000). Intrinsic resting-state oscillation amplitudes recorded over fronto-parietal areas showed strong correlations with both verbal and spatial WM scores. Using MEG, Brookes, Wood, et al. (2011b) show an increase in theta power in the mPFC during both n-back and Sternberg tasks in a similar spatial location of our results.

### **Relationship with previous task-based WM studies: the frequency patterns**

Our results suggest the coexistence of narrow-band and broadband effects. Broadband correlations (i.e. correlation effects observed in successive frequency bands and located in the same anatomical cluster) may be interpreted in two different ways. One possibility is that oscillations in multiple bands reflect distinct mechanisms (and represent a common node across different functional networks) that are all relevant for WM. Alternatively, it is also possible that oscillatory amplitude across a wide range of frequencies reflects a single functional mechanism important for WM capacities. The present study was not designed to disentangle the two options. In addition, a combination of both explanations is in theory possible. By contrast, narrow-band correlations are thought to reflect a functionally specific involvement of brain oscillations within a restricted bandwidth. In particular, alpha band oscillations have been tightly linked to top-down functional inhibition that can suppress for instance, the processing of distracting sensory information (Bonnefond & Jensen, 2013; Klimesch, 2012; Klimesch, Sauseng & Hanslmayr, 2007). The localization in the paracentral gyrus (sensori-motor area) of the resting state correlation

cluster may reflect that a stronger top down inhibitory control of the sensorimotor region is associated with a better performance in WM tasks. Moreover, our results from the resting state MEG are in line with changes in the alpha band in active WM tasks. For instance, a modified Sternberg task alpha peak amplitude was shown to increase with the number of items held in WM, especially over posterior and bilateral central brain regions (Jensen et al., 2002). More recently, alpha oscillations have been proposed to shield WM maintenance from anticipated distractors (Bonfond & Jensen, 2012). The alpha increase with memory load (Jensen et al., 2002; Scheeringa et al., 2009; Tuladhar et al., 2007) has been proposed to either reflect active memory maintenance (Klimesch, Pfurtscheller, Mohl, & Schimke, 1990; Klimesch, Schimke, & Pfurtscheller, 1993; Klimesch et al. 1999; Palva & Palva, 2007) or active inhibition of regions not required for the task (Jensen & Mazaheri, 2010; Klimesch et al., 2007). In addition to the prominent alpha effects, statistically significant results were seen across delta, theta, beta and gamma frequencies, with the same areas often being significant across several adjacent frequency bands (i.e. what we referred to as broadband effects). These frequencies have also been found to play a key role during performance of WM tasks. For instance, theta band power is known to increase in task-based EEG/MEG studies, such as the investigations of changes in memory load in different verbal and visuospatial tasks (e.g., Gevins et al., 1997, 1998; Jensen & Tesche, 2002; Onton, Delorme, & Makeig, 2005; Missonnier et al., 2006; Sauseng, Griesmayr, Freunberger, & Klimesch, 2010; Brookes, Wood et al., 2011b). A delta range parieto-frontal correlation cluster we found is also in line with earlier findings of task-based power modulations in the 2-4Hz range, found during performance of a Sternberg paradigm (Harmony et al., 1996). The gamma band is also known to be involved in visuospatial and auditory WM tasks, and several studies have demonstrated a parametric relationship between the number of items to be memorized and the amplitude of gamma band oscillations (Kaiser & Lutzenberger, 2003; Morgan et al., 2011; Meeuwissen et al., 2011; Roux, Wibral, Mohr, Singer, & Uhlhaas, 2012; Medendorp et al., 2007; Howard et al., 2003; Bonfond & Jensen, 2013; Lozano- Soldevilla et al., 2014; Honkanen et al., 2015; Lundqvist et al., 2016).



### **Links to findings from lesion studies**

A lesion study by Barbey, Koenigs, and Grafman (2013) suggests that the left dorsolateral prefrontal cortex (dlPFC) supports manipulating representations in WM, and the right dlPFC supports the manipulation of information in a broader range of reasoning contexts. More specifically, the authors argue that this lateralization pattern is consistent with the hypothesis that the left dlPFC supports cognitive processes that are temporally bound within WM (e.g. LNS), whereas the right dlPFC supports more global cognitive processes enabling goal-directed behavior and adaptive decision-making (e.g. arithmetic reasoning). This is in agreement with the left dlPFC cluster detected here through correlation with LNS subtask scores. In a more recent study, Barbey, Colom, Paul, and Grafman (2014) reported that impairments in verbal/numeric WM are associated with damage primarily within the left hemisphere, including left angular gyrus (BA 39), left superior parietal cortex (BA 7) and left superior temporal gyrus (BA 41/42/22). In line with these lesion-based results, the MEG data reported here also show a left-lateralized correlation cluster specifically for the SA scores.

## Conclusions

Taken together, and to the best of our knowledge, our findings provide the first evidence for a direct relationship between cortical spectral power, measured with MEG at rest, and WM performance, as assessed by standardized neuropsychological tests outside the scanner. In particular, we report significant correlations between WM abilities and spectral power in distinct prefrontal, parietal and temporal brain areas. While a subset of the significant correlation clusters were frequency selective (e.g. alpha-band power in paracentral lobule), other areas were present across a wide range of frequencies, indicating that they may reflect broadband power effects, i.e. not driven by distinct oscillations. This was observed in dmPFC. These results complement previous findings from neuroimaging and lesion studies and represent a step forward in understanding the link between spontaneous oscillatory dynamics in fronto-parietal networks and WM. Future work will have to extend the current study to assessment of links between other properties of resting-state networks (e.g. connectivity) and WM indices.

Importantly, scores derived from standardized intelligence scales are stable over time (e.g. Estevis, Basso & Combs, 2012; Wechsler, 2008a, 2008b). Likewise, MEG resting-state network properties also show a fair degree of stability and long-term test-retest reliability in healthy adults (Colclough et al., 2016; Deuker et al., 2009; Garces, Martín-Buro & Maestú, 2016; Wens et al., 2014). Hence, our main findings of correlations between the two measures may be interpreted as indicative of a long-lasting trait effect rather than a short-lived state effect. In fact, this can be considered one of the advantages of the approach used here, compared to task-based studies of active working-memory tasks where individual performance could be more context-dependent. Nevertheless, because some degree of variability over time in resting state and standardized intelligence measures do exist, testing the long-term reliability of the correlations reported here would be an important venue for future research. Critically, the data reported here open new questions about the interpretation of modulations in neuronal oscillations observed during WM tasks, where a task-free rest period (e.g. pre-stimulus interval) is often used as a baseline. If the oscillatory properties already differ at baseline as a function of WM capacities, as our data suggest, then comparisons of active tasks with such baselines need to be taken with a lot of caution. For instance, it would be important to verify whether stronger event-related power

suppression (e.g. in the alpha band) are entirely dependent on the brain's response to a stimulus, or whether they are at least in part due to differing levels of power during the period used as a baseline. At minimum, the baseline window needs to be compared across conditions or individuals (or correlated with behavioral performance) in order to rule out significant differences at rest that could impact or invalidate subsequent analyses. Finally, our results may have promising implications for the development of novel cognitive enhancement procedures and clinical rehabilitation therapies. This, for instance, may be achieved by using neurofeedback, neuromodulation, or carefully chosen cognitive tasks that may specifically boost ongoing neuronal oscillations in distinct brain regions and frequency bands.

### **Acknowledgements**

This work was supported by the CIRSH [255074, 2014]; KJ acknowledges funding from the Canada Research Chairs program and NSERC Discovery Grant [RGPIN-2015-04854] and FRQNT New Researcher Grant [RQT00121]. VO acknowledges support by the Marc Bougie Foundation, the Faculty of Medicine of the University of Montreal and CIRSH [255074, 2014].

## References

- Axmacher, N., Henseler, M. M., Jensen, O., Weinreich, I., & Elger, C. E. (2010). Cross-frequency coupling supports multi-item working memory in the human hippocampus. *Journal Proceedings of National Academic Sciences the United States of America*, 107(7), 3228–3233. Epub 2010 Jan 26.
- Baillet, S., Mosher, J. C., & Leahy, R. M. (2001). Electromagnetic brain mapping. *IEEE Signal Processing Magazine*, 18, 14e3010.1109/79.962275.
- Barbey, A. K., Colom, R., Paul, E. J., & Grafman, J. (2014). Architecture of fluid intelligence and working memory revealed by lesion mapping. *Brain Structure and Function*, 219(2), 485–494.
- Barbey, A. K., Koenigs, M., & Grafman, J. (2013). Dorsolateral prefrontal contributions to human working memory. *Cortex*, 49(5), 1195–1205.
- Biswal, B., Zerrin Yetkin, F., Haughton, V. M., & Hyde, J. S. (1995). Functional connectivity in the motor cortex of resting human brain using echo-planar MRI. *Magnetic Resonance in Medicine*, 34, 537–541.
- Bonnefond, M., & Jensen, O. (2012). Alpha oscillations serve to protect working memory maintenance against anticipated distracters. *Current Biology*, 22(20), 1969–1974. <https://doi.org/10.1016/j.cub.2012.08.029>.
- Bonnefond, M., & Jensen, O. (2013). The role of gamma and alpha oscillations for blocking out distraction. *Communicative & Integrative Biology*, 16(1), e22702.
- Brookes, M. J., Wood, J. R., Stevenson, C. M., Zumer, J. M., White, T. P., Liddle, P. F., et al. (2011b). Changes in brain network activity during working memory tasks: A magnetoencephalography study. *NeuroImage*, 55, 1804–1815.
- Brookes, M. J., Woolrich, M., Luckhoo, H., Price, D., Hale, J. R., Stephenson, M. C., et al. (2011a). Investigating the electrophysiological basis of resting state networks using magnetoencephalography. *Proceedings of the National Academy of Sciences of the United States of America*, 4; 108(40), 16783–16788.
- Broyd, S. J., Demanuele, C., Debener, S., Helps, S. K., James, C. J., & Sonuga-Barke, E. J. S. (2009). Default-mode brain dysfunction in mental disorders: A systematic review. *Neuroscience and Biobehavioral Reviews*, 33(3), 279–296.
- Buckner, R. L., Andrews-Hanna, J. R., & Schacter, D. L. (2008). The Brain's default network anatomy, function, and relevance to disease. *Annals of the New York Academic Sciences*, 1124, 1–38. <https://doi.org/10.1196/annals.1440.011>.
- Bullmore, E., & Sporns, O. (2009). Complex brain networks: Graph theoretical analysis of structural and functional systems. *Nature Reviews Neurosciences*, 10, 186–198. <https://doi.org/10.1038/nrn2575>.

- Buzsaki, G., & Silva, F. L. (2012). High frequency oscillations in the intact brain. *Progress in Neurobiology*, 98(3), 241–249.
- Chang, L., Speck, O., Miller, E., Braun, A., Jovicich, J., Koch, C., et al. (2001). Neural correlates of attention and working memory deficits in HIV patients. *Neurology*, 57, 1001–1007.
- Chen, S. H., & Desmond, J. E. (2005). Temporal dynamics of cerebro-cerebellar network recruitment during a cognitive task. *Neuropsychologia*, 43, 1227–1237.
- Colclough, G. L., Woolrich, M. W., Tewarie, P. K., Brookes, M. J., Quinn, A. J., & Smith, S. M. (2016). How reliable are MEG resting-state connectivity metrics? *NeuroImage*, 138.
- Dalal, S. S., Vidal, J. R., Hamame, C. M., Ossandon, T., Bertrand, O., Lachaux, J. P., et al. (2011). Spanning the rich spectrum of the human brain: Slow waves to gamma and beyond. *Brain Structure & Function*, 216(2), J77–J84.
- Deuker, L., Bullmore, E. T., Smith, M., Christensen, S., Nathan, P. J., Rockstroh, B., et al. (1 October 2009). Reproducibility of graph metrics of human brain functional networks. *NeuroImage*, 47(4), 1460–1468. <https://doi.org/10.1016/j.neuroimage.2009.05.035>. ISSN 1053e8119.
- Estevis, E., Basso, M. R., & Combs, D. (2012). Effects of practice on the Wechsler adult intelligence scale-IV across 3- and 6-month intervals. *The Clinical Neuropsychologist*, 26(2), 239–254.
- Fischl, B., Salat, D. H., Busa, E., Albert, M., Dieterich, M., Haselgrove, C., et al. (2002). Whole brain Segmentation: Automated labeling of neuroanatomical structures in the human brain. *Neuron*, 33(3), 341–355. [https://doi.org/10.1016/S0896-6273\(02\)00569-X](https://doi.org/10.1016/S0896-6273(02)00569-X). ISSN 0896e6273.
- Foster, B. L., He, B. J., Honey, C. J., Jerbi, K., Maier, A., & Saalman, Y. B. (2016). Spontaneous neural dynamics and multi-scale network organization. *Frontiers in Systems Neuroscience*, 10(7). <https://doi.org/10.3389/fnsys.2016.00007>.
- Fox, M. D., & Greicius, M. (2010). Clinical applications of resting state functional connectivity. *Frontiers in Systems Neuroscience*, 4, 19.
- Fox, M. D., & Raichle, M. E. (2007). Spontaneous fluctuations in brain activity observed with functional magnetic resonance imaging. *Nature Reviews Neurosciences*, 8, 700–711. <https://doi.org/10.1038/nrn2201>.
- Garces, P., Martín-Buro, M. C., & Maestú, F. (2016 Jul). Quantifying the test-retest reliability of magnetoencephalography resting- state functional connectivity. *Brain Connectivity*, 6(6), 448–460.
- Gevins, A., Smith, M. E., Leong, H., McEvoy, L., Whitfield, S., Du, R., et al. (1998). Monitoring working memory load during computer-based tasks with EEG pattern recognition methods. *Human Factors*, 40, 79–91.
- Gevins, A., Smith, M. E., McEvoy, L., & Yu, D. (1997). High- resolution EEG mapping of cortical activation related to working memory: Effects of task difficulty, type of processing, and practice. *Cerebral Cortex*, 7, 374–385.

- Ghuman, A. S., McDaniel, J. R., & Martin, A. (2011). A wavelet-based method for measuring the oscillatory dynamics of resting-state functional connectivity in MEG. *NeuroImage*. ISSN: 1053-8119, 56(1), 69–77. <https://doi.org/10.1016/j.neuroimage.2011.01.046>.
- Greicius, M. D. (2008 Aug). Resting-state functional connectivity in neuropsychiatric disorders. *Current Opinion in Neurology*, 24(4), 424–430.
- Güntekin, B., & Basar, E. (2014). A review of brain oscillations in perception of faces and emotional pictures. *Neuropsychologia*, 58, 33–51.
- Harmony, T., Fernandez, T., Silva, J., Bernal, J., Diaz-Comas, L., Reyes, A., et al. (1996). EEG delta activity: An indicator of attention to internal processing during performance of mental tasks. *International Journal of Psychophysiology*, 24(1e2), 161–171.
- Haut, M. W., Kuwabara, H., Leach, S., & Arias, R. G. (2000). Neural activation during performance of number-letter sequencing. *Applied Neuropsychology*, 7(4), 237–242. [https://doi.org/10.1207/S15324826AN0704\\_5](https://doi.org/10.1207/S15324826AN0704_5).
- Heister, D., Diwakar, M., Nichols, S., Robb, A., Angeles, A. M., Gal, O., et al. (2013). Resting-state neuronal oscillatory correlates of working memory performance. *PLoS One*, 8(6), e66820. <https://doi.org/10.1371/journal.pone.0066820>.
- Hinkley, L. B. N., Vinogradov, S., Guggisberg, A. G., Fisher, M., Findlay, A. M., & Nagarajan, S. S. (2011). Clinical symptoms and alpha band resting-state functional connectivity imaging in patients with Schizophrenia: Implications for novel approaches to treatment. *Biological Psychiatry*, 70(12), 1134–1142.
- Honkanen, R., Rouhinen, S., Wang, S. H., Palva, J. M., & Palva, S. (2015). Gamma oscillations underlie the maintenance of feature-specific information and the contents of visual working memory. *Cerebral Cortex*, 25(10), 3788–3801.
- Howard, M. W., Rizzuto, D. S., Caplan, J. B., Madsen, J. R., Lisman, J., Aschenbrenner-Scheibe, R., et al. (2003). Gamma oscillations correlate with working memory load in humans. *Cerebral Cortex*, 13(12), 1369–1374. <https://doi.org/10.1093/cercor/bhg084>.
- Huang, M. X., Mosher, J. C., & Leahy, R. M. (1999). A sensor-weighted overlapping-sphere head model and exhaustive head model comparison for MEG. *Physics in Medicine and Biology*, 44(2), 423. <http://stacks.iop.org/0031-9155/44/i1/42/a1/4010>.
- Jensen, O., Gelfand, J., Kounios, J., & Lisman, J. E. (2002). Oscillations in the alpha band (9-12 Hz) increase with memory load during retention in a short-term memory task. *Cerebral Cortex*, 12, 877–882.
- Jensen, O., Gips, B., Bergmann, T. O., & Bonnefond, M. (2014). Temporal coding organized by coupled alpha and gamma oscillations prioritize visual processing. *Trends in Neurosciences*, 37(7), 357–369.

- Jensen, O., & Mazaheri, A. (2010). Shaping functional architecture by oscillatory alpha activity: Gating by inhibition. *Frontiers in Human Neuroscience*, 4(186). <https://doi.org/10.3389/fnhum.2010.00186>.
- Jensen, O., & Tesche, C. D. (2002). Frontal theta activity in humans increases with memory load in a working memory task. *The European Journal of Neuroscience*, 1395–1399.
- Jerbi, K., Ossandon, T., Hamame, C. M., Senova, S., Dalal, S. S., Jung, J., et al. (2009). Task-related gamma-band dynamics from an intracerebral perspective: Review and implications for surface EEG and MEG. *Human Brain Mapping*, 30(6), 1758–1771.
- Jerbi, K., Vidal, J. R., Ossandon, T., Dalal, S. S., Jung, J., Hoffmann, D., et al. (2010 Jun 28). Exploring the electrophysiological correlates of the default-mode network with intracerebral EEG. *Frontiers in System Neuroscience*, 4, 27. <https://doi.org/10.3389/fnsys.2010.00027>.
- Kaiser, J., & Lutzenberger, W. (2003). Induced gamma-band activity and human brain function. *The Neuroscientist*, 9(6), 475–484.
- Keller, J. B., Hedden, T., Thompson, T. W., Anteraper, S. A., Gabrieli, J. D. E., & Whifiles-Gabrieli, S. (2015). Resting-state anticorrelations between medial and lateral prefrontal cortex: Association with working memory, aging, and individual differences. *Cortex*, 64, 271–280.
- Kirschen, M. P., Chen, S. H., Schraedley-Desmond, P., & Desmond, J. E. (2005). Load- and practice-dependent increases in cerebro-cerebellar activation in verbal working memory: An fMRI study. *NeuroImage*, 24, 462–472.
- Klimesch, W. (2012).  $\alpha$ -Band oscillations, attention, and controlled access to stored information. *Trends in Cognitive Science*, 16(12), 606e617.
- Klimesch, W., Doppelmayr, M., Schwaiger, J., Auinger, P., & Winkler, T. (1999). ‘Paradoxical’ alpha synchronization in a memory task. *Brain Research. Cognitive Brain Research*, 7, 493–501.
- Klimesch, W., Pfurtscheller, G., Mohl, W., & Schimke, H. (1990). Event-related desynchronization, erd-mapping and hemispheric differences for words and numbers. *International Journal of Psychophysiology*, 8, 297–308.
- Klimesch, W., Sauseng, P., & Hanslmayr, S. (2007). EEG alpha oscillations: The inhibition-timing hypothesis. *Brain Research Reviews*, 53, 63–88.
- Klimesch, W., Schimke, H., & Pfurtscheller, G. (1993). Alpha frequency, cognitive load and memory performance. *Brain Topography*, 5, 241–251.
- Leszczynski, M., Fell, J., & Axmacher, N. (2015). Rhythmic working memory activation in the human Hippocampus. *Cell Reports [Electronic Resource]*, 13(6), 1272e1282. <https://doi.org/10.1016/j.celrep.2015.09.081>.
- Liang, X., Zou, Q., He, Y., & Yang, Y. (2013). Coupling of functional connectivity and regional cerebral blood flow reveals a physiological basis for network hubs of the human brain.

Proceedings of the National Academy of Sciences of the United States of America, 110(5), 1929–1934.

- Linden, D. E., Bittner, R. A., Muckli, L., Waltz, J. A., Kriegeskorte, N., Goebel, R., et al. (2003). Cortical capacity constraints for visual working memory: Dissociation of fMRI load effects in a fronto- parietal network. *NeuroImage*, 20, 1518–1530.
- Liuzzi, L., Gascoyne, L. E., Tewarie, P. K., Barratt, E. L., Boto, E., & Brookes, M. J. (2016 Nov 26). Optimising experimental design for MEG resting state functional connectivity measurement. *NeuroImage*. pii: S1053-8119(16), 30680–30682.
- Lozano-Soldevilla, D., ter Huurne, N., Cools, R., & Jensen, O. (2014). GABAergic modulation of visual gamma and alpha oscillations and its consequences for working memory performance. *Current Biology: CB*, 24(24), 2878–2887.
- Lundqvist, M., Rose, J., Herman, P., Brincat, S. L., Buschman, T. J., & Miller, E. K. (2016). Gamma and beta bursts underlie working memory. *Neuron*, 90(1), 152–164.
- Majerus, S., Attout, L., D'Argembeau, A., Degueldre, C., Fias, W., Maquet, P., et al. (2012). Attention supports verbal short-term memory via competition between dorsal and ventral attention networks. *Cerebral Cortex*, 22, 1086–1097.
- Majerus, S., Bastin, C., Poncelet, M., Van der Linden, M., Salmon, E., Collette, F., et al. (2007). Short-term memory and the left intraparietal sulcus: Focus of attention? Further evidence from a face short-term memory paradigm. *NeuroImage*, 35, 353–367.
- Majerus, S., Belayachi, S., De, S. B., Leclercq, A. L., Martinez, T., Schmidt, C., et al. (2008). Neural networks for short-term memory for order differentiate high and low proficiency bilinguals. *NeuroImage*, 42, 1698–1713.
- Majerus, S., D'Argembeau, A., Martinez, P. T., Belayachi, S., Van der Linden, M., Collette, F., et al. (2010). The commonality of neural networks for verbal and visual short-term memory. *Journal of Cognitive Neuroscience*, 22, 2570–2593.
- Majerus, S., Poncelet, M., Van der Linden, M., Albouy, G., Salmon, E., Sterpenich, V., et al. (2006). The left intraparietal sulcus and verbal short-term memory: Focus of attention or serial order? *NeuroImage*, 32, 880–891.
- Majerus, S., Salmon, E., & Attout, L. (2013). The importance of encoding-related neural dynamics in the prediction of inter- individual differences in verbal working memory performance. *PLoS One*, 8, e69278.
- Maris, E., & Oostenveld, R. (2007). Nonparametric Statistical testing of EEG- and MEG-data. *Journal of Neuroscience Methods*, 164(2007), 177–190.
- Medendorp, W. P., Kramer, G. F. I., Jensen, O., Oostenveld, R., Schoffelen, J. N., & Fries, P. (2007). Oscillatory activity in human parietal and occipital cortex shows hemispheric lateralization and memory effects in a delayed double-step saccade task. *Cerebral Cortex*, 17(10), 2364e2374. [https:// doi.org/10.1093/cercor/bhl145](https://doi.org/10.1093/cercor/bhl145).



- Meeuwissen, E. B., Takashima, A., Fernandez, G., & Jensen, O. (2011). Evidence for human fronto-central gamma activity during long-term memory encoding of word sequences. *PLoS One*, 6(6), e21356.
- Missonnier, P., Deiber, M. P., Gold, G., Millet, P., Gex-Fabry Pun, M., Fazio-Costa, L., et al. (2006). Frontal theta event-related synchronization: Comparison of directed attention and working memory load effects. *Journal of Neural Transmission*, 113, 1477–1486. <https://doi.org/10.1007/s00702-005-0443-9>.
- Morgan, H. M., Muthukumaraswamy, S. D., Hibbs, C. S., Shapiro, K. L., Bracewell, R. M., Singh, K. D., et al. (2011). Feature integration in visual working memory: Parietal gamma activity is related to cognitive coordination. *Journal of Neurophysiology*, 106(6), 3185–3194.
- Onton, J., Delorme, A., & Makeig, S. (2005). Frontal midline EEG dynamics during working memory. *NeuroImage*, 27, 341–356.
- Ossandon, T., Jerbi, K., Vidal, J. R., Bayle, D. J., Henaff, M. A., Jung, J., et al. (2011 Oct 12). Transient suppression of broadband gamma power in the default-mode network is correlated with task complexity and subject performance. *The Journal of Neuroscience*, 31(41), 14521–14530.
- Owen, A. M., McMillan, K. M., Laird, A. R., & Bullmore, E. (2005). N-back working memory paradigm: A meta-analysis of normative functional neuroimaging studies. *Human Brain Mapping*, 25, 46–59. <https://doi.org/10.1002/hbm.20131>.
- Palva, S., & Palva, J. M. (2007 Apr). New vistas for alpha-frequency band oscillations. *Trends in Neurosciences*, 30(4), 150e158.
- Park, H., Kang, E., Kang, H., Kim, J. S., Jensen, O., Chung, C. K., et al. (2011). Cross-frequency power correlations reveal the right superior temporal gyrus as a hub region during working memory maintenance. *Brain Connectivity*, 1(6), 460–472. Epub 2012 Mar 8.
- de Pasquale, F., Della Penna, S., Snyder, A. Z., Lewis, C., Mantini, D., Marzetti, L., et al. (2010 Mar 30). Temporal dynamics of spontaneous MEG activity in brain networks. *Proceedings of the National Academy of Sciences of the United States of America*, 107(13), 6040–6045.
- de Pasquale, F., Della Penna, S., Sporns, O., Romani, G. L., & Corbetta, M. A. (2016 Oct). Dynamic core network and global efficiency in the resting human brain. *Cerebral Cortex*, 26(10), 4015–4033.
- Raichle, M. E., MacLeod, A. M., Snyder, A. Z., Powers, W. J., Gusnard, D. A., & Shulman, G. L. (2001). A default mode of brain function. *Proceedings of the National Academy of Sciences of the United States of America*, 98, 676e682. <https://doi.org/10.1073/pnas.98.2.676>.
- Richard, C. C., Veltmeyer, M. D., Hamilton, R. J., Simms, E., Paul, R., Hermens, D., et al. (2004). Spontaneous alpha peak frequency predicts working

memory performance across the age span. *International Journal of Psychophysiology*, 53, 1–9.

- Rottschy, C., Langner, R., Dogan, I., Reetz, K., Laird, A. R., Schulz, J. B., et al. (2012). Modelling neural correlates of working memory: A coordinate-based meta-analysis. *NeuroImage*, 60(1), 830e846. <https://doi.org/10.1016/j.neuroimage.2011.11.050>. ISSN 1053–8119.
- Roux, F., & Uhlhaas, P. J. (2014). Working memory and neural oscillations: a-g versus q-g codes for distinct WM information? *Trends in Cognitive Science*, 18(1), 16–25.
- Roux, F., Wibral, M., Mohr, H. M., Singer, W., & Uhlhaas, P. J. (2012). Gamma-band activity in human prefrontal cortex codes for the number of relevant items maintained in working memory. *Journal of Neuroscience*, 32(36), 12411–12420. <https://doi.org/10.1523/JNEUROSCI.0421-12.2012>.
- Ruhnau, P., Hauswald, A., & Weisz, N. (2014 Oct 30). Investigating ongoing brain oscillations and their influence on conscious perception e network states and the window to consciousness. *Front Psychol*, 5, 1230.
- Sauseng, P., Griesmayr, B., Freunberger, R., & Klimesch, W. (2010). Control mechanisms in working memory: A possible function of EEG theta oscillations. *Neuroscience & Biobehavioral Reviews*, 34(7), 1015–1022.
- Scheeringa, R., Petersson, K. M., Oostenveld, R., Norris, D. G., Hagoort, P., & Bastiaansen, M. C. (2009). Trial by-trial coupling between EEG and BOLD identifies networks related to alpha and theta EEG power increases during working memory maintenance. *NeuroImage*, 44, 1224–1238.
- Tadel, F., Baillet, S., Mosher, J. C., Pantazis, D., & Leahy, R. M. (2011). Brainstorm: A user-friendly application for MEG/EEG analysis. *Computational Intelligence and Neuroscience*, 2011. ID 879716.
- Tomasi, D., Ernst, T., Caparelli, E. C., & Chang, L. (2006). Common deactivation patterns during working memory and visual attention tasks: An intra-subject fMRI study at 4 Tesla. *Human Brain Mapping*, 27, 694–705.
- Tuladhar, A. M., ter Huurne, N., Schoffelen, J. M., Maris, E., Oostenveld, R., & Jensen, O. (2007). Parieto-occipital sources account for the increase in alpha activity with working memory load. *Human Brain Mapping*, 28, 785–792.
- Uusitalo, M. A., & Ilmoniemi, R. J. (1997). Signal-space projection method for separating MEG or EEG into components. *Medical & Biological Engineering & Computing*, 35, 135–140.
- Vlahou, E. L., Thurm, F., Kolassa, I. T., & Schlee, W. (2014 May 29). Resting-state slow wave power, healthy aging and cognitive performance. *Scientific Reports*, 4, 5101.
- Wager, T. D., & Smith, E. E. (2003). Neuroimaging studies of working memory: A meta-analysis cognitive, affective, & behavioral. *Neuroscience*, 3(4), 255–274.

- Wechsler, D. (2008a). Wechsler Adult Intelligence Scaled Fourth Edition: Canadian (WAIS-IV CDN). Toronto, Ontario: Pearson.
- Wechsler, D. (2008b). Wechsler Adult Intelligence Scaled Fourth Edition. San Antonio, TX: The Psychological Corporation.
- Wens, V., Bourguignon, M., Goldman, S., Marty, B., Op de Beeck, M., Clumeck, C., et al. (2014 Sep 29). Inter- and intra- subject variability of neuromagnetic resting state networks. *Brain Topography*, 27(5), 620–634.
- Yamashita, M., Kawato, M., & Imamizu, H. (2015). Predicting learning plateau of working memory from whole-brain intrinsic network connectivity patterns. *Scientific Reports*, 5, 7622.
- Zou, Q., Ross, T. J., Gu, H., Geng, X., Zuo, X.-N., Hong, L. E., et al. (2013). Intrinsic resting-state activity predicts working memory brain activation and behavioral performance. *Human Brain Mapping*, 34, 3204–3215. <https://doi.org/10.1002/hbm.22136>.

# Chapitre 3 — Resting-state cortical activity in MEG reveals the neural correlate of executive and phonological complexity of verbal fluency

Victor Oswald<sup>1,2</sup>, Philippe Robaey<sup>1,7,8,9</sup>, Younes Zerouali<sup>3,4</sup>, Aubrée Boulet-Craig<sup>5</sup>, Maja Krajinovic<sup>1</sup>, Caroline Laverdière<sup>6</sup>, Daniel Sinnett<sup>1</sup>, Pierre Jolicoeur<sup>5</sup>, Sarah Lippé<sup>1,5</sup>, Karim Jerbi

5.

<sup>1</sup>*Service hématologie-oncologie, Charles-Bruneau Cancer Center, Sainte-Justine Hospital, Montreal, QC, Canada;*

<sup>2</sup>*Department of Neuroscience, Faculty of Medicine, University of Montreal, Montreal, Qc, Canada;*

<sup>3</sup>*Department of Biomedical Engineering, École Polytechnique de Montréal, Montreal, QC, Canada;*

<sup>4</sup>*Department of Neurology, CHU Notre-Dame Research Center, University of Montreal, Montreal Qc, Canada*

<sup>5</sup>*Department of Psychology, University of Montreal, Montreal, QC, Canada*

<sup>6</sup> *Department of Pediatric, CHU Sainte-Justine Research Center, Montreal, QC, Canada;*

<sup>7</sup> *Department de Psychiatrie, University of Montreal, Montreal, QC, Canada;*

<sup>8</sup> *Children’s Hospital of Eastern Ontario, Ottawa, ON, Canada;*

<sup>9</sup> *Department de Psychiatrie, University of Ottawa, Ottawa, ON, Canada;*

*Article Accepted dans le journal Scientific Reports*

## Abstract

Verbal fluency (VF) is a heterogeneous cognitive function that requires executive functions as well as language abilities. The purpose of this study was to elucidate the specificity of the resting state MEG correlates of the executive and language components. To this end, we administered a VF test, another verbal test (Vocabulary), and another executive test (Trail Making Test), and we recorded 5-min eyes-open resting-state MEG data in 28 healthy participants. We used source-reconstructed spectral power estimates to compute correlation/anticorrelation MEG clusters with the performance at each test, as well as with the advantage in performance between tests, across individuals using cluster-level statistics in the standard frequency bands. By obtaining conjunction clusters between verbal fluency scores and factor loading obtained for verbal fluency and each of the two other tests, we showed a core of slow clusters (delta to beta) localized in the right hemisphere, in adjacent parts of the premotor, pre-central and post-central cortex in the mid-lateral regions related to executive monitoring. We also found slow parietal clusters bilaterally and a cluster in the gamma 2 and 3 bands in the left inferior frontal gyrus likely associated with phonological processing involved in verbal fluency.

Keywords: Executive function, Magnetoencephalography (MEG), Neuronal oscillations, Resting State, Verbal Fluency.

## Introduction

One way to evaluate executive functions is through verbal fluency (VF) testing. In a Verbal Fluency Letter (VFL) test, the participant is instructed to name as many words as possible starting with specific letters (F, A, and S in English), while following several binding instructions. VF is a test widely used in the clinic in order to detect executive impairment, for example to document deficits following traumatic brain injury (Henry & Crawford, 2004b) or neurotoxic treatment in oncology (Boulet-Craig et al., 2018), focal cortical lesions (Henry & Crawford, 2004a), and disease progression in different forms of dementia (Henry et al., 2004; McDonnell et al., 2020; Paek et al., 2020). Among all executive functions, cognitive flexibility, inhibition and processing speed are the best predictors of verbal fluency performance (Amunts et al., 2020).

Executive functions are high-level cognitive processes that control lower-level processes in the service of goal-directed behavior. They include abilities such as response inhibition, interference control, working memory updating, and set shifting. Based on the factorization of different behavioral tests,, the unity and diversity framework describes a common factor related to inhibition and specific factors, such as updating and switching (Friedman & Miyake, 2017; Miyake et al., 2000; Miyake & Friedman, 2012). Executive functioning is often associated with the frontal lobes. A meta-analysis found better executive functions was associated with larger volume and greater thickness in prefrontal cortex (Yuan & Raz, 2014). Functional neural correlates of executive functioning revealed by another meta-analysis has shown a common pattern of activation in the prefrontal, dorsal anterior cingulate, and parietal cortices across executive function domains (Niendam et al., 2012). In general, executive tests appear to be sensitive but not specific for measuring frontal lobe functioning. In other words, other brain regions are needed to perform executive tests. One explanation for this contrast is that executive tests are complex and combine high-level control processes with lower-level non-executive processes that they control. Impairment of these lower-level processes will also affect performance on executive tests. Thus, frontal lobe involvement in virtually any executive process is probably a necessary but insufficient condition for optimal performance (Alvarez & Emory, 2006).

With regard to VF tests in particular, previous neuroimaging and lesioning studies have suggested that they primarily reflect the frontal cortex functioning (Baldo et al., 2006; Paek et al., 2020). Prefrontal cortex volume was correlated with VF in a meta-analysis (Yuan & Raz, 2014). A meta-analysis of coordinate-based activation likelihood estimation (ALE) of brain activation during VF tasks in healthy volunteers showed that the main activation clusters are found in left frontal cortex inferior/middle gyri (BA 6, 9, 44 & 45) and right frontal lobe (BA 44, 47) the left precuneus (BA 7), as well as in bilateral insula (BA 13) and anterior cingulate gyrus (BA 24, 32) (Wagner et al., 2014). Lesions or perturbation studies have reinforced this view. Phonemic word fluency was more severely impaired in patients with lesions in the right frontal lobe than in the left frontal lobe, but lesions in both frontal lobes have shown significant decrease in fluency performance compared to control (Robinson et al., 2012). Cortical modulation excitability of the left dorsolateral prefrontal cortex via transcranial direct current stimulation (tDCS) showed a significant increase in the number of words produced after a letter cue (Ghanavati et al., 2019). Thus, performance in VFL shows great sensitivity to frontal lobe damage and executive functions impairment; this sensitivity is only slightly lower than that of the Wisconsin Card Sorting Task, which is a typical test for executive functions (Alvarez & Emory, 2006).

However, as every executive function test, VFL is a hybrid test, due to its verbal nature. Regression analyses clearly demonstrated the hybrid nature of verbal fluency tests by showing that both executive control abilities (such as working memory updating and inhibition) and verbal abilities (such as vocabulary or lexical access) explained the number of words produced in fluency tasks (Shao et al., 2014). In another study, scores from fluency tasks were entered into an exploratory factorial analysis with the scores of language tests (WAIS Vocabulary subtest and Boston Naming Test) and executive functioning tests (Wisconsin Card-Sorting Test and Trail-Making Test Part B). A two-factor solution was obtained: language tests logically loaded on the language factor, and executive tests loaded on the other executive factor. However, scores of verbal fluency loaded exclusively on the language factor (Whiteside et al., 2016). Among the frontal brain neural correlate of VF, the left inferior frontal gyrus (BA 44, 45) as well as the left premotor cortex (BA 6) are involved in speech production through the well establish language functional network (Hickok & Poeppel, 2007; Indefrey & Levelt, 2004). This raises the question of

whether the frontal lobe functional correlates of verbal fluency are attributed to language or executive function. This question especially arises for the left hemisphere, where language is dominant.

One of the main limitations in studying brain activity of the executive and language component of VF is the difficulty of recording this brain activity while the participants name words. An overt approach produces motion artifacts, whereas a covert approach does not allow for assessment of task performance. It is therefore difficult to generalize conclusions between the overt and covert paradigms. Moreover, the cognitive processes may be different in the two approaches. The same difficulty arises for the baseline condition, which can vary considerably from overt or covert word repetition to a resting state. For this reason, we turned to the resting state magnetoencephalography (MEG) correlation cluster analysis method, as we had previously done on the same group of subjects to map the neural correlates of working memory in the resting state (Oswald et al., 2017). The objective of this study was to distinguish clusters associated with language or executive components of VF on the basis of correlations between MEG activity and performance on executive and/or language tests. In the present study, we first map the resting state neural correlates of Verbal Fluency Letter (VFL) scores. Then we entered the VFL and another neuropsychological test scores into a factor analysis to extract a factor that measures a relative advantage for VFL over this other test. Specifically, we measured the relative advantage for VFL over another verbal test (Vocabulary-VOC), and over another executive test (Trail Making Test-Condition 4- TMT). Using conjunction maps, we identified which clusters among those initially obtained for VFL were associated with better performance for VFL compared to VOC, or compared to TMT, or compared to both. This method using relative comparison with two neuropsychological tests allowed us identifying more specific clusters of VFL. We hypothesize that these correlation clusters could separate executive-related processes from speech production processes. Furthermore, during a task, gamma oscillations increase in the regions recruited by the task due to a neuronal synchronization of local activity, while an inhibition mechanism supported by alpha oscillations increases in non-task specific regions. This raises the question of whether i) the same mechanism is present at rest and ii) whether one of the two is more robust in predicting task performance. As verbal fluency requires a strong language network and



executive possessing, we hypothesis that alpha oscillations will be right dominant and supported by the dorsal stream, while gamma oscillations will be held on the left language network.

## **Method**

### **Participants**

Twenty-eight healthy subjects (13 males and 15 females,  $25.76 \pm 4.84$  years old) with no reported history of neurological or psychiatric disorders took part in this study. The project was reviewed and approved by the University of Montreal and the CHU Sainte-Justine Research Ethics Board. Informed consent was obtained before the experiment and financial compensation was given upon completion of the experiment.

### **Neuropsychological Assessment**

A neuropsychological evaluation was carried out the same day as the MEG recordings. For verbal fluency, we used the Verbal Fluency-letter (VFL) subtest from the Delis-Kaplan Executive Function System (C. Delis et al., 2001). In this test, participants are asked to generate as many words as possible for 60 seconds beginning with a given letter. This test assesses the ability to rapidly generate words by letter, following specific rules: words cannot be repeated, cannot be names or people or places, numbers, or grammatical variants of previous responses. To assess verbal abilities, we used the Vocabulary subtests (VOC) from the Wechsler Adult Intelligence Scale - 4<sup>th</sup> Edition (Wechsler, 2008). In the Vocabulary subtest, participants have to define up to thirty words presented orally by the tester. Participants can define the given word by using synonyms, by its use, a general category to which the word belongs, a clear or primary characteristic, some concrete example of action or causal relationship. Each word is scored 2, 1 or 0, depending on the degree of comprehension of the word. In order to have another measure executive functioning, we use the Trail Making Test Condition 4 (TMT4) from the Delis-Kaplan Executive Function System Trail Making Test (C. Delis et al., 2001) to assess cognitive flexibility. In the condition 4, participants have to draw lines alternating between letters and numbers printed on a page, but in their alphabetical or numerical order as quickly and accurately as they can. The response is scored as completed within the time limit. The three tests did not show any significant correlation between them, VFL and TMT4 ( $r=-.013$ ;  $p=.947$ ), VFL and VOC ( $r=.211$ ;  $p=.282$ ), and TMT4 with VOC ( $r=.350$ ;  $p=.068$ ).

## **MEG and Anatomical MRI Data Acquisition**

All 28 subjects were comfortably seated with eyes open, fixating a back-illuminated screen located 75 cm in front of them. Two 5-minute periods of resting state were recorded at a sampling rate of 1200 Hz, using a CTF-VSM whole head 275-sensor MEG system (MEG core facility, Psychology Department, University of Montreal, QC, Canada). Following standard procedures, third-order gradiometer noise reduction was computed based on twenty-nine reference channels. Bipolar EOG (Vertical EOG and Horizontal EOG) was recorded in order to monitor eye blinks and ocular movements. ECG was also recorded to monitor heartbeats. Three head coils fixed at the nasion and the bilateral preauricular points were used for head localization and were monitored at the beginning and the end of each session. Particular care was taken to ensure that head displacement across sessions remained below 5 mm. The neuropsychological assessments were done in the morning at the Ste-Justine Hospital (Montreal, QC, Canada). Later in the afternoon, the participants went to the MEG facility, located in the Psychology Department of the University of Montreal, for the MEG recordings.

Structural MRI images were obtained for each subject with a 3-T General Electric (GE) scanner (Saint-Justine Hospital, Montreal, QC, Canada). The individual surfaces were used to carry out the co-registration between the MEG fiducial markers (LAP, NAS, RAP) and the MRI structural image. The exact position of the head was refined based on head shape position files obtained using a 3D-localization Polhemus system.

## **Data Pre-Processing**

MEG data pre-processing was performed using the Matlab-based Brainstorm open-source software. The data was first notch filtered at 60 Hz, and then between 0.5 Hz and 120 Hz. Cardiac artefacts, eye blinks, and eye movements were corrected using the Signal-Space-Projection method (SSP). Fifty signal epochs, centred on each artefact, were selected, and a singular value decomposition was applied to each artefact using built-in Matlab functions. Eigenvectors explaining at least 10 % of the variance of the artefacts were discarded and the remaining eigenvectors were used to define the SSP. The SSP method relies on a signal space decomposition procedure, where the statistical characteristics of the measured signals are used to determine

the two subspaces spanned by the MEG brain signals and the unwanted artifacts, respectively. Projecting the continuous MEG data onto the signal subspace effectively removes the components belonging to the artifact subspace.

## **MEG Sources Estimation**

MEG source reconstruction was performed using a standard weighted minimum-norm approach, with the Brainstorm software. T1-weighted brain volumes were acquired in all participants and were used to generate a cortical surface model, using the FreeSurfer software package. Forward modelling of the magnetic field was defined based on an overlapping-sphere method. The weighted minimum norm solution was computed using a loose dipolar orientation constraint (set at 0.5), a signal-to-noise ratio of 3, whitening PCA and a depth weighting of 0.5. The noise covariance matrix for each participant was estimated from a 2 min empty room recording performed earlier the same day (same acquisition parameters but with no subject in the shielded room), the source time series were initially reconstructed on a 15000-vertex individual brain tessellation, and then spatially interpolated to the MNI ICBM152 brain template and down-sampled to a 10000-vertices template.

## **Spectral Power Analysis**

Resting-state power spectral density (PSD) was measured using the modified Welch periodogram technique (1-s Hamming window and 50 % time-window overlap). The mean PSD for each frequency band of interest was obtained for each subject by averaging the PSD values across the frequency bins of each band. Power estimates were computed for all elemental cortical sources and all participants in the following frequency bands: Delta (1–4 Hz), theta (4–8 Hz), alpha (8–13 Hz), beta (13–30 Hz), gamma 1 (30–60 Hz), gamma 2 (60–90 Hz) and gamma 3 (90–120 Hz). Next, for each participant, the PSD values (i.e. oscillatory power) were standardized using a z-score transformation (computed at each vertex using the mean and standard deviation of the power values across all vertices within the same frequency band).

## Correlation Analyses and Cluster-Level Statistics

A correlation analysis was carried out to probe the putative relationship across individuals between spontaneous brain oscillation power (separately for each frequency band) and neuropsychological tests and factors scores (see below).

The computation and assessment of correlation were achieved via a two-step procedure. First, the Pearson correlation coefficients were computed between resting-state power (z-scores) at each cortical vertex and scores from the neuropsychological tests. Next, the statistical significance of the correlation results was evaluated using t-statistics and nonparametric cluster-wise correction for multiple testing. More specifically, the correlation was computed using MATLAB's built-in *corrcoef* function at each cortical node (vertex), for each frequency band and each subject (n=28).

In addition to computing the Pearson correlation coefficient, the correlation function also returns p-values obtained by transforming the correlation to create a t-statistic with n-2 degrees of freedom. Setting the threshold for the first-level statistical significance to  $p < 0.05$  (uncorrected) provides a spatial mask in source space.

Next, within this mask (i.e. significant correlation coefficients, uncorrected), we determined clusters of spatially contiguous (neighbouring) vertices, which were identified based on the FreeSurfer adjacency matrix. The correlation coefficients within each cluster were then added up, in order to obtain a cluster mass (cluster mass statistics).

To assess the statistical significance of the obtained clusters, we used nonparametric permutation testing. We randomly shuffled the subjects' neuropsychological scores, while keeping the MEG source power data across subjects intact. This essentially creates random associations that destroy any putative correlation between the two types of observations. Using 1000 permutations of the data (and replicating the cluster mass computation described above for each set of permuted data) provides for an estimate for the null distribution against, which we then allows for testing the significance of the truly observed clusters in the original data.

Statistically significant correlation clusters at  $p_{\text{corr}} < 0.001$  were then defined as those with a cluster mass larger than the correlation value ranked 999 on the null distribution. By choosing such a restrictive significance threshold (i.e.  $p < 0.001$ ), not only do we minimize the type-I errors, but we also ensure that the reported results would remain significant—for instance, at a level of  $p < 0.05$ , accounting for up to 50 multiple tests—based on a regular Bonferroni correction. In other words, all our results remain significant at  $p < 0.05$  if we correct for tests across all frequency bands, and all the WAIS-IV subtests and indices used (as the number of comparisons does not exceed 50).

The results reported here are therefore statistically significant at  $p < 0.001$  levels, corrected across space, for each frequency band and neuropsychological test, but they are all also significant at  $p < 0.05$  when corrected for comparisons across space, frequency bands, and subtests.

## **Steps for conjunction analysis**

**In order to differentiate verbal component and executive to the complex and sparse neural correlates of verbal fluency, we used a three-step method illustrated in Figure 1.**

### Step 1: Cluster analyses with individual scaled tests scores

This first step was to perform the cluster-level analysis of brain-test score correlation and anticorrelation patterns for each test (i.e. VFL, TMT4 and VOC). Figure 2 shows spatial distribution of correlation clusters between resting state source-space MEG power and scores on the VFL test; the correlation clusters obtained with VOC and TMT4 scores are presented in supplementary material (Figure S1 and S2 respectively).

### Step 2: Cluster analyses with factor loadings combining test scores

In this second step, we first entered the scores of VFL and VOC in a principal analysis component (PCA). The scores in both tests depend on verbal responses. In VOC, the subject is asked to give the meaning of words and the score (0, 1 or 2) reflects the comprehension of the word as well as the precision and the clarity of the response. In VFL, the subject has to say in 60 sec as many words as possible starting with a specific letter while complying with a set of rules (words cannot be repeated, be names or people or places, numbers, or grammatical variants of previous responses.). The difference between VFL and VOC scores reflects a relative advantage in lexical

access and word production monitoring over word knowledge and verbal concept formation, in other terms the relative advantage in executive over semantic abilities, both in the language domain. Due to the correlation between scores their difference are relatively unreliable (Caruso, 2001). Therefore, we decomposed their variance using a principal component analysis (PCA), which by construction yielded two factors. One factor is correlated with the average scores between the tests while the other factor is correlated with their difference, but the individual loadings are more reliable than averages or differences between scores. The first factor (F1-VOC) represented 60.5 % of the total variance, while the second factor (F2-VOC) 39.5%. F1-VOC was highly and equally correlated with both the VFL and the VOC scaled scores ( $r = .778$ ;  $p < .001$ ), and with their mean scores ( $r = .928$ ;  $p < .001$ ). F2-VOC was also equally correlated with both tests, but in opposite directions:  $r = .628$ ;  $p < .001$  with VFL, and  $r = -.628$ ;  $p < .001$  with VOC. As a consequence, this factor was highly correlated with the difference between the VF and VOC scores ( $r = .846$ ;  $p < .001$ ). Then we computed the MEG clusters with positive and negative correlations with the individual factor loadings on the difference factor (F2-VOC), which for positively correlated clusters reflect a better performance in VFL than in VOC. Results also presented in the supplementary figure S3.

We used the same approach for VFL and TMT4. In both tests, the subject had to produce and monitor a sequence of actions. In VFL, the subject had to self-generate a series of words while monitoring the compliance with a set of rules. In TMT4, the subject had to draw lines alternating between letters and numbers printed on a page, in their alphabetical or numerical order. During the production of a sequence of responses, the difference between VFL and TMT4 scores reflects a relative advantage in lexical access in long-term memory while checking for compliance with a set of rules over attention to external cues using two overlearned orders and switching between them. In this PCA, the first factor (F1-TMT) represented 50.6 % of the total variance, while the second factor (F2-TMT) 49.3%. F1-TMT was equally correlated with both tests, but in opposite directions:  $r = .712$ ;  $p < .001$  with TMT4, and  $r = -.712$ ;  $p < .001$  with VFL. F2-TMT was also correlated with the difference between VFL and TMT4 scores ( $r = .94$ ;  $p < .001$ ). F2-TMT was highly and equally correlated with both the VFL and the TMT4 scaled scores ( $r = .702$ ;  $p < .001$ ), and with their mean scores ( $r = .702$ ;  $p < .001$ ). We computed the MEG clusters with positive and negative correlations

with the individual factor loadings on the difference factor (F2-TMT), which for positively correlated clusters reflect a better performance in VFL than in TMT4. Results also presented in the supplementary figure S4.

### Step 3: Conjunction analysis

Finally, in order to compare the pattern obtained with the two difference factors (F2-VOC and F1-TMT) and the initial pattern of VFL, the third step was to compute conjunction maps of cluster correlations.

To this end, we computed the overlap between each vertex (10003) across each frequencies band (70). We compute three conjunction maps. For the first map (Conjunction 1), we used the clusters that correlated both positively with VFL in F2-VOC (Fig. S3) and with VFL scores in the initial pattern. For the second map (Conjunction 2), we used the clusters that correlated both positively with VFL in F1-TMT (Fig. S4) and with VFL scores in the initial pattern. For the third map (Conjunction 3), we computed the conjunction between conjunction 1 and conjunction 2. Conjunction 1 and Conjunction 2 are respectively presented in figures 3 and 4, and Conjunction 3 in figure 5.



## Results

### Verbal Fluency Letter (initial brain behaviour pattern)

Figure 2 presents the brain behaviour neural pattern correlation/anticorrelation. The lateral face shows correlation clusters in parietal, sensorimotor and frontal regions on the right for lower frequency bands (delta to beta range), as well as in the same regions on the left for high frequency bands (gamma 2 and 3 bands). Specifically, on the right side, we found clusters in the superior parietal (delta to beta range); in the inferior parietal (theta band) lobe; in the postcentral and precentral gyri (delta, alpha and beta bands); and in the caudal part of the superior frontal (delta and alpha bands) as well in the caudal middle frontal gyri (delta, alpha and beta bands). On the left side, we detected clusters in the superior parietal (gamma 2 band) and the supramarginal (gamma 2 and 3 bands); in the postcentral (gamma 2 and 3 bands) and precentral (gamma 3 band); and in the caudal (gamma 2 and 3 bands) and rostral (gamma 3 band) middle frontal gyri.

On the medial hemispheres, the correlation clusters were mostly bilateral in the paracentral lobule (delta, alpha and beta bands), the precuneus (theta band), and the rostral superior frontal gyrus (delta to beta range). Additional clusters were observed in the left precuneus (theta band), in the left rostral anterior cingulate (delta and beta bands). Anticorrelation clusters were fewer and mostly found on the left temporal/occipital areas: in the middle temporal (delta to beta range), inferior temporal (alpha band) and lateral occipital (beta, gamma 1 and 2 bands) cortex. Medial anticorrelation clusters were also observed in the isthmus cingulate in the right (alpha and beta band) and left (alpha, beta and gamma 2 bands) hemispheres.

### Conjunction 1

Conjunction 1 (figure 3) maps analysis shows clusters between factors (F2\_VOC) and the initial pattern of VF. These clusters were found in the right premotor in delta alpha and beta band, in the caudal part of right pre- and post-central gyrus, in the right dmPFC in theta to beta band, in the left inferior dorsolateral in gamma 3 band, in the left anterior cingular in delta and beta band, and also in the left dmPFC theta to beta band.

## **Conjunction 2**

Conjunction 2 (figure 4) map analysis shows clusters between factors (F1\_TMT) and the initial pattern of VF. These clusters were found in the right superior parietal lobule in delta to alpha band, in the right post dorsal part of pre-central gyrus in the delta, alpha and beta band, in the right premotor in alpha and beta band, in the right caudal part of post-central gyrus in alpha band, in the bilateral paracentral lobule in delta and alpha band and only on the left side in the beta band, in the bilateral precuneus in theta band and right side for alpha band in the left angular, post central in gamma 2 and 3, in the left superior parietal lobule in gamma 2 band and in the left premotor in gamma 3 band.

## **Conjunction 3**

The result of conjunction 3 map analysis (figure 5) shows clusters only in the right hemisphere, with clusters found in the caudal part of the pre- and post-central gyrus as well as in the premotor gyrus in alpha band. Another cluster in the delta band was found more dorsal in the premotor cortex; a cluster overlapping alpha and beta was also found in the same area, in the right premotor cortex.

## Discussion

The aim of this study was to provide the resting state MEG correlates of verbal fluency. Our results revealed a complex correlation pattern showing bilateral fronto-parietal clusters, right dominant in slow oscillations (delta to beta bands) and left dominant in highest oscillations frequency (gamma 2 and 3 bands). Anticorrelation clusters were also found in the left hemisphere temporal and occipital regions, in the right isthmus cingulate. Our results are in line with previous results report obtained during task-based approach of verbal fluency: similar activation was found in the left IFG/MFG (BA 6, 9, 44 & 45), the left precuneus (BA 7), and bilateral anterior cingulate gyrus (BA 24, 32). However, we did not find the right frontal lobe (BA 44, 47) nor the bilateral insula (BA 13) whereas we did find additional clusters in the bilateral motor cortex with paracentral lobule (BA 4), in the right premotor (BA 6, 8) and bilateral post central gyrus (BA 1, 2, 3) (Wagner et al., 2014). MEG fields are induced by synchronized neuronal currents, caused by synaptic transmission. Our results show that EEG/MEG power at rest may be correlated with performance during a test for different cortical sources and frequency bands.

Our results demonstrate inter-individual differences in spontaneous brain activity in MEG. These differences arise from local oscillatory activity and seem to reflect a large-scale organization of brain dynamics. Previous work in fMRI and more recent work in electrophysiology has shown that this brain organization is a stable and discriminating feature across several demographic characteristics (age, clinical conditions, gender etc...)(XX). Our previous study (Oswald et al, 2017), this results and other work (X) support the idea that oscillatory resting state neural activity should be consider as a brain trait which target a relationship between this activity and cognition performance. If resting state oscillatory neural organization plays a role in the deployment of cognitive functions, then some organization (here level of resting power) would favor cognitive performance compared to others. Furthermore, our approach allows us to isolate among resting state oscillatory neural organization, spatial-frequential patterns specific to verbal fluency compared to others cognitive functions (i.e. verbal vs. non-verbal, executive vs. non-executive). The clusters of cortical sources where the resting MEG power correlates with the scores on a specific test reveal a spatial-frequency unit in the brain regions associated with the competence assessed by the test. However, one should not expect that all regions actually

activated in a task will yield resting state MEG clusters, and vice versa, all clusters found in resting state pattern will play a role during active task because these two brain states can share some common spatial-frequency pattern or not. Interindividual difference related to oscillatory brain traits can be different according to the brain state, for example in the case where compensative brain mechanism was recruited to achieve a task, or distinct strategies support by distinct brain oscillatory mechanism to achieve a similar task. Moreover, some of these regions may give rise to resting state MEG clusters but are not specific enough, activated in other processes, and subtracted from a closely matched control task in task-based brain imaging. In the resting-state MEG cluster approach, the relationship between inter-individual differences in test scores and in relative power at different cortical sources must fit a defined function (e.g., linear) for these clusters in the sample of subjects to be observed. These differences could account for discrepancies between resting states clusters and regions activated in tasks. Nevertheless, resting state clusters can complement the activity patterns and are relevant to provide a new perspective on the set of regions activated in VFL.

With conjunction 1, we aimed at identifying among the initial VFL clusters those accounting for a better performance in VFL as compared to VOC, thus for a relative advantage in executive over semantic abilities. A first group of clusters was found in the right premotor, motor and dorsolateral prefrontal cortex in the slow bands, most clearly in the alpha band. In early studies of executive function localization (Stuss, 2011; Stuss & Alexander, 2007), right lateral brain lesions, including the dorsolateral prefrontal cortex (BA9/46), thus overlapping some conjunction 1 clusters, had been linked to a deficit in monitoring ongoing performance in different executive tasks. This suggests that the relative advantage in executive abilities over semantic abilities is likely in monitoring verbal production. The second set of clusters was found in the dorsomedial prefrontal cortex, specifically in the bilateral rostral superior frontal and left rostral and caudal anterior cingulate, also in the slow frequency bands. This localization is consistent with lesions observed in patients whose performance deficits in various tasks have been described as an energization failure (Stuss, 2011; Stuss & Alexander, 2007). These patients showed lesions in superior medial cortex, primarily in BA areas 24, 32, 9, and 6. In the VFL task, these patients showed a marked decrease in the number of words in the last 45 seconds, compared with the

first 15. This failure to energize is thus one of initiation and maintenance of performance. Moreover, these clusters are found in the alpha (8–13 Hz) and beta (13–30 Hz) oscillations, which are known to support inhibition mechanism (Klimesch, 2012; Klimesch, Sauseng, & Hanslmayr, 2007), which may be required to for maintenance of performance. These two clusters (right frontal lateral and dorsomedial frontal) correspond to the dual control network hypothesis (Dosenbach et al., 2007). The fronto-parietal network is optimized for rapid adaptive control and the other cingulo-opercular for stable set-maintenance. It also fits with the conjunction analyses across different executive functions (flexibility, inhibition and working memory), which also reveal activation in dorsolateral prefrontal (BAs 9, 46) and anterior cingulate (BA 32) cortex (Niendam et al., 2012). However, contrary to Wagner's et al (2014) previous meta-analysis, we did not find any parietal clusters in this conjunction 1.

The last set of clusters in conjunction 1 was found in the left inferior frontal gyrus (BA 44) in the gamma band. In phonemic and semantic verbal fluency tasks, activation in the left inferior frontal gyrus overlapped the same regions (BA 9, 45), but BA 47 appeared in the semantic condition, and BA 44 in the phonemic condition only (Wagner et al., 2014). This left inferior frontal gyrus was found in gamma band (90–120 Hz). Gamma band oscillations have been observed during word production and auditory perception. They reflect synchronized firing of neuronal assemblies and task-related cortical activation. Using electro-corticography (CoG), an increase in gamma range (70–120 Hz), activity was also observed continuously in the inferior frontal gyrus starting 500 msec prior to the onset of syllable-articulation and stopping at vocalization. The gamma-augmentation may thus be predominantly driven and/or monitored phonological processing (Brown et al., 2008).

We first discussed, the conjunction 1 clusters that correlated positively both with the VFL scores and with the individual factor loadings on the difference factor, and reflected an advantage in executive over semantic abilities. We also found clusters that were positively correlated with vocabulary scores (Figure S1) but negatively correlated with individual factor loadings of the difference factor. They reflected an advantage of semantic abilities over executive abilities, (Figure S3) and appeared to constitute a semantic knowledge network. These clusters were found for the low frequency bands in the left lateral temporo-parietal region: in the transverse, superior

and middle temporal gyri, the inferior parietal and supramarginal gyri, the post-central gyrus as well as in the lateral occipital regions. According to the “embodied” view of semantic information, a word is associated with different representations of an object, for example how it looks like, or how it is used. The meaning of a word is then based on a network of visual, auditory, somato-motor representations. These widely distributed regions, and the various connections between them, constitute the semantic network (Barsalou, 1999, 2008; Martin, 2007; Pulvermuller, Hauk, Nikulin, & Ilmoniemi, 2005). Semantic representations can be based on different types of relations (Mirman, Landrigan, & Britt, 2017). For example, similarity can use shared features (taxonomic, e.g. coat for dog-bear), or contiguity which relies on the co-occurrence in events or scenarios (thematic, e.g., dog - leash). By performing voxel-based lesion-symptom mapping on taxonomic and thematic errors separately in individual with poststroke aphasia, thematic errors were located in the left temporoparietal junction, and taxonomic errors in the left anterior temporal lobe (Schwartz et al., 2011). The left temporo-parietal junction, where thematic knowledge has been proposed to be grounded, is the core of the F2 anticorrelation clusters we found. The temporo-parietal region (especially the posterior middle temporal cortex and the inferior parietal lobule) might be involved in mental simulation of events, or re-enactement of the subject’s own perceptual and motor experience. Using a picture matching task in which participants had to identify taxonomic and thematic relations between objects thematic processing specifically recruited a bilateral temporo-parietal network including the inferior parietal lobules and middle temporal gyri (Kalénine et al., 2009). The clusters we found also include postcentral and occipital regions, which is consistent with the role of visual and sensorimotor regions in visuo-motor processes supporting thematic representations. In sum, the stronger the traces left by language experience in this thematic semantic network, the better the individuals perform in the Vocabulary test. Relying on the thematic semantic network would optimize the score at Vocabulary as participants can define the given word by using synonym, by its use, a clear characteristic, some concrete example of action or causal relationship, and not necessarily by providing a general or more abstract category to which the word belongs.

Going back to the VFL correlation clusters, Conjunction 2 has two main differences from conjunction 1. The first difference was in slow frequencies, with bilateral clusters in the precuneus

and paracentral lobule, and in the right superior parietal lobe. At the same time, clusters in the bilateral dorsomedial frontal cortex and in the right superior frontal gyrus disappeared. The second difference were additional gamma clusters in the left parietal, sensory-motor and premotor regions. These changes in resting state activity account for an advantage for VFL over TMT, as compared to VOC. VFL and TMT mainly assess two different executive functions, fluency and flexibility, and differ mainly on two aspects. First, VFL requires the production of a verbal sequence, whereas TMT requires an eye-hand coordinated sequence. Second, in VFL the subject must keep in memory the entire verbal sequence as it is spoken to check that it conforms to a set of rules (first letter of the word, no repetition, etc.), but without following a pre-established order. On the other hand, in the TMT, the subject must follow a pre-established sequence (the alphabetical and numerical orders), and switch between them, but without keeping in memory the entire sequence since the test sheet provides a visual support. We suggest that the changes in predominantly right parietal slow oscillations may reflect the fact that the subject must pay attention to items in episodic memory (a form of working memory) during the fluency task. On the other hand, larger left frontal gamma clusters may be attributed to the speech production itself.

According to the attention-to-memory model, the dorsal parietal cortex is most active when top-down monitoring of memory content is maximal (Cabeza, 2008). The dorsal parietal cortex corresponds approximately to BA7 and includes the superior parietal lobule, but also the precuneus and part of the paracental lobule. The additional parietal clusters in conjunction 2 may therefore correspond to top-down attentional processes in accordance with internal goals as per VFL instructions, and thus account for an advantage in performance in VFL over TMT, as compared to VOC. The presence of a medial parietal structure (precuneus) in the slow oscillation clusters is likely related to the fact that the task requires the subject to monitor his or her own verbal output, given that the precuneus supports the recall of memories from a first-person perspective (Cavanna & Trimble, 2006; Fretton et al., 2014). The dorsal parietal cortex is part of a dorsal frontoparietal pathway that includes the midlateral prefrontal cortex and enables the selection of internal goals and links them to appropriate responses (Nee et al., 2013). The absence of dorsomedial prefrontal clusters which were present in conjunction 1 may reflect the fact that the

energization component of executive functioning is no longer an advantage for VFL when comparing with TMT over VOC, as initiation and maintenance of performance is greatly helped in TMT by the availability of the test sheet with the different letters and numbers to connect.

The rapid oscillatory cluster on the left corresponds with the word production sequence, from the left phonological store (i.e. left supramarginal gyrus) and then to pre-motor for the syllabification and ending in the pre-central gyrus for articulation (Indefrey & Levelt, 2004). Moreover, this cluster is found in the gamma bands, gamma 2 (60–90 Hz) and gamma 3 (90–120 Hz). As described previously, the gamma band were found in the left pre-central gyrus after onset of vocalization process (Brown et al., 2008) and reflects local synchronized firing of neuronal assemblies.

Finally, the conjunction 3 (fig 5) shows the overlap between conjunction 1 and conjunction 2, highlighting a set of anterior frontal clusters related to the executive monitoring process and a set of more posterior frontal clusters related to phonological sequence implementation. Conjunction 3 thus reflects regions that must coordinate activity in order to perform in the fluency task. This overlap is localized in the right hemisphere, in adjacent parts of the premotor, pre-central and post-central cortex in the mid-lateral regions. Previous lesions study shown these regions are implicated in monitoring and control of speech production (Stuss & Alexander, 2007).

To conclude, we first showed a complex set of correlation clusters, for the slow frequencies, in the right parietal and frontal regions, and in the bilateral medial frontal regions, bilateral paracentral and precuneus, as well as anticorrelation clusters in the left medial temporal lobe. By examining which of these clusters were related to a relative advantage in VFL as compared to two other tests (one verbal and one executive), we retained the core clusters of VFL. These core clusters clearly present verbal fluency as an executive test, related to word production and performance monitoring. Despite the verbal nature of verbal fluency, these clusters were located in the right hemisphere, which seems to reflect right-hemisphere dominance for executive control of attention (Spagna, Kim, Wu, & Fan, 2020). This study confirms the value of the cluster analysis method based on correlations between resting MEG and cognitive skills, such as working memory or verbal fluency.



These results and this method require replication and further internal and external validation. The sample was small and susceptible to sampling bias effects. As MEG temporal dynamics mainly include oscillatory and non-oscillatory ( $1/f$  noise-like) brain activities, the nature of the correlation needs to be elucidated. Although we have observed correlation clusters for various cognitive abilities (working memory, verbal fluency, and vocabulary), it is not known which other cognitive skills may generate such clusters. It is also not known whether differences in performance beyond the normal range can be detected by MEG clusters at rest, or whether other than linear functions should be used. This approach of cluster analysis is thus nascent, and requires much further research, but may have great potential.

## Figures

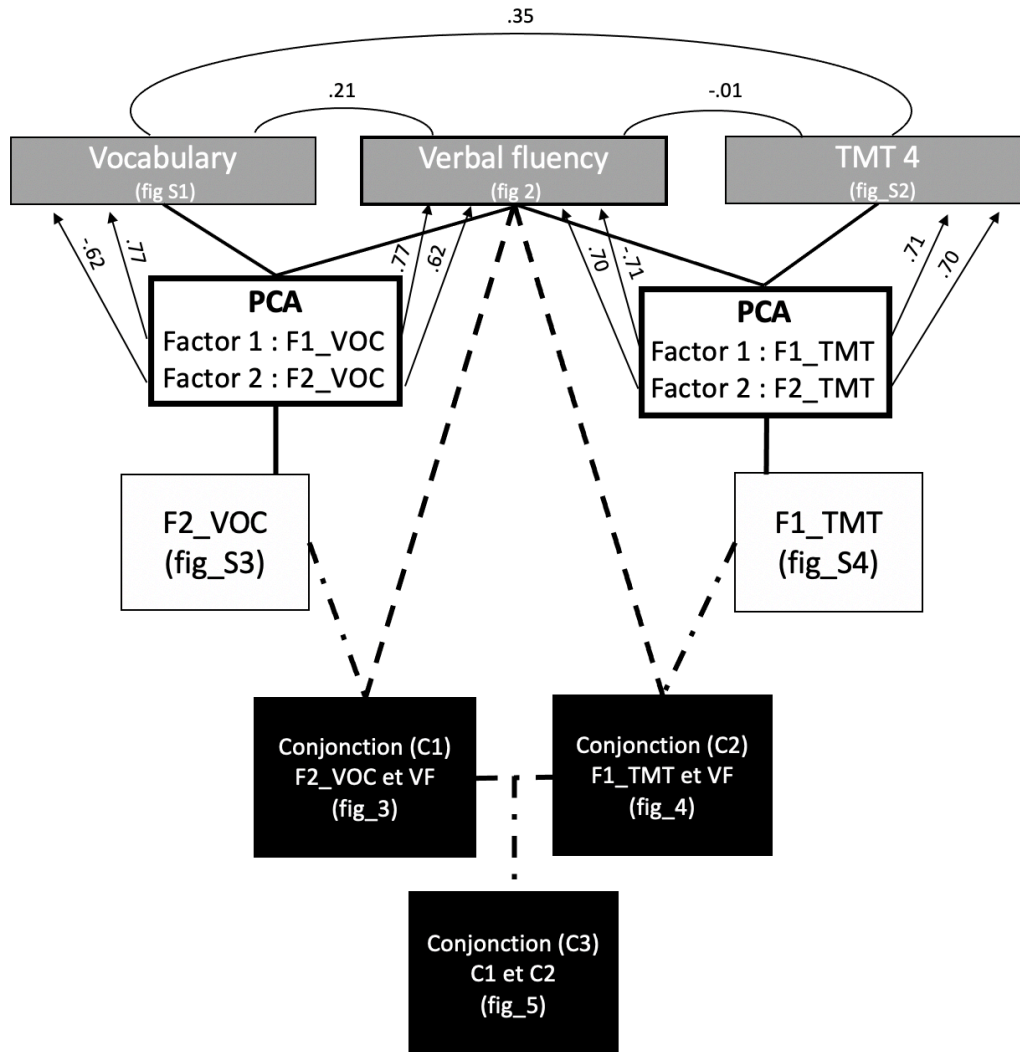


Figure 20. – Figure 1: Schema showing the 3 steps methods used to explore relative specificity and different neural correlates of verbal fluency. The first step is to perform brain-behavior correlation/anticorrelation pattern between rsMEG power and each neuropsychological test independently (VOC, VF, TMT4). The second step consists of factorizing Voc and VF and TMT4 and VF, from this factorization brain-behavior correlation/anticorrelation pattern was performed with residual regression from F2\_VOC and F1\_TMT. The third step was to make conjunction maps between F2\_VOC & VF (conjunction 1) and F1\_TMT & VF (conjunction 2). Conjunction 3 is the overlapping cluster between conjunction 1 & conjunction 2.

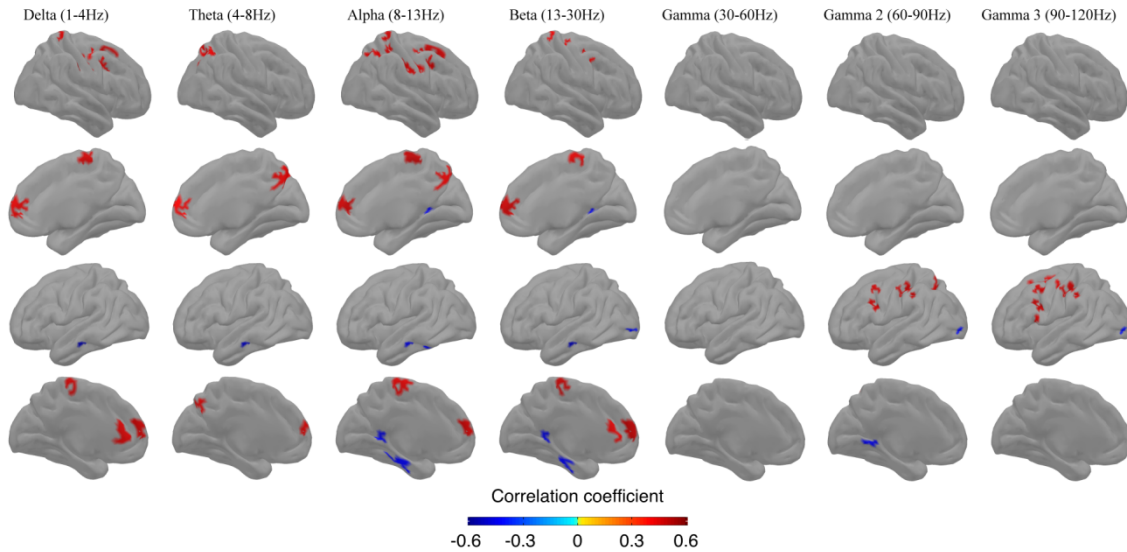


Figure 21. – Figure 2: Spatial distribution of clusters with statistically significant correlations ( $p < .001$ ) between resting MEG source-space power (z-scores across vertices) and neuropsychological performance on the **Verbal Fluency** test. Each column shows the significant correlations for a given range of frequencies, in both hemispheres (right lateral and medial view, followed by left lateral and medial views). The results are corrected across space using cluster-level corrections. All results remain significant at  $p < .05$ , correction for multiple comparisons across space and frequency bands.

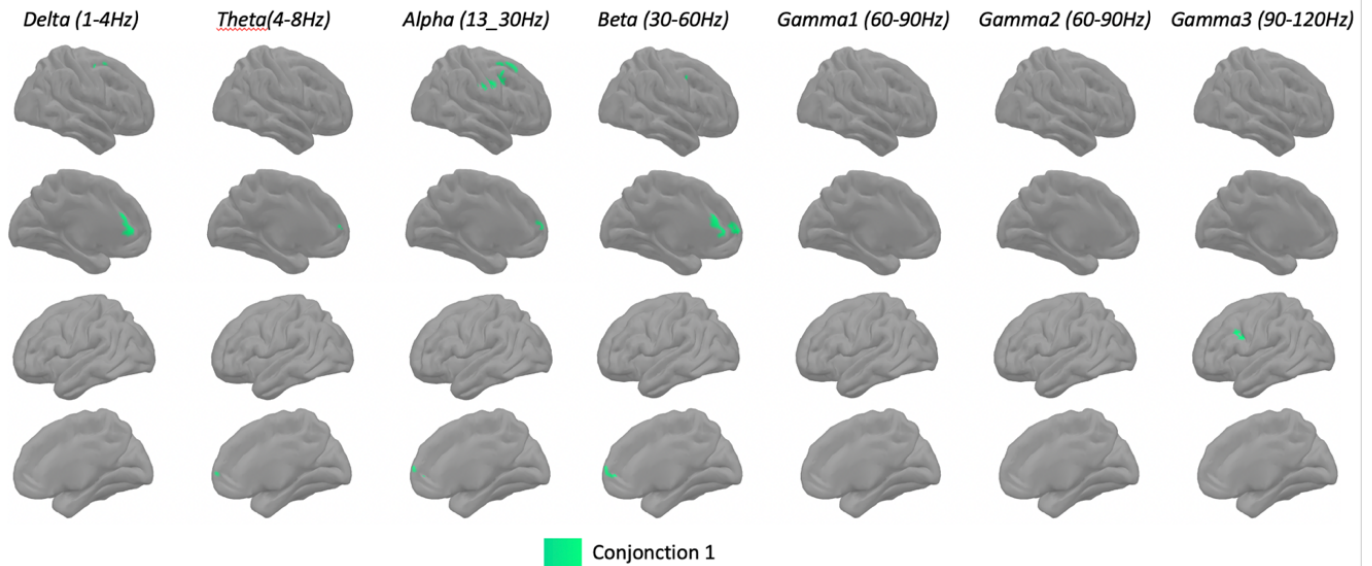


Figure 22. – Figure 3: Spatial distribution of clusters with statistically significant correlations ( $p < .001$ ) in resting MEG source-space power (z-scores across vertices) on the **Conjunction 1**. Each column shows the significant correlations for a given range of frequencies, in both hemispheres (right lateral and medial view, followed by left lateral and medial views). The results are corrected across space using cluster-level corrections. All results remain significant at  $p < .05$ , correction for multiple comparisons across space and frequency bands.

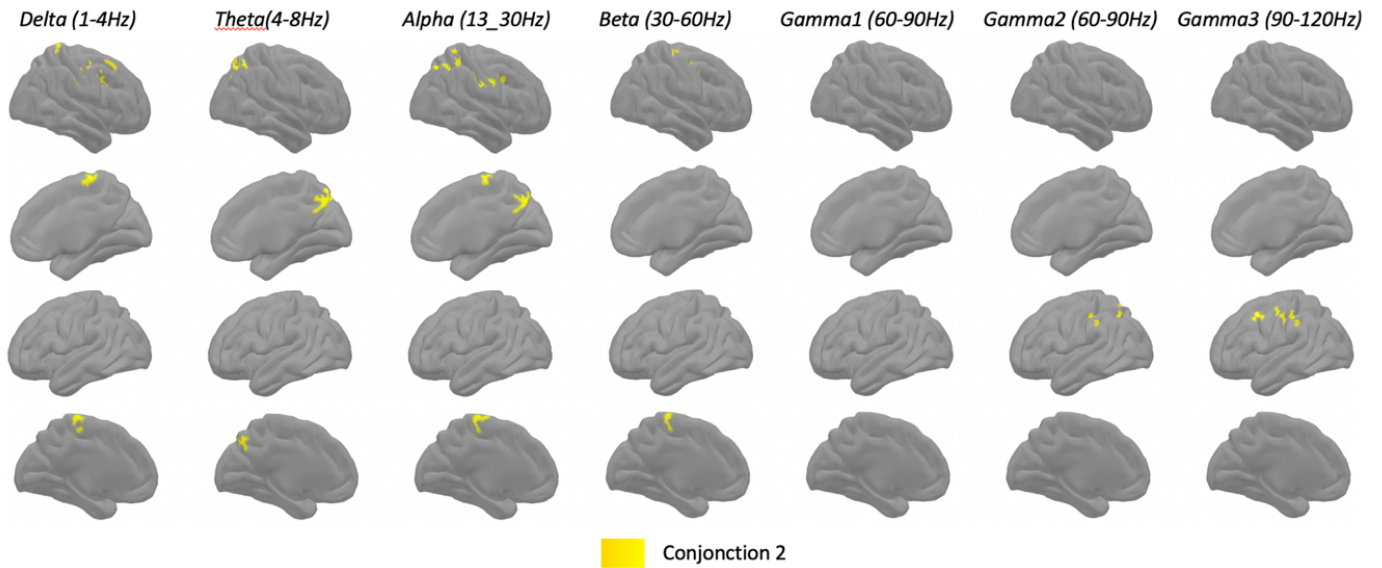


Figure 23. – Figure 4: Spatial distribution of clusters with statistically significant correlations ( $p < .001$ ) in resting MEG source-space power (z-scores across vertices) on the **Conjunction 2**. Each column shows the significant correlations for a given range of frequencies, in both hemispheres (right lateral and medial view, followed by left lateral and medial views). The results are corrected across space using cluster-level corrections. All results remain significant at  $p < .05$ , correction for multiple comparisons across space and frequency bands.

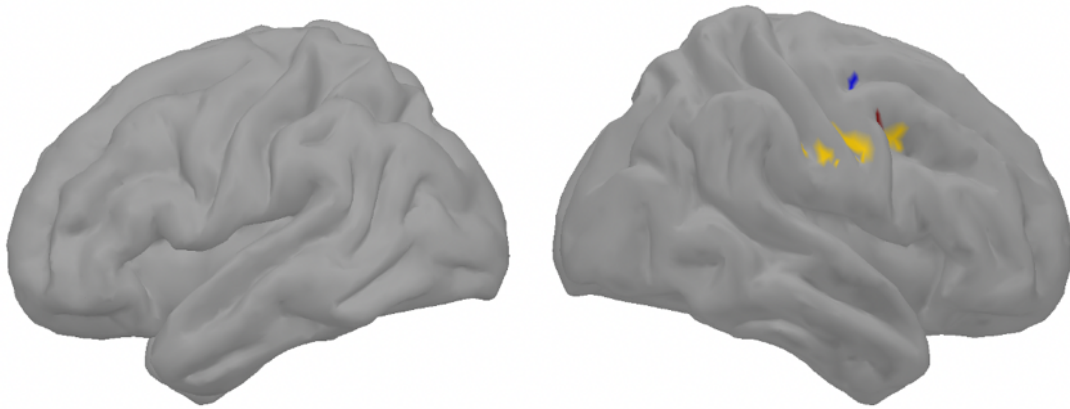


Figure 24. – Figure 5: Spatial distribution of clusters with statistically significant correlations ( $p < .001$ ) in resting MEG source-space power (z-scores across vertices) on the **Conjunction 3**. Spatial frequencies are described as following: delta band (1–4 Hz) in blue, alpha band (8–13 Hz) in yellow, clusters found in both (alpha (8–13 Hz) band and beta (13–30 Hz) band) are in red.

## References

- Alvarez, J. A., & Emory, E. (2006). Executive function and the frontal lobes: A meta-analytic review. *Neuropsychology Review*, *16*(1), 17–42. <https://doi.org/10.1007/s11065-006-9002-x>
- Amunts, J., Camilleri, J. A., Eickhoff, S. B., Heim, S., & Weis, S. (2020). Executive functions predict verbal fluency scores in healthy participants. *Scientific Reports*, *10*(1), 1–11. <https://doi.org/10.1038/s41598-020-65525-9>
- Baldo, J. V., Schwartz, S., Wilkins, D., & Dronkers, N. F. (2006). Role of frontal versus temporal cortex in verbal fluency as revealed by voxel-based lesion symptom mapping. *Journal of the International Neuropsychological Society*, *12*(6), 896–900. <https://doi.org/10.1017/S1355617706061078>
- Barsalou, L. W. (1999). Perceptual symbol systems. *Behav Brain Sci*, *22*(4), 577-609; discussion 610-560.
- Barsalou, L. W. (2008). Grounded cognition. *Annu Rev Psychol*, *59*, 617-645. doi:10.1146/annurev.psych.59.103006.093639
- Boulet-Craig, A., Robaey, P., Laniel, J., Bertout, L., Drouin, S., Krajinovic, M., Laverdière, C., Sinnett, D., Sultan, S., & Lippé, S. (2018). DIVERGT screening procedure predicts general cognitive functioning in adult long-term survivors of pediatric acute lymphoblastic leukemia: A PETALE study. *Pediatric Blood and Cancer*, *65*(9), 1–9. <https://doi.org/10.1002/pbc.27259>
- Brown, E. C., Rothermel, R., Nishida, M., Juhász, C., Muzik, O., Hoechstetter, K., Sood, S., Chugani, H. T., & Asano, E. (2008). In vivo animation of auditory-language-induced gamma-oscillations in children with intractable focal epilepsy. *NeuroImage*, *41*(3), 1120–1131. <https://doi.org/10.1016/j.neuroimage.2008.03.011>
- Cabeza, R. (2008). Role of parietal regions in episodic memory retrieval: The dual attentional processes hypothesis. *Neuropsychologia*, *46*(7), 1813-1827. doi:<https://doi.org/10.1016/j.neuropsychologia.2008.03.019>
- C. Delis, Kaplan, E., & Kramer, J. H. (2001). Delis Kaplan Executive Function System. San Antonio, TX. *The Psychological Corporation*.
- Corbetta, M., Patel, G., & Shulman, G. L. (2008). The Reorienting System of the Human Brain: From Environment to Theory of Mind. *Neuron*, *58*(3), 306–324. <https://doi.org/10.1016/j.neuron.2008.04.017>
- Caruso, J. C. (2001). Increasing the Reliability of the Fluid/Crystallized Difference Score from the Kaufman Adolescent and Adult Intelligence Test with Reliable Component Analysis. *Assessment*, *8*(2), 155-166. doi:10.1177/107319110100800204
- Cavanna, A. E., & Trimble, M. R. (2006). The precuneus: a review of its functional anatomy and behavioural correlates. *Brain*, *129*(3), 564-583. doi:10.1093/brain/awl004
- Dosenbach, N. U., Fair, D. A., Miezin, F. M., Cohen, A. L., Wenger, K. K., Dosenbach, R. A., . . . Petersen, S. E. (2007). Distinct brain networks for adaptive and stable task control in humans. *Proc. Natl. Acad Sci. U. S. A*, *104*(26), 11073-11078.

Freton, M., Lemogne, C., Bergouignan, L., Delaveau, P., Lehericy, S., & Fossati, P. (2014). The eye of the self: precuneus volume and visual perspective during autobiographical memory retrieval. *Brain Structure and Function*, *219*(3), 959-968. doi:10.1007/s00429-013-0546-2

Friedman, N. P., & Miyake, A. (2017). Unity and diversity of executive functions: Individual differences as a window on cognitive structure. *Cortex*, *86*, 186–204. <https://doi.org/10.1016/j.cortex.2016.04.023>

Ghanavati, E., Salehinejad, M. A., Nejati, V., & Nitsche, M. A. (2019). Differential role of prefrontal, temporal and parietal cortices in verbal and figural fluency: Implications for the supramodal contribution of executive functions. *Scientific Reports*, *9*(1), 1–10. <https://doi.org/10.1038/s41598-019-40273-7>

Hampshire, A., Chamberlain, S. R., Monti, M. M., Duncan, J., & Owen, A. M. (2010). The role of the right inferior frontal gyrus: inhibition and attentional control. *NeuroImage*, *50*(3), 1313–1319. <https://doi.org/10.1016/j.neuroimage.2009.12.109>

Henry, J. D., & Crawford, J. R. (2004a). A Meta-Analytic Review of Verbal Fluency Performance Following Focal Cortical Lesions. *Neuropsychology*, *18*(2), 284–295. <https://doi.org/10.1037/0894-4105.18.2.284>

Henry, J. D., & Crawford, J. R. (2004b). A meta-analytic review of verbal fluency performance in patients with traumatic brain injury. *Neuropsychology*, *18*(4), 621–628. <https://doi.org/10.1037/0894-4105.18.4.621>

Henry, J. D., Crawford, J. R., & Phillips, L. H. (2004). Verbal fluency performance in dementia of the Alzheimer's type: A meta-analysis. *Neuropsychologia*, *42*(9), 1212–1222. <https://doi.org/10.1016/j.neuropsychologia.2004.02.001>

Hickok, G., & Poeppel, D. (2007). The cortical organization of speech understanding. *Nature*, *8*(May), 393–402. [www.nature.com/reviews/neuro%0Ahttps://www-nature-com.ezp-prod1.hul.harvard.edu/articles/nrn2113.pdf](http://www.nature.com/reviews/neuro%0Ahttps://www-nature-com.ezp-prod1.hul.harvard.edu/articles/nrn2113.pdf)

Indefrey, P., & Levelt, W. J. M. (2004). The spatial and temporal signatures of word production components. *Cognition*, *92*(1–2), 101–144. <https://doi.org/10.1016/j.cognition.2002.06.001>

Kalénine, S., Peyrin, C., Pichat, C., Segebarth, C., Bonthoux, F., & Baciú, M. (2009). The sensory-motor specificity of taxonomic and thematic conceptual relations: A behavioral and fMRI study. *Neuroimage*, *44*(3), 1152-1162. doi:<https://doi.org/10.1016/j.neuroimage.2008.09.043>

Klimesch, W., Schimke, H., & Pfurtscheller, G. (1993). Alpha frequency, cognitive load and memory performance. *Brain Topography*, *5*(3), 241–251. <https://doi.org/10.1007/BF01128991>

Klimesch, Wolfgang. (2012). Alpha-band oscillations, attention, and controlled access to stored information. *Trends in Cognitive Sciences*, *16*(12), 606–617. <https://doi.org/10.1016/j.tics.2012.10.007>

Klimesch, Wolfgang, Sauseng, P., & Hanslmayr, S. (2007). EEG alpha oscillations: The inhibition-timing hypothesis. *Brain Research Reviews*, *53*(1), 63–88. <https://doi.org/10.1016/j.brainresrev.2006.06.003>



Martin, A. (2007). The representation of object concepts in the brain. *Annu Rev Psychol*, 58, 25-45. doi:10.1146/annurev.psych.57.102904.190143

Martin, A., & Chao, L. L. (2001). *Semantic memory and the brain: structure and processes*. 194–201.

McDonnell, M., Dill, L., Panos, S., Amano, S., Brown, W., Giurgius, S., Small, G., & Miller, K. (2020). Verbal fluency as a screening tool for mild cognitive impairment. *International Psychogeriatrics*, 32(9), 1055–1062. <https://doi.org/10.1017/S1041610219000644>

Mirman, D., Landrigan, J.-F., & Britt, A. E. (2017). Taxonomic and thematic semantic systems. *Psychological Bulletin*, 143(5), 499-520. doi:10.1037/bul0000092

Miyake, A., & Friedman, N. P. (2012). The nature and organization of individual differences in executive functions: Four general conclusions. *Current Directions in Psychological Science*, 21(1), 8–14. <https://doi.org/10.1177/0963721411429458>

Miyake, A., Friedman, N. P., Emerson, M. J., Witzki, A. H., Howerter, A., & Wager, T. D. (2000). The Unity and Diversity of Executive Functions and Their Contributions to Complex “Frontal Lobe” Tasks: A Latent Variable Analysis. *Cognitive Psychology*, 41(1), 49–100. <https://doi.org/10.1006/cogp.1999.0734>

Nee, D. E., Brown, J. W., Askren, M. K., Berman, M. G., Demiralp, E., Krawitz, A., & Jonides, J. (2013). A meta-analysis of executive components of working memory. *Cerebral cortex (New York, N.Y. : 1991)*, 23(2), 264-282. doi:10.1093/cercor/bhs007

Niendam, T. A., Laird, A. R., Ray, K. L., Dean, Y. M., Glahn, D. C., & Carter, C. S. (2012). Meta-analytic evidence for a superordinate cognitive control network subserving diverse executive functions. *Cognitive, Affective and Behavioral Neuroscience*, 12(2), 241–268. <https://doi.org/10.3758/s13415-011-0083-5>

Oswald, V., Zerouali, Y., Boulet-Craig, A., Krajcinovic, M., Laverdière, C., Sinnett, D., Jolicoeur, P., Lippé, S., Jerbi, K., & Robaey, P. (2017). Spontaneous brain oscillations as neural fingerprints of working memory capacities: A resting-state MEG study. *Cortex*, 97, 109–124. <https://doi.org/10.1016/j.cortex.2017.09.021>

Owen, A. M., McMillan, K. M., Laird, A. R., & Bullmore, E. (2005). N-back working memory paradigm: A meta-analysis of normative functional neuroimaging studies. *Human Brain Mapping*, 25(1), 46–59. <https://doi.org/10.1002/hbm.20131>

Paek, E. J., Murray, L. L., & Newman, S. D. (2020). Neural Correlates of Verb Fluency Performance in Cognitively Healthy Older Adults and Individuals With Dementia: A Pilot fMRI Study. *Frontiers in Aging Neuroscience*, 12(March), 1–12. <https://doi.org/10.3389/fnagi.2020.00073>

Palva, S., & Palva, J. M. (2007). New vistas for  $\alpha$ -frequency band oscillations. *Trends in Neurosciences*, 30(4), 150–158. <https://doi.org/10.1016/j.tins.2007.02.001>

Pulvermuller, F., Hauk, O., Nikulin, V. V., & Ilmoniemi, R. J. (2005). Functional links between motor and language systems. *Eur J Neurosci*, 21(3), 793-797. doi:10.1111/j.1460-9568.2005.03900.x

Robinson, G., Shallice, T., Bozzali, M., & Cipolotti, L. (2012). The differing roles of the frontal cortex in fluency tests. *Brain*, 135(7), 2202–2214. <https://doi.org/10.1093/brain/aws142>

Sadaghiani, S., Dombert, P. L., Løvstad, M., Funderud, I., Meling, T. R., Endestad, T., Knight, R. T., Solbakk, A. K., & D'Esposito, M. (2019). Lesions to the Fronto-Parietal Network Impact Alpha-Band Phase Synchrony and Cognitive Control. *Cerebral Cortex*, *29*(10), 4143–4153. <https://doi.org/10.1093/cercor/bhy296>

Sadaghiani, S., & Kleinschmidt, A. (2016). Brain Networks and  $\alpha$ -Oscillations: Structural and Functional Foundations of Cognitive Control. *Trends in Cognitive Sciences*, *20*(11), 805–817. <https://doi.org/10.1016/j.tics.2016.09.004>

Sadaghiani, S., Scheeringa, R., Lehongre, K., Morillon, B., Giraud, A. L., D'Esposito, M., & Kleinschmidt, A. (2012). Alpha-band phase synchrony is related to activity in the fronto-parietal adaptive control network. *Journal of Neuroscience*, *32*(41), 14305–14310. <https://doi.org/10.1523/JNEUROSCI.1358-12.2012>

Sauz on, H., Raboutet, C., Rodrigues, J., Langevin, S., Schelstraete, M. A., Feyereisen, P., . . . N'Kaoua, B. (2011). Verbal Knowledge as a Compensation Determinant of Adult Age Differences in Verbal Fluency Tasks over Time. *Journal of Adult Development*, *18*(3), 144-154. doi:10.1007/s10804-010-9107-6

Schwartz, M. F., Kimberg, D. Y., Walker, G. M., Brecher, A., Faseyitan, O. K., Dell, G. S., . . . Coslett, H. B. (2011). Neuroanatomical dissociation for taxonomic and thematic knowledge in the human brain. *Proc Natl Acad Sci U S A*, *108*(20), 8520-8524. doi:10.1073/pnas.1014935108

Shao, Z., Janse, E., Visser, K., & Meyer, A. S. (2014). What do verbal fluency tasks measure? Predictors of verbal fluency performance in older adults. *Frontiers in Psychology*, *5*(JUL), 1–10. <https://doi.org/10.3389/fpsyg.2014.00772>

Stuss, D. T., & Alexander, M. P. (2007). Is there a dysexecutive syndrome? *Philosophical Transactions of the Royal Society B: Biological Sciences*, *362*(1481), 901–915. <https://doi.org/10.1098/rstb.2007.2096>

Stuss, D. T. (2011). Functions of the Frontal Lobes: Relation to Executive Functions. *Journal of the International Neuropsychological Society*, *17*(5), 759-765. doi:10.1017/S1355617711000695

Spagna, A., Kim, T. H., Wu, T., & Fan, J. (2020). Right hemisphere superiority for executive control of attention. *Cortex*, *122*, 263-276. doi:<https://doi.org/10.1016/j.cortex.2018.12.012>

Veltman, D. J., Rombouts, S. A. R. B., & Dolan, R. J. (2003). Maintenance versus manipulation in verbal working memory revisited: An fMRI study. *NeuroImage*, *18*(2), 247–256. [https://doi.org/10.1016/S1053-8119\(02\)00049-6](https://doi.org/10.1016/S1053-8119(02)00049-6)

Wagner, S., Sebastian, A., Lieb, K., Tüscher, O., & Tadić, A. (2014). A coordinate-based ALE functional MRI meta-analysis of brain activation during verbal fluency tasks in healthy control subjects. *BMC Neuroscience*, *15*. <https://doi.org/10.1186/1471-2202-15-19>

Wechsler, D. (2008). Wechsler Adult Intelligence Scale - Fourth Edition. San Antonio, TX. *The Psychological Corporation*.

Weckerly, J., Wulfeck, B., & Reilly, J. (2001). Verbal Fluency Deficits in Children With Specific Language Impairment: Slow Rapid Naming or Slow to Name? *Child Neuropsychology*, *7*(3), 142-152. doi:10.1076/chin.7.3.142.8741

Whiteside, D. M., Kealey, T., Semla, M., Luu, H., Rice, L., Basso, M. R., & Roper, B. (2016). Verbal Fluency: Language or Executive Function Measure? *Applied Neuropsychology:Adult*, 23(1), 29–34. <https://doi.org/10.1080/23279095.2015.1004574>

Yuan, P., & Raz, N. (2014). Prefrontal cortex and executive functions in healthy adults: A meta-analysis of structural neuroimaging studies. *Neuroscience and Biobehavioral Reviews*, 42, 180–192. <https://doi.org/10.1016/j.neubiorev.2014.02.005>

# Supplementary material

## Supplementary Figures

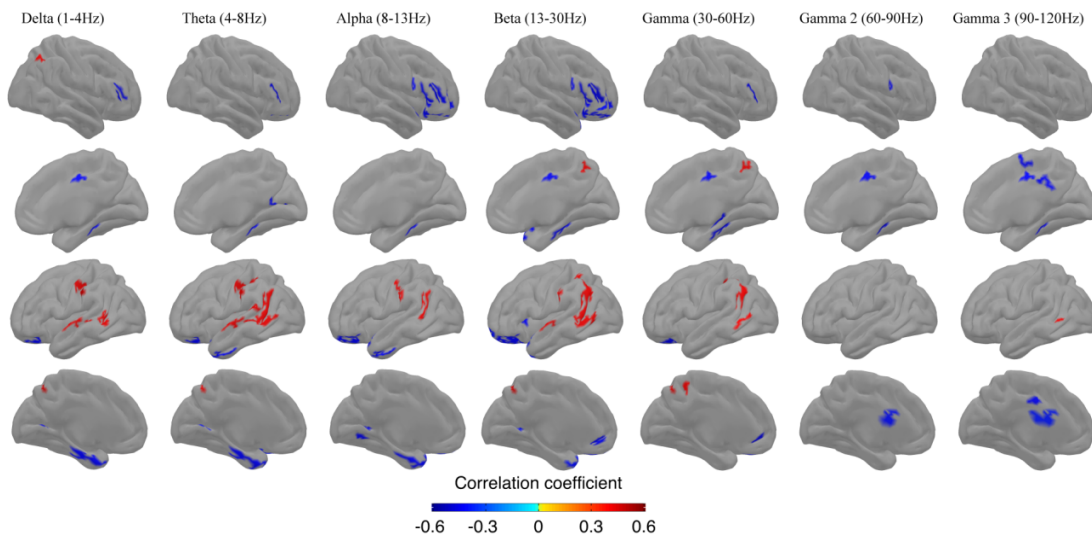


Figure 25. – Figure S1: Spatial distribution of clusters with statistically significant correlations ( $p < .001$ ) between resting MEG source-space power (z-scores across vertices) and neuropsychological performance on the **Vocabulary** test. The formatting of the figure and statistical significance of the results are identical to those in Fig. 1.

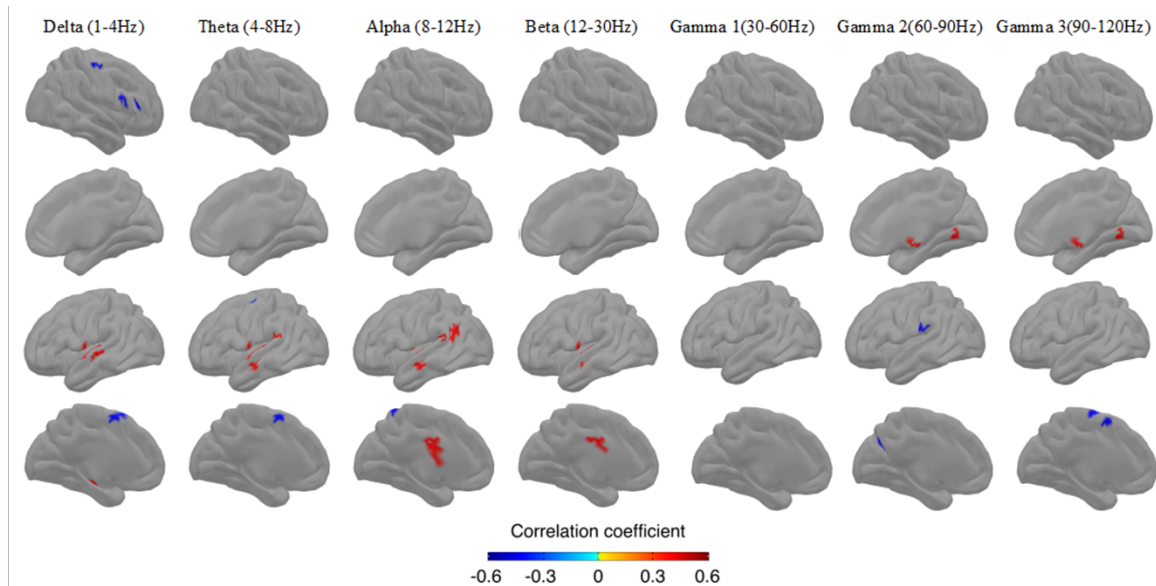


Figure 26. – Figure S2: Spatial distribution of clusters with statistically significant correlations ( $p < .001$ ) between resting MEG source-space power (z-scores across vertices) and neuropsychological performance on the **Trail Making Test (Condition 4)** test. The formatting of the figure and statistical significance of the results are identical to those in Fig. 1.

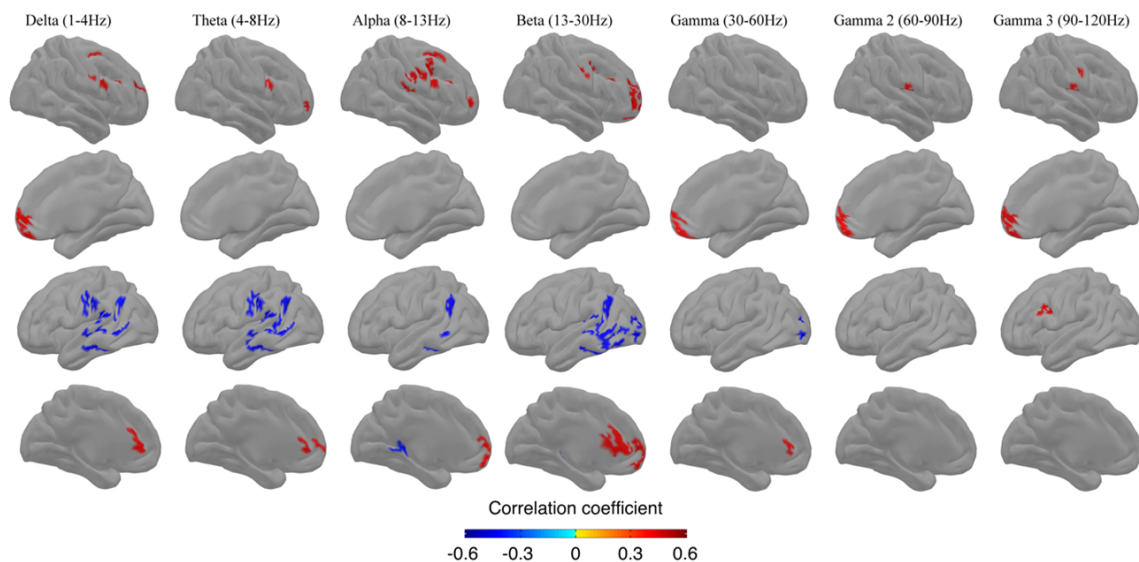


Figure 27. – Figure S3: Spatial distribution of clusters with statistically significant correlations ( $p < .001$ ) between resting MEG source-space power (z-scores across vertices) and individual regression of **F2\_VOC**. The formatting of the figure and statistical significance of the results are identical to those in Fig. 1.

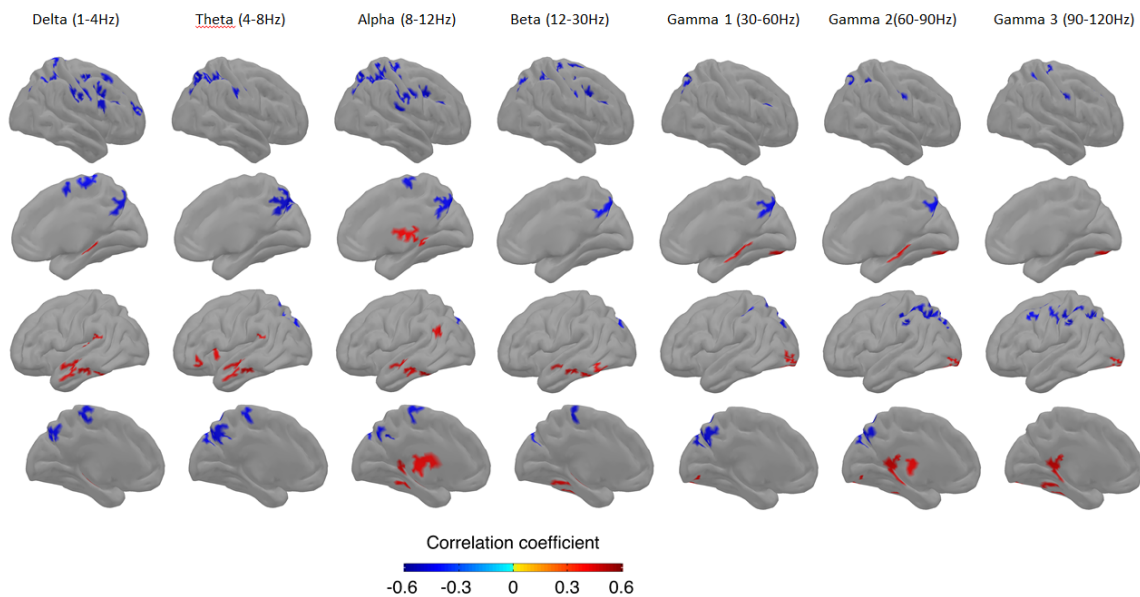


Figure 28. – Figure S4: Spatial distribution of clusters with statistically significant correlations ( $p < .001$ ) between resting MEG source-space power (z-scores across vertices) and individual regression of **F1\_TMT**. The formatting of the figure and statistical significance of the results are identical to those in Fig. 1.

## Chapitre 4 — Resting state MEG power correlates of semantic and serial strategy in learning a list of words

Victor Oswald<sup>1,2</sup>, Philippe Robaey<sup>1,7,8,9</sup>, Younes Zerouali<sup>3,4</sup>, Aubrée Boulet-Craig<sup>5</sup>, Maja Krajinovic<sup>1</sup>, Caroline Laverdière<sup>6</sup>, Daniel Sinnett<sup>1</sup>, Pierre Jolicoeur<sup>5</sup>, Sarah Lippé<sup>1,5</sup>, Karim Jerbi<sup>5</sup>

<sup>1</sup>*Service hématologie-oncologie, Charles-Bruneau Cancer Center, Sainte-Justine Hospital, Montreal, QC, Canada;*

<sup>2</sup>*Department of Neuroscience, Faculty of Medicine, University of Montreal, Montreal, Qc, Canada;*

<sup>3</sup>*Department of Biomedical Engineering, École Polytechnique de Montréal, Montreal, QC, Canada;*

<sup>4</sup>*Department of Neurology, CHU Notre-Dame Research Center, University of Montreal, Montreal Qc, Canada*

<sup>5</sup>*Department of Psychology, University of Montreal, Montreal, QC, Canada*

<sup>6</sup> *Department of Pediatric, CHU Sainte-Justine Research Center, Montreal, QC, Canada;*

<sup>7</sup> *Department de Psychiatrie, University of Montreal, Montreal, QC, Canada;*

<sup>8</sup> *Children's Hospital of Eastern Ontario, Ottawa, ON, Canada;*

<sup>9</sup> *Department de Psychiatrie, University of Ottawa, Ottawa, ON, Canada;*

## Abstract

In order to perform in a learning environment, it is necessary to use strategies. In a verbal learning task, many strategies are already known that can be used, some of which are more effective than others, but the neural substrates to which they are linked are not known. Here we investigate the neural underpinning related to a verbal learning test and their inter-individual strategy scores (semantic and serial clustering). We used The California Verbal Learning Test (CVLT-2) to obtain a behavioural standardized measure of verbal learning for each participant (n=28). In addition, we obtained semantic and serial clustering score associated with verbal learning score. We perform brain-behaviour correlation/anticorrelation pattern with a cluster analysis method based on resting state MEG power in the canonical frequency bands. Results demonstrate that semantic clustering and serial clustering shows two distinct patterns. Semantic clustering was associated with a left lateralized pattern including frontal, parietal and temporal cortex while serial clustering showed correlation clusters in the right hemisphere in fronto-parietal cortex. Clusters in the left inferior frontal gyrus, left ventral premotor, left caudal part of pre- and post-central gyrus, left supramarginal gyrus dominant in alpha band (8–13 Hz) were linked to a bias of semantic over serial clustering whereas clusters in the left parahippocampal gyrus in delta band (1–4 Hz), mid cingulate gyrus in beta band (13–30 Hz) and occipital cortex in theta band (4–8 Hz) were associated with a bias of serial over semantic clustering. We also found that verbal learning performance was related to semantic clustering in behavioural scores, as well as with the correlation/anticorrelation clusters similar to the semantic clustering correlation pattern. Our results suggest that the spontaneous brain activity at rest is predictive of the strategy employed to achieve a verbal memory task.

Keywords: Semantic clustering, serial clustering, learning strategy, CVLT-2, verbal learning memory, Magnetoencephalography (MEG), Neuronal oscillations, Resting State.



## Introduction

The study of learning and memory frequently relies on the use of word lists that are longer than the memory span. Given the limited capacity for short-term information storage, the organization of material used during learning could compensate for such memory limitations. We can distinguish between the primary and secondary organization of a word list (Tulving, 1972). An individual's experience with the word list as presented constitutes the primary organization. For example, a better recall of words at the beginning (primacy effect) or end (recency effect) of the list compared to those in the middle reflects the primary organization. On the other hand, when an individual uses his or her prior experience with the words presented in the list, for example by grouping them into common associations (such as words that are names of fruits), he or she appeals to the secondary organization of the list. Among the supraspan word-list tests available, the California Verbal Learning Test (D.C. Delis, J.H. Kramer, E. Kaplan, 2000) provides measures of short- and long-term recall and recognition, vulnerability to proactive and retroactive interference, and learning ability. Therefore, the primary measure of learning on the CVLT is the total recall of correct responses over the five learning trials of list A. However, it also evaluates the encoding strategies that may have been used by subjects by counting the number of words clusters by semantic association (semantic clustering), or by the order they were presented and their serial association (serial clustering), while correcting for chance.

Brain imaging of CVLT has mostly focused on measures of short- and long-term recall and recognition. The neural correlates of the CVLT have revealed that the recall is dependent on the hippocampus. Verbal learning, free immediate – and delayed recall scores were shown to be specifically correlated with the volumes of the left Cornu Ammonis (CA) 1–4 subfields (Aslaksen et al., 2018). More specifically, measures of learning and early retrieval (Immediate Free Recall Discriminability and Short Free Recall Discriminability) were linked to CA3 and DG volume, while a measure of consolidation (Delayed Recall Discriminability) was associated with CA1 volume (Mueller et al., 2011). Hippocampus has also been shown to be implicated in the short-term memory and the working memory, especially if precision and relational binding are required (Olsen et al., 2012; Yonelinas, 2013). A fundamental feature of the hippocampus during encoding is to link features into a memory trace or engram (Dudai, 2012; Josselyn et al., 2015; Tonegawa

et al., 2015). However, it is at the cortical level that the representations that will finally be encoded in longer-term memory. This interaction between hippocampus and medial temporal lobe, frontal lobe and ventral parietal lobe is described as a loop to build memory trace and is highly context dependent (Moscovitch et al., 2016).

Using the CVLT, findings related to the learning strategies were serendipitous. For example, verbal learning, recall performance and semantic clustering were found to be correlated with the volume of left hippocampal in healthy controls. By contrast, in depressed individuals, the volume of both hippocampi, but especially in the right hemisphere, were correlated with serial clustering indices, which may reflect the use of a less effective learning strategy (Turner et al., 2012). Other studies have been explored the effect of training learning strategy on the brain. When comparing encoding during verbal learning with list of word structure (by thematic category) to unstructured related word, significant activation was found in the occipital cortex, the left orbitofrontal cortex, and the left parietal cortex. When the participants were explicitly trained to use a semantic strategy, the activation in bilateral dorsolateral prefrontal cortex, bilateral inferior frontal gyrus, right orbitary gyrus, occipital cortex and precuneus increased (Miotto et al., 2006). With a similar design, similar result were obtained in older healthy participants (Miotto et al., 2014). However, there is not study of brain activity differences in participants who spontaneously use more a semantic or a serial strategy when actively learning a list of words. However, as both strategies are used concurrently and parsing the brain activities related to each strategy may prove challenging. Therefore, we turned to brain activity at rest before participants learned the word list and measured inter-individual differences in the use of each strategy.

Rhythmic neuronal activity is a hallmark of brain function that is prominent during rest (Buzsaki & Silva, 2012; Dalal et al., 2011; Guntekin & Basar, 2014; Jensen, Gips, Bergmann, & Bonnefond, 2014; Jerbi et al., 2009; Klimesch, 2012; Palva & Palva, 2007; Ruhnau, Hauswald, & Weisz, 2014). Remarkably, beyond refuting the view that spontaneous brain activity consists of irrelevant noise, we have previously showed that cortical spontaneous oscillatory activity can correlate in the spatial and in the frequency domains with cognitive performance, like working memory (Oswald et al., 2017) or verbal fluency (Oswald et al., 2020). As the serial and semantic strategy are used concurrently when learning a list of words, and reflect distinct cognitive abilities, spontaneous

brain activity may also show different correlation cluster at rest. Therefore, we recorded the resting state brain magnetoencephalography, used the CVLT-2 as a test of verbal learning memory to obtain the total recall of correct responses and measures of semantic and serial clustering over the five learning trials, to compute brain task free neural correlates of verbal learning. Our hypothesis was that the semantic and serial strategies would have distinct neural “fingerprints” at the cortical level, similar to the correlation clusters obtained for the free immediate recall measures.

## **Method**

### **Participants**

Twenty-eight healthy subjects (15 females,  $25.76 \pm 4.84$  years old) with no reported history of neurological or psychiatric disorders took part in this study. The project was reviewed and approved by the University of Montreal and the CHU Sainte-Justine Research Ethics Board. Informed consent was obtained before the experiment, and financial compensation was given upon completion of the experiment.

### **Neuropsychological Assessment**

A neuropsychological evaluation was carried out the same day as the MEG recordings. To assess verbal learning, we used the California Verbal Learning Test (CVLT-2), Second Edition, Adult version (Dean C. Delis, Joel H. Kramer, Edith Kaplan, Beth A. Ober, 2000). This test is composed by two lists of words (A&B), each list being composed of sixteen words which can be placed in one of the following 4 semantic categories: transportation, vegetables, animals and furniture. The list was presented by mixing words (i.e. two words following each other do not belong to the same semantic category) and enunciated by the examiner to the participant five times (trials 1 to 5). The participant is asked to recite the list back in the order of their choice after every examiner listing. The list enunciated by the examiner is still in the same order with no semantic grouping. The answers from each trial were calculated for every subject to evaluate their performance (number of words) and, on the other hand, strategy employed to give back the word could be calculated based on the subject list order: three main strategies could be employed by the subject — namely serial (number of words given in the same order as the list was presented to the subject), semantic (number of groupings the subject formed) and subjective (a strategy developed by the subject). After the fifth trial, a new list (B) was introduced to the subjects and two recalls were done of list A with both a short and a long delay. In the protocol, participants did other neuropsychological tests between recalls, the time between recalls was maintained for all participants. The performance score and the strategy scores were standardized in scale score with age. This test allowed the evaluation participants verbal learning skills and the related strategy used to perform.

## **MEG and Anatomical MRI Data Acquisition**

All 28 subjects were comfortably seated with eyes open, fixating a back-illuminated screen located 75 cm in front of them. Two 5-minute periods of resting-state were recorded at a sampling rate of 1200 Hz, using a CTF-VSM whole head 275-sensor MEG system (MEG core facility, Psychology Department, University of Montreal, QC, Canada). Following standard procedures, third-order gradiometer noise reduction was computed based on twenty-nine reference channels. Bipolar EOG (Vertical EOG and Horizontal EOG) was recorded in order to monitor eye blinks and ocular movements. ECG was also recorded to monitor heartbeats. Three head coils fixed at the nasion and the bilateral preauricular points were used for head localization and were monitored at the beginning and the end of each session. Particular care was taken to ensure that head displacement across sessions remained below 5 mm. The neuropsychological assessments were done in the morning at the Sainte-Justine Hospital (Montreal, QC, Canada). Later in the afternoon, the participants went to the MEG facility, located in the Psychology Department of the University of Montreal, for the MEG recordings.

Structural MRI images were obtained for each subject with a 3-T General Electric (GE) scanner (Saint-Justine Hospital, Montreal, QC, Canada). The individual surfaces were used to carry out the co-registration between the MEG fiducial markers (LAP, NAS, RAP) and the MRI structural image. The exact position of the head was refined based on head shape position files obtained using a 3D-localization Polhemus system.

## **Data Pre-Processing**

MEG data pre-processing was performed using the Matlab-based Brainstorm open-source software. The data was first notch filtered at 60 Hz, and then between 0.5 Hz and 120 Hz. Cardiac artefacts, eye blinks, and eye movements were corrected using the Signal-Space-Projection method (SSP). Fifty signal epochs, centered on each artefact, were selected, and a singular value decomposition was applied to each artefact using built-in Matlab functions. The eigenvectors explaining at least 10 % of the variance of the artefacts were discarded, and the remaining eigenvectors were used to define the SSP. The SSP method relies on a signal space decomposition procedure, where the statistical characteristics of the measured signals are used to determine

the two subspaces spanned by the MEG brain signals and the unwanted artifacts, respectively. Projecting the continuous MEG data onto the signal subspace effectively removes the components belonging to the artifact subspace.

### **MEG Sources Estimation**

MEG source reconstruction was performed using a standard weighted minimum-norm approach, with the Brainstorm software. T1-weighted brain volumes were acquired in all participants and were used to generate a cortical surface model, using the FreeSurfer software package. Forward modelling of the magnetic field was defined based on an overlapping-sphere method. The weighted minimum norm solution was computed using a loose dipolar orientation constraint (set at 0.5), a signal-to-noise ratio of 3, whitening PCA and a depth weighting of 0.5. The noise covariance matrix for each participant was estimated from a 2-min empty room recording performed earlier the same day (same acquisition parameters but with no subject in the shielded room) e.g., The source time series were initially reconstructed on a 15000-vertex individual brain tessellation, and then spatially interpolated to the MNI ICBM152 brain template and down-sampled to a 10000-vertices template.

### **Spectral Power Analysis**

Resting-state power spectral density (PSD) was measured using the modified Welch periodogram technique (1-s Hamming window and 50 % time-window overlap). The mean PSD for each frequency band of interest was obtained for each subject by averaging the PSD values across the frequency bins of each band. Power estimates were computed for all elemental cortical sources and all participants in the following frequency bands: Delta (1–4Hz), theta (4–8 Hz), alpha (8–13 Hz), beta (13–30 Hz), gamma 1 (30–60 Hz), gamma 2 (60–90 Hz) and gamma 3 (90–120 Hz). Next, for each participant, the PSD values (i.e. oscillatory power) were standardized using a z-score transformation (computed at each vertex using the mean and standard deviation of the power values across all vertices within the same frequency band).

## Correlation Analyses and Cluster-Level Statistics

A correlation analysis was carried out to probe the putative relationship across individuals between spontaneous brain oscillation power (separately for each frequency band) and neuropsychological score. The computation and assessment of correlation were achieved via a two-step procedure. First, the Pearson correlation coefficients were computed between resting-state power (z-scores) at each cortical vertex and scores from the neuropsychological tests. Next, the statistical significance of the correlation results was evaluated using t-statistics and nonparametric cluster-wise correction for multiple testing. More specifically, the correlation was computed using MATLAB's built-in *corrcoef* function at each cortical node (vertex), for each frequency band and each subject ( $n=28$ ). In addition to computing the Pearson correlation coefficient, the correlation function also returns p-values obtained by transforming the correlation to create a t-statistic with  $n-2$  degrees of freedom. Setting the threshold for the first-level statistical significance to  $p < 0.05$  (uncorrected) provides a spatial mask in source space. Next, within this mask (i.e. significant correlation coefficients, uncorrected), we determined clusters of spatially contiguous (neighbouring) vertices, which were identified based on the FreeSurfer adjacency matrix. The correlation coefficients within each cluster were then added up to obtain a cluster mass (cluster mass statistics). To assess the statistical significance of the obtained clusters, we used nonparametric permutation testing. We randomly shuffled the subjects' neuropsychological scores, while keeping the MEG source power data across subjects intact. This essentially creates random associations that destroy any putative correlation between the two types of observations. The 1000 permutations of the data (and replicating the cluster mass computation described above for each set of permuted data) provides an estimate for the null distribution against which we can then test the significance of the truly observed clusters in the original data. Statistically significant correlation clusters at  $p_{\text{corr}} < 0.001$  were then defined as those with a cluster mass larger than the correlation value ranked 999 on the null distribution. By choosing such a restrictive significance threshold (i.e.  $p < 0.001$ ), not only do we minimize the type I errors, but we also ensure that the reported results would remain significant — for instance, at a level of  $p < 0.05$ , accounting for up to 50 multiple tests — based on a regular Bonferroni correction. In other words, all our results remain significant at  $p < 0.05$  if we correct for tests across

all frequency bands, and all the WAIS-IV subtests and indices used (as the number of comparisons does not exceed 50). The results reported here are therefore statistically significant at  $p < 0.001$  level, corrected across space, for each frequency band and neuropsychological test, but they are all also significant at  $p < 0.05$  when corrected for comparisons across space, frequency bands, and subtests.

### **Comparison Between Brain-Behaviour Pattern**

We compared pattern correlation/anticorrelation between brain-behaviour result by using the transferred between correlation coefficients into z scores using Fisher's r method. (<http://core.ecu.edu/psyc/wuenschk/docs30/CompareCorrCoeff.pdf>). We then corrected p\_value with an FDR correct across brain space.



## Results

### Behavioural performance

Neuropsychological assessment shows normal behavioural performance at the CVLT. Subjects retain a means of 58 words (table 2) when we cumulate the words retain at each trial, from first trial to the fifth trial with the list A. Table 2 show the mean performance across the fifth trial for each learning strategy (i.e. semantic, serial backward, serial forward). Results show that semantic is the most used by participants (mean= 1.95) following by serial backward (mean = 0.61) and by the serial forward (mean= 0.45).

Table 3 show correlation between mean row performance across trial and mean indices of each strategy used across the fifth trial. Results show that only semantic strategy strongly correlates with mean learning performance ( $r = .49$ ;  $p = 0.007$ ), where serial strategy does not correlate with mean performance (serial backward ( $r = -.15$ ;  $p = 0.43$ ) and forward ( $r = -.07$ ;  $p = 0.70$ )).

### Brain Behaviour Correlation for Mean Performance Across Trials 1 to 5

#### Correlation Pattern

In the parietal lobe (Fig. 29), we found cluster correlation in the bilateral superior lobule (beta band), Left superior parietal lobule and angular gyrus (all frequency bands) and in the Left post-central gyrus (delta, theta, gamma 1, gamma 2 bands). In the temporal lobe, we found clusters in the right superior temporal sulcus (delta, theta and beta band), in the left posterior middle temporal gyrus (all frequency bands), in the left superior temporal gyrus and sulcus (delta, theta, alpha, beta band) as well as in the left inferior temporal sulcus (gamma 1, gamma 2, gamma 3 bands). In the frontal lobe, we found significant clusters in the left pre-central gyrus (delta, alpha, beta, gamma1 band) and left middle frontal gyrus (alpha band)

#### Anticorrelation Pattern

In the parietal lobe (Fig. 29), we found anticorrelation clusters in the left post cingular gyrus (delta, theta, alpha, beta band). In the temporal lobe, we found clusters in the right inferior temporal gyrus and temporal pole (beta, gamma 1 and gamma 2 bands), as well as in the right lingual and

para hippocampal gyrus (beta band). In the frontal lobe, we found significant clusters in the\_right dmPFC (theta and alpha band), in the Left dmPFC (gamma 1, gamma 2, gamma 3 bands), in the Right pre-central (gamma 3 band), in the right dIPFC (beta and gamma 1 bands), in the left dIPFC (delta, theta, alpha, beta bands), in the right anterior cingular (gamma 1 band), in the left anterior cingular (beta, gamma 1, gamma 2 and gamma 3 bands) and in the right middle Cingular gyrus (gamma 1, gamma 2, gamma 3 bands).

### **Brain Behaviour Correlation for Semantic Strategy Across Trials 1 to 5**

#### Correlation Pattern

In the parietal lobe (Fig. 30), we found correlation clusters in the left superior lobule (Delta, theta, alpha, beta band), in the left superior parietal lobule angular gyrus (Delta, theta, alpha, beta band) and in the left post-central gyrus (all frequency bands). In the temporal lobe, we found significant results in the left posterior middle temporal gyrus (all frequency bands), in the left superior temporal gyrus and sulcus (all frequency bands) and in the left inferior temporal sulcus (beta, gamma 1, gamma 2, gamma 3 bands). In the frontal lobe, we found correlation clusters in the left pre-central gyrus (delta, theta, alpha, beta, gamma 1, gamma 2 bands), in the left middle frontal gyrus (delta, alpha, gamma 1 bands) and in the left dIPFC (alpha, gamma 1, gamma 2 bands). In the occipital lobe, we found clusters in the right cuneus (gamma 2 et gamma 3 bands).

#### Anticorrelation pattern

In the parietal lobe (Fig. 30), we found anticorrelation clusters in the left post cingular gyrus (delta, theta, alpha, beta bands) and in the right post cingular gyrus (delta, beta gamma 1 bands).

### **Brain Behaviour Correlation for Serial Backward Strategy Across Trials 1 to 5**

#### Correlation Pattern

In the parietal lobe (Fig. 31), we found clusters correlation in the right parieto-occipital gyrus (gamma 2 band) and in the right post cingular gyrus (delta, beta bands). In the temporal lobe, significant clusters were found in the right posterior middle temporal gyrus (gamma 1 band). In

the frontal lobe, we found clusters in the right middle frontal gyrus (gamma 3 band) and in the occipital lobe in the right occipital gyrus (beta band).

#### Anticorrelation Pattern

In the parietal lobe (Fig. 31), we found clusters significant in the left supramarginal gyrus (delta, theta, alpha, beta, gamma 1, gamma 3 bands) and in the left post-central gyrus (delta, theta, alpha, beta, gamma 1 band). In the temporal lobe, we found clusters in the left middle temporal gyrus (beta, gamma 1 band), in the left inferior temporal sulcus (gamma 2, gamma 3 bands) and in the left posterior middle temporal gyrus (alpha, beta, gamma 2, gamma 3 bands). In the frontal lobe, we found clusters in the left dlPFC (all frequency bands, in the left middle frontal gyrus (delta, alpha, beta, gamma 1 band) and in the left pre-central gyrus (delta, theta, alpha, beta, gamma 1, gamma 2 bands).

### **Brain Behaviour Correlation for Serial Forward Strategy Across Trials 1 to 5**

#### Correlation Pattern

In the parietal lobe (Fig. 32), we found correlation clusters in the right superior lobule (delta, theta, alpha band), in the right parieto-occipital gyrus (delta, theta, alpha, gamma 1, gamma 2, gamma 3 bands) and in the right angular gyrus (gamma 2 and gamma 3 bands). In the temporal lobe, we found clusters in the right posterior middle temporal gyrus (gamma 1 and gamma 2 bands). In the frontal lobe, we found significant clusters in the right pre-central gyrus (beta, gamma 1, gamma 2, gamma 3 band), in the right middle frontal gyrus (delta, theta, beta, gamma 1, gamma 2, gamma 3 band), and in the left middle frontal gyrus (gamma 3 band).

#### Anticorrelation Pattern

In the parietal lobe (Fig. 32), we found anticorrelations clusters in the left p cingular gyrus (gamma 3 band) and in the left supramarginal gyrus (delta, theta, alpha, beta band). In the temporal lobe, we found the left middle temporal gyrus (delta, theta, alpha, beta, gamma 2 bands), in the left inferior temporal sulcus (gamma 1, gamma 2, gamma 3 bands) and in the left posterior middle temporal gyrus (theta, alpha, beta, gamma 1, gamma 3 bands). In the frontal lobe, we found clusters in the left dlPFC (delta, theta band).

### **Difference of brain-behaviour pattern between both strategies (semantic versus serial)**

Figure 33 shows the difference between correlation/Anticorrelation pattern found with strategies used. We tested the significance difference between the correlation coefficient obtained on each cluster from brain-behaviour pattern for each strategy. We found positive difference of coefficient correlation between semantic and serial strategies. Positive difference was found with an extended left cluster across all frequencies including dorsolateral prefrontal cortex, angular and supramarginal gyrus, pre- and post-central gyrus, posterior middle temporal gyrus, and superior temporal gyrus. We found negative difference in correlation in bilateral middle cingular gyrus, left entorhinal gyrus and right visual cortex. Figure 34 show scatter plot for the left cluster found in difference correlations shown in (Fig. 33). The scatter plot shows that semantic strategy used strongly correlated with normalized power at rest ( $r=.73$ ) while serial strategy strongly anti-correlated with it (serial Backward ( $r=-.41$ ); serial Forward  $-.57$ ).

## Discussion

### Behavioural Result

At the behavioural level, we found that semantic clustering strategy correlated with the global learning performance over the first five trials while the serial (backward or forward) strategy did not. Our results are in line previous results showing the link between semantic strategy and learning performance (Miotto et al., 2006, 2014). Our functional neuroimaging results explored the neural substrates related to learning strategies and showed that the two learning strategies explored in this study are supported by different neural networks. This suggests that cortical oscillations at rest reflect different neural organizations supporting these learning strategies.

### Semantic Strategies Neural Correlate

Semantic strategy is related to a left dominant pattern that includes premotor, post- and pre-central gyrus, superior and inferior parietal lobule, superior temporal gyrus and posterior middle and inferior temporal gyrus. This large pattern is in line with the literature on semantic memory. Semantic representation is grounded in a sparse and distributed neural network supporting different cognitive components: (1) the left superior temporal sulcus and the left inferior lateral frontal gyrus for language processing (Halgren et al., 2002; Lopes et al., 2016; Mousavi et al., 2020), (2) the middle temporal gyrus, anterior temporal gyrus and posterior temporal gyrus are core regions for conceptual and knowledge (Elger et al., 1997; Kapur et al., 1996; Saykin et al., 1999) and (3) the pre-motor, motor and somatosensory cortex for motor planning (Binder et al., 2009; Binder & Desai, 2011). According to the embodied view of semantic representation, sensory-motor regions are the core of a network of semantic representations. These authors suggest that conceptual knowledge is encoded in sensory regions linked to action motor representations (Binder et al., 2016; Gallese & Cuccio, 2018; Gallese & Lakoff, 2005). The presence of neural correlates related to semantic memory can be explained by the fact the sixteen words are grouped into four categories (*vegetables, furniture, animals, transportation*), and that the participants can use this structure and use a semantic strategy in learning the list of words. Although words from the same category are never consecutive, the subject can identify the categories by himself very quickly and use a unique abstract representation per category.

Moreover *vegetables, furniture, animals, transportation* are exactly the type of information that the semantic memory encodes (Binder et al., 2016; Gallese & Cuccio, 2018; Gallese & Lakoff, 2005).

### **Neural Correlates of Serial Clustering**

The serial strategy (backward and forward) yielded a correlation pattern including the right superior parietal lobule, the right pre-central, and the bilateral middle frontal gyrus across frequency bands but especially in the gamma bands. These clusters are located on the fronto-parietal stream and could be linked to short-term and working memory networks. The number of serial clusters corrected for chance during recall measures the association of items in memory as a function of their position in the list A, regardless of whether the subject recalls them in forward or reverse order. When monkeys had to encode in working memory the spatial location and presentation order of visual stimuli (Carpenter, Baud-Bovy, Georgopoulos, & Pellizzer, 2018), many neurons in the motor, premotor and lateral prefrontal cortex regions showed activity related to both positions in the series and spatial location. These neurons encoded serial position in working memory in a relative rather than an absolute manner, i.e. the relative position of items between them (before, after, etc.) rather than according to an invariant order (first, second, etc.). The parietal, precentral and frontal location of the clusters associated with the serial strategy could therefore indicate the brain regions encoding the relative serial position of words in the list A.

With a similar method and in the same participants, the resting MEG-based clusters correlated with verbal working memory performance were similar to those correlated with serial strategy (i.e. right parietal and premotor clusters) (Oswald et al., 2017). This is in line with a growing body of literature linking fronto-parietal circuits to working memory using various methods. A fronto-parieto-cerebellar network has repeatedly been identified with fMRI with various types of working memory tasks using letter or number stimuli (e.g. (Chen & Desmond, 2005; Linden et al., 2003; Majerus et al., 2012; Majerus et al., 2007; Majerus et al., 2008; Majerus et al., 2010; Majerus et al., 2006; Majerus, Salmon, & Attout, 2013). The involvement of the parietal cortex, in particular the dorsal part of the parietal cortex, is consistent with the role of this region in top-

down attentional processes to guide the recall process of stored items (Cabeza, 2008; Ciaramelli, Grady, & Moscovitch, 2008). In the case of a serial strategy, one word serves as a cue to recall the contiguous word in the list. It has been shown that in a memory recognition task the presence of a cue functionally connects the dorsal parietal cortex with the dorsal attentional network, in particular the premotor cortex and the middle frontal gyrus (Burianová, Ciaramelli, Grady, & Moscovitch, 2012). We found correlation clusters for the serial strategy in the latter two regions.

In a previous study, with a similar approach and the same participants, we calculated clusters of correlations between the relative power of the MEG at rest and factors obtained by PCA. These factors reflected the subjects' advantage in performance on the verbal fluency test, compared, on the one hand, to a non-executive verbal test (Vocabulary) and, on the other hand, to a non-executive verbal test (Trail Making Test). A relatively better performance in the verbal fluency test compared to the other two tests (i.e. a better ability to check that an action sequence conforms to a set of rules as it is executed) was correlated with a cluster in the right premotor cortex (Oswald et al., 2020). The role of the right premotor cortex in speech production was also illustrated in a study in which subjects were asked to learn a series of eight digits and letters over a period of one month and then manipulate them in working memory (by segmenting the series and linking the segments together). Segmentation activated the dorsolateral prefrontal cortex bilaterally, whereas linking was associated with activity in the dorsal premotor cortex on the left. The functional coupling of these two regions seems to allow the serial execution of these two executive functions (Abe et al., 2007). Again, these results are consistent with the clusters of MEG relative power correlations in premotor regions and dorsolateral prefrontal cortex obtained with the serial strategy of word recall.

### **Verbal Performance Memory and Semantic Verbal Memory Sharing Common Neural Substrate**

Our results show that the semantic clustering is correlated with the number of words recalled in the first five trials. Moreover, the correlation and anticorrelation clusters obtained for semantic clustering largely overlapped with those obtained for the number of correct words recalled in the first five trials, but were strikingly different from those obtained for serial clustering. The

correlation between the semantic strategy and the learning indices for a list of words has been reported in the literature (Gsottschneider et al., 2011; Miotto et al., 2014, 2020). A meta-analysis has identified a semantic network of seven parietal, temporal and prefrontal areas in the left hemisphere: (1) posterior inferior parietal lobe, (2) middle temporal gyrus, (3) fusiform and parahippocampal gyri, (4) dorsomedial prefrontal cortex, (5) inferior frontal gyrus, (6) ventromedial prefrontal cortex, and (7) posterior cingulate gyrus (Binder, Desai, Graves, & Conant, 2009). In addition, brain imaging studies reported that activation of this semantic network was related to word recall performance (Bruffaerts et al., 2019; Casasanto et al., 2002; Heinze et al., 2006; Miotto et al., 2006). This suggests that the same left-lateralized verbal semantic distributed networks support learning performance and the use of a semantic encoding and retrieval strategies.

Previous studies have already reported a link between learning performances and left lateralized neural correlates similar to the regions identified by our semantic correlation pattern. For example, by comparing successful with unsuccessful learning, widespread activity was observed in the left prefrontal and posterior temporal gyrus as well as in the left superior parietal lobe (Heinze et al., 2006). Moreover, better performance during recognition testing was associated with activation in left-hemisphere prefrontal and temporoparietal structures and in bilateral medial temporal lobe structures (Casasanto et al., 2002). The performance-related hemispheric effects that we report appear consistent with levels of processing effects reported in previous neuroimaging studies of verbal long-term memory (Kapur et al., 1996) and may correspond to differences in individual subjects' encoding strategies. The degree of left lateralization of brain activity seems related to the semantic complexity of the task. If two semantic criteria are to be used instead of one to classify an auditory word, the lateralization index is shifted significantly to the left hemisphere, when contrasting the whole brain and Broca's area, or Wernicke's area and Broca's area. Similarly, the left superior and middle frontal gyri, angular gyrus, and left posterior cingulate gyrus (all regions involved in semantic processing) were more activated in the 2-criterion condition than in the 1-criterion condition (Lopes et al., 2016).



## **Language network as key component for learning performance, through the semantic strategies**

Some clusters of semantic and serial correlation are of opposite sign. In these regions a relative increase in MEG signal strength is positively correlated with one strategy, and negatively correlated with the other. The regions where the differences in correlations were statistically significant are shown in Figure 5, separately for the comparison between semantic clustering, on the one hand, and serial clustering, on the other hand, forward or backward. The corresponding scatter plots are presented in Figure 6. The regions where the MEG relative power at rest is positively correlated with a semantic strategy at the expense of a serial strategy were all located in the left hemisphere: the inferior lateral frontal gyrus (pars opercularis), the ventral part of the pre- and post-central gyri, the transverse temporal gyrus, the supramarginal cortex and the adjacent part of the inferior parietal cortex. The regions that predict more semantic clusters and fewer serial clusters during the 5 recalls of list A form a left linguistic network supporting speech perception and production (Hickok & Poeppel, 2007). A functional area known as the left sylvian-parietal-temporal area (in the posterior planum temporale/supramarginal gyrus) on the one hand and Broca's area, on the other hand, act as input and output short-term memory buffers in a reverberating bidirectional dorsal stream for perceiving and producing phonemes (Herman, Houde, Vinogradov, & Nagarajan, 2013). The relative resting power in these regions is critical for language, as well as for learning a list of words repeated aloud, especially when preferentially using a semantic strategy over a serial strategy.

Inversely, a preferential use of a serial strategy over a semantic strategy is linked to smaller clusters of significant difference between correlation in the left entorhinal, bilateral posterior cingulate, right occipital and right inferior parietal cortex. The hippocampus receives inputs from all brain neocortices via the entorhinal cortex. Through the output from the hippocampus back to the neocortex, the hippocampus is involved in the retrieval of episodic memory. In addition, when the same sequence is repeated multiple times, the hippocampus may associate the beginning of the sequence with the rest of the sequence before it is presented. This forward prediction via a hippocampal predictive model could be an important feature of sequence learning (Davachi & DuBrow, 2015). The hippocampus could therefore anticipate upcoming

sensory information using recent sensory inputs as well as memory representations of internally generated sequences. This predictive activity suggests that the hippocampus can produce an internal model to anticipate the consequences of an action before sensorimotor feedback is available (Barron, Auztulewicz, & Friston, 2020). This ability may explain why the relative MEG power of the left entorhinal cortex may predict the use of a serial strategy at the expense of a semantic strategy, since it represents the main input to a hippocampal system capable of creating and learning sequences, especially when they are repeated, as in the case of a word list learning test. There are few examples of differential activity in brain regions according to the cognitive strategy. For example, to solve a navigation task, subjects can spontaneously adopt a spatial memory strategy or develop habitual responses by developing stimulus-response associations. It has been shown that the hippocampus is involved when spatial memory is used, but that the habitual approach is associated with activation in the basal ganglia (Iaria, Petrides, Dagher, Pike, & Bohbot, 2003). However, to our knowledge, this is the first time that the opposition between learning strategies has been linked to the activity of different brain regions at rest.

## **Conclusion**

Taken together, and to the best of our knowledge, our findings provide the first evidence for a direct relationship between cortical spectral power, measured with MEG at rest, and verbal learning strategy as assessed by standardized neuropsychological tests (CVLT-2) outside the scanner. Resting state MEG power showed specific positive and negative correlation clusters as a function of the strategy that the subject later used when performing a verbal memory task. Semantic clustering and global verbal learning performance showed a closely related brain correlation pattern, which suggests a common semantic neural network. Auditory regions in the left hemisphere predicted a semantic advantage over serial strategy, while hippocampal regions predicted a serial advantage over semantic strategy. The next step would be to record the brain activity during a verbal learning task and test whether the prediction using the resting state MEG would be confirmed by a relative greater use of the hippocampus or the semantic network.

## References

- Abe, M., & Hanakawa, T. (2009). Functional coupling underlying motor and cognitive functions of the dorsal premotor cortex. *Behavioural Brain Research*, 198(1), 13–23. <https://doi.org/10.1016/j.bbr.2008.10.046>
- Abe, M., Hanakawa, T., Takayama, Y., Kuroki, C., Ogawa, S., & Fukuyama, H. (2007). Functional Coupling of Human Prefrontal and Premotor Areas during Cognitive Manipulation. *The Journal of Neuroscience*, 27(13), 3429. doi:10.1523/JNEUROSCI.4273-06.2007
- Alexander, M. P., Stuss, D. T., & Fansabedian, N. (2003). California Verbal Learning Test: Performance by patients with focal frontal and non-frontal lesions. *Brain*, 126(6), 1493–1503. <https://doi.org/10.1093/brain/awg128>
- Aslaksen, P. M., Bystad, M. K., Ørbo, M. C., & Vangberg, T. R. (2018). The relation of hippocampal subfield volumes to verbal episodic memory measured by the California Verbal Learning Test II in healthy adults. *Behavioural Brain Research*, 351(January), 131–137. <https://doi.org/10.1016/j.bbr.2018.06.008>
- Atkinson, R. C., & Shiffrin, R. M. (1968). *Human Memory: A Proposed System and its Control Processes* This research was supported by the National Aeronautics and Space Administration, Grant No. NGR-05-020-036. The authors are indebted to W. K. Estes and G. H. Bower who provided many valuable suggestions (K. W. Spence & J. T. B. T.-P. of L. and M. Spence (eds.); Vol. 2, pp. 89–195). Academic Press. [https://doi.org/https://doi.org/10.1016/S0079-7421\(08\)60422-3](https://doi.org/https://doi.org/10.1016/S0079-7421(08)60422-3)
- Baldo, J. V., Delis, D., Kramer, J., & Shimamura, A. P. (2020). *Memory performance on the California Verbal Learning Test – II : Findings from patients with focal frontal lesions*. 2002, 539–546.
- Barron, H. C., Auztulewicz, R., & Friston, K. (2020). Prediction and memory: A predictive coding account. *Progress in Neurobiology*, 192, 101821. doi:<https://doi.org/10.1016/j.pneurobio.2020.101821>
- Binder, J. R., Conant, L. L., Humphries, C. J., Fernandino, L., Simons, S. B., Aguilar, M., & Desai, R. H. (2016). Toward a brain-based componential semantic representation. *Cognitive*

- Neuropsychology*, 33(3–4), 130–174. <https://doi.org/10.1080/02643294.2016.1147426>
- Binder, J. R., & Desai, R. H. (2011). The neurobiology of semantic memory. *Trends in Cognitive Sciences*, 15(11), 527–536. <https://doi.org/10.1016/j.tics.2011.10.001>
- Binder, J. R., Desai, R. H., Graves, W. W., & Conant, L. L. (2009). Where is the semantic system? A critical review and meta-analysis of 120 functional neuroimaging studies. *Cerebral Cortex*, 19(12), 2767–2796. <https://doi.org/10.1093/cercor/bhp055>
- Bruffaerts, R., De Deyne, S., Meersmans, K., Liuzzi, A. G., Storms, G., & Vandenberghe, R. (2019). Redefining the resolution of semantic knowledge in the brain: Advances made by the introduction of models of semantics in neuroimaging. *Neuroscience and Biobehavioral Reviews*, 103(March), 3–13. <https://doi.org/10.1016/j.neubiorev.2019.05.015>
- Buchsbaum, B. R., & D’Esposito, M. (2008). The search for the phonological store: From loop to convolution. *Journal of Cognitive Neuroscience*, 20(5), 762–778. <https://doi.org/10.1162/jocn.2008.20501>
- Buchsbaum, B. R., & D’Esposito, M. (2019). A sensorimotor view of verbal working memory. *Cortex*, 112, 134–148. <https://doi.org/10.1016/j.cortex.2018.11.010>
- Burianová, H., Ciaramelli, E., Grady, C. L., & Moscovitch, M. (2012). Top-down and bottom-up attention-to-memory: Mapping functional connectivity in two distinct networks that underlie cued and uncued recognition memory. *Neuroimage*, 63(3), 1343–1352. doi:<https://doi.org/10.1016/j.neuroimage.2012.07.057>
- Cabeza, R. (2008). Role of parietal regions in episodic memory retrieval: The dual attentional processes hypothesis. *Neuropsychologia*, 46(7), 1813–1827. doi:<https://doi.org/10.1016/j.neuropsychologia.2008.03.019>
- Carpenter, A. F., Baud-Bovy, G., Georgopoulos, A. P., & Pellizzer, G. (2018). Encoding of serial order in working memory: Neuronal activity in motor, premotor, and prefrontal cortex during a memory scanning task. *Journal of Neuroscience*, 38(21), 4912–4933. <https://doi.org/10.1523/JNEUROSCI.3294-17.2018>
- Casasanto, D. J., Killgore, W. D. S., Maldjian, J. A., Glosser, G., Alsop, D. C., Cooke, A. M., Grossman,

- M., & Detre, J. A. (2002). Neural correlates of successful and unsuccessful verbal memory encoding. *Brain and Language*, *80*(3), 287–295. <https://doi.org/10.1006/brln.2001.2584>
- Chen, S. H., & Desmond, J. E. (2005). Temporal dynamics of cerebro-cerebellar network recruitment during a cognitive task. *Neuropsychologia*, *43*(9), 1227-1237. doi:S0028-3932(05)00010-2 [pii];10.1016/j.neuropsychologia.2004.12.015 [doi]
- Ciaramelli, E., Grady, C. L., & Moscovitch, M. (2008). Top-down and bottom-up attention to memory: A hypothesis (AtoM) on the role of the posterior parietal cortex in memory retrieval. *Neuropsychologia*, *46*(7), 1828-1851. doi:<https://doi.org/10.1016/j.neuropsychologia.2008.03.022>
- Crosson, B., Novack, T. A., Trenerry, M. R., Craig, P. L., Crosson, B., Novack, T. A., Trenerry, M. R., Craig, P. L., & Crosson, B. (2008). *California verbal learning test ( CVLT ) performance in severely head-injured and neurologically normal adult males California Verbal Learning Test ( CVLT ) Performance in Severely Head-Injured and Neurologically Normal Adult Males \**. 8634. <https://doi.org/10.1080/01688638808402812>
- Davachi, L., & DuBrow, S. (2015). How the hippocampus preserves order: the role of prediction and context. *Trends in cognitive sciences*, *19*(2), 92-99. doi:<https://doi.org/10.1016/j.tics.2014.12.004>
- D.C. Delis, J.H. Kramer, E. Kaplan, B. A. O. (2000). California Verbal Learning Test – second edition. Adult version. Manual. *Psychological Corporation, San Antonio, TX*.
- Dudai, Y. (2012). The restless engram: Consolidations never end. *Annual Review of Neuroscience*, *35*, 227–247. <https://doi.org/10.1146/annurev-neuro-062111-150500>
- Elger, C. E., Grunwald, T., Lehnertz, K., Kutas, M., Helmstaedter, C., Brockhaus, A., Van Roost, D., & Heinze, H. J. (1997). Human temporal lobe potentials in verbal learning and memory processes. *Neuropsychologia*, *35*(5), 657–667. [https://doi.org/10.1016/S0028-3932\(96\)00110-8](https://doi.org/10.1016/S0028-3932(96)00110-8)
- Herman, A. B., Houde, J. F., Vinogradov, S., & Nagarajan, S. S. (2013). Parsing the Phonological Loop: Activation Timing in the Dorsal Speech Stream Determines Accuracy in Speech

Reproduction. *The Journal of Neuroscience*, 33(13), 5439. doi:10.1523/JNEUROSCI.1472-12.2013

Gallese, V., & Cuccio, V. (2018). The neural exploitation hypothesis and its implications for an embodied approach to language and cognition: Insights from the study of action verbs processing and motor disorders in Parkinson's disease. *Cortex*, 100, 215–225. <https://doi.org/10.1016/j.cortex.2018.01.010>

Gallese, V., & Lakoff, G. (2005). The brain's concepts: The role of the sensory-motor system in conceptual knowledge. *Cognitive Neuropsychology*, 22(3–4), 455–479. <https://doi.org/10.1080/02643290442000310>

Gsottschneider, A., Keller, Z., Pitschel-Walz, G., Froböse, T., & Jahn, T. (2011). The role of encoding strategies in the verbal memory performance in patients with schizophrenia. *Journal of Neuropsychology*, 5(1), 56–72. <https://doi.org/10.1348/174866410X497382>

Halgren, E., Dhond, R. P., Christensen, N., Van Petten, C., Marinkovic, K., Lewine, J. D., & Dale, A. M. (2002). N400-like magnetoencephalography responses modulated by semantic context, word frequency, and lexical class in sentences. *NeuroImage*, 17(3), 1101–1116. <https://doi.org/10.1006/nimg.2002.1268>

Hanakawa, T., Honda, M., Okada, T., Fukuyama, H., & Shibasaki, H. (2003). Differential activity in the premotor cortex subdivisions in humans during mental calculation and verbal rehearsal tasks: A functional magnetic resonance imaging study. *Neuroscience Letters*, 347(3), 199–201. [https://doi.org/10.1016/S0304-3940\(03\)00692-X](https://doi.org/10.1016/S0304-3940(03)00692-X)

Healey, M. K., Long, N. M., & Kahana, M. J. (2019). Contiguity in episodic memory Basic properties of the contiguity effect Finding 1 : Temporal contiguity in free recall. *Psychonomic Bulletin and Review*, 699–720.

Heinze, S., Sartory, G., Müller, B. W., de Greiff, A., Forsting, M., & Jüptner, M. (2006). Neural encoding correlates of high and low verbal memory performance. *Journal of Psychophysiology*, 20(2), 68–78. <https://doi.org/10.1027/0269-8803.20.2.68>

Hickok, G., & Poeppel, D. (2007). The cortical organization of speech understanding. *Nature*,

8(May), 393–402. [www.nature.com/reviews/neuro](http://www.nature.com/reviews/neuro)<https://www-nature-com.ezp-prod1.hul.harvard.edu/articles/nrn2113.pdf>

Iaria, G., Petrides, M., Dagher, A., Pike, B., & Bohbot, V. D. (2003). Cognitive strategies dependent on the hippocampus and caudate nucleus in human navigation: variability and change with practice. *J Neurosci*, *23*(13), 5945-5952.

Josselyn, S. A., Köhler, S., & Frankland, P. W. (2015). Finding the engram. *Nature Reviews Neuroscience*, *16*(9), 521–534. <https://doi.org/10.1038/nrn4000>

Kapur, S., Tulving, E., Cabeza, R., McIntosh, A. R., Houle, S., & Craik, F. I. M. (1996). The neural correlates of intentional learning of verbal materials: A PET study in humans. *Cognitive Brain Research*, *4*(4), 243–249. [https://doi.org/10.1016/S0926-6410\(96\)00058-4](https://doi.org/10.1016/S0926-6410(96)00058-4)

Kibby, M. Y., Schmitter-Edgecombe, M., & Long, C. J. (1998). Ecological validity of neuropsychological tests: focus on the California Verbal Learning Test and the Wisconsin Card Sorting Test. *Archives of Clinical Neuropsychology : The Official Journal of the National Academy of Neuropsychologists*, *13*(6), 523–534.

Linden, D. E., Bittner, R. A., Muckli, L., Waltz, J. A., Kriegeskorte, N., Goebel, R., . . . Munk, M. H. (2003). Cortical capacity constraints for visual working memory: dissociation of fMRI load effects in a fronto-parietal network. *Neuroimage*, *20*(3), 1518-1530. doi:S1053811903004725 [pii]

Lopes, T. M., Yasuda, C. L., Campos, B. M. de, Balthazar, M. L. F., Binder, J. R., & Cendes, F. (2016). Effects of task complexity on activation of language areas in a semantic decision fMRI protocol. *Neuropsychologia*, *81*, 140–148. <https://doi.org/10.1016/j.neuropsychologia.2015.12.020>

Majerus, S., Attout, L., D'Argembeau, A., Degueldre, C., Fias, W., Maquet, P., . . . Balteau, E. (2012). Attention supports verbal short-term memory via competition between dorsal and ventral attention networks. *Cereb. Cortex*, *22*(5), 1086-1097. doi:bhr174 [pii];10.1093/cercor/bhr174 [doi]



- Majerus, S., Bastin, C., Poncelet, M., Van der Linden, M., Salmon, E., Collette, F., & Maquet, P. (2007). Short-term memory and the left intraparietal sulcus: focus of attention? Further evidence from a face short-term memory paradigm. *Neuroimage*, *35*(1), 353-367. doi:S1053-8119(06)01200-6 [pii];10.1016/j.neuroimage.2006.12.008 [doi]
- Majerus, S., Belayachi, S., De, S. B., Leclercq, A. L., Martinez, T., Schmidt, C., . . . Maquet, P. (2008). Neural networks for short-term memory for order differentiate high and low proficiency bilinguals. *Neuroimage*, *42*(4), 1698-1713. doi:S1053-8119(08)00723-4 [pii];10.1016/j.neuroimage.2008.06.003 [doi]
- Majerus, S., D'Argembeau, A., Martinez, P. T., Belayachi, S., Van der Linden, M., Collette, F., . . . Maquet, P. (2010). The commonality of neural networks for verbal and visual short-term memory. *J. Cogn Neurosci*, *22*(11), 2570-2593. doi:10.1162/jocn.2009.21378 [doi]
- Majerus, S., Poncelet, M., Van der Linden, M., Albouy, G., Salmon, E., Sterpenich, V., . . . Maquet, P. (2006). The left intraparietal sulcus and verbal short-term memory: focus of attention or serial order? *Neuroimage*, *32*(2), 880-891. doi:S1053-8119(06)00240-0 [pii];10.1016/j.neuroimage.2006.03.048 [doi]
- Majerus, S., Salmon, E., & Attout, L. (2013). The importance of encoding-related neural dynamics in the prediction of inter-individual differences in verbal working memory performance. *PLoS. One*, *8*(7), e69278. doi:10.1371/journal.pone.0069278 [doi];PONE-D-13-10509 [pii]
- Miotto, E. C., Balardin, J. B., da Graça M Martin, M., Polanczyk, G. V., Savage, C. R., Miguel, E. C., & Batistuzzo, M. C. (2020). Effects of semantic categorization strategy training on episodic memory in children and adolescents. *PLoS ONE*, *15*(2), 1–17. <https://doi.org/10.1371/journal.pone.0228866>
- Miotto, E. C., Balardin, J. B., Savage, C. R., Martin, M. da G. M., Batistuzzo, M. C., Amaro Junior, E., & Nitrini, R. (2014). Brain regions supporting verbal memory improvement in healthy older subjects. *Arquivos de Neuro-Psiquiatria*, *72*(9), 663–670. <https://doi.org/10.1590/0004-282X20140120>

- Miotto, E. C., Savage, C. R., Evans, J. J., Wilson, B. A., Martins, M. G. M., Iaki, S., & Amaro, E. (2006). Bilateral activation of the prefrontal cortex after strategic semantic cognitive training. *Human Brain Mapping, 27*(4), 288–295. <https://doi.org/10.1002/hbm.20184>
- Moscovitch, M., Cabeza, R., Winocur, G., & Nadel, L. (2016). Episodic memory and beyond: The hippocampus and neocortex in transformation. *Annual Review of Psychology, 67*, 105–134. <https://doi.org/10.1146/annurev-psych-113011-143733>
- Mousavi, N., Nazari, M. A., Babapour, J., & Jahan, A. (2020). Electroencephalographic characteristics of word finding during phonological and semantic verbal fluency tasks. *Neuropsychopharmacology Reports, 40*(3), 254–261. <https://doi.org/10.1002/npr2.12129>
- Mueller, S. G., Chao, L. L., Berman, B., & Weiner, M. W. (2011). Evidence for functional specialization of hippocampal subfields detected by MR subfield volumetry on high resolution images at 4T. *NeuroImage, 56*(3), 851–857. <https://doi.org/10.1016/j.neuroimage.2011.03.028>
- Olsen, R. K., Moses, S. N., Riggs, L., & Ryan, J. D. (2012). The hippocampus supports multiple cognitive processes through relational binding and comparison. *Frontiers in Human Neuroscience, 6*(MAY 2012), 1–13. <https://doi.org/10.3389/fnhum.2012.00146>
- Oswald, V., Zerouali, Y., Boulet-Craig, A., Krajcinovic, M., Laverdière, C., Sinnett, D., Jolicoeur, P., Lippé, S., Jerbi, K., & Robaey, P. (2017). Spontaneous brain oscillations as neural fingerprints of working memory capacities: A resting-state MEG study. *Cortex, 97*, 109–124. <https://doi.org/10.1016/j.cortex.2017.09.021>
- Rabin, L. A., Barr, W. B., & Burton, L. A. (2005). *Assessment practices of clinical neuropsychologists in the United States and Canada : A survey of INS , NAN , and APA Division 40 members & . 20*, 33–65. <https://doi.org/10.1016/j.acn.2004.02.005>
- Reber, P. J., Siwiec, R. M., Gitleman, D. R., Parrish, T. B., Mesulam, M. M., & Paller, K. A. (2002). Neural correlates of successful encoding identified using functional magnetic resonance imaging. *Journal of Neuroscience, 22*(21), 9541–9548. <https://doi.org/10.1523/jneurosci.22-21-09541.2002>

- Saykin, A. J., Johnson, S. C., Flashman, L. A., McAllister, T. W., Sparling, M., Darcey, T. M., Moritz, C. H., Guerin, S. J., Weaver, J., & Mamourian, A. (1999). Functional differentiation of medial temporal and frontal regions involved in processing novel and familiar words: An fMRI study. *Brain*, *122*(10), 1963–1971. <https://doi.org/10.1093/brain/122.10.1963>
- Serruya, M. D., Sederberg, P. B., & Kahana, M. J. (2014). Power shifts track serial position and modulate encoding in human episodic memory. *Cerebral Cortex*, *24*(2), 403–413. <https://doi.org/10.1093/cercor/bhs318>
- Tonegawa, S., Liu, X., Ramirez, S., & Redondo, R. (2015). Memory Engram Cells Have Come of Age. *Neuron*, *87*(5), 918–931. <https://doi.org/10.1016/j.neuron.2015.08.002>
- Tulving, E. (1972). Episodic and semantic memory. In *Organization of memory*. (pp. xiii, 423–xiii, 423). Academic Press.
- Turner, A. D., Furey, M. L., Drevets, W. C., Zarate, C., & Nugent, A. C. (2012). Association between subcortical volumes and verbal memory in unmedicated depressed patients and healthy controls. *Neuropsychologia*, *50*(9), 2348–2355. <https://doi.org/10.1016/j.neuropsychologia.2012.06.003>
- Yonelinas, A. P. (2013). The hippocampus supports high-resolution binding in the service of perception, working memory and long-term memory. *Behavioural Brain Research*, *254*, 34–44. <https://doi.org/10.1016/j.bbr.2013.05.030>

## Table and Figures

<b>Neuropsychological Results score tests (n=28)</b>	<b>Score mean (SD) [min-max]</b>
CVLT mean performance trial 1 to 5 (words)	58.89 (7.37) [42-69]
CVLT learning slope trial 1 to 3	2.55 (1.14) [0.5-4.5]
CVLT learning slope trial 3 to 5	0.64 (1.03) [-1.5-3.5]
CVLT mean performance trial 1 to 5 semantic strategy	1.95 (2.58) [-0.9-6.9]
CVLT mean performance trial 1 to 5 serial Backward	0.61 (1.40) [-1.4-3.3]
CVLT mean performance trial 1 to 5 serial Forward	0.45 (1.10) [-0.8-3.6]

Tableau 2. – Table 1: Learning performance and strategy correlation trial by trial in CVLT-2 (n=28)

<b>Correlation with mean row performance trial 1 to 5 (n=28)</b>	<b>Pearson coefficient (p_value)</b>
Semantic strategy	.49 (0.007)
Serial Backward	-.15 (0.43)
Serial forward	-.07 (0.70)

Tableau 3. – Table 2: Correlation between mean performance and strategy used across the fifth trial correlation trial (n=28)

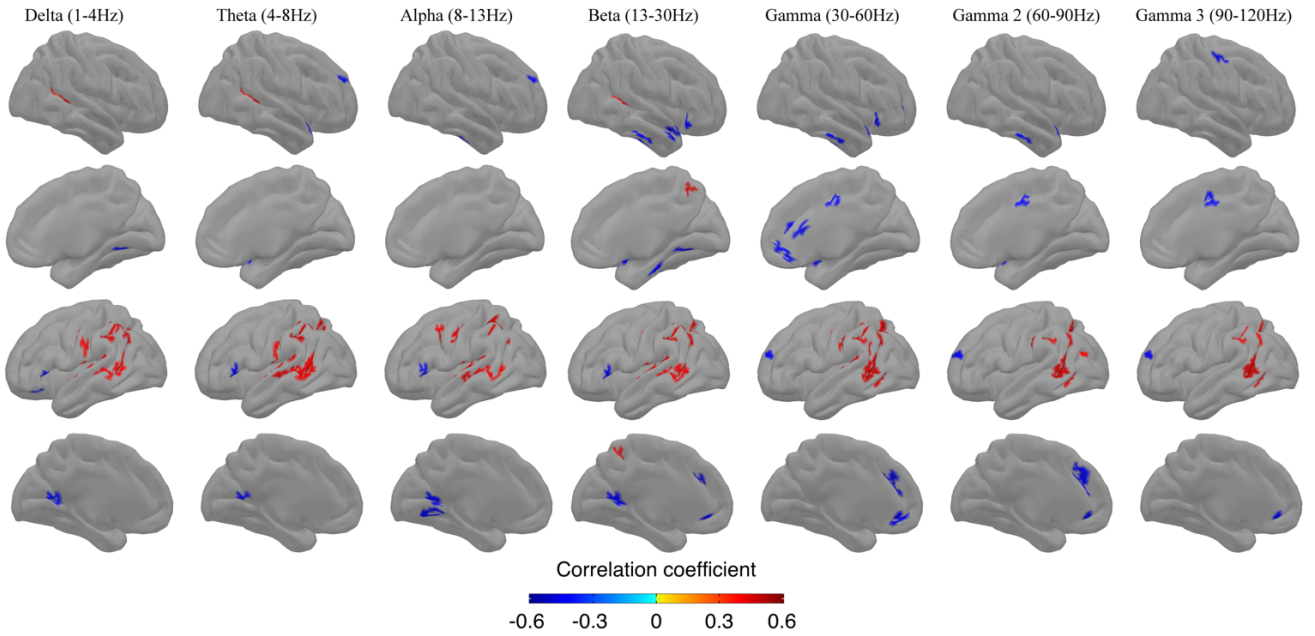


Figure 29. – Brain-behaviour correlation/anticorrelation pattern (corrected:  $p > 0,001$ ) with mean raw performance between trial 1 to 5 in CVLT-2.

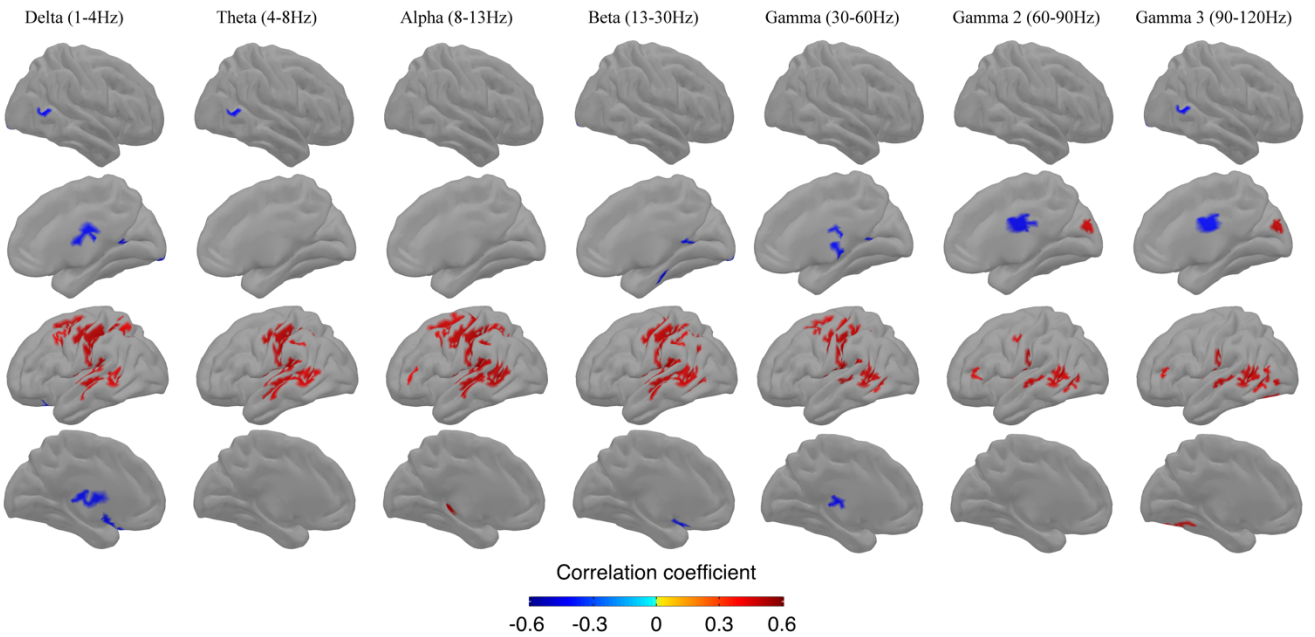


Figure 30. – Brain-behaviour correlation/anticorrelation pattern (corrected:  $p > 0,001$ ) with Semantic strategy indices grouping related to performance in trial 1 to 5 in CVLT-2.

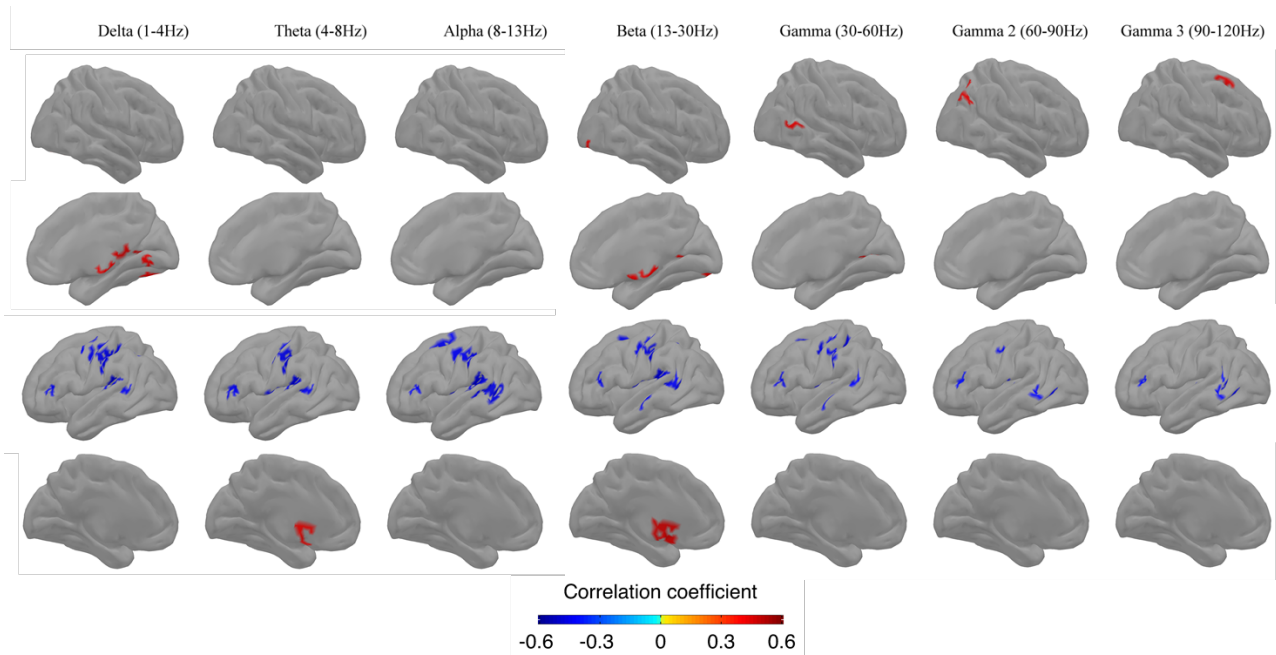


Figure 31. – Brain-behaviour correlation/anticorrelation pattern (corrected:  $p > 0,001$ ) with Serial Backward strategy indices grouping related to performance in trial 1 to 5 in CVLT-2.

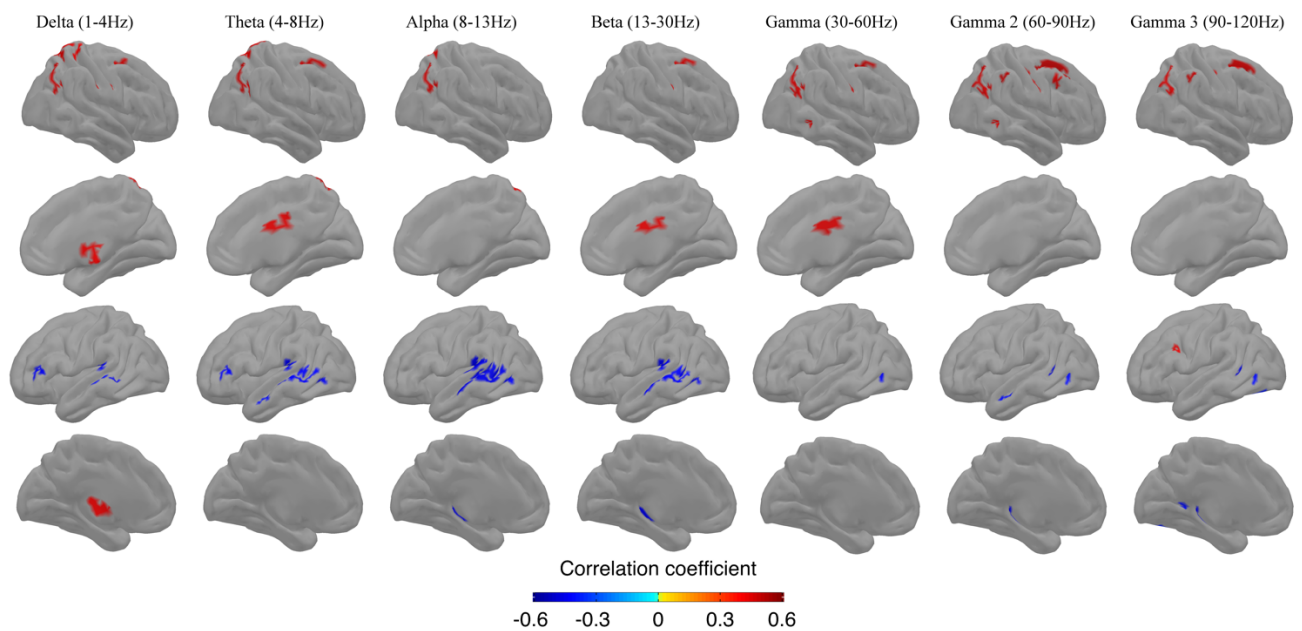


Figure 32. – Brain-behaviour correlation/anticorrelation pattern (corrected:  $p > 0,001$ ) with Serial Forward strategy indices grouping related to performance in trial 1 to 5 in CVLT-2.

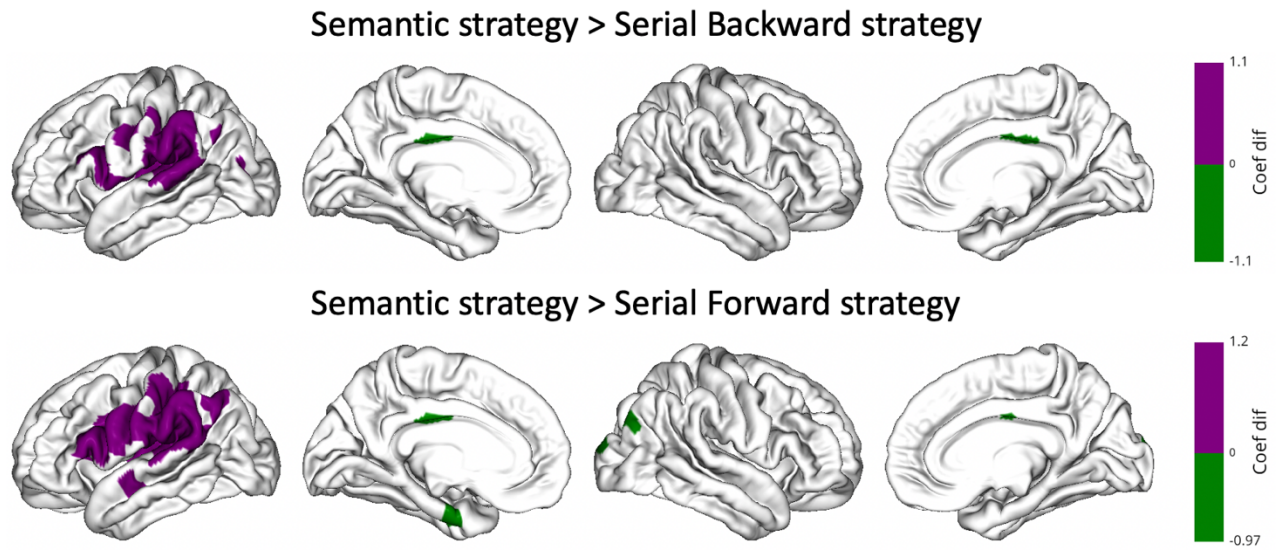


Figure 33. – Comparison between Correlation/Anticorrelation pattern in strategy: Significant difference (FDR  $p > 0,05$ ) between correlation pattern between strategies across all frequencies, upper line show difference between semantic strategies minus serial backward strategies, lower line show difference between semantic strategies minus serial forward strategies.

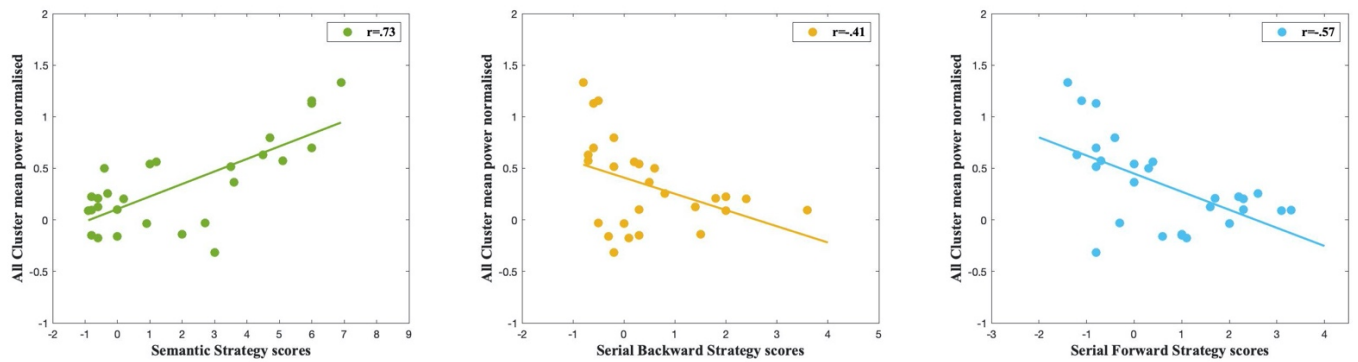


Figure 34. – Scatter plot between normalized power and strategies scores: mean across clusters and frequencies show correlation relationship with semantic scores (left), Serial backward scores (middle) and serial forward scores (right). The spatial mask is spatial

## Supplementary figures

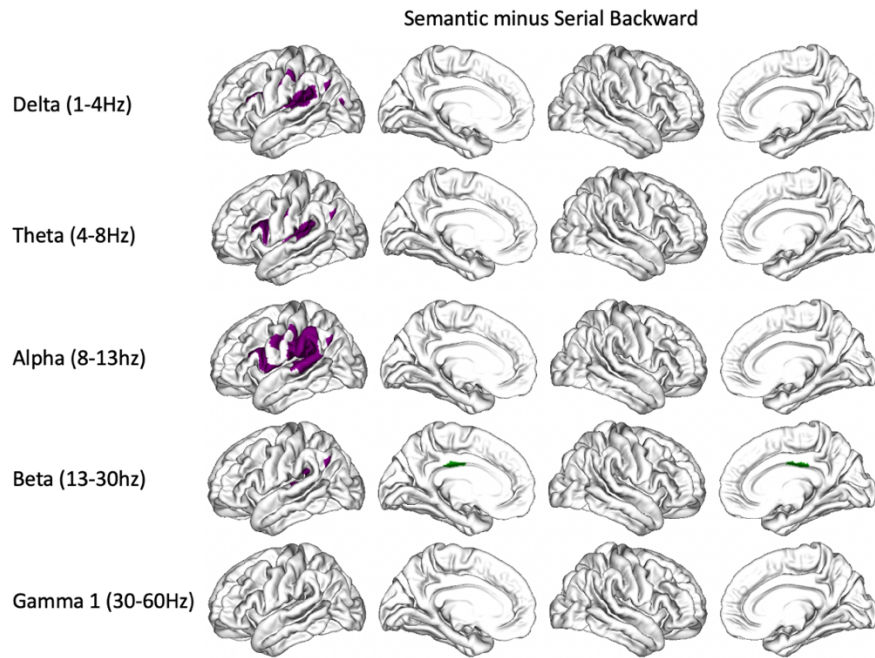


Figure 35. – Figure Supplementary 1: Comparison between Correlation/Anticorrelation pattern in strategy in all frequency: Significant difference (FDR  $p > 0,05$ ) between correlation pattern in semantic strategies minus serial backward strategies



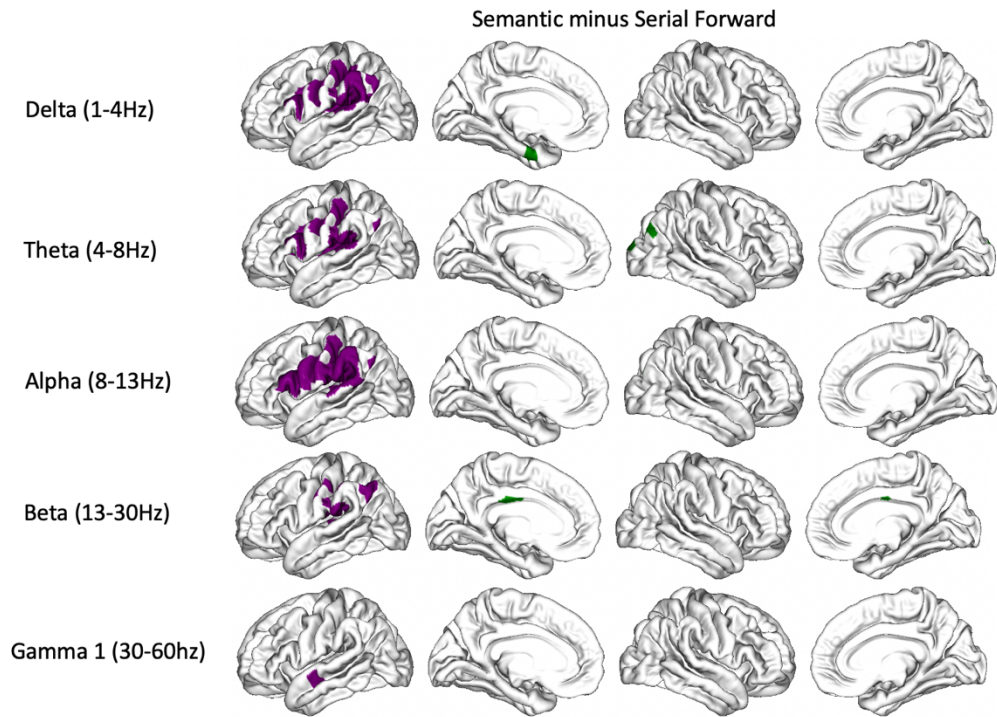


Figure 36. – Figure Supplementary 2: Comparison between Correlation/Anticorrelation pattern in strategy in all frequency: Significant difference (FDR  $p > 0,05$ ) between correlation pattern in semantic strategies minus serial forward strategies

# **Chapitre 5 — Enhanced alpha long-range brain synchrony mediates the long-term effects of intrathecal methotrexate on executive deficits in ALL survivors**

Victor Oswald<sup>1,2</sup>, David Meunier<sup>3</sup>, Tarek Lanef<sup>4</sup>, Aubrée Boulet-Craig<sup>4</sup>, Maja Krajinovic<sup>1</sup>, Caroline Laverdière<sup>6</sup>, Daniel Sinnett<sup>1</sup>, Pierre Jolicoeur<sup>4</sup>, Sarah Lippé<sup>1,4</sup>, Karim Jerbi<sup>2,4</sup>, Philippe Robaey<sup>1,6</sup>

<sup>1</sup>Service hématologie-oncologie, Charles-Bruneau Cancer Center, CHU Sainte-Justine, Montréal, QC, Canada.

<sup>2</sup>Department of Neuroscience, Faculty of Medicine, University of Montreal, Montreal, Qc, Canada.

<sup>3</sup>Aix Marseille Univ, CNRS, INT, Institut de Neurosciences de la Timone, Marseille, France

<sup>4</sup>Department of Psychology, University of Montreal, Montreal, QC, Canada

<sup>5</sup>Department of Pediatric, CHU Sainte-Justine Research Center, Montreal, QC, Canada.

<sup>6</sup>Children's Hospital of Eastern Ontario, Ottawa, ON, Canada.

## Abstract

**Purpose:** To determine whether MEG-based spectral connectivity could be a marker of the mechanisms linking cumulative dose of chemotherapy and executive deficits in long-term acute lymphoblastic leukemia (ALL) survivors.

**Patients and Method:** We recruited controls and long term ALL survivors 5 or more years after diagnosis ( $\geq 18$  years). Both groups performed neuropsychological assessments and a recording of passive resting state (5 min) in magnetoencephalography neuroimaging. We measured long-range brain synchrony (LRS) in the canonical frequencies bands at rest. We compared brain LRS between controls and patients with or poor cognitive performance respectively, based on the scores of the DIVERGT battery tests. We computed the correlations between LRS and cognitive performance and chemotherapy cumulative doses during treatment. Finally, we tested the hypothesis that LRS mediated the relationships between chemotherapy cumulative doses and long-term neuropsychological performance.

**Results:** We found that ALL survivors had higher LRS than controls for the theta band (4–8 Hz) in 4 resting state networks (control, default, dorsal attention and visual). ALL survivors with poor DIVERGT scores showed an increase in LRS in alpha band (8–13 Hz) across the whole brain. Higher cumulative dose of IT-MTX correlated with lower DIVERGT scores, more specifically with scores at cognitive flexibility and working memory tests. This effect was partially mediated by increased whole-brain LRS at rest in the alpha band, but not in the theta band.

**Conclusions:** In ALL survivors, excess in alpha LRS at rest is a functional marker for executive deficits. This marker may be useful to monitor brain health and as a target for remediation.

**Keywords:** long-term Acute Lymphoblastic Leukemia (ALL) survivors, magnetoencephalography (MEG), spectral connectivity, long-range synchrony, resting state, IT methotrexate, cognitive impairment.

## Introduction

A sizable proportion (15 to 30%) of long-term survivors of childhood Acute Lymphoblastic Leukemia (ALL) has severe deficits in executive functions, attention and memory<sup>1</sup>. These deficits increase in rate with cranial radiation therapy (CRT) dose, earlier age at diagnosis, longer time elapsed from diagnosis, and female sex<sup>2, 3</sup>. However, even in absence of CRT, or after controlling for CRT, chemotherapy, c also increases the risk of cognitive impairment, especially for attention and executive functions<sup>1</sup>. CRT and MTX impair plasticity of synapse structure and function, and of myelin, through microglial activation<sup>4, 5</sup>. As a consequence, long-term ALL survivors show white matter (WM) microstructural anomalies. Magnetic Resonance Imaging (MRI) studies mostly reported decreased  $c^{6-10}$  and increased radial diffusivity (RD)<sup>7</sup>, but sometimes increased FA/decreased RD<sup>11</sup>, in different WM structures. CRT doses definitely contributed to these microstructural anomalies<sup>6, 9-11</sup>, but exposure to high dose of MTX was also associated with increased axial diffusivity<sup>12</sup>. In addition, both cognitive deficits<sup>1</sup> and WM microstructural anomalies<sup>6</sup> are worse when children are younger at diagnosis. White matter tracts are organized at birth and their microstructure develops rapidly in infancy and early childhood, largely driven by increasing myelination. WM microstructure continues to develop at a slower pace into adulthood, primarily by increasing axonal packing<sup>13</sup>. Pubertal processes affect WM microstructure differently in boys and girls, at least partially through the effect of sex steroids<sup>14-16</sup>. Moreover, pubertal stage partly mediated the effect of environment on WM microstructure in brain regions such as the anterior cingulate, especially in girls<sup>17</sup>.

Microstructural WM anomalies alter brain anatomical and functional connectivity. At rest, functional connectivity can be assessed by the temporal correlations between BOLD signals from separate regions. For example, brain regions that mature earliest showed hyperconnectivity in survivors with executive deficits<sup>18</sup>. Connectivity networks can be further characterized by graph-based approaches. Efficiency indexes how effectively information is integrated locally between immediate neighbours, or globally across the whole brain. Global efficiency was decreased for both structural and functional connectomes in ALL survivors with executive impairments, as compared with those without<sup>18</sup>. Global efficiency was also lower for those who were younger at di

agnosis, or treated with a greater number of intrathecal MTX<sup>18</sup>. However the BOLD signal measures the neuronal activity through slow neurovascular coupling, while the magnetic field produced by current flows along neurons provides a more direct measure on a millisecond timescale<sup>19</sup>. Brain oscillatory activities reflect cyclic inhibition, and only neuronal groups that coherently oscillate can interact effectively<sup>20</sup>. For example, controlling the phase lag of alpha oscillations (9–12 Hz) between distant neural populations would enable fast-changing long-distance cortical coordination, and support adaptive control in executive functions<sup>21</sup>. Measures of spectral synchrony as phase-lag coupling should allow detecting possible abnormal or compensatory mechanisms in ALL survivors.

Our hypothesis is that WM microstructure should have direct effects on the synchronization of oscillations across distant cortical regions. We recorded resting-state MEG in long-term survivors and healthy controls matched on age and sex. First, we tested the differences in a phase lag coupling index for the different MEG frequency bands between controls and survivors (at least 5 years after treatment) with and without cognitive deficits. Second, we computed the correlations between cumulative doses of chemotherapeutic drugs (MTX, GC, leucovorin), spectral synchrony and the cognitive deficits, and finally tested whether spectral synchrony mediated the relationships between cumulative doses and cognitive impairment. To further control WM changes related to age, specifically to puberty, we only included ALL patients diagnosed until the age of 12 - before menarche<sup>22</sup>, which still represent 82% of all pediatric ALL diagnoses<sup>23</sup>.

## **Population**

This study was included in the PETALE study conducted at Sainte-Justine University Health Center. We recruited 50 ALL survivors who were treated on DFCI-ALL 87-01 to 2005-01 protocols, at least five years' post-diagnosis and with no history of refractory ALL, relapse, or hematopoietic stem cells transplant. Intensive intrathecal chemotherapy (ITC) substituted CRT in low-risk patients. Patients that were not irradiated received more frequently triple ITC composed of methotrexate, cytarabine and hydrocortisone. We computed the cumulative dose of intrathecal MTX (IT-MTX), intravenous MTX (IV-MTX), leucovorin and glucocorticosteroid (GCS), using the equity rule:

0.75 mg/m<sup>2</sup>, DEX=5 mg/m<sup>2</sup> PRED. Age of diagnosis was negatively correlated with IT-MTX ( $r=-.446$ ;  $p=0.027$ ), but not with IV-MTX ( $r=.33$ ;  $p=0.05$ ) or GCS ( $r=-.047$ ;  $p=0.786$ ).

We also recruited 45 age and sex-matched healthy adult subjects, with no reported history of neurological or psychiatric disorder through social networks, online advertising and posters on hospital billboards. Participants were mostly of European descent (97% of ALL survivors and 90% of controls) and were French-speaking. The study was approved by SJUHC Institutional Review Board. All participants agreed to participate in the study and signed an informed consent form.

### **Neuropsychological Assessment**

The participants completed a neuropsychological evaluation, equivalent to the DIVERGT screening procedure<sup>24</sup>. We described the procedure in a previous paper<sup>25</sup>. We a priori selected 4 specific conditions: Trail Making Test – Condition 4: Number-Letter Switching, Verbal Fluency – Letter, Digit Span-Global Score and Grooved Pegboard –Dominant Hand. Follow-up evaluation included French-Canadian versions of Similarities, Vocabulary, Block design, Matrix Reasoning, Code and Symbol Search (WAIS-IV)<sup>26, 27</sup>.

### **MEG & MRI Acquisition and Pre-Processing**

All subjects were comfortably seated with eyes open, fixating on a back-illuminated screen located 75 cm in front of them. Two 5-minute periods of resting state were recorded at a sampling rate of 1200 Hz, using a CTF-VSM whole head 275-sensor MEG system, as described previously<sup>28</sup>. MEG data pre-processing was performed using the Matlab-based Brainstorm open-source software<sup>28</sup>.

### **Cortical Sources Estimation and Spectral Connectivity Analysis**

MEG source reconstruction was performed using a standard weighted minimum-norm approach, with the Brainstorm software<sup>29</sup>. T1-weighted brain volumes were acquired in all participants and were used to generate a cortical surface model, using the FreeSurfer software package<sup>30</sup>. Forward modelling of the magnetic field was defined based on an overlapping-sphere method<sup>31</sup>. The weighted minimum norm solution was computed using a loose dipolar orientation constraint (set at 0.5), a signal-to-noise ratio of 3, whitening PCA and a depth weighting of 0.5<sup>32</sup>. The noise

covariance matrix for each participant was estimated from a 2-min empty room recording performed earlier the same day (same acquisition parameters but with no subject in the shielded room, e.g.<sup>33</sup>). The source time series were initially reconstructed on a 15000-vertex individual brain tessellation, and then spatially interpolated to the MNI ICBM152 brain template and down-sampled to a 4000-vertices template.

Resting state spectral connectivity was measured using the Weighted Phase Lag Index (wPLI) method. In WPLI the contribution of the observed phase leads and lags is weighted by the magnitude of the imaginary component of the cross-spectrum<sup>34</sup>. Here, we used the package `neuropype_ephy` (<https://github.com/davidmeunier79>) which used `mne.connectivity.spectral_connectivity` function from `mne` toolbox (<https://mne.tools/stable/index.html>) to perform spectral connectivity. A sliding window (3 sec) was used to analyze 4 minutes of resting state recording for all frequency bands (except for the delta band, we used 5 sec window) and we computed the mean connectivity value across the window for all participants in the following frequency bands: delta (1–4 Hz), theta (4–8 Hz), alpha (8–13 Hz), beta (13–30 Hz), gamma 1 (30–60 Hz), gamma 2 (60–90 Hz) and gamma 3 (90–120 Hz). The whole brain connectivity was first computed over 4000 nodes. Second, we averaged edges value using the parcellation of 7 resting state networks<sup>35</sup>.

## Statistical Analyses

We tested normality of data with the Shapiro–Wilk test. To test the difference between group in network spectral connectivity, we used t-test with 1000 permutations and we corrected for multiple comparison across networks with FDR correction ( $p < 0.05$ ). Individual correlations between spectral connectivity, medication doses, cognitive performance and age at diagnosis were performed with Spearman correlation tests. Finally, we performed mediation analyses using the toolbox PROCESS v3.5 implemented in SPSS V26<sup>36</sup>.

## Results

### Neuropsychological results (Table 2)

The test scores were significantly lower in ALL survivors than in controls, although within the normal range in both groups. IT-MTX was negatively correlated with the DIVERGT ( $r_s = -.34$ ;  $p = 0.042$ ) but not with FSIQ scores. IV-MTX was correlated neither with the DIVERGT nor the FSIQ scores. The correlations between GCS and the DIVERGT or the FSIQ scores were not significant. We didn't find any significant difference in DIVERGT or FSIQ scores between the ALL patients treated with or without the CRT. Younger age at diagnostic was associated with lower DIVERGT ( $r_s = .49$ ;  $p = 0.002$ ) and FSIQ scores ( $r_s = .58$ ;  $p = 0.001$ ). The correlations remained significant for the DIVERGT ( $r_s = .39$ ;  $p = 0.023$ ) and the FSIQ ( $r_s = .53$ ;  $p < 0.001$ ) after controlling for the total cumulative dose of IT-MTX and of GCS.

### Spectral connectivity

Spectral connectivity in ALL survivors and controls

On average, wPLIs were significantly higher in ALL survivors than in healthy controls for the theta band (4–8 Hz) in different networks: control ( $-0.011$ ,  $p = 0.011$  FDR), default mode ( $-0.014$ ,  $p = 0.011$  FDR-corrected), dorsal attention ( $-0.011$ ,  $p = 0.006$  FDR-corrected) and visual networks ( $-0.022$ ,  $p = 0.019$  FDR-corrected). No significant statistical difference was found between survivors and healthy controls for any other frequency band (Appendix Figure A1).

#### Neuropsychological Scores and Spectral Connectivity

In ALL survivors, the DIVERGT scores were significantly correlated with the wPLI in the alpha band (8–13 Hz) at the whole brain level ( $r_s = -.39$ ;  $p = 0.02$ ). Across resting state networks, the correlations ranged from  $-0.30$  to  $-0.42$ . By contrast the correlations between the DIVERGT scores and wPLI in the theta band were lower (ranging from  $-0.02$  to  $-.27$ ), and not significant at the whole brain level ( $r_s = -.14$ ;  $p = 0.41$ ). In the control group, the correlation between the DIVERGT scores and the whole-brain alpha-wPLI was almost null ( $r_s = -.07$ ;  $p = 0.65$ ), ranging from  $-0.25$  to  $-0.05$  across networks. The correlation with the whole brain theta-wPLI was also very low ( $r_s = .07$ ;  $p = 0.68$ ), with large differences between networks (range:  $-0.35$  to  $0.23$ ).



In order to further explore the differences in wPLI as a function of the DIVERGT scores between the alpha and the theta band, we separated the survivors according to whether their scores overlapped with those of the healthy controls (N=27) or not (N=9): Figure 2. In each network, and at the whole brain level, the alpha-wPLI was significantly stronger in the non-overlap group than in the overlap and the control groups, which were non-distinguishable. By contrast for the theta-wPLI the two patient groups were indistinguishable, but the overlap group showed significantly stronger wPLI than the control group for the same networks as for the whole survivor group (control, default, dorsal attention, visual), but not at the whole brain level. When taking into account the FSIQ, the correlation tended to be significant with alpha-wPLI at the whole brain level in healthy controls ( $r_s = -.31$ ;  $p = 0.05$ ) and in ALL survivors ( $r_s = -.30$ ;  $p = 0.06$ ). The correlation between the FSIQ and the theta-wPLI at the whole brain level was lower and did not reach significance neither in ALL survivors ( $r_s = -.054$ ;  $p = 0.76$ ) nor in healthy controls ( $r_s = -.28$ ;  $p = 0.09$ ).

#### Chemotherapy and Spectral Connectivity

The cumulative dose of IT-MTX was significantly correlated with wPLI in the alpha band at the whole brain level ( $r_{s(36)} = .36$ ;  $p = 0.03$ ) (fig supplementary 2). Across the different networks, this correlation ranged from .27 to .40. GCS was significantly correlated with the spectral connectivity in the gamma3 band at the whole brain level ( $r_{s(36)} = -.37$ ;  $p = 0.02$ ). Across the different networks, correlations ranged from -.13 to -.35.

#### Mediation models (Table 3)

The cumulative dose of IT-MTX was positively correlated to the whole-brain alpha wPLI, which in turn was higher in survivors with lower DIVERGT scores. Therefore we tested whether wPLI mediates the effect of the cumulative dose of IT-MTX on the DIVERGT score by using Hayes' PROCESS macro for SPSS 22 (Model 4). A patient who received 1 SD more IT-MTX (about 40 mg/m<sup>2</sup>) relative to the mean showed in the long-term follow-up a decrease of 1/3 SD in her DIVERGT score ( $t = -2.11$ ,  $p = 0.04$ ). After the introduction of the mediator, the indirect effect was significantly different from zero: for every 1 standard deviation increase of IT-MTX, the whole brain alpha phase locking increase would account for about 0.1 standard deviation decrease in

DIVERGT score (-.0961, BootIC=-.2117, -.0030), thus almost a third of the total effect. The direct effect decreased and was no longer significant ( $t=-1.56$ ,  $p=0.13$ ).

Among the different tests contributing to the DIVERGT score, the completely standardized indirect effect of ITMTX via alpha wPLI were significant for both the Trail Making Test (-.1122, BootIC=-.2632, -.0033), and the Digit Span scores (-.1029, BootIC=-.2148, -.0082). But the scores of the Verbal Fluency or the Grooved Pegboard were better described as a constant. Both direct and indirect effects of IT-MTX were thus specific to cognitive flexibility and working memory. As the theta phase locking was also higher in the survivors than in the controls, we tested whether the effect of IT-MTX on the DIVERGT score could be mediated by the whole brain wPLI in the theta band. After introducing the mediator the direct effect of IT-MTX on the DIVERGT score ( $t=-2.26$ ,  $p=0.03$ ) was the same as the total effect, and the confidence interval of the indirect effect included zero.

In order to test whether this partial indirect effect of IT-MTX may be increased by other factors, we also conducted a moderated mediation analysis using Hayes' PROCESS macro for SPSS 22 (Model 8). We first tested the moderation by cranial irradiation (absent vs. present) of both the direct and indirect paths from IT-MTX to DIVERGT. The direct effect of IT-MTX on the DIVERGT score was not significantly different from zero, regardless of the presence of cranial irradiation. However, the indirect effect was almost null in the group without irradiation (0.0007, Boot CI: -0.076, 0.0215), but negative and significantly different zero for patients with brain irradiation (-.0063, Boot CI: -.0165, -.0007). The pairwise contrast, however, failed to support a moderated mediation (-.0070, Boot CI:-0.0312, 0.0023). Age at diagnosis, time elapsed since diagnosis, leucovorin cumulative doses and sex did not moderate the mediation.

## Discussion

We found that the IT-MTX cumulative dose was negatively correlated to the global DIVERGT score, and that increased alpha band whole-brain phase-locking at rest partly mediated this effect. This indirect effect was specific for the tests of the DIVERGT battery that require cognitive flexibility and working memory. We also found a whole-brain phase locking increase for the theta band in survivors. However, this increase was not related to later cognitive functioning and appears only as a marker of past treatment or illness in itself.

Methotrexate is an essential drug in ALL treatment but it can cause acute and long-term neurotoxicity. MTX disrupts folate homeostasis, which can induce durable inflammatory microglia which in turn leads to neurotoxic astrocyte reactivity, and disruption of oligodendroglial lineage dynamics and myelin microstructure. It also blocks neuronal differentiation of hippocampal stem cells, disrupts hippocampal neurogenesis, and contributes to aberrantly exuberant pruning of synapses<sup>37</sup>. As a result MTX use was linked to neuropsychological deficits, especially in executive functions, both in clinical studies<sup>12, 38</sup> and in animal models<sup>39</sup>.

Enhanced long-range alpha phase synchrony has been shown to support adaptive cognitive processes, especially when top-down control was required, both in humans<sup>40–42</sup> and in animal model<sup>43</sup>. Locking the phase of alpha oscillations between distant neural populations was proposed to enable long-distance coordination and to subtend phasic adaptive control<sup>44</sup>. Changes in global synchrony in the upper alpha band correlated positively with activity measured by fMRI in the frontoparietal network<sup>21</sup>. Alpha resting state connectivity has been found to correlate with improved attention working memory and executive functioning within the right frontoparietal network 6 months after surgical resection of low-grade glioma (without radiation or chemotherapy)<sup>45</sup>.

By contrast, we found increased alpha connectivity at rest and for the whole brain, which suggests a persistent and nonspecific state of enhanced adaptive control in survivors. This brain state fits with Grady's model of compensatory activity which ultimately impairs performance<sup>50, 51</sup>. At rest survivors would activate top-down adaptive control at the whole brain level, and when a task requires further adaptation, additional resources would be limited, and result in lower score in

executive tests. Using a short-term memory task (VSTM), we previously described over- and under-activation of regions usually involved in VSTM but also recruitment of additional regions<sup>52</sup>, for the same level of performance. However, further research is needed to test whether alpha phase-locking at rest would compromise additional adaptation with increasing difficulty, for example in the frontoparietal network. Such a deficit in adaptive control has been shown in individuals with a mild traumatic brain injury (mTBI) commonly who also show WM microstructural alterations<sup>46-48</sup>. In a task where participants were asked to indicate which of two candidate images matched a third probe, normal controls showed an increase in MEG alpha band connectivity (150–250 mg after stimulus onset) when they have to shift from one dimension to another (for example from colour to shape), as compared to changes within the same dimension (colour or shape). Within 2 months of the trauma, mTBI patients failed to boost alpha connectivity between occipital and all other brain regions and showed poorer performance during extradimensional shifting<sup>49</sup>.

We also found that the indirect effect of IT-MTX through alpha phase-locking was significantly different from zero after irradiation, but not in survivors without CRT. Brain irradiation essentially ablates neurogenesis in the hippocampus but can also impact all brain regions through neurovascular disruption and microglial inflammation<sup>53</sup>. There is a clear dose-response curve for the neurotoxic effect of CRT<sup>1</sup>, but even lower dose (18 Gy) was associated with IQ decline when preceded by a high dose of MTX<sup>54</sup>. However, the difference between the direct and indirect effects was not large enough to conclude that CRT increased the indirect effect of MTX through increased alpha connectivity.

This study has limitations. The number of participants was relatively low, and conclusions may not be generalizable to those diagnosed after age 12. However, we identified whole brain increased alpha synchrony as a marker of executive deficit related to IT-MTX cumulative dose. If increased alpha long-range synchrony is a dysfunctional compensatory mechanism, longitudinal studies before, during and after treatment will inform about its prognostic value to identify at risk survivors. Moreover, different techniques have been shown to modify alpha synchrony such as transcranial magnetic stimulation<sup>55</sup>, neurofeedback<sup>56, 57</sup> or meditation practice<sup>58</sup> might be used as rehabilitation treatment.

Authors' disclosures of potential conflicts of interest

Author contributions

Conception and design: Victor Oswald, Maja Krajinovic, Caroline Laverdière, Daniel Sinnett, Pierre Jolicoeur, Sarah Lippé, Karim Jerbi, Philippe Robaey

Provision of study materials or patients: Maja Krajinovic, Caroline Laverdière, Daniel Sinnett, Pierre Jolicoeur, Sarah Lippé, Karim Jerbi, Philippe Robaey

Financial support: Maja Krajinovic, Caroline Laverdière, Daniel Sinnett, Sarah Lippé, Philippe Robaey

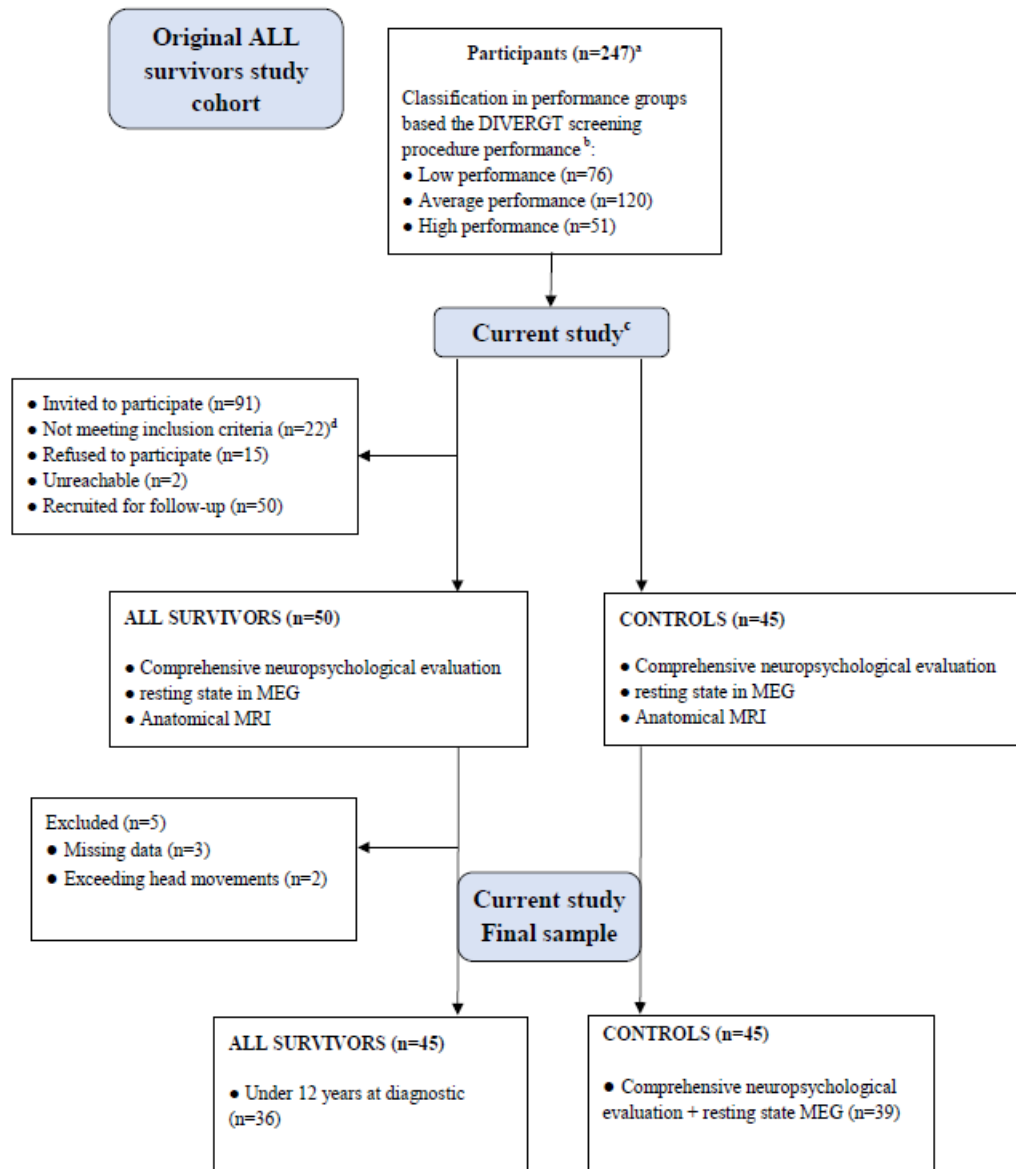
Administrative support: Maja Krajinovic, Caroline Laverdière, Daniel Sinnett, Pierre Jolicoeur, Sarah Lippé, Karim Jerbi, Philippe Robaey

Collection and assembly of data: Victor Oswald, Tarek Lanef, Aubrée Boulet-Craig, Maja Krajinovic, Caroline Laverdière, Daniel Sinnett, Pierre Jolicoeur, Sarah Lippé, Karim Jerbi, Philippe Robaey

Data analysis and interpretation: Victor Oswald, David Meunier, Karim Jerbi, Philippe Robaey

Manuscript writing: All authors

Final approval of manuscript: All authors



<sup>a</sup> For comprehensive information about participant’s characteristics and recruitment in the original cohort (PETALE project), see Marcoux et al. (2017).

<sup>b</sup> For comprehensive information about group classification process, see Boulet-Craig et al. (2018).

<sup>c</sup> Current study was a follow-up evaluation included in a broader research project (PETALE).

<sup>d</sup> Exclusion criteria included any metallic foreign body (the most common being metallic dental wired braces).

Figure 37. – CONSORT diagram for PETALE study

Tableau 4. – Survivor Demographic and Treatment Characteristics

	<b>Control</b>	<b>ALL Survivors</b>
Female; Male	22; 24	21; 24
Mean age (std)	25,5 (4,6)	25 (5,5)
Educations years (std)	14,1 (3,8)	12,5 (2,04)
Age of diag yrs (std)		6 (4,9)
Time since treatment end yrs (std)		7,5 (15,5)
<b>Cumulative pharmacologic doses</b>		
IT: methotrexate mg/m <sup>2</sup>		133.62 (51.32)
Methotrexate mg/m <sup>2</sup>		5895.32 (1796.8)
Equivalent corticosteroid mg/m <sup>2</sup>		12043 (5125.66)
IT: Cytarabine mg/m <sup>2</sup>		542.14 (187.78)
L-asparaginase UI/m <sup>2</sup>		540197.33 (179040.27)
Radiotherapy (Gray) with (33)/without (12)		n=2 (12 G); n=31 (18 G)

Tableau 5. – Neurocognitive performance data

Neuropsychological tests	Control (n=39) Mean (SD)	ALL survivors (N=36) Mean (SD)	Student t test	p_val	ALL survivors		IT-MTX		IV-MTX		Corticosteroid				
					CRT+ n=25	CRT- n=11	t test d01=34	p_val	coef corr	p_val	coef corr	p_val	coef corr	p_val	
Vocabulary	12.33 (1.65)	10.13 (2.19)	<b>-4.8</b>	<0.001	9.88 (2.29)	10.72 (1.90)	-1.07	.29	-0.10	.56	.02	.91	-.32	.05	
Similarities	11.41 (2.42)	8.36 (2.29)	<b>-5.5</b>	<0.001	8.44 (2.14)	8.18 (2.71)	.30	.76	.012	.94	-.02	.90	-.23	.16	
Block Design	11.87 (2.71)	8.47 (2.83)	<b>-5.3</b>	<0.001	8.56 (2.81)	8.27 (3.00)	.27	.78	-.32	.05	-.13	.45	-.24	.15	
Matrix Reasoning	11.92 (2.51)	10.80 (2.45)	-1.9	0.056	10.84 (2.47)	10.72 (2.53)	.12	.90	-.20	.22	-.02	.89	-.04	.78	
Code	11 (2.88)	8.5 (2.33)	<b>-4.1</b>	<0.001	8.20 (2.08)	9.1 (2.82)	-1.16	.25	-.11	.50	.09	.61	-.20	.23	
Symbol search	12.53 (2.25)	9.11 (2.92)	<b>-5.7</b>	<0.001	9.28 (2.86)	8.72 (3.16)	.51	.60	-.07	.67	.18	.31	-.04	.80	
Letter Number Sequencing	10.71 (3.41)	8.91 (3.22)	<b>-2.3</b>	0.022	8.56 (3.33)	9.72 (2.96)	-.99	.32	-.21	.20	-.02	.88	-.30	.07	
Full Scale IQ	111.61 (14.23)	92.86 (13.62)	<b>5.8</b>	<0.001	91.16 (12.58)	94.45 (14.54)	-.69	.49	-.24	.14	.01	.94	-.27	.10	
Verbal fluency letter	9.41 (2.90)	7.8 (2.86)	<b>2.4</b>	0.019	7.36 (2.69)	8.81 (3.12)	-1.4	.16	-.15	.36	.006	.97	-.21	.21	
Groove Pegboard (Dominant hand)	.12 (1.03)	-0.37 (1.18)	1.9	0.053	-.54 (1.04)	-.002 (1.43)	-1.2	.21	-.04	.77	.11	.52	-.21	.20	
Digit Span	9.76 (2.66)	9.38 (3.49)	1.9	0.06	8.08 (3.67)	9.09 (3.11)	-.79	.43	-.35	.03	-.02	.89	-.22	.18	
Trail making test condition 4	11.35 (1.34)	9.58 (3.07)	<b>3.1</b>	0.003	9.72 (2.85)	9.27 (3.66)	.39	.69	-.31	.06	.07	.70	-.008	.96	
DIVERGT (n=36)	7.66 (1.37)	6.48 (2.08)	<b>2.8</b>	0.006	6.15 (1.93)	6.79 (2.01)	.89	.37	-.34	.04	0.03	.86	-.20	.22	
Subgroup															
DIVERGT low (n=9)		3.8 (.51)	<b>13.7</b>	<0.001	7.05 (1.49)	7.48 (1.52)	-.70	.48	.42	.25	.16	.69	.22	.57	
DIVERGT normal (n=28)		7.15 (1.47)	1.2	0.201	3.83 (0.18)	3.67 (1.38)	.37	.72	-.24	.21	-.05	.81	-.20	.31	



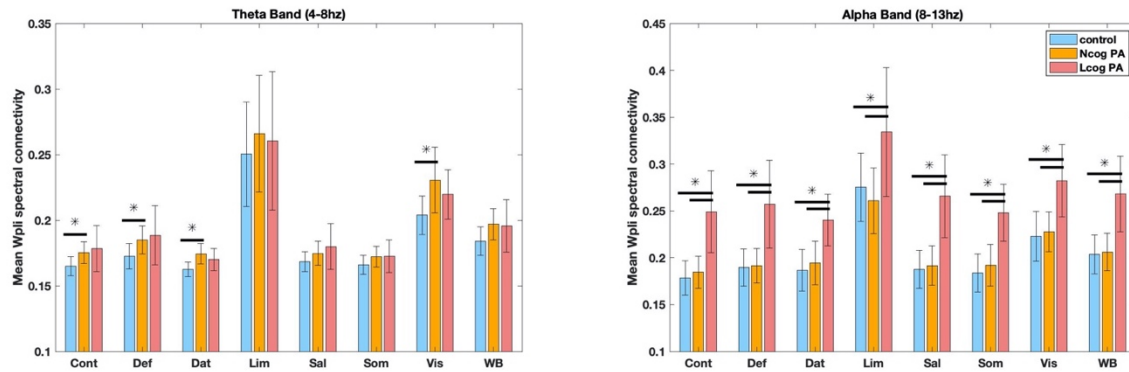


Figure 38. – Mean weighted phase lag index (Wpli) in ALL non-overlapping, overlapping and healthy control groups in 7 resting state networks and across the whole brain. A: Theta band, B: Alpha band. The horizontal grey bars indicate significant difference between groups ( $p < .01$  after FDR) (Ncog: Normal cognitive performance; Lcog: Low cognitive performance).

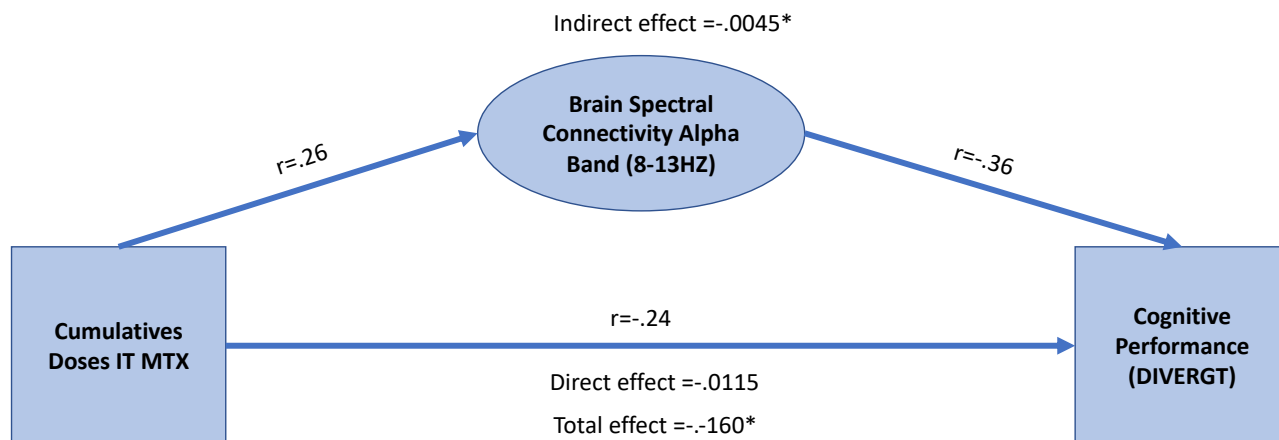


Figure 39. – Mediation models between cumulative doses of IT:MTX and cognitive performance (DIV). After introducing whole brain connectivity in alpha band (8–13 Hz) as mediator direct pathways found nonsignificant (effect=-0.0115,  $p = 0.12$ ) while total effect found to be significant (-0.0045,  $p = 0.04$ ), the total accounted variance in indirect pathways is 28,12%.

Tableau 6. – Mediation analysis

Consequent								
		M (WB- $\alpha$ -wPLI)			Y (DIVERGT)			
Antecedent		Coeff	SE	P		Coeff	SE	P
X (IT-MTX)*	$a$	0.0004	0.0002	0.1247	$c'$	-0.0115	0.0074	0.1291
M (WB- $\alpha$ -wPLI)		-	-	-	$b$	-12.5193	5.3274	0.0249
Constant	$i_M$	.2216	.0095	<.0001	$i_Y$	9.1240	1.2171	<.0001
		R <sup>2</sup> =.0679			R <sup>2</sup> =.2426			
		F(1,34)=2.4777, $p$ =0.1247			F(2,33)=5.2847, $p$ =0.0102			
		M (WB- $\alpha$ -wPLI)			Y (DS)			
Antecedent		Coeff	SE	P		Coeff	SE	P
X (IT-MTX)*	$a$	.0004	0.0002	0.1247	$c'$	-0.0206	0.0128	0.1184
M (WB- $\alpha$ -wPLI)		-	-	-	$b$	-23.6624	9.2456	0.0153
Constant	$i_M$	0.2216	0.0095	<.0001	$i_Y$	13.6323	2.1122	<.0001
		R <sup>2</sup> =.0679			R <sup>2</sup> =.2680			
		F(1,34)=2.4777, $p$ =0.1247			F(2,33)=6.0402, $p$ =0.0058			
		M (WB- $\alpha$ -wPLI)			Y (TMT4)			
Antecedent		Coeff	SE	P		Coeff	SE	P
X (IT-MTX)*	$a$	0.0004	0.0002	0.1247	$c'$	-0.0149	0.0112	0.1943
M (WB- $\alpha$ -wPLI)		-	-	-	$b$	-22.6637	8.0969	0.0085
Constant	$i_M$	0.2216	0.0095	<.0001	$i_Y$	14.6054	1.8498	<.0001
		R <sup>2</sup> =.0679			R <sup>2</sup> =.2725			
		F(1,34)=2.4777, $p$ =0.1247			F(2,33)=6.1816, $p$ =0.0052			
		M (WB- $\alpha$ -wPLI)			Y (TMT4)			
Antecedent		Coeff	SE	P		Coeff	SE	P
X (IT-MTX)*	$a_1$	-0.0001	0.0005	0.9114	$c'_1$	-0.0149	0.0112	0.1943
M (WB- $\alpha$ -wPLI)		-	-	-	$b$	-12.1991	5.3877	0.0307
W (CRT)	$a_2$	-0.0020	0.0223	0.9307	$c'_2$	-0.9985	0.6792	0.1516
X x W	$a_3$	0.0006	0.0006	0.3096	$c'_3$	-0.0015	0.0171	0.9291
Constant	$i_M$	0.2256	0.0189	<.0001	$i_Y$	9.7393	1.3456	<.0001
		R <sup>2</sup> =.0987			R <sup>2</sup> =.2963			
		F(3,32)=1.1683, $p$ =0.3371			F(4,31)=3.2636, $p$ =0.0241			

\* Mean centered prior to analysis

## References

1. Krull KR, Brinkman TM, Li C, Armstrong GT, Ness KK, Srivastava DK, Gurney JG, Kimberg C, Krasin MJ, Pui CH, Robison LL, Hudson MM. Neurocognitive Outcomes Decades After Treatment for Childhood Acute Lymphoblastic Leukemia: A Report From the St. Jude Lifetime Cohort Study. *J. Clin. Oncol.* 2013;31(35):4407–4415.
2. Jain N, Brouwers P, Okcu MF, Cirino PT, Krull KR. Sex-specific attention problems in long-term survivors of pediatric acute lymphoblastic leukemia. *Cancer.* 2009;115(18):4238–4245.
3. Cheung YT, Krull KR. Neurocognitive outcomes in long-term survivors of childhood acute lymphoblastic leukemia treated on contemporary treatment protocols: A systematic review. *Neurosci Biobehav Rev.* 2015;53:108-120.
4. Geraghty AC, Gibson EM, Ghanem RA, Greene JJ, Ocampo A, Goldstein AK, Ni L, Yang T, Marton RM, Paşca SP, Greenberg ME, Longo FM, Monje M. Loss of Adaptive Myelination Contributes to Methotrexate Chemotherapy-Related Cognitive Impairment. *Neuron.* 2019;103(2):250–265.e258.
5. Gibson EM, Nagaraja S, Ocampo A, Tam LT, Wood LS, Pallegar PN, Greene JJ, Geraghty AC, Goldstein AK, Ni L, Woo PJ, Barres BA, Liddelov S, Vogel H, Monje M. Methotrexate Chemotherapy Induces Persistent Tri-gliaial Dysregulation that Underlies Chemotherapy-Related Cognitive Impairment. *Cell.* 2019;176(1):43-55.e13.
6. Schuitema I, Deprez S, Van Hecke W, Daams M, Uyttebroeck A, Sunaert S, Barkhof F, van Dulmen-den Broeder E, van der Pal HJ, van den Bos C, Veerman AJ, de Sonnevill LM. Accelerated aging, decreased white matter integrity, and associated neuropsychological dysfunction 25 years after pediatric lymphoid malignancies. *J Clin Oncol.* 2013;31(27):3378–3388.
7. Zou L, Su L, Xu J, Xiang L, Wang L, Zhai Z, Zheng S. Structural brain alteration in survivors of acute lymphoblastic leukemia with chemotherapy treatment: A voxel-based morphometry and diffusion tensor imaging study. *Brain Research.* 2017;1658:68-72.
8. Dellani PR, Eder S, Gawehn J, Vucurevic G, Fellgiebel A, Muller MJ, Schmidberger H, Stoeter P, Gutjahr P. Late structural alterations of cerebral white matter in long-term survivors of childhood leukemia. *J. Magn Reson. Imaging.* 2008;27(6):1250–1255.
9. Khong PL, Leung LH, Fung AS, Fong DY, Qiu D, Kwong DL, Ooi GC, McAlonan G, Cao G, Chan GC. White matter anisotropy in post-treatment childhood cancer survivors: preliminary evidence of association with neurocognitive function. *J. Clin. Oncol.* 2006;24(6):884–890.
10. Porto L, Preibisch C, Hattingen E, Bartels M, Lehrnbecher T, Dewitz R, Zanella F, Good C, Lanfermann H, DuMesnil R, Kieslich M. Voxel-based morphometry and diffusion-tensor MR imaging of the brain in long-term survivors of childhood leukemia. *Eur. Radiol.* 2008;18(11):2691–2700.
11. Edelmann MN, Krull KR, Liu W, Glass JO, Ji Q, Ogg RJ, Sabin ND, Srivastava DK, Robison LL, Hudson MM, Reddick WE. Diffusion tensor imaging and neurocognition in survivors of childhood acute lymphoblastic leukaemia. *Brain.* 2014;137(Pt 11):2973–2983.
12. Krull KR, Cheung YT, Liu W, Fella S, Reddick WE, Brinkman TM, Kimberg C, Ogg R, Srivastava D, Pui CH, Robison LL, Hudson MM. Chemotherapy Pharmacodynamics and Neuroimaging and

- Neurocognitive Outcomes in Long-Term Survivors of Childhood Acute Lymphoblastic Leukemia. *J Clin Oncol*. 2016.
13. Lebel C, Deoni S. The development of brain white matter microstructure. *NeuroImage*. 2018;182:207-218.
  14. Herting MM, Maxwell EC, Irvine C, Nagel BJ. The Impact of Sex, Puberty, and Hormones on White Matter Microstructure in Adolescents. *Cerebral Cortex*. 2012;22(9):1979–1992.
  15. Chahal R, Vilgis V, Grimm KJ, Hipwell AE, Forbes EE, Keenan K, Guyer AE. Girls' pubertal development is associated with white matter microstructure in late adolescence. *NeuroImage*. 2018;181:659-669.
  16. Menzies L, Goddings A-L, Whitaker KJ, Blakemore S-J, Viner RM. The effects of puberty on white matter development in boys. *Developmental Cognitive Neuroscience*. 2015;11:116-128.
  17. Thijssen S, Collins PF, Luciana M. Pubertal development mediates the association between family environment and brain structure and function in childhood. *Development and Psychopathology*. 2019;32(2):687–702.
  18. Kesler SR, Ogg R, Reddick WE, Phillips N, Scoggins M, Glass JO, Cheung YT, Pui C-H, Robison LL, Hudson MM, Krull KR. Brain Network Connectivity and Executive Function in Long-Term Survivors of Childhood Acute Lymphoblastic Leukemia. *Brain connectivity*. 2018;8(6):333–342.
  19. Hall EL, Robson SE, Morris PG, Brookes MJ. The relationship between MEG and fMRI. *NeuroImage*. 2014;102:80-91.
  20. Fries P. A mechanism for cognitive dynamics: neuronal communication through neuronal coherence. *Trends in Cognitive Sciences*. 2005;9(10):474–480.
  21. Sadaghiani S, Scheeringa R, Lehongre K, Morillon B, Giraud A-L, Esposito M, Kleinschmidt A. Alpha-Band Phase Synchrony Is Related to Activity in the Fronto-Parietal Adaptive Control Network. *The Journal of Neuroscience*. 2012;32(41):14305.
  22. Al-Sahab B, Ardern CI, Hamadeh MJ, Tamim H. Age at menarche in Canada: results from the National Longitudinal Survey of Children & Youth. *BMC Public Health*. 2010;10(1):736.
  23. Hossain MJ, Xie L, McCahan SM. Characterization of pediatric acute lymphoblastic leukemia survival patterns by age at diagnosis. *Journal of cancer epidemiology*. 2014;2014:865979-865979.
  24. Krull KR, Okcu MF, Potter B, Jain N, Dreyer Z, Kamdar K, Brouwers P. Screening for neurocognitive impairment in pediatric cancer long-term survivors. *J. Clin. Oncol*. 2008;26(25):4138–4143.
  25. Boulet-Craig A, Robaey P, Laniel J, Bertout L, Drouin S, Krajinovic M, Laverdière C, Sinnett D, Sultan S, Lippé S. DIVERGT screening procedure predicts general cognitive functioning in adult long-term survivors of pediatric acute lymphoblastic leukemia: A PETALE study. *Pediatric Blood & Cancer*. 2018;65(9):e27259.
  26. Wechsler D. *Wechsler Intelligence Scale for Children-Fourth Edition*. San Antonio, TX: The Psychological Corporation; 2003.

27. Wechsler D. *WISC-IV Canadian Manual*. Toronto: Harcourt Assessment; 2004.
28. Oswald V, Zerouali Y, Boulet-Craig A, Krajinovic M, Laverdiere C, Sinnott D, Jolicoeur P, Lippe S, Jerbi K, Robaey P. Spontaneous brain oscillations as neural fingerprints of working memory capacities: A resting-state MEG study. *Cortex*. 2017;97:109-124.
29. Tadel F, Baillet S, Mosher JC, Pantazis D, Leahy RM. Brainstorm: a user-friendly application for MEG/EEG analysis. *Comput Intell Neurosci*. 2011;2011:879716.
30. Fischl B, Salat DH, Busa E, Albert M, Dieterich M, Haselgrove C, van der Kouwe A, Killiany R, Kennedy D, Klaveness S, Montillo A, Makris N, Rosen B, Dale AM. Whole Brain Segmentation: Automated Labeling of Neuroanatomical Structures in the Human Brain. *Neuron*. 2002;33(3):341–355.
31. Huang MX, Mosher JC, Leahy RM. A sensor-weighted overlapping-sphere head model and exhaustive head model comparison for MEG. *Physics in Medicine and Biology*. 1999;44(2):423–440.
32. Baillet S, Mosher JC, Leahy RM. Electromagnetic brain mapping. *IEEE Signal Processing Magazine*. 2001;18(6):14–30.
33. Ghuman AS, McDaniel JR, Martin A. A wavelet-based method for measuring the oscillatory dynamics of resting-state functional connectivity in MEG. *NeuroImage*. 2011;56(1):69–77.
34. Vinck M, Oostenveld R, van Wingerden M, Battaglia F, Pennartz CMA. An improved index of phase-synchronization for electrophysiological data in the presence of volume-conduction, noise and sample-size bias. *NeuroImage*. 2011;55(4):1548–1565.
35. Schaefer A, Kong R, Gordon EM, Laumann TO, Zuo X-N, Holmes AJ, Eickhoff SB, Yeo BTT. Local-Global Parcellation of the Human Cerebral Cortex from Intrinsic Functional Connectivity MRI. *Cerebral Cortex*. 2018;28(9):3095–3114.
36. Hayes JF, Khandaker GM, Anderson J, Mackay D, Zammit S, Lewis G, Smith DJ, Osborn DP. Childhood interleukin-6, C-reactive protein and atopic disorders as risk factors for hypomanic symptoms in young adulthood: a longitudinal birth cohort study. *Psychol Med*. 2017;47(1):23–33.
37. Filbin M, Monje M. Developmental origins and emerging therapeutic opportunities for childhood cancer. *Nature medicine*. 2019;25(3):367–376.
38. Krull JL, Cheong J, Fritz MS, MacKinnon DP. Moderation and Mediation in Interindividual Longitudinal Analysis. *Developmental Psychopathology*: John Wiley & Sons, Inc.; 2016.
39. Wen J, Maxwell RR, Wolf AJ, Spira M, Gulinello ME, Cole PD. Methotrexate causes persistent deficits in memory and executive function in a juvenile animal model. *Neuropharmacology*. 2018;139:76-84.
40. Mima T, Oluwatimilehin T, Hiraoka T, Hallett M. Transient Interhemispheric Neuronal Synchrony Correlates with Object Recognition. *The Journal of Neuroscience*. 2001;21(11):3942.

41. Sauseng P, Klimesch W, Doppelmayr M, Pecherstorfer T, Freunberger R, Hanslmayr S. EEG alpha synchronization and functional coupling during top-down processing in a working memory task. *Human Brain Mapping*. 2005;26(2):148–155.
42. Zanto TP, Rubens MT, Thangavel A, Gazzaley A. Causal role of the prefrontal cortex in top-down modulation of visual processing and working memory. *Nature neuroscience*. 2011;14(5):656–661.
43. von Stein A, Chiang C, König P. Top-down processing mediated by interareal synchronization. *Proceedings of the National Academy of Sciences of the United States of America*. 2000;97(26):14748–14753.
44. Sadaghiani S, Kleinschmidt A. Brain Networks and  $\alpha$ -Oscillations: Structural and Functional Foundations of Cognitive Control. *Trends in Cognitive Sciences*. 2016;20(11):805–817.
45. Dellen E, De Witt Hamer P, Douw L, Klein M, Heimans JJ, Stam CJ, Reijneveld J, Hillebrand A. Connectivity in MEG resting-state networks increases after resective surgery for low-grade glioma and correlates with improved cognitive performance. *NeuroImage: clinical*. 2012;2:1-7.
46. Sasaki T, Pasternak O, Mayinger M, Muehlmann M, Savadjiev P, Bouix S, Kubicki M, Fredman E, Dahlben B, Helmer KG, Johnson AM, Holmes JD, Forwell LA, Skopelja EN, Shenton ME, Echlin PS, Koerte IK. Hockey Concussion Education Project, Part 3. White matter microstructure in ice hockey players with a history of concussion: a diffusion tensor imaging study. *Journal of neurosurgery*. 2014;120(4):882–890.
47. Pasternak O, Koerte IK, Bouix S, Fredman E, Sasaki T, Mayinger M, Helmer KG, Johnson AM, Holmes JD, Forwell LA, Skopelja EN, Shenton ME, Echlin PS. Hockey Concussion Education Project, Part 2. Microstructural white matter alterations in acutely concussed ice hockey players: a longitudinal free-water MRI study. *Journal of neurosurgery*. 2014;120(4):873–881.
48. Helmer KG, Pasternak O, Fredman E, Preciado RI, Koerte IK, Sasaki T, Mayinger M, Johnson AM, Holmes JD, Forwell LA, Skopelja EN, Shenton ME, Echlin PS. Hockey Concussion Education Project, Part 1. Susceptibility-weighted imaging study in male and female ice hockey players over a single season. *Journal of neurosurgery*. 2014;120(4):864–872.
49. Pang EW, Dunkley BT, Doesburg SM, da Costa L, Taylor MJ. Reduced brain connectivity and mental flexibility in mild traumatic brain injury. *Annals of Clinical and Translational Neurology*. 2016;3(2):124–131.
50. Grady C. The cognitive neuroscience of ageing. *Nature Reviews Neuroscience*. 2012;13:491.
51. Grady CL. Cognitive Neuroscience of Aging. *Annals of the New York Academy of Sciences*. 2008;1124(1):127–144.
52. Boulet-Craig A, Robaey P, Barlaam F, Laniel J, Oswald V, Jerbi K, Sultan S, Affret-Bertout L, Drouin S, Krajcinovic M, Laverdière C, Sinnett D, Jolicoeur P, Lippé S. Visual short-term memory activation patterns in adult survivors of childhood acute lymphoblastic leukemia. *Cancer*. 2019;0(0).
53. Monje M. Cranial radiation therapy and damage to hippocampal neurogenesis. *Dev Disabil Res Rev*. 2008;14(3):238–242.

54. Waber DP, Tarbell NJ, Fairclough D, Atmore K, Castro R, Isquith P, Lussier F, Romero I, Carpenter PJ, Schiller M, . Cognitive sequelae of treatment in childhood acute lymphoblastic leukemia: cranial radiation requires an accomplice. *J Clin. Oncol.* 1995;13(10):2490–2496.
55. Plewnia C, Rilk A, Soekadar S, Arfeller C, Huber H, Sauseng P, Hummel F, Gerloff C. Enhancement of long-range EEG coherence by synchronous bifocal transcranial magnetic stimulation. *The European journal of neuroscience.* 2008;27:1577-1583.
56. Berhanu CNAP. *Connectivity-based EEG-neurofeedback in VR: pipeline development and experimental validation*, Institute for Systems and Robotics at Instituto Superior Tecnico; 2019.
57. Bruña R, Maestú F, Pereda E. Phase locking value revisited: teaching new tricks to an old dog. *Journal of Neural Engineering.* 2018;15(5):056011.
58. Hebert R, Lehmann D, Tan G, Travis F, Arenander A. Enhanced EEG alpha time-domain phase synchrony during Transcendental Meditation: Implications for cortical integration theory. *Signal Processing.* 2005;85(11):2213–2232.

# Appendix

## Supplementary figure

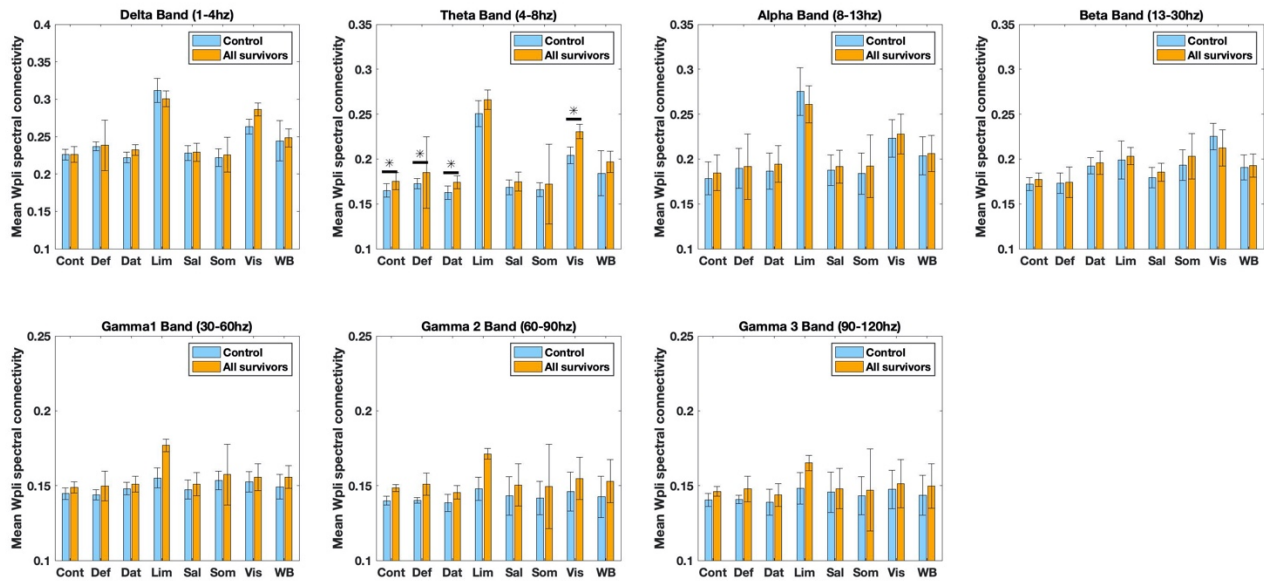


Figure 40. – Supplementary figure 1 (SF1): mean wPLI in healthy controls (N=39) and ALL survivors (N=36) for each resting state network and whole brain level. \* indicates significant difference (p=0.05 FDR corrected. Cont: control (frontoparietal), Def: default, Dat: dorsal attention, Lim: limbic, Sal: Salience (ventral attention), Som: somato-motor, Vis: visual.

1.



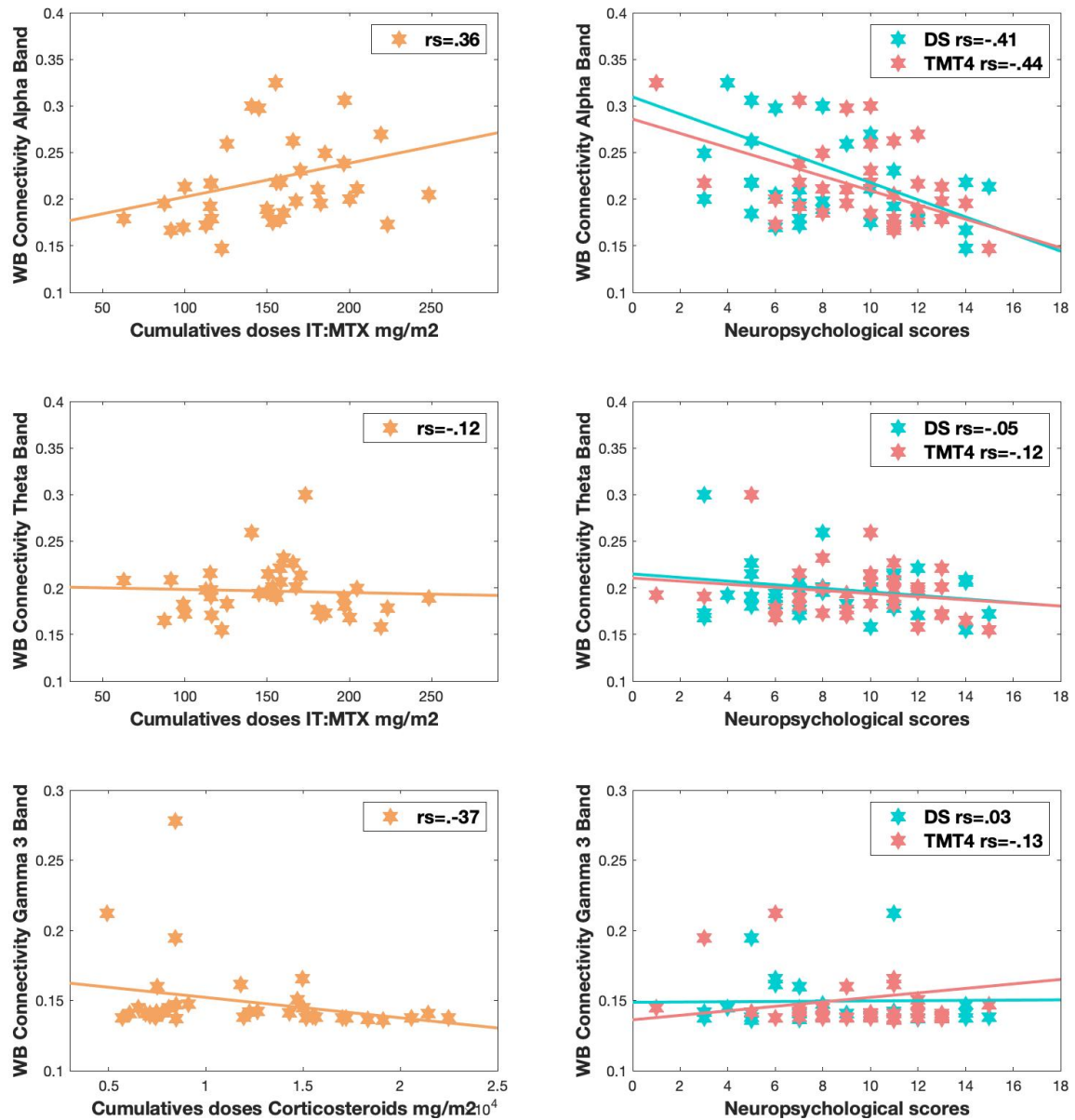


Figure 41. – Supplementary figure 2 (SF2): Scatter plot of correlation between Cumulative IT:MTX and Alpha band spectral connectivity (8–13 Hz) at Whole brain (upper left). Scatter plot of correlation between performance in digit span (DS) and trail Making test condition 4 (TMT-4) and Alpha band spectral connectivity (8–13 Hz) at Whole brain (upper right). Scatter plot of correlation between Cumulative IT:MTX and Theta band spectral connectivity (4–8 Hz) at Whole brain (middle left). Scatter plot of correlation between performance in digit span (DS) and trail Making test condition 4 (TMT-4) and Alpha band spectral connectivity (4–8 Hz) at Whole brain (middle right). Scatter plot of correlation between Cumulative Corticosteroids and Gamma band spectral connectivity (90–120 Hz) at Whole brain (lower left). Scatter plot of correlation between performance in digit span (DS) and trail Making test condition 4 (TMT-4) and Gamma band spectral connectivity (90–120 Hz) at Whole brain (lower right).



## Chapitre 6 : Synthèse des résultats et discussion

### Résumé des résultats

Le but de ces recherches était de caractériser l'activité spontanée au repos en magnétoencéphalographie, au niveau des sources corticales. Notre approche par clusters, qui permettait un découpage des régions d'intérêt, a permis d'identifier des patrons significatifs. Ces patrons se sont aussi montrés relativement différents suivant les processus cognitifs explorés : la mémoire de travail, les fonctions exécutives puis l'apprentissage verbal. Globalement, la méthode utilisée semble spécifique à différents processus cognitifs et permet d'identifier des patrons différents dans le domaine spatial et fréquentiel.

Dans le chapitre 2, nous avons trouvé que la performance en mémoire de travail (index de mémoire de travail issu du WAIS-IV) corrèle positivement avec les régions suivantes : la partie dorso-médiale du cortex frontal, le lobule para-central, le lobule supérieur pariétal ainsi que la partie caudale du gyrus somesthésique gauche. Lorsqu'on cherche à isoler les substrats spécifiques de la mémoire de travail, nous avons trouvé que les cortex cingulaire antérieur et postérieur sont corrélés significativement avec cette performance comportementale. En testant différents types de mémoire de travail (addition spatiale issue du Weschler) utilisant d'autres modalités, nous avons trouvé que des régions similaires se retrouvaient comme la partie dorso-médiale du cortex frontal, le lobule para-central, alors que d'autres régions s'ajoutaient, notamment les cortex prémoteur, moteur et somesthésique à gauche, ainsi que le lobule inférieur et la partie postérieure du lobe temporal dans l'hémisphère gauche.

Dans le chapitre 3, nous avons investigué les corrélats de la fluence verbale, qui est un test très largement utilisé en clinique pour évaluer les fonctions exécutives. Nous avons encore retrouvé un ensemble de clusters, précédemment identifié dans la mémoire de travail, qui inclut des clusters fronto-pariétaux dans les oscillations lentes (1–30 Hz), ainsi qu'un ensemble de clusters à gauche uniquement dans les régions frontales prémotrice, motrice et somesthésique, et ce, dans les oscillations à haute fréquence (gamma 60–120 Hz). En cherchant les régions spécifiques à la fluence verbale, nous avons trouvé une région incluant la partie caudale du cortex moteur et

somesthésique à droite, ainsi que plusieurs clusters dans le cortex prémoteur dans l'hémisphère droit. En contrastant la fluence verbale avec un test exécutif non verbal (*Trail Making Test condition 4*) de flexibilité cognitive, nous avons observé que les principales régions impliquées dans la séquence phonologique de la fluence verbale étaient les régions postérieures pariétales, incluant le précuneus, le lobule pariétal supérieur et le cortex somesthésique à droite, ainsi que les cortex moteur et prémoteur. Au contraire, en contrastant la fluence verbale avec un test non exécutif verbal sémantique testant la richesse du vocabulaire (Vocabulaire issu de batterie WAIS-IV), nos résultats montrent que les régions prémotrices à droite ainsi que le pôle frontal et cingulaire antérieur supportent la dimension exécutive, plus particulièrement l'inhibition utilisée dans une tâche de fluence verbale. Finalement, une région dite pivot se trouve à la jonction entre ces deux contrastes : cette région est latéralisée à droite, partagée entre la partie caudale du cortex sensori-moteur et prémoteur. Elle serait impliquée dans le contrôle et le monitoring des différents sous-ensembles fonctionnels montrés précédemment (c'est-à-dire : la mise en place de la séquence phonologique/articulatoire, l'inhibition et mémoire de travail).

Dans le chapitre 4, nous avons exploré les corrélats neuronaux de l'activité spontanée associée à la performance d'apprentissage d'une série de mots, ainsi qu'aux stratégies d'apprentissage utilisées au cours de cet apprentissage. L'hémisphère gauche principalement a été trouvé corrélérer avec la performance d'apprentissage. Les régions incluent le cortex pariétal droit, la partie supérieure et postérieure du lobe temporal, le gyrus somesthésique gauche, ainsi qu'un cluster dans le cortex prémoteur gauche. Au contraire, un patron d'anti-corrélation a été trouvé dans le gyrus cingulaire bilatéralement de sa partie la plus antérieure à la plus postérieure. Nous avons ensuite investigué les indices sémantique et sériel d'apprentissage, tous deux relatifs aux stratégies d'apprentissage; nous n'avons trouvé que deux patrons de corrélation qui s'opposent ; le centre de ce patron est un ensemble de régions latéralisées à gauche qui corrélerent positivement avec la stratégie sémantique et négativement avec les stratégies sérielles. Il comprend le lobule pariétal inférieur, le gyrus somesthésique, la partie caudale du gyrus pré-central, ainsi que la partie latérale inférieure du gyrus frontal. À l'opposé, les régions à gauche para-hippocampique et cingulaire médiane ainsi que des régions occipitales à droite, corrélerent positivement pour la stratégie sérielle et négativement pour la stratégie sémantique. L'ensemble

de ces régions, qui semblent cruciales pour la mise en place de la stratégie sémantique, semble être le substrat d'un réseau dédié à la compréhension et production verbale, très généralement attribué dans la littérature au réseau du langage.

Les trois chapitres 2, 3 et 4 utilisent exactement le même échantillon de 28 participants et les mêmes méthodes : les patrons sont donc comparables ; le seul aspect qui varie réside dans les tests comportementaux utilisés, ainsi que les méthodes de contrastes pour comparer ou différencier des patrons d'activation combinant soustraction, conjonction et factorisation.

## **Synthèse des résultats**

### **Discussion générale**

Dans la discussion générale, nous allons synthétiser les résultats obtenus, tels que décrits dans les différents chapitres de cette thèse. L'objectif de cette section est de discuter d'une classification qui permet d'interpréter les résultats des puissances dans un même niveau d'interprétation. Pour cela, nous avons utilisé le modèle qui sépare le néocortex en deux voies, une dorsale et une ventrale. La voie dorsale comprend cortex préfrontal dorsolatéral, les régions cingulaires, l'ensemble du cortex prémoteur, moteur, sensorimoteur et pariétal, ainsi que le cortex rétrosplénial (Goodale & Milner, 2014). La voie ventrale comprend les cortex orbitofrontal, gustatif et viscéral, le cortex limbique et le lobe temporal (Goodale & Milner, 2014). Ces voies ont une origine phylogénétique différente; elles se sont différenciées au cours de l'évolution des mammifères et sont présentes chez chacun d'entre eux (Cisek, 2019). De plus, elles se différencient par leur organisation neuronale: la voie dorsale est organisée de manière spatialement topographique alors que la voie ventrale ne l'est pas (Cisek, 2019). Cette taxonomie des voies dorsale et ventrale a été d'abord étudiée à travers le système visuel (Goodale & Milner, 2014) ; puis un modèle auditif plus récent pour la compréhension du langage a été développé (Hickok & Poeppel, 2004).

Le tableau 7 propose une synthèse des clusters trouvés pour tous les différents tests cognitifs à travers les chapitres 2, 3 et 4. Ce tableau présente aussi l'information sur la latéralité (par la lettre indiquée dans le tableau) et indique si les clusters démontrent une corrélation positive ou

négative (par le code couleur). Plusieurs observations peuvent être faites. La première est que l'ensemble des clusters se répartissent au sein de ces deux voies, ventrale et dorsale (tableau 7). Lorsque des clusters sont présents dans une des deux voies, l'autre voie montre systématiquement soit une absence de cluster, soit des clusters montrant une corrélation de signe opposé ; ce résultat se vérifie pour tous les tests, à deux exceptions près : le *CVLT performance* (figure 1, article 4) et le *CVLT stratégie sémantique* (figure 2, article 4).

Cela traduit qu'à l'état de repos, l'organisation de l'activité spontanée cérébrale en lien avec les processus cognitifs est préférentiellement partagée entre les deux voies. De plus, la répartition des tests neuropsychologiques et des clusters ne correspond pas forcément à la taxonomie neuropsychologique classique. Par exemple, pour les fonctions exécutives présentes dans cette thèse (c'est-à-dire la mémoire de travail, le test des tracés ou TMT, et la fluence verbale), nos expériences démontrent des résultats en partie similaires entre la fluence verbale et la mémoire de travail. Les régions communes sont les régions frontales qui incluent le cortex dorso-latéral préfrontal (dlPFC), le cortex dorso-médial préfrontal (dmPFC), le lobule para-central, ainsi que le lobule pariétal supérieur.

Cette voie fronto-pariétale est souvent décrite dans la littérature dans des études en connectivité, bien que nous retrouvions les mêmes résultats pour la mémoire de travail en connectivité avec le réseau fronto-pariétal (FPN) (chapitre 2 annexe) ou le réseau d'attention dorsal (DAN). Nos résultats avec les clusters sur les puissances spectrales se situent le long de cette voie, mais sont davantage localisés dans le cortex moteur (lobule para-central) et dans la frontière entre le cortex prémoteur et cortex frontal dorsal médial.

Ces mêmes clusters se retrouvent dans nos résultats en mémoire de travail et avec la fluence verbale. Il a déjà été montré que le cortex prémoteur dans sa partie rostrale était en lien avec des tâches cognitives non motrices, de manipulation de l'information impliquant souvent les chiffres via des tâches de calcul mental ainsi qu'un traitement sériel de l'information plus généralement (Abe & Hanakawa, 2009). Ces régions sont proéminentes à droite et davantage en lien avec la représentation visuo-spatiale (Hanakawa et al., 2003). De plus, on retrouve ces mêmes clusters avec la stratégie sérielle d'apprentissage (*endroit et envers*). L'interprétation de cette voie dorsale

peut être multiple, mais d'après (Graziano, 2016), il résume l'interaction entre les régions pariétales et frontales sur la voie dorsale, suivant une organisation d'après le type d'action appelé des « cartes d'action ». Ces cartes d'action sont un ensemble de circuits fronto-pariétaux dédiés à différentes classes d'actions typiques de l'espèce (Graziano, 2016; Kaas & Stepniewska, 2016). Chacun de ces circuits traitait l'information sensorielle d'une manière idiosyncrasique spécialisée pour son type d'action spécifique (par exemple, l'espace près des pattes pour la locomotion, l'espace près du museau pour l'ingestion), et chacun se projetait vers un ensemble spécifique d'effecteurs pertinents (Cisek, 2019). Nos résultats suggèrent donc ce lien entre action et processus cognitifs ; de plus, tous les tests démontrant des clusters sur la voie dorsale impliquent un type d'action « conceptuel », comme la mémoire de travail — qui consiste à manipuler de l'information — ou la fluence verbale — qui consiste à dire le plus rapidement possible un grand nombre de mots.

	<i>Voie Dorsale</i>	<i>Voie Ventrale</i>
<u>Mémoire de travail (WMI-Wais-IV)</u>	B	
<u>Fluence verbale (VF1)</u>	B	
CVLT – Stratégie <i>serial backward</i>	R L	L
CVLT – Stratégie <i>serial forward</i>	R	L
CVLT – Stratégie sémantique	L	L
CVLT– Performance	R L	L
<u>Trail making test (condition 4)</u>		L
Vocabulaire (Voc-Wais-IV)		L

Légende : fonction exécutive ; rouge : corrélation, bleu : anti-corrélation; R = droite, L = gauche, B = bilatérale. **Voie dorsale** : *dmPFC-premotor-motor-superior lobule (parietal cortex)- precuneus*; **Voie ventrale** : *Inf lateral frontal-angular/supramarginal gyrus (inferior parietal cortex), Anterior temporal lobe, MTG, STG, pMTG*

Tableau 7. – Tableau récapitulatif des résultats puissance des clusters à travers tous les tests comportementaux

Au contraire, le TMT-4, qui est aussi considéré comme un test exécutif, ne montre pas du tout le même patron de corrélation ; il montre davantage des régions latéralisées à gauche, incluant le gyrus angulaire, le gyrus temporal médian et supérieur, et l'extrémité caudale du cortex moteur. Ces régions font partie d'une voie ventrale, caractérisée en connectivité par le réseau de l'attention ventral, ou *ventral attention network* (VAN). À partir des deux tests connus pour tester des habilités exécutives, l'imagerie montre deux patrons de corrélation différents au repos : l'un montre la voie dorsale pour la fluence verbale ou la mémoire de travail et l'autre (TMT-4) montre une voie ventrale latéralisée à gauche. Dans ce cas-ci, le détail amené par l'imagerie par repos en électrophysiologie ainsi que sa finesse spectrale permettent de distinguer des patrons spatiaux fréquentiels différents, tandis que les fonctions exécutives en général peuvent être réduites aux lobes frontaux (Alvarez & Emory, 2006). Au chapitre 3, nos résultats montrent un facteur de contraste (F1\_TMT) opposant la fluence verbale à TMT (figure S4, article 3) : on voit plus clairement apparaître l'opposition entre la voie dorsale latéralisée à droite favorisant la fluence verbale et la voie ventrale latéralisée à gauche favorisant TMT-4.

De plus, la modalité semble plus importante que le type de tâche, ce qui suggère que ces patrons tendent à décrire prioritairement des caractéristiques comportementales liées au contexte de la tâche, plutôt que l'habileté en tant que telle. C'est notamment ce que montrent les résultats sur le TMT-4 : ce dernier est un test visuo-moteur, et il aurait été attendu que la voie dorsale domine dans ces compétences de planification motrice, mais cela n'est pas le cas. Les autres études en tâche vont dans le même sens que nos résultats au repos et démontrent une dominance de la voie ventrale (Varjadic et al., 2018), ce qui pousse à affirmer que cela n'est pas relié à la condition de l'état de repos. De plus, dans une étude qui compare plusieurs résultats en neuro-imagerie à propos du TMT (Varjadic et al., 2018), trois études ont été retenues pour montrer des activations pour la différence entre TMTA et TMTB (TMTB > TMTA). Deux d'entre elles (Jacobson et al., 2011; Zakzanis et al., 2005) démontrent des activations frontales (du cortex moteur au cortex préfrontal) ainsi que des activations dans la voie ventrale à gauche (insula/gyrus médian temporal/gyrus supérieur temporal) semblables à nos résultats. Par contre, la troisième étude (Moll et al., 2002), qui a adapté le TMT pour les besoins expérimentaux, a modifié la tâche sous forme verbale, alors que ce test normalement visuo-moteur s'effectue à l'aide d'un papier et d'un



crayon ; cette étude ne rapporte aucune activité dans la voie ventrale et seulement des activations dans la voie dorsale complète (lobe pariétal au lobe frontal). Ce résultat unique demande à être reproduit, mais si un même test comportemental démontre des patrons d'activations différents suivant la modalité (visuel, verbal, etc.) utilisée, cela indique que la modalité est une condition importante au niveau des entrées et des voies de traitement de l'information dans le cerveau.

Dans cette même idée, un récent modèle de fonctions exécutives a été développé par factorisation à travers plusieurs tests comportementaux ; il propose un modèle unifié/diversifié des fonctions exécutives contenant un facteur commun et deux facteurs spécifiques — un facteur de mise à jour de la mémoire de travail spécifique et un facteur de changement entre les tâches spécifique. (Miyake & Friedman, 2012). Ce modèle comportemental semble très bien expliquer les tests. Cependant, leurs corrélats neurophysiologiques restent faibles. Peu d'études démontrent les mécanismes cérébraux sous-tendant ces facteurs (Friedman & Miyake, 2017). Dans le modèle d'unité et de diversité de la fonction exécutive, l'un des facteurs spécifiques est le changement spécifique (*switching*) ; le type de tests exécutifs qui sont représentés par ce facteur sont tous des tâches impliquant des changements entre des catégories de stimulus (par exemple catégoriser la forme et la couleur des stimuli). Dans ces tâches les participants doivent rapidement passer d'une sous-tâche à l'autre en fonction d'indices aléatoires, ce qui est lié avec ce que le participant doit faire pendant le TMT-4. Le facteur spécifique de *switching* bénéficie de plusieurs de résultats en neuro-imagerie, ce dernier est notamment soutenu par des résultats reliés à un réseau d'attention somatomotrice/ventrale qui inclut le gyrus angulaire gauche (Friedman & Miyake, 2017), ce qui est en concordance avec nos résultats sur TMT-4. Nos résultats concernant ce modèle pourraient confirmer que le facteur spécifique de *switching* est relié à la voie ventrale dans nos résultats latéralisée à gauche.

Dans le chapitre 3, le test Vocabulaire présente des clusters principalement sur la voie ventrale latéralisée à gauche. En effet, ces clusters ont été trouvés dans les régions pariétales (supramarginale et angulaire), temporales (supérieure, moyenne et inférieure) et occipitales (fusiforme), principalement sur la face externe de l'hémisphère gauche. Ces clusters ont été trouvés principalement pour les bandes de fréquences plus basses (delta à bêta). Des groupes de

corrélation très similaires ont été trouvés pour le facteur de contraste (F1-VOC, figure S3, article 3) de l'hémisphère gauche : dans cette figure, le contraste entre la latéralité est dominant, la fluence verbale se révèle comme un test principalement dans l'hémisphère droit très frontal, alors que le Vocabulaire se montre comme un test très postéro-inferieur à gauche. La dimension phonologique associée au cluster à droite ayant déjà été discutée dans l'article 3, nous discuterons ici des clusters associés au test de vocabulaire. Comme Vocabulaire est un test verbal sémantique, il évalue la richesse du vocabulaire et la capacité à faire des liens sémantiques à partir d'un mot.

Nous proposons que les clusters qui sont associés à ce test reflètent le rôle d'un réseau sémantique. De nombreux chercheurs ont proposé une vision « incarnée » de l'information sémantique. Selon ce point de vue, la signification d'un mot est basée sur un réseau de représentations visuelles, auditives et somato-motrices, de sorte qu'un mot est associé à des représentations de l'apparence de l'objet et de son utilisation, par exemple. Ces régions largement distribuées, ainsi que les diverses connexions entre elles, constituent le réseau sémantique (Barsalou, 1999, 2008; Martin, 2007; Pulvermüller et al., 2005). Les représentations sémantiques peuvent reposer sur différents types de relations (Mirman et al., 2017) basées sur des caractéristiques partagées (relations taxonomiques, par exemple chien-ours), ou des relations de contiguïté basées sur la co-occurrence dans des événements ou des scénarios (relations thématiques, par exemple chien-laisse). En réalisant une cartographie des symptômes et des lésions basées sur les voxels pour les erreurs taxonomiques et thématiques séparément chez des personnes atteintes d'aphasie post-AVC, on a constaté que les erreurs thématiques étaient localisées dans la jonction temporo-pariétale gauche et les erreurs taxonomiques dans le lobe temporal antérieur gauche (Schwartz et al., 2011). De plus, dans une tâche d'appariement d'images dans laquelle les participants devaient identifier les relations taxonomiques et thématiques entre les objets, il a été démontré que le traitement thématique recrute spécifiquement un réseau temporo-pariétal bilatéral comprenant les lobules pariétaux inférieurs et les gyri temporaux moyens (Kalénine et al., 2009). Il a été proposé que la connaissance thématique soit ancrée dans la jonction temporo-pariétale gauche, qui est au centre du patron des clusters que nous avons trouvé. Les régions temporo-pariétales (en particulier le cortex

temporal moyen postérieur et le lobule pariétal inférieur) pourraient être impliquées dans la simulation mentale d'événements, ou dans la reconstitution de la propre expérience perceptive et motrice du sujet. Les clusters que nous avons trouvés comprennent également des régions post-centrales et occipitales, ce qui est cohérent avec le rôle des régions visuelles et sensorimotrices dans les processus visuo-moteurs soutenant les représentations thématiques. Ces groupes ont été spécifiquement trouvés dans l'hémisphère gauche, ce qui est cohérent avec la nature verbale du test de vocabulaire. En somme, plus un individu s'appuierait sur ce réseau thématique sémantique, plus il serait performant dans le test de vocabulaire. Cette approche permettrait d'optimiser le score à ce test, puisque les participants obtiennent un score plus élevé lorsqu'ils définissent un mot donné en utilisant un synonyme, ou par son utilisation, une caractéristique claire, ou un exemple concret d'action ou de relation causale, et pas nécessairement une catégorie générale ou plus abstraite à laquelle le mot appartient. De plus, ces clusters reflèteraient l'avantage d'utiliser la représentation thématique au niveau du vocabulaire. Dans le contraste entre la fluence verbale et le test de vocabulaire (F2-VOC; figure S3-article 3), les clusters qui corrèlent avec la fluence verbale étaient associés à des représentations plus abstraites et taxonomiques (situées dans le lobe temporal antérieur), qui nécessitent davantage de contrôle sémantique (situé dans le gyrus frontal inférieur gauche et le cortex cingulaire) et étaient liés à de moins bonnes performances dans le test de vocabulaire.

Dans le chapitre 4, nous avons répliqué ces analyses, mais avec un autre type de test, le CVLT, qui est un test d'apprentissage verbal. Le patron de corrélations trouvé en lien avec la performance d'apprentissage, autrement dit la capacité à restituer le plus grand nombre de mots possible, est un patron de corrélation qui présente des clusters à la fois le long de la voie dorsale (cortex prémoteur/moteur/lobule pariétal supérieur) et de la voie ventrale (lobule pariétal inférieur, gyrus temporal médian et supérieur/partie caudale gyrus post et précentral). Secondairement, les stratégies d'apprentissages ont été testées et deux patrons apparaissent opposés entre eux, les stratégies sérielles (par ordre croissant ou décroissant) montrent des clusters de corrélation tout au long de la voie dorsale latéralisée à droite et au contraire corrélée négativement avec les régions qui prédisent la performance d'apprentissage du nombre de mots (*CVLT performance*) et ces clusters ont été trouvés principalement à gauche. Quant à elle, la stratégie sémantique

d'apprentissage démontre un patron de corrélation similaire à celui trouvé avec la performance d'apprentissage, mais davantage étendu spatialement. Les clusters trouvés avec les indices sériels à droite sont très similaires à ceux trouvés avec la fluence verbale et la mémoire de travail, ce qui renforce encore l'idée d'un traitement de l'information sériel supporté par le réseau dorsal supérieur droit (pariéto-frontal). En revanche, la performance de l'apprentissage semble latéralisée à gauche et représente une conjonction du réseau ventral et du réseau dorsal dans l'hémisphère gauche, ce qui est similaire aux corrélats trouvés avec l'indice dit sémantique (CVLT sémantique). Nous suggérons dans ce cas que la voie dorsale conjointe à la voie ventrale semble être un ensemble de régions soutenant un mécanisme d'apprentissage. Nous n'avons pas trouvé de résultats en connectivité pour le CVLT, le TMT et la fluence verbale, mais il serait intéressant dans le cas du CVLT d'investiguer davantage pour évaluer si la connectivité entre la voie dorsale et ventrale reflétait une plus grande performance dans l'apprentissage.

Finalement, très peu de clusters se sont retrouvés dans les régions du réseau par défaut classique (partie centrale), bien établi en IRM fonctionnelle (Buckner et al., 2008). En effet, quelques clusters ont été retrouvés dans la partie postérieure du réseau par défaut, notamment le cortex cingulaire postérieur dans la fluence verbale ainsi qu'avec la performance globale au CVLT (*CVLT performance*). Ces clusters montrent des corrélations négatives et sont alignés avec des résultats précédents qui montrent une corrélation négative au repos entre l'activité du réseau par défaut et la performance cognitive (Jerbi et al., 2010).

En somme, nos résultats sur les fonctions cognitives supportent les hypothèses que la neuro-imagerie reflète des aspects comportementaux, et que l'état de repos qui possède sa propre organisation y participe aussi. Cependant, les analyses de l'organisation de repos peuvent s'effectuer à plusieurs niveaux (capteurs, sources, réseaux, graphes, etc.), avec plusieurs types de caractéristiques (puissance spectrale,  $1/f$ , type de métrique de connectivité, métrique de graphe, etc.), et ce, à chaque niveau d'analyse. Ici, nos résultats rapportent un lien entre le comportement et le niveau d'activité corticale caractérisée par les puissances spectrales normalisées. D'un point de vue global, chaque test comportemental montre des spécificités spatio-fréquentielles. Cependant, il est aussi possible de dégager une lecture de ces clusters à travers tous les tests, par les grandes voies anatomo-fonctionnelles (ventrale et dorsale). Cette perspective semble pointer

vers des fonctions cognitives à plus large échelle et être en lien avec le type d'action qu'implique le test comportemental utilisé, et ce, via la modalité où s'effectue la tâche, mais aussi avec la nature ou le type d'action même abstraite que requiert la tâche.

Cette notion est souvent décrite dans la littérature de la cognition incarnée. Les modèles de cognition incarnée varient d'un auteur à l'autre (Ziemke, 2016), mais tous s'accordent à reconnaître l'aspect situé (*Embedded*) de la cognition (Newen, 2018). La dimension située de la cognition fait appel à son contexte ou environnement. Ce dernier est décrit par (Gibson, 1981) comme une opportunité ou une demande d'action appelée « *affordance* », mots issu de l'anglais, mais on retrouve dans cette idée dans le concept d'intentionnalité de la conscience (Brentano, 1924; Husserl, 1917).

« L'activité neuronale dans le circuit répondant à cette *affordance* n'est pas la représentation d'une chose dans le monde, mais la spécification d'une action à entreprendre dans le monde. Nous pouvons l'appeler une représentation pragmatique de l'action, par opposition à une représentation descriptive de la connaissance explicite. » (Cisek & Kalaska, 2010)

Dans un récent article, une perspective évolutionniste du comportement en fonction de la physiologie et de la phylogénie a été décrite, afin de proposer une manière d'interpréter les comportements issus des processus de sélection en lien avec les circonstances. De cette manière, la voie dorsale a été associée aux planifications simples ou complexes en rapport avec toutes les séquences pour tous les types d'actions (locomotion, déplacement, saisie d'objet, se nourrir, mordre ou parler). De manière différente, la voie ventrale a été associée à toute la sélection, la pertinence, la hiérarchisation et l'attribution de la valence, et la reconnaissance d'objets (Cisek, 2019). Nos résultats vont dans ce sens. La voie dorsale est associée autant à la performance en mémoire de travail, à la fluence verbale ainsi qu'à l'apprentissage verbal de manière sérielle. Ces trois tests ont comme action commune la planification verbale, malgré une représentation interne différente (utilisation des chiffres ou de mots) ; en revanche le TMT 4, Vocabulaire et l'apprentissage verbal sémantique sont supportés par un substrat de la voie ventrale. La planification d'action dans ces trois tests est davantage portée sur une hiérarchisation, une sélection ou un changement catégoriel. Finalement, nos résultats montrent que la performance à l'apprentissage verbal combine un substrat utilisant les deux voies (ventrale et dorsale),

contrairement aux autres fonctions cognitives testées ici. Cela suggère que l'apprentissage serait une manière de hiérarchiser l'information dans une perspective de planification motrice, et que l'encodage à long terme le plus efficient serait la combinaison de ces deux voies, contrairement à une voie dorsale seule (comme cela est montré avec les résultats de la stratégie sérielle).

## **Contribution**

Dans ce travail, nous avons développé une méthode originale pour explorer la structure et l'organisation de l'activité spontanée cérébrale au repos. Le but a été de combiner une série de méthodes déjà existantes afin d'avoir une approche précise, spécifique et reproductible. En effet, les patrons d'activations spatio-fréquentielles caractérisés au niveau des sources corticales avaient déjà été utilisés dans d'autres études en tâche pour caractériser des activations spécifiques, mais jamais à l'état de repos et sur les sources corticales en même temps.

De plus, combiner cette méthode avec les tests comportementaux neuropsychologiques n'a jamais été fait auparavant; Quelques études l'ont fait avec des analyses de connectivité, mais généralement les tests comportementaux neuropsychologiques sont utilisés pour contrôler les déficits dans des études où l'outil principal est une tâche, alors que ces tests donnent des mesures très précises du comportement, qui sont fiables, reproductibles et standardisées. Elles permettent aussi de cibler des aspects comportementaux ou domaines cognitifs précis, notamment en utilisant des contrastes, des factorisations ou des différences relatives, comme nous l'avons fait dans les chapitres précédents. La pertinence de ces tests est principalement clinique pour l'évaluation, mais nos résultats démontrent leur utilité aussi dans la recherche en sciences cognitives, lorsque combinés à l'imagerie cérébrale.

Nos analyses comblent un manque dans la littérature en imagerie cérébrale sur l'activité locale au niveau des sources corticales, entre les études sur les capteurs — qui possédaient une faible résolution spatiale — et la connectivité fonctionnelle — qui, quand elle était calculée à partir des sources corticales, représente un niveau d'interactions entre les régions corticales. Le niveau d'activité corticale au niveau local était quasiment absent, surtout concernant les différentes fonctions cognitives abordées dans cette thèse.

De plus, les résultats de cette recherche ont permis d'autres avancées dans les connaissances. D'une manière générale, nos résultats ont montré une spécificité des processus des patrons d'activations associées au différents tests neuropsychologiques, ce qui suggère bien une organisation de l'activité cérébrale au repos, dans certaines régions et fréquences qui prédisposent à certaines fonctions cognitives. Ces avancées sont avant tout spatiales, c'est-à-dire concernant le découpage cortical de chaque région. En effet, ces patrons n'avaient pas été montrés auparavant. Parmi les patrons d'activation, une partie était déjà connue, soit parce qu'il y a un recoupement avec l'activité en tâche, soit parce qu'il y a un recoupement avec des régions impliqués en connectivité lors de tâches ou au repos. De plus, le fait que tous nos patrons aient été observés sur un même échantillon renforce leur validité externe.

En général, nos résultats vont dans le sens de la littérature, mais à chaque processus cognitif, nos résultats ajoutent des régions ou révèlent des contrastes permettant de nouvelles interprétations pour ces processus cognitifs. Par exemple, concernant les régions motrices pour la mémoire de travail (chapitre 2), pour la fluence verbale (chapitre 3) et pour l'apprentissage verbal ainsi que les stratégies d'apprentissages (chapitre 4), nos résultats montrent des régions originales trouvées dans le cortex prémoteur et dans le gyrus pré et post central qui n'ont jamais été rapportées pour la fluence verbale dans l'hémisphère droit. De même, pour les résultats du chapitre 4, les clusters trouvés en lien avec la performance d'apprentissage ou encore les stratégies d'apprentissages n'ont jamais été rapportés dans la littérature, à notre connaissance.

Ce projet rapporte aussi des résultats intéressants quant à l'utilisation de la MEG ainsi que de l'état de repos dans la caractérisation des processus cognitifs déficitaires. En effet, le chapitre 5 montre comment l'état de repos en électrophysiologie permet, à travers la connectivité fonctionnelle, de cibler des dysfonctions cognitives spécifiques, ce qui permet ainsi d'expliquer des changements métaboliques, comme ici l'impact neurotoxique à long terme. Ces résultats, qui ciblent un mécanisme précis, permettent aussi d'envisager de nouveaux traitements pour cette population, et contribuent plus généralement à mieux décrire des marqueurs spécifiques de la cognition en santé.

Finalement, nos résultats démontrent que les informations contenues dans les patrons spatial et fréquentiel contiennent ainsi une partie de l'information dont l'état de repos dispose pour décrire les processus cognitifs ; cela suggère aussi que chaque niveau d'analyse (c.-à.-d. source, connectivité fonctionnelle, topologie des réseaux, etc.) peut contenir des informations différentes et qu'ils devraient tous être considérés et peuvent être intégrés ensemble.

## Limites

### Participants et populations

Ce projet a principalement été réalisé sur 28 sujets pour les chapitres 2, 3 et 4 ; cette petite taille d'échantillon peut suggérer des limites méthodologiques d'interprétation des résultats. Il serait donc intéressant de répliquer l'étude sur de plus grands échantillons, afin de vérifier si les résultats demeurent présents, tout en obtenant une puissance statistique plus élevée.

Dans cette étude, la population pédiatrique survivant à la leucémie a été recrutée dans le cadre d'un grand projet multidisciplinaire qui cherchait à mieux comprendre les effets tardifs de la leucémie sur différents volets (neuropsychologique, génétique, métabolique, cardiovasculaire, etc.). Le recrutement de la phase 3 (imagerie cérébrale et évaluation neuropsychologie complète) était fait d'après les scores obtenus à la phase 2, sur lequel trois (3) groupes de performance ont été regroupés (faible, moyen et fort) ; ce recrutement peut avoir mené à un biais dans la représentation de la population.

### Composante oscillatoire ou effet de large bande

Nos résultats sur les clusters de puissance montrent des corrélations entre des mesures comportementales et des puissances spectrales. Dans nos résultats, nous observons deux types de clusters : des clusters que nous retrouvons uniquement dans une seule bande de fréquence, ainsi que d'autres clusters que nous observons dans les mêmes régions spatiales, mais dans plusieurs bandes de fréquences. On pourrait parler de cluster spatio-fréquentiel spécifique ou alors de clusters à large bande de fréquences (c.-à.-d. *delta-to-beta*). Notre interprétation suggérait que certains de ces clusters seraient liés au phénomène oscillatoire de la puissance, tandis que les clusters trouvés à travers les larges bandes de fréquences seraient reliés à la partie



linéaire ( $1/f$ ) du spectre de puissance. Une récente étude a utilisé la puissance dans la bande alpha dans deux conditions (yeux ouverts et yeux fermés) au repos ; ils ont dissocié la composante linéaire ( $1/f$ ) et la composante oscillatoire dans la bande alpha (8–12 Hz), ce qui leur a permis de trouver que la puissance au repos corrèle avec la vitesse de traitement les yeux ouverts. Cependant, lorsqu'ils décomposent la puissance entre la partie oscillatoire « pure » et la partie linéaire  $1/f$ , seulement la partie  $1/f$  corrèle encore significativement avec la performance en vitesse de traitement ; plus précisément c'est l'exposant et non la magnitude de la partie linéaire  $1/f$  qui corrèle avec la performance comportementale (Ouyang et al., 2020). Cette étude a été uniquement réalisée sur la bande alpha (8–12 Hz) et avec une seule habileté comportementale. Il serait intéressant d'évaluer si des résultats similaires se retrouveraient avec d'autres bandes de fréquences au niveau comportemental avec différentes habiletés cognitives ; il serait aussi intéressant d'évaluer s'il est possible d'isoler des régions spécifiques au niveau cortical. La dissociation des deux permettra sans aucun doute de dresser un tableau plus détaillé des signatures fonctionnelles des activités cérébrales en cours. En effet, les circuits ou systèmes neuronaux qui génèrent des oscillations structurées peuvent reposer sur des architectures physiologiques différentes de celles qui génèrent la partie linéaire ( $1/f$ ) de la puissance (Buzsáki, 2009).

### **Corrélation et Variabilité Inter-individuelle**

La méthode développée dans cette thèse est une approche qui utilise la corrélation. La corrélation est un des outils majeurs utilisés en science : elle permet d'établir une relation entre deux variables, cependant elle ne permet pas de prouver la causalité (Buzsáki, 2019). Les méthodes de perturbation de système sont alors des outils plus efficaces pour cela ; cependant, d'autres contraintes surviennent aussi avec ces méthodes.

Une autre problématique liée à la corrélation est la variabilité liée aux données, principalement sur de petits échantillons ; il faut donc bien comprendre que les phénomènes dont rend compte cette méthode sont principalement liés à la variabilité interindividuelle ; autrement dit, les patrons de corrélation trouvés ici représentent davantage ce qui caractérise la relation entre les

performances cognitives à un des tests associés et ce qui représente le plus de différence entre les individus.

Cela signifie qu'une partie entière du mécanisme qui ne contiendrait pas de variabilité interindividuelle ne serait pas révélée par ce type de méthode. Ceci représente une limite méthodologique à l'interprétation des résultats ; cependant, une littérature conséquente aujourd'hui soutient que les différences interindividuelles dans la variabilité neurale permettent de bien caractériser l'aspect comportemental. En effet, en électrophysiologie, McIntosh et ses collègues (2008) ont examiné les relations entre la variabilité du signal et le comportement à l'aide de l'EEG dans un échantillon de jeunes de 8 à 33 ans, lors d'une tâche de reconnaissance faciale. Les auteurs ont constaté que l'EEG était associé à une plus grande précision de la reconnaissance des visages et à un temps de réaction plus constant des réponses. (Voytek et al., 2015) ont également montré que des pentes plus raides basées sur l'EEG en  $1/f$  étaient typiques des jeunes, plus précises, et plus rapides, plus stables dans une tâche de mémoire visuelle de travail. Il est important de noter qu'une étude récente a pu démontrer la compensation des baisses de la performance de la mémoire de travail liées à l'âge, en augmentant la variabilité neurale sous la forme d'oscillations de faible fréquence, et ce, par une stimulation cérébrale non invasive (Reinhart & Nguyen, 2019). Le paradigme idéal serait de combiner plusieurs types de méthodes comme la corrélation interindividuelle, la corrélation intra-individuelle ainsi que les approches qui consistent à perturber le système pour valider le rôle et la nécessité de chacun de ces composants.

### **Bases d'interprétations psychologiques du comportement**

Dans les chapitres 2, 3 et 4, nous avons utilisé une méthode par clusters pour identifier des patrons de corrélations entre l'activité spontanée en électrophysiologie au niveau cortical. Pour obtenir ces patrons, nous avons utilisé des tests comportementaux, tels que la mémoire de travail, la fluence verbale, l'apprentissage verbal, ainsi que les stratégies d'apprentissages.

Il apparaît que les patrons de corrélation changent en fonction du type de tests comportementaux utilisés pour établir les patrons de corrélation. Il est possible que la variabilité introduite entre les tests comportementaux mette en avant des régions qui elles aussi varient dans leur organisation

entre les individus ; par exemple, plus la puissance dans la bande alpha est élevée au repos dans le lobule para central, et plus cela est associé à une meilleure performance en mémoire de travail. Il serait possible ici de questionner ce que la mémoire de travail représente pour un cerveau, l'origine de ce comportement complexe qui inclut, si on le détaille, beaucoup de processus cognitifs différents. Plusieurs modèles de la mémoire de travail existent (A. D. Baddeley, 1978; A. D. Baddeley & Hitch, 1974). Certains auteurs vont décrire ou le décomposer comme une série d'actes dits « cognitifs » en le décomposant en différents sous-modules cognitifs (par exemple dans la mémoire de travail ici utilisé, la modalité d'encodage (auditive), puis la rétention et la manipulation de l'information et la restitution, etc.). Cette manière d'interpréter les résultats est dominante en neuro-imagerie, mais elle repose sur un entendement conceptuel du comportement. L'avantage de cet angle d'approche est clinique, car il permet de cibler la fonction comportementale symptomatologique (ou de « l'esprit »). Une taxonomie du comportement est donc ainsi souvent décrite entre les trois aspects de perception-cognition-action, auquel des sous-processus cognitifs sont ajoutés et spécialisés (figure 42). L'origine de cette influence dans les sciences cognitives a été très bien mise en évidence par (Buzsáki, 2019), qui décrit dès la fondation de la psychologie dans l'ouvrage « *The Principles of Psychology* » écrit par William James en 1890.

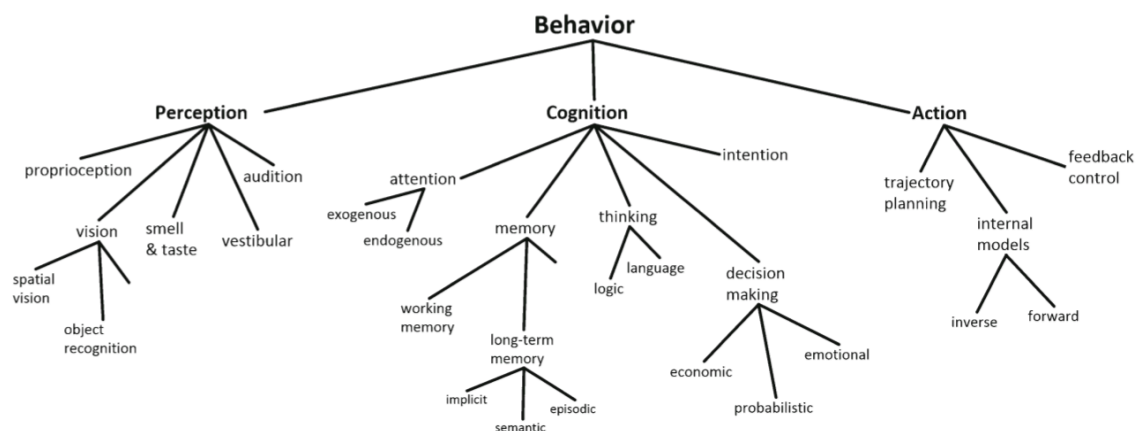


Figure 42. – Esquisse partielle d'une taxonomie conceptuelle implicite dans les sciences cognitives et les neurosciences courantes extraites. Tiré de (Cisek, 2019)

Dans cette perspective, des aspects comportementaux très précis sont isolés, et on cherche leurs corrélats physiologiques. Le principal problème est que cette approche est fondée sur les

fondations de la psychologie comme science descriptive du comportement, alors que le comportement est déjà un produit de la physiologie. En d'autres mots, on fait l'hypothèse, dans cette perspective, que le comportement existe de la manière dont nous l'avons décrit par observation ou conceptualisation, effectué souvent à la première personne ou à la troisième personne. C'est l'esprit caractérisant l'esprit et cherchant son corrélat physiologique, mais il n'y a aucune certitude quant au fait que cette caractérisation est fondée de la même manière dans la physiologie et, dans notre cas, dans l'activité spontanée cérébrale. Plusieurs auteurs ont évoqué cette problématique (Buzsáki, 2019; Cisek, 1999, 2019; Varela, F. J., Thompson, E., & Rosch, 1991). Un récent article entièrement consacré à cette problématique s'intitule « *No one knows what attention is* » (Hommel et al., 2019), dans son récent ouvrage « *the brain inside out* », (Buzsáki, 2019) évoque dès le début cette problématique appelée « *outside-in approach* » qui consiste à chercher les corrélats neuronaux à partir des concepts psychologiques. Interpréter la fonction cérébrale comme corrélats comportementaux amène alors dans une impasse explicative, surtout si la taxonomie comportementale n'est pas adéquatement décrite.

Un autre angle d'interprétation possible se comporterait en deux étapes : la première étape serait d'interpréter le comportement à partir de l'activité cérébrale, donc d'utiliser l'activité cérébrale comme référence et non comme activité à décoder ; la deuxième étape serait d'ancrer l'interprétation comportementale cognitive dans une perspective sensori-motrice et phylogénétique et non pas psychologique. La perspective sensori-motrice se voit formuler les premières fois par (Piaget, 1937) puis par (Merleau Ponty, 1942, 1945) mais réinterprétée plus récemment par (Varela, F. J., Thompson, E., & Rosch, 1991) qui ont fondé la perspective de la cognition incarnée. Une littérature abondante existe fondée sur cette théorie, autant dans les sciences de l'esprit qu'en neuro-imagerie ; cela dépasserait le cadre de ce travail d'en faire la revue. Cependant, une perspective incluant les fondations sensori-motrices du comportement, ou plutôt le comportement comme fondé sur une physiologie ayant une fonction sensori-motrice, peut aider à interpréter certains résultats et mécanismes en neuroscience comportementale. Cette perspective est notamment soutenue par une explication phylogénétique du comportement (Cisek, 2019). En effet, une interprétation possible de notre pensée conceptuelle serait issue de fonctions biologiques qui étaient nécessaires dans l'évolution et qui sont apparues

dans un certain contexte qui n'est plus le même de nos jours ; par exemple la vision était nécessaire pour se prévenir de danger pour pouvoir prendre la fuite, amorcer le combat ou encore pour chasser et augmenter les chances d'attraper des proies. Avec la sélection biologique au cours du temps, cette faculté est restée, mais le contexte a changé ; la vision est un sens qui dans la théorie sensori-motrice est considéré comme un des sens d'action « *We propose that seeing is a way of acting* » (O'Regan & Noë, 2001). Cette perspective pourrait servir à faire un pont entre, d'une part, des fonctions cognitives abstraites telles que la mémoire de travail ou la sémantisation de l'information lors d'un apprentissage, et d'autre part, les corrélats neuronaux fonctionnels trouvés en imagerie. De plus, le niveau d'analyse (activation, connectivité, organisation fonctionnelle des réseaux, dynamique des réseaux) pourrait aussi représenter plusieurs stades des spécialisations fonctionnelles apparues au cours du temps, et donc, un niveau de complexité et d'interprétation différents. Ces hypothèses seraient des avenues à explorer dans de futurs travaux.

## **Conclusions**

Cette recherche aura approfondi les connaissances sur l'état de repos et principalement fourni les premiers travaux qui mettent en lien l'activité cérébrale spontanée au repos au niveau des sources corticales avec plusieurs tests neuropsychologiques comportementaux. Les résultats ont amené des patrons d'activations spatio-fréquentielles différents, démontrant des spécificités reliées à certains tests comportementaux ou des traitements de l'information (sériel ou sémantique). Ces résultats permettent de compléter la compréhension fonctionnelle du niveau de l'activité corticale locale, en lien avec le comportement cognitif, contrairement à d'autres niveaux comme inter-cortical (connectivité) ou à l'activité en tâche. Finalement, les travaux sur les survivants de la leucémie ont montré que l'état de repos pouvait caractériser le fonctionnement des déficits cognitifs à long terme et être un marqueur de remédiation pour de futurs traitements.

## Annexes

## **Annexe 1 — chapitre 2**

### **Methods**

#### **Population**

We recruited 39 healthy adult subjects, with no reported history of neurological nor psychiatric disorder, through social networks, online advertising and posters on hospital billboards. Participants were mostly of European descent (90%) and were French speaking. The study was approved by the SJUHC Institutional Review Board. All participants agreed to participate in the study and signed an informed consent form.

#### **Neuropsychological Assessment**

A neuropsychological evaluation was carried out on the same day as the MEG recordings. The battery of neuropsychological tests consisted of subtests from the WAIS e 4th edition (Wechsler, 2008a, 2008b): Letter-Number Sequencing (LNS) and DS. In the DS subtest, the participants must recall a series of numbers in order. This subtest involves WM, attention, encoding, and auditory processing. LNS requires the participants to recall a series of numbers in increasing order, and letters in alphabetical order. This subtest assesses WM, attention, and mental control. Since the participants were all francophone, the French Canadian versions of the tests were used, and all the subtests from the neuropsychological evaluation were compiled and transformed to normative scale scores using Canadian norms (Wechsler, 2008a, 2008b). We calculated different indices: WMI with its LNS and DS components, and the Full-Scale IQ Index with all its subtests. We used scaled scores of the different subtests and indices to compute the correlations with MEG data. The WAIS-IV was standardized on a sample of 2200 people in the United States, ranging in age from 16 to 90. The derived scaled scores (z-scores) allow for a direct numerical comparison between individuals (Wechsler, 2008a, 2008b). To avoid any bias caused by the presence of outliers, only participants with scaled scores on all tests that were fewer than three standard deviations from the mean were included in the correlation analyses. This only led us to exclude five (5) participants out of the 39 for the correlation computations.

## MEG & MRI Acquisition and Pre-Processing

All subjects were comfortably seated with eyes open, fixating on a back-illuminated screen located 75 cm in front of them. Two 5-minute periods of resting state were recorded at a sampling rate of 1200 Hz, using a CTF-VSM whole head 275-sensor MEG system, as described previously. MEG data pre-processing was performed using the Matlab-based Brainstorm open-source software.

## Cortical Sources Estimation and Spectral Connectivity Analysis

MEG source reconstruction was performed using a standard weighted minimum-norm approach, with the Brainstorm software. T1-weighted brain volumes were acquired in all participants and were used to generate a cortical surface model, using the FreeSurfer software package. Forward modelling of the magnetic field was defined based on an overlapping-sphere method. The weighted minimum norm solution was computed using a loose dipolar orientation constraint (set at 0.5), a signal-to-noise ratio of 3, whitening PCA and a depth weighting of 0.5. The noise covariance matrix for each participant was estimated from a 2-min empty room recording performed earlier the same day (same acquisition parameters but with no subject in the shielded room, e.g.). The source time series were initially reconstructed on a 15000-vertex individual brain tessellation, and then spatially interpolated to the MNI ICBM152 brain template and down-sampled to a 4000-vertices template. Resting state spectral connectivity was measured using the Weighted Phase Lag Index (wPLI) method. In WPLI the contribution of the observed phase leads and lags is weighted by the magnitude of the imaginary component of the cross-spectrum. Here, we used the *neurotype\_ephy* package (<https://github.com/davidmeunier79>) which used *mne.connectivity.spectral\_connectivity* function from mne toolbox (<https://mne.tools/stable/index.html>) to perform spectral connectivity. A 3-sec sliding window was used to analyze four (4) minutes of resting state recording for all frequency band (except for the delta band, we used 5-seconds window) and we computed the mean connectivity value across the window for all participants in the following frequency bands: delta (1–4 Hz), theta (4–8 Hz), alpha (8–13 Hz), beta (13–30 Hz), gamma 1 (30–60 Hz), gamma 2 (60–90 Hz) and gamma 3 (90–120 Hz). The whole brain connectivity was first computed over 4000 nodes. Second, we averaged edges value using the parcellation of 7 resting state networks.



## Statistical Analyses

We tested normality of data with the Shapiro-Wilk test. Individual correlations between spectral connectivity and cognitive performance were performed with Spearman correlation test, we corrected for multiple comparison across networks with FDR correction ( $p < 0.05$ ).

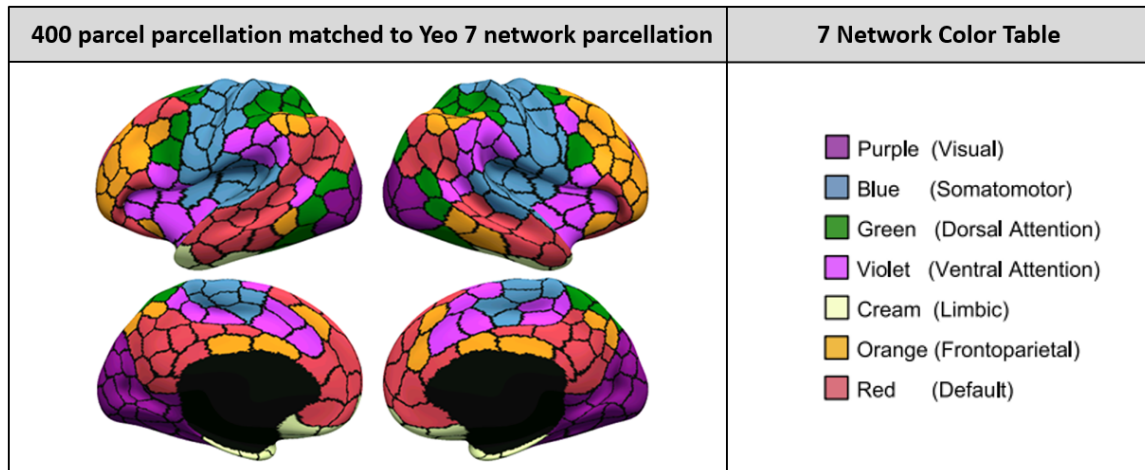


Figure 43. – Parcellations used from Schaffer et al. (2018) 7 networks

## Results

### Neuropsychological assessment

Table 1 summarizes the mean and standard deviation, and min/max values for the scaled scores on the neuropsychological tests. The participants' IQs were in the average range ( $108.35 \pm 12.01$ ) and all subtest scores fell within normal limits. The participants' scores were normally distributed, and no clinically meaningful cognitive deficits were found in any of the participants.

<i>n=34</i>	<i>Mean</i>	<i>Std</i>	<i>Min-max</i>
<i>Digit span</i>	<i>9.11</i>	<i>2.11</i>	<i>4–15</i>
<i>Letter number sequencing</i>	<i>9.58</i>	<i>1.7</i>	<i>6–12</i>
<i>Working memory Index</i>	<i>95.79</i>	<i>9.22</i>	<i>76–117</i>
<i>Full IQ</i>	<i>108.35</i>	<i>12.01</i>	<i>74–142</i>

Tableau 8. – Table 1: Scaled score, mean, standard deviation, minimum and maximum value of neuropsychological assessments for 34 subjects. The WAIS-IV battery includes subtest DS and LNS form WMI. Note that all standardized indices (i.e. WMI and FSIQ) are designed such that  $m=100$  &  $SD=15$ , while the subtests have  $m=10$  and  $SD=3$ .

### Neuropsychological scores and spectral connectivity

Table 2 summarizes coefficient correlation across all network and their frequency bands and uncorrected p-value. After FDR correction, working memory index scores were significantly correlated with the wPLI in the alpha band (8–13 Hz) in the frontoparietal (Con,  $r_s=-0.41$ ,  $p=0.02$ ), in the default network (Def,  $r_s=-0.40$ ,  $p=0.02$ ), in the limbic network (Lim,  $r_s=-0.50$ ,  $p=0.01$ ) and in the visual network (Vis,  $r_s=-0.47$ ,  $p=0,01$ ). Figure 1 show scatter plot of these significant correlation.

	Cont	Dat	Def	Lim	Sal	Som	Vis
	<i>Cc (p_val)</i>	<i>Cc (p_val)</i>	<i>CC (p_val)</i>	<i>Cc (p_val)</i>	<i>Cc (p_val)</i>	<i>Cc (p_val)</i>	<i>Cc (p_val)</i>
Delta	-0.20 (0.24)	0.06 (0.73)	-0.10 (0.53)	-0.22 (0.20)	-0.06 (0.70)	0.04 (0.81)	0.10 (0.55)
Thêta	-0.32 (0.05)	-0.06 (0.73)	-0.25 (0.14)	-0.26 (0.13)	-0.17 (0.32)	-0.04 (0.81)	-0.07 (0.67)
Alpha	<b>-0.41 (0.01)</b>	-0.31 (0.07)	<b>-0.40 (0.01)</b>	<b>-0.50 (0.002)</b>	-0.33 (0.05)	-0.34 (0.04)	<b>-0.47 (0.004)</b>
Beta	-0.10 (0.55)	-0.05 (0.75)	-0.15 (0.39)	-0.23 (0.17)	-0.13 (0.46)	-0.18 (0.30)	-0.08 (0.64)
Gamma1	0.07 (0.66)	-0.08 (0.62)	0.10 (0.54)	-0.18 (0.28)	0.14 (0.42)	0.04 (0.80)	-0.12 (0.46)
Gamma2	0.13 (0.43)	0.13 (0.45)	0.20 (0.23)	-0.01 (0.95)	-0.03 (0.83)	0.20 (0.24)	0.11 (0.50)
Gamma3	-0.08 (0.62)	0.23 (0.17)	0.06 (0.71)	-0.03 (0.82)	0.03 (0.53)	0.04 (0.83)	-0.02 (0.89)

Tableau 9. – Table 2: Correlation between mean spectral connectivity (wPLI)and working memory index performance across the 7 resting state network pour Working memory index ( $n=34$ ;p-value uncorrected)

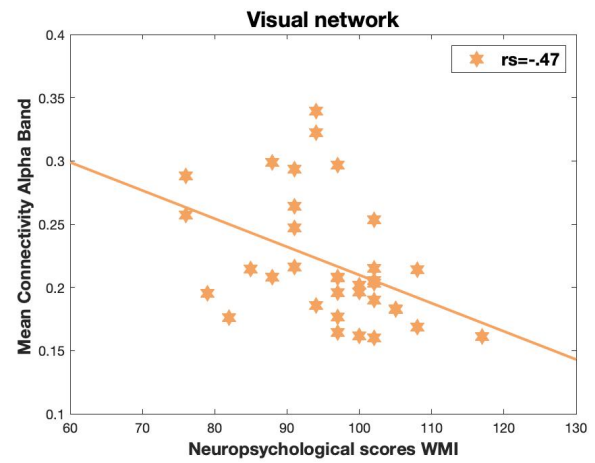
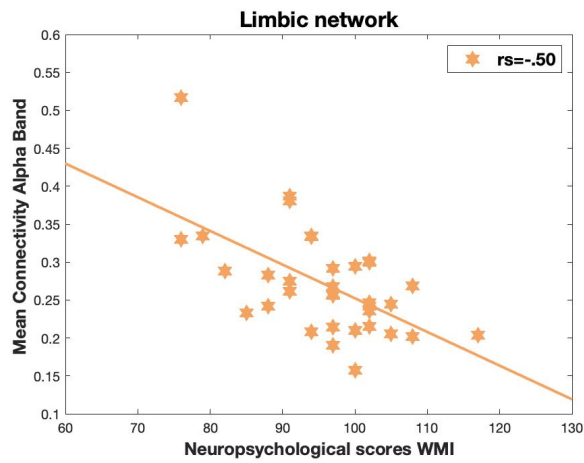
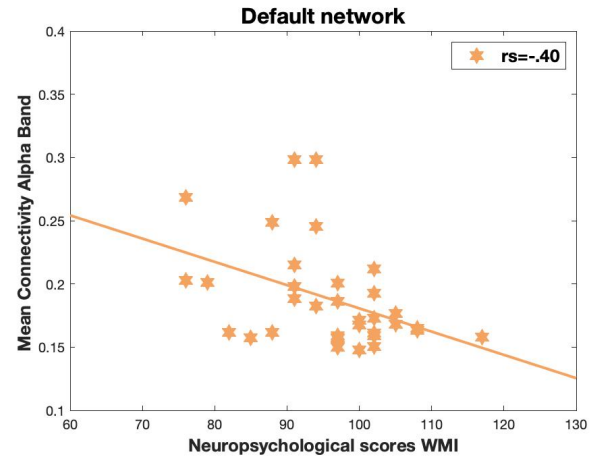
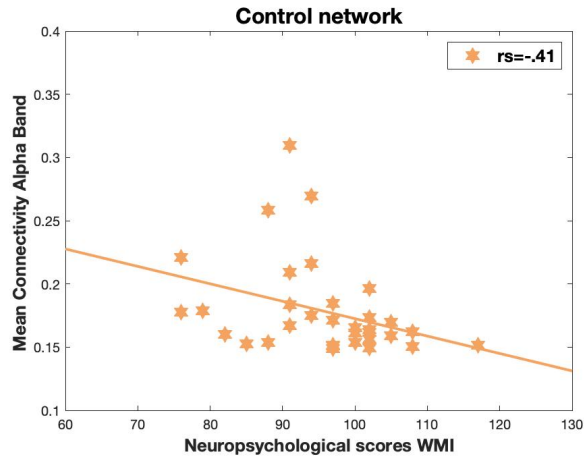


Figure 44. – Figure 1: Scatter plot with significant network (Cont, Def, Lim, Vis) between mean spectral connectivity (wPLI) and working memory index performance



## Annexe 2 — chapitre 3

### Additional results

#### Vocabulary

Correlation clusters were found in neighboring areas in the parietal and temporal areas almost exclusively in the left hemisphere. In the parietal region, these clusters were localized in the postcentral (alpha to beta band), superior parietal (beta band), inferior parietal (theta to gamma 1 bands) and supramarginal (delta to gamma 1) gyri. In the temporal regions, we found clusters in the middle temporal (delta to gamma 1 and gamma 2), superior temporal (delta, theta and beta bands), transverse temporal (theta band), as well as more posteriorly in the lateral occipital cortex (beta and gamma 1 bands). Medially, clusters were observed in the left precuneus (delta, theta, beta and gamma 1 bands). In the right hemisphere, correlation clusters were found for the delta band in the superior and inferior parietal gyri, and for the beta and gamma 1 bands in the precuneus.

Anticorrelation clusters were found bilaterally in the temporal and frontal/cingulate areas. In the left temporal regions, clusters were found for the theta to beta range in the superior temporal pole and the anterior inferior temporal gyri. On the right side, temporal clusters were restricted to the superior temporal pole for the alpha and beta bands. In the left frontal regions, we detected clusters in the lateral orbitofrontal cortex (delta to gamma 1 range), the inferior frontal gyrus pars orbitalis (alpha and beta bands) and in the insula (beta band). On the right hemisphere, we found clusters in homologous regions: in the lateral orbitofrontal (theta to beta range) and the inferior frontal gyrus pars orbitalis (alpha and beta bands). But we also detected clusters in the inferior frontal gyrus pars triangularis (alpha and beta bands) and opercularis (alpha, beta and gamma 2 bands), and in the rostral middle frontal gyrus (delta to gamma 1 range).

On the left medial face, in the lower frequency bands, anticorrelation clusters were detected in the occipito-temporal regions: in the lingual (delta to alpha range), fusiform (delta and theta bands), parahippocampal (delta to alpha range), entorhinal gyri (delta to alpha range), as well as

in the superior (delta to beta range) and inferior (delta to alpha range) temporal poles. In addition, anticorrelation clusters were found in the medial orbitofrontal cortex (theta to gamma 1 range), the caudal anterior cingulate (gamma 2 and 3 bands), the posterior cingulate (gamma 3 band) and the isthmus cingulate (alpha and beta bands). On the medial face of the right hemisphere, the anticorrelation clusters were located in the fusiform (delta to gamma 3 range), the parahippocampal (beta and gamma 1 range) and the superior temporal pole (beta band). In addition, right medial clusters were also found in the posterior cingulate (delta band, beta to gamma 3 range), the isthmus cingulate (theta band) and the paracentral lobule (gamma 3 band).

#### **Trail Making Test (Condition 4)**

On the right hemisphere we found anticorrelation clusters in the motor cortex and in the lateral inferior frontal gyrus (delta band). We also found correlation clusters in right lingual gyrus in the highest frequencies (gamma2 and gamma 3 band). On the left hemispheres, we found clusters correlation in the superior temporal gyrus and sulcus (delta to beta band), we also found left inferior post central gyrus (delta to beta band), we found a cluster correlation in middle temporal gyrus (theta and alpha band), and a supramarginal clusters (theta and alpha band) as well as a left angular gyrus in alpha band. In gamma 2 we found an anticorrelation clusters in the left supramarginal gyrus. We also found a anticorrelation clusters in the left superior frontal gyrus (delta, theta and gamma3 band), and finally anticorrelation clusters in the left cuneus and left superior lobule respectively in gamma 2 and alpha band.

#### **F2\_VOC (second factors between verbal fluency and vocabulary)**

In this section, we describe clusters arise from the contrast factors and compared them with the original clusters obtained with Verbal Fluency Letter (initial brain behaviour pattern) correlation/anticorrelation pattern, to better show what contrast factors bring, we divided description into similar cluster, disappearing and added clutters. Cluster description is only focused on the cluster account for verbal fluency variance.

#### Similar clusters between F2\_VOC and VF initial pattern

Similar clusters were found in the right premotor in delta alpha and beta band, in the caudal part of right pre- and post-central gyrus, in the right dmPFC in theta to beta band, in the left inferior dorsolateral in gamma 3 band, in the left anterior cingulate in delta and beta band, and also in the left dmPFC theta to beta band.

#### Disappearing clusters between F2\_VOC and VF initial pattern

Compare to the initial VF pattern, clusters disappearing with the contrast factors with vocabulary, we found these clusters in the right superior parietal lobule and precuneus delta to beta band, in the bilateral paracentral lobule in delta, alpha, beta band, in the caudal part of the dmPFC on the right hemisphere in delta to beta band, in the left superior parietal lobule in gamma 2, in the left post and pre-central gyrus in gamma 2 and 3 and in the upper part of premotor cortex in left hemisphere in gamma 3 band.

#### Added clusters between F2\_VOC and VF initial pattern

New clusters were found with the contrast factors (F2\_VOC) compare to initial pattern in the bilateral rostral part of dmPFC in theta to beta, in the right dlPFC delta to beta and in the right inferior dlPFC in gamma 2 and gamma 3.

### **F1\_TMT (first factor between verbal fluency and TMT4)**

#### Similar clusters between F1\_TMT and VF initial pattern

Similar clusters were found between contrast factors (VF-TMT4) and the initial pattern of VF, these clusters were found in the right superior parietal lobule in delta to alpha band, in the right post dorsal part of pre central gyrus in delta, alpha and beta band, in the right premotor in alpha and beta band, in the right caudal part of post central gyrus in alpha band, in the bilateral paracentral lobule in delta and alpha band and only on the left side in beta band, in the bilateral precuneus in theta band and right side for alpha band in the left angular, post central in gamma 2 and 3, in the left superior parietal lobule in gamma 2 band and in the left premotor in gamma 3 band.

### Disappearing clutters between F1\_TMT and VF initial pattern

Compare to the initial VF pattern, cluster disappearing with the contrast factors with vocabulary, we found these cluster in the bilateral dmPFC in delta alpha, right para central in beta band, in the right pre -motor and right superior lobule in gamma 2 and gamma 3 respectively and in the left anterior cingular in delta and beta band.

### Added clusters between F1\_TMT and VF initial pattern

New clusters were found with the contrast factors (VF-TMT4) compare to initial pattern in the right pre- and post-central gyrus in delta, theta, beta, gamma 2, gamma 3, in the bilateral superior parietal lobule (including precuneus) in all frequency bands, in the right dlPFC in delta band and in the right precuneus in beta to gamma 2 band.

### Supplementary Figures

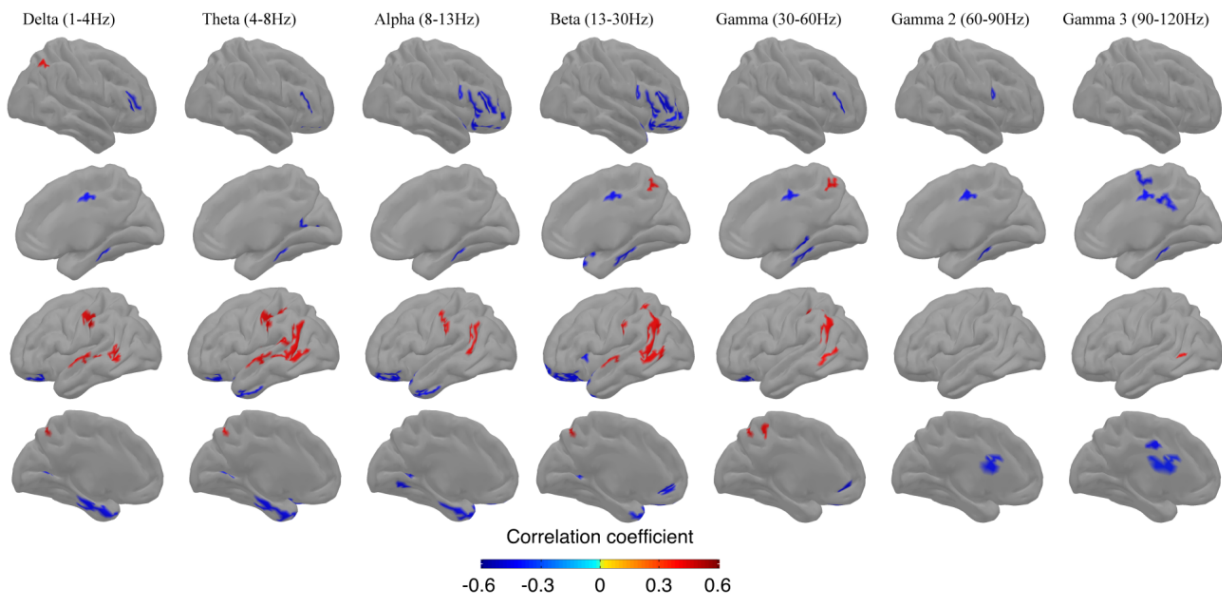


Figure 45. – Figure 2. — Spatial distribution of clusters with statistically significant correlations ( $p < .001$ ) between resting MEG source-space power (z-scores across vertices) and neuropsychological performance on the **Vocabulary** test. The formatting of the figure and statistical significance of the results are identical to those in Fig. 1.



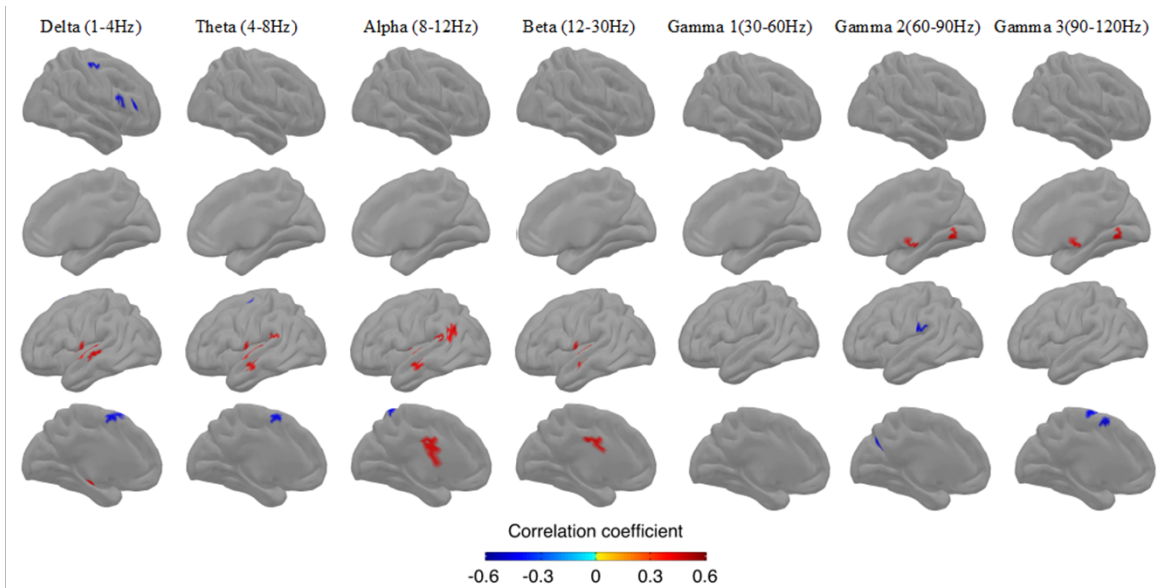


Figure 46. – Figure 3. — Spatial distribution of clusters with statistically significant correlations ( $p < .001$ ) between resting MEG source-space power (z-scores across vertices) and neuropsychological performance on the **Trail Making Test (Condition 4)** test. The formatting of the figure and statistical significance of the results are identical to those in Fig. 1.

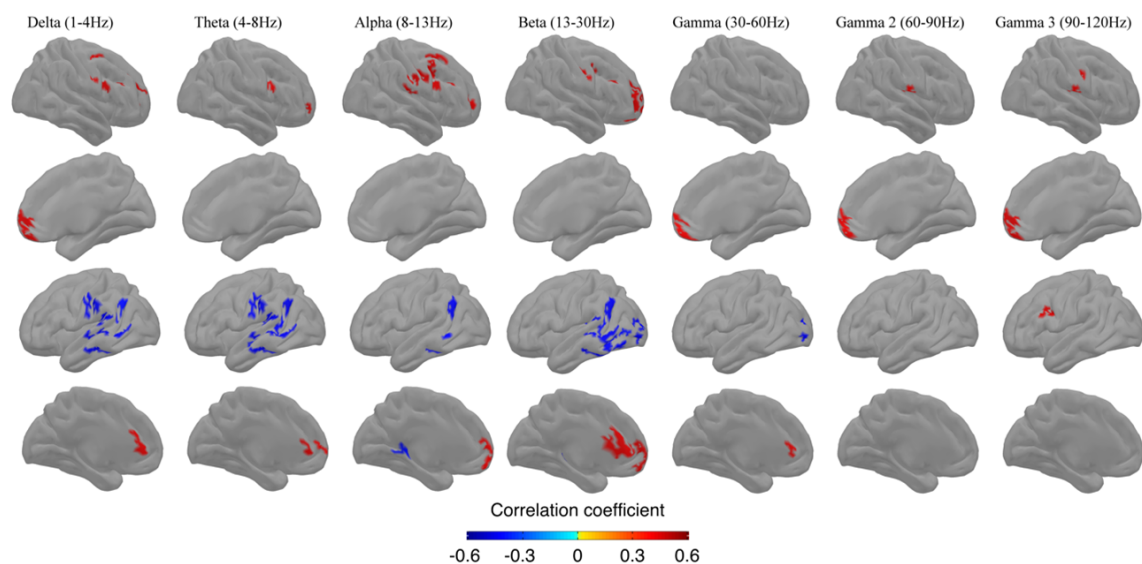


Figure 47. – Figure 4: Spatial distribution of clusters with statistically significant correlations ( $p < .001$ ) between resting MEG source-space power (z-scores across vertices) and neuropsychological performance on the Contrast factor (F2\_VOC) between **Verbal**

**Fluency and Vocabulary.** The formatting of the figure and statistical significance of the results are identical to those in Fig. 1.

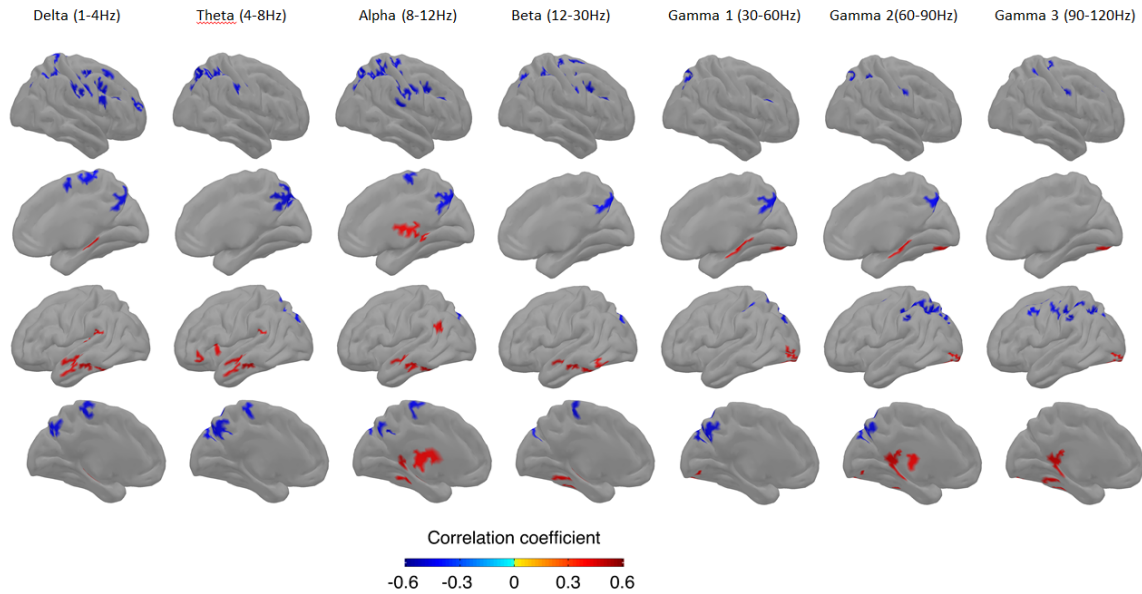


Figure 48. – Figure 5: Spatial distribution of clusters with statistically significant correlations ( $p < .001$ ) between resting MEG source-space power (z-scores across vertices) and neuropsychological performance on the Contrast factor (F1\_TMT) between **Verbal Fluency** and **Trail Making Test (Condition 4)**. The formatting of the figure and statistical significance of the results are identical to those in Fig. 1.

## Annexe 3 — chapitre 4

### Additional results

#### Neuropsychological performance

Tab 1 summarizes the mean and standard deviation, and min/ max values for the scores on the neuropsychological tests from CVLT-2. The participants' scores were normally distributed and no clinically meaningful cognitive deficits were found in any of the participants.

<b>Neuropsychological tests CVLT-2 (N=28)</b>	<b>Results Raw Score mean (SD) [min-max]</b>
<i>Verbal performance (trial 1)</i>	7,64 (1,31) [6-10]
<i>Verbal performance (trial 2)</i>	10,92 (1,96) [6-14]
<i>Verbal performance (trial 3)</i>	13,03 (2,38) [8-16]
<i>Verbal performance (trial 4)</i>	13,21 (1,96) [9-16]
<i>Verbal performance (trial 5)</i>	14,07 (1,65) [10-16]
<i>Verbal performance (trial B)</i>	7,07 (1,78) [5-11]
<i>Verbal performance (trial short recall)</i>	13,03 (2,54) [8-16]
<i>Verbal performance (trial long recall)</i>	13,5 (2,41) [7-16]
<i>Verbal performance (trial 1 to 5 T-score)</i>	57,32 (8,63) [36-71]
<i>Verbal learning slope (trial 1 to 3)</i>	1,5 (0,51) [0,7-2,30]
<i>Verbal learning slope (trial 3 to 5)</i>	0,64 (1,03) [-1,5-3,50]
<i>Semantic Strategy (trial 1 to 5)</i>	1,95 (2,58) [-0,90-6,90]
<i>Serial Forward Strategy (trial 1 to 5)</i>	0,45 (1,10) [-0,80-3,60]

Tableau 10. – Summarizes the mean and standard deviation, and min/ max values for the scores on the neuropsychological tests from CVLT-2

Figure 1A shows the mean performance across trials and evaluates short and long term recall. The score presented here are the raw (ie the number of word memorised), Participants performance improved consistently trial after trial. Up until trial 3, the sequence was encoded, while between trials 3 to 5, a memory consolidation process occurs that is reflect by a plateau in performance in between trial 3 and 4. Across participants the learning occurs in a similar and constantly manner, trial after trial showing a progressive learning process. This is confirmed by the performance during recall (short and long delay).

### **Trial by trial correlation for learning performance**

Figure 3 shows the sequential pattern of correlation trial by trial from CVLT, where the verbal learning memory was tested.

During the first trial, the participants show a correlation pattern with the dominant right hemisphere (the right hemisphere is illustrated in figure Supplementary 1), contrarily to the rest of the sequence which is supported by the left hemisphere. The trial shows correlation patterns with right sensory-motor and pre motor areas (BA 1, 2, 3, 4, 6), right superior temporal sulcus and gyrus (BA 22, 41, 42), these patterns are broad band in the right hemisphere while only the gamma band in the left hemisphere shows clusters correlation in premotor area (BA6) and somatosensory gyrus (BA2) and the dorso medial pre-frontal cortex (Dmpfc) (BA9).

The second trial highlights regions involved in language processing in the left hemisphere, we found clusters in the left inferior and superior parietal lobule, in the medial temporal gyrus and sulcus (BA22) mainly in posterior portion and we also found a cluster in the occipito-temporal area (BA37).

The process of encoding turned into consolidation during Trial 3, this process is supported by the left supplementary motor areas (SMA), premotor area (PMA) and sensorimotor regions appearing solely in trial 3, the performance begins to slow down at this point as is illustrated in figure 1. A second set of regions appear in this trial are parietal regions with the left parietal lobule and a cluster of in the angular gyrus (BA 7, 39, 40). Moreover, the same clusters related to language was found in this trial including superior temporal gyrus and sulcus and posterior middle temporal gyrus. No specific frequency band seems to play a role in linking specific regions at this level Trial 3 notes a large increase in correlation patterns in both size and number of clusters found.

In Trial 4, we found a similar pattern to the second trial with clusters in the left temporo-occipital junction, left superior temporal gyrus and sulcus, a left somatosensory gyrus with whom we also find a cluster in the left superior and left inferior parietal lobule.

For the trial 5, only slow frequency delta and theta band show clusters in left superior parietal areas. A broadband frequency clusters were found on the left side of the middle temporal gyrus and delta to beta for the left superior temporal gyrus.

Trial B, is an interference list, a new list is introduced to perturb the semantic memory process, Figure 1 show the drastic decrease of performance during this trial. Neural correlations for this trial show clusters in the same regions in alpha to gamma band than trial 2, 3 and 4 in the posterior middle temporal sulcus and gyrus, there is also medial cluster found in left parietal cortex with a left occipital cluster found in beta to gamma band. We also found in this trial a left Broca areas cluster (BA44) in highest gamma band.

The short term recall is administrated after trial B and show how the participants is able to recall the first list (list A) repeated 5 five times during trial 1 to 5. Our result show clusters in the left supplementary motor areas (SMA), pre central gyrus (motor) and post central (somatosensory) dominant in alpha band but extended between delta to gamma band.

For the long term recall, we only found a positive correlation clusters in the left central sulcus, left superior temporal gyrus and sulcus, and posterior middle temporal gyrus, distributed in alpha and gamma band respectively.

Overall correlation at rest with verbal learning show a coherent pattern with three sets of regions: temporal, central and parietal. Everyone appears at a selective step, temporal regions appear during learning step (trial 2 to 5, trial B) and long term recalls were mostly sustained by broad band frequency even if the strongest correlation is supported by the gamma band, whereas premotor motor, motor and somatosensory regions appears when the consolidation memory begins and with the short term recall mostly supported by the alpha band and their frequency neighbors. Finally, the parietal regions seem to support the cognitive effort during verbal learning, only appears in trial 3 and 4 and not in the recall with a broad band effect through all frequencies.

## **Two distinct learning slope correlation pattern**

As we just saw in trial by trial verbal learning performance, we saw that third trial is a turning point in the learning process. This suggested by performance curve and also by neural correlate found in trial 3.

Here we performed correlation with individual learning slope between trial 1 to 3 and trial 3 to 5. Figure 4 show pattern correlation between learning slope from trial 1 to 3 and neural oscillations power at rest. These results show pattern correlation with left hemisphere only including superior parietal lobule, premotor motor, motor and somatosensory areas in slowest frequency (delta to beta), and superior temporal gyrus, sulcus in the alpha band and posterior middle temporal gyrus in the gamma band.

On another hand Figure 5 show pattern correlations between learning slope from trial 3 to 5 and neural oscillations power at rest. We found cluster in both hemisphere, in bilateral dmPFC, in left dlPFC and left vmPFC. We also found cluster in left insula and left temporal pole, in bilateral parahippocampal gyrus and bilateral cingulate gyrus (frontal, medial and posterior), All these results are distributed across broad band frequencies.

The learning slope pattern correlations show clearly two distinct correlation pattern, the first one between trial 1 to 3 including all regions found in performance correlations in figure 2 and 3 whereas the second pattern correlation with learning slope between trial 3 to 5 show a new set of regions mostly supported by frontal, cingulate and temporal pole areas.

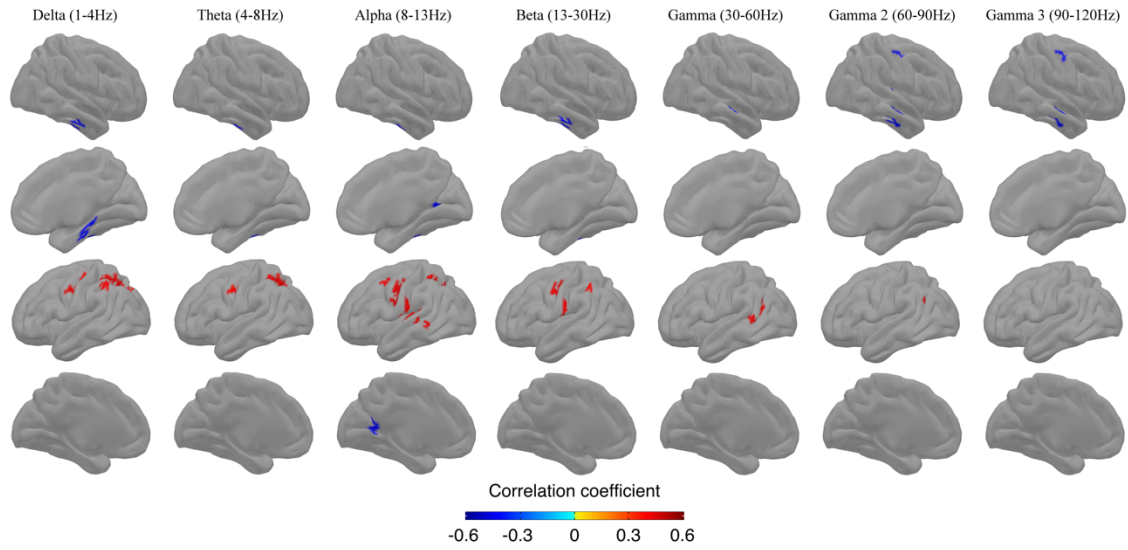


Figure 49. – Correlation Pattern with learning slope trial 1 to 3

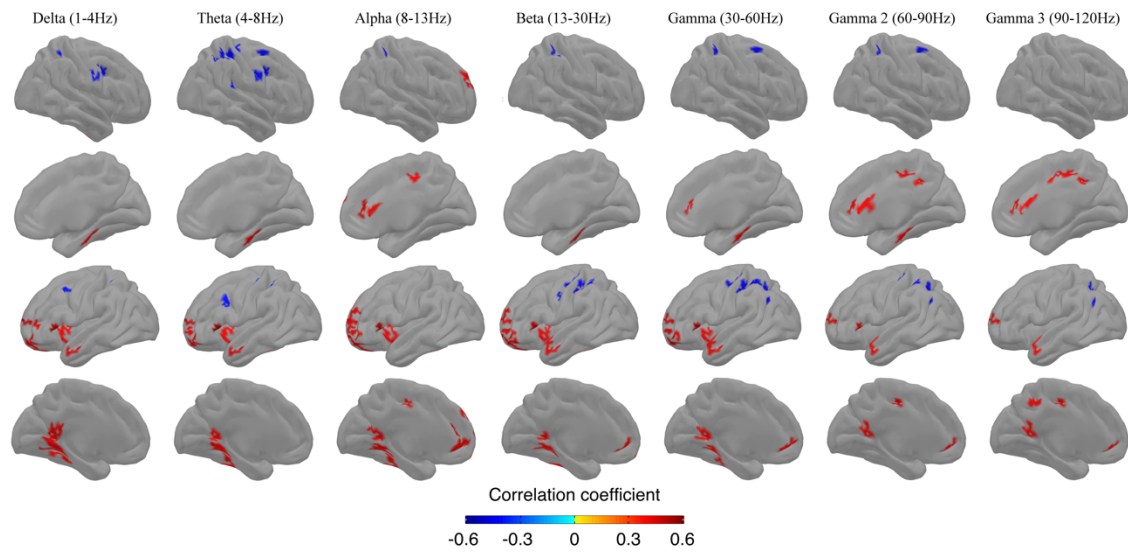


Figure 50. – Correlation Pattern with learning slope trial 3 to 5



Figure 51. – Strategy uses and correlation with performance trial by trial. Left panel shows the mean performance across trials and evaluates short- and long-term recall. The score presented here are the raw (ie the number of word memorized), Participants performance improved consistently trial after trial. Up until trial 3, the sequence was encoded, while between trials 3 to 5, a memory consolidation process occurs that is reflect by a plateau in performance in between trial 3 and 4. Across participants the learning occurs in a similar and constantly manner, trial after trial showing a progressive learning process. This is confirmed by the performance during recall (short and long delay). Right panel show correlation between raw score and strategy used trial by trial. Semantic strategy show and increase in performance until the fifth trial and for the recall.



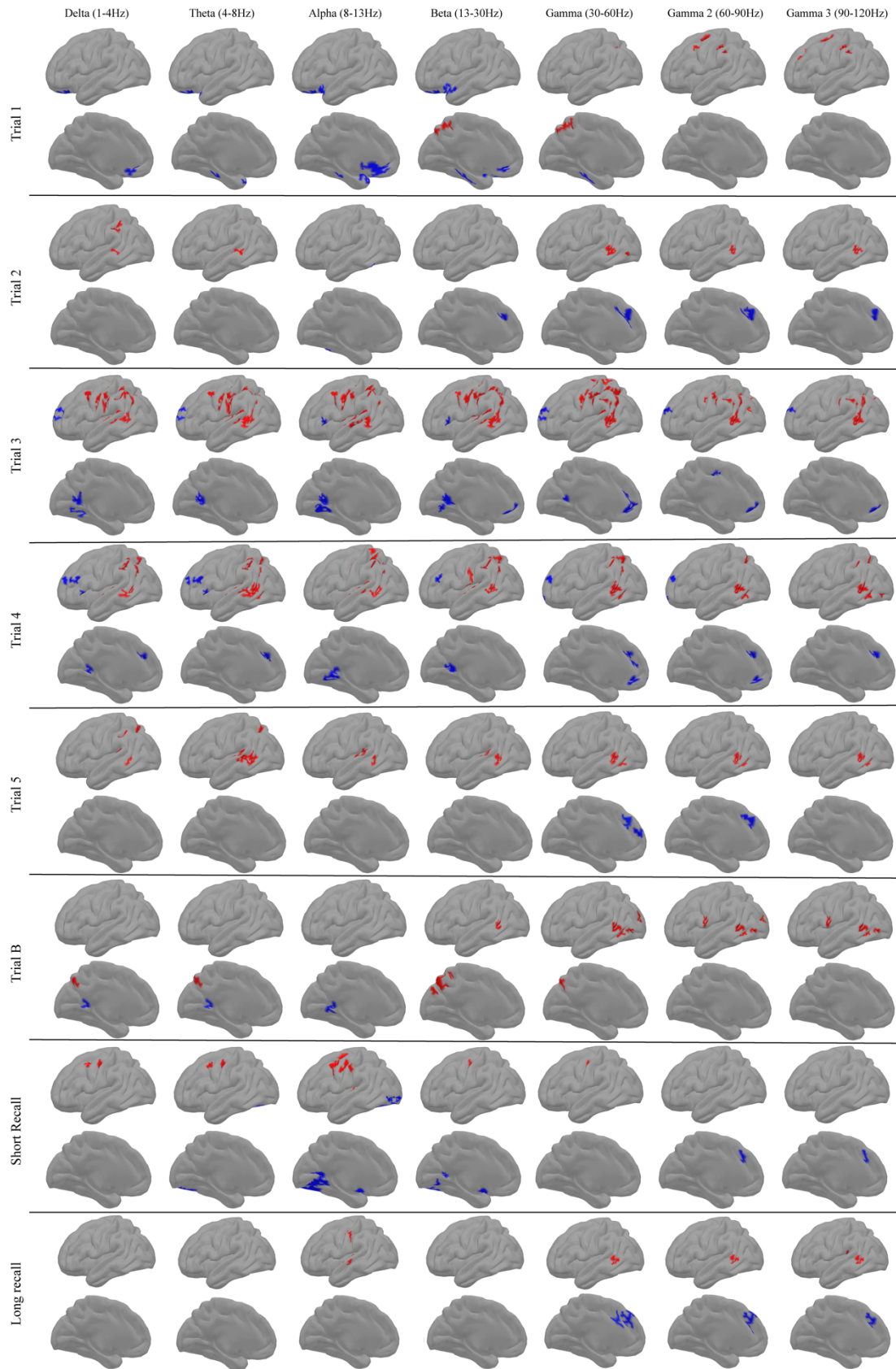


Figure 52. – Correlation Pattern with performance trial by trial and recall of CVLT-2, for the Left hemisphere

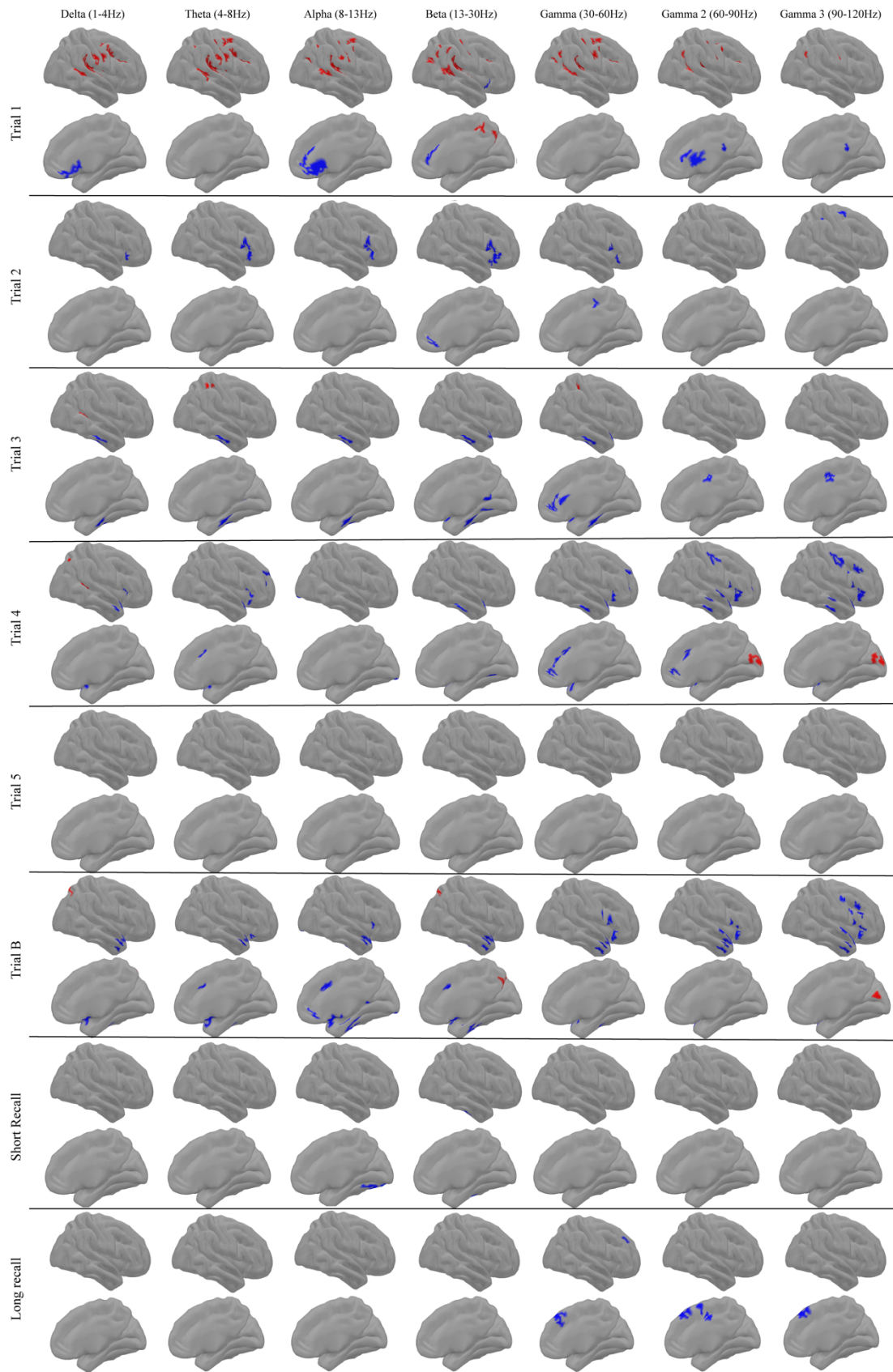


Figure 53. – Correlation Pattern with performance trial by trial and recall of CVLT-2 for the right hemisphere

## Références bibliographiques

- Abe, M., & Hanakawa, T. (2009). Functional coupling underlying motor and cognitive functions of the dorsal premotor cortex. *Behavioural Brain Research*, *198*(1), 13–23. <https://doi.org/10.1016/j.bbr.2008.10.046>
- Alexander, M. P., Stuss, D. T., & Fansabedian, N. (2003). California Verbal Learning Test: Performance by patients with focal frontal and non-frontal lesions. *Brain*, *126*(6), 1493–1503. <https://doi.org/10.1093/brain/awg128>
- Alexander, T. C., Simecka, C. M., Kiffer, F., Groves, T., Anderson, J., Carr, H., Wang, J., Carter, G., & Allen, A. R. (2018). Changes in cognition and dendritic complexity following intrathecal methotrexate and cytarabine treatment in a juvenile murine model. *Behavioural Brain Research*, *346*(December 2017), 21–28. <https://doi.org/10.1016/j.bbr.2017.12.008>
- Alvarez, J. A., & Emory, E. (2006). Executive function and the frontal lobes: A meta-analytic review. *Neuropsychology Review*, *16*(1), 17–42. <https://doi.org/10.1007/s11065-006-9002>
- Anastassiou, C. A., Montgomery, S. M., Barahona, M., Buzsáki, G., & Koch, C. (2010). The effect of spatially inhomogeneous extracellular electric fields on neurons. *Journal of Neuroscience*, *30*(5), 1925–1936. <https://doi.org/10.1523/JNEUROSCI.3635-09.2010>
- Andersen, P., Bliss, T. V. P., & Skrede, K. K. (1971). Lamellar organization of hippocampal excitatory pathways. *Experimental Brain Research*, *13*(2), 222–238. <https://doi.org/10.1007/BF00234087>
- Arnett, J. A., & Labovitz, S. S. (1995). Effect of Physical Layout in Performance of the Trail Making Test. *Psychological Assessment*, *7*(2), 220–221. <https://doi.org/10.1037//1040-3590.7.2.220>
- Atkinson, R. C., & Shiffrin, R. M. (1968). *Human Memory: A Proposed System and its Control Processes*. This research was supported by the National Aeronautics and Space Administration, Grant No. NGR-05-020-036. The authors are indebted to W. K. Estes and G. H. Bower who provided many valuable suggestions (K. W. Spence & J. T. B. T.-P. of L. and M. Spence (eds.); Vol. 2, pp. 89–195). Academic Press. <https://doi.org/https://doi.org/10.1016/S0079->

7421(08)60422-3

Baddeley, A. (2000). The episodic buffer: a new component of working memory? *Trends in Cognitive Sciences*, 4(11), 6267–6279. <https://doi.org/10.1016/j.apm.2016.02.027>

Baddeley, A. D. (1978). The trouble with levels: A reexamination of Craik and Lockhart's framework for memory research. *Psychological Review*, 85(3), 139–152. <https://doi.org/10.1037/0033-295X.85.3.139>

Baddeley, A. D., & Hitch, G. (1974). *Working Memory* (G. H. B. T.-P. of L. and M. Bower (ed.); Vol. 8, pp. 47–89). Academic Press. [https://doi.org/https://doi.org/10.1016/S0079-7421\(08\)60452-1](https://doi.org/https://doi.org/10.1016/S0079-7421(08)60452-1)

Baillet, S., Mosher, J. C., & Leahy, R. M. (2001). *Sylvain Baillet, John C. Mosher, and Richard M. Leahy. November.*

Baldo, J. V., Delis, D., Kramer, J., & Shimamura, A. P. (2020). *Memory performance on the California Verbal Learning Test – II : Findings from patients with focal frontal lesions. 2002*, 539–546.

Barsalou, L. W. (1999). Perceptual symbol systems and emotion. *Behavioral and Brain Sciences*, 22(4), 612–613. <https://doi.org/10.1017/S0140525X99252144>

Barsalou, L. W. (2008). Grounded cognition. *Annual Review of Psychology*, 59, 617–645. <https://doi.org/10.1146/annurev.psych.59.103006.093639>

Basti, A., Pizzella, V., Chella, F., Romani, G. L., Nolte, G., & Marzetti, L. (2018). Disclosing large-scale directed functional connections in MEG with the multivariate phase slope index. *NeuroImage*, 175(May 2017), 161–175. <https://doi.org/10.1016/j.neuroimage.2018.03.004>

Bastiaansen, M. C. M., Van Der Linden, M., Ter Keurs, M., Dijkstra, T., & Hagoort, P. (2005). Theta responses are involved in lexical-semantic retrieval during language processing. *Journal of Cognitive Neuroscience*, 17(3), 530–541. <https://doi.org/10.1162/0898929053279469>

Beber, B. C., & Chaves, M. L. F. (2014). The Basis and Applications of the Action Fluency and Action Naming Tasks. *Dementia & Neuropsychologia*, 8(1), 47–57. <https://doi.org/10.1590/s1980-57642014dn81000008>

- Beggs, J. M. (2008). The criticality hypothesis: How local cortical networks might optimize information processing. *Philosophical Transactions of the Royal Society A: Mathematical, Physical and Engineering Sciences*, 366(1864), 329–343. <https://doi.org/10.1098/rsta.2007.2092>
- Beggs, J. M., & Plenz, D. (2003). Neuronal Avalanches in Neocortical Circuits. *The Journal of Neuroscience*, 23(12), 2489–2493. <https://doi.org/10.1523/JNEUROSCI.4453-03.2003>
- Bennett, M. V. L., & Zukin, R. S. (2004). Electrical Coupling and Neuronal Synchronization in the Mammalian Brain. *Neuron*, 41(4), 495–511. [https://doi.org/10.1016/S0896-6273\(04\)00043-1](https://doi.org/10.1016/S0896-6273(04)00043-1)
- Billiet, T., Elens, I., Sleurs, C., Uyttebroeck, A., D’Hooge, R., Lemièrre, J., & Deprez, S. (2018). Brain connectivity and cognitive flexibility in nonirradiated adult survivors of childhood leukemia. *Journal of the National Cancer Institute*, 110(8), 905–913. <https://doi.org/10.1093/jnci/djy009>
- Biswal, B., Zerrin Yetkin, F., Haughton, V. M., & Hyde, J. S. (1995). Functional connectivity in the motor cortex of resting human brain using echo-planar mri. *Magnetic Resonance in Medicine*, 34(4), 537–541. <https://doi.org/10.1002/mrm.1910340409>
- Bonnefond, M., & Jensen, O. (2012). Alpha oscillations serve to protect working memory maintenance against anticipated distracters. *Current Biology*, 22(20), 1969–1974. <https://doi.org/10.1016/j.cub.2012.08.029>
- Boulet-Craig, A., Robaey, P., Laniel, J., Bertout, L., Drouin, S., Krajinovic, M., Laverdière, C., Sinnett, D., Sultan, S., & Lippé, S. (2018). DIVERGT screening procedure predicts general cognitive functioning in adult long-term survivors of pediatric acute lymphoblastic leukemia: A PETALE study. *Pediatric Blood and Cancer*, 65(9), 1–9. <https://doi.org/10.1002/pbc.27259>
- Brentano, F. (1924). Psychologie vom empirischen standpunkt. In *leipzig f. Meiner*.
- Brookes, M. J., Woolrich, M., Luckhoo, H., Price, D., Hale, J. R., Stephenson, M. C., Barnes, G. R., Smith, S. M., & Morris, P. G. (2011). Investigating the electrophysiological basis of resting state networks using magnetoencephalography. *Proceedings of the National Academy of Sciences*, 108(18), 7993–7998. <https://doi.org/10.1073/pnas.1014613108>

*Sciences of the United States of America*, 108(40), 16783–16788.  
<https://doi.org/10.1073/pnas.1112685108>

Buchsbaum, B. R., & D'Esposito, M. (2008). The search for the phonological store: From loop to convolution. *Journal of Cognitive Neuroscience*, 20(5), 762–778.  
<https://doi.org/10.1162/jocn.2008.20501>

Buchsbaum, B. R., Padmanabhan, A., & Berman, K. F. (2011). The neural substrates of recognition memory for verbal information: Spanning the divide between short- and long-term memory. *Journal of Cognitive Neuroscience*, 23(4), 978–991.  
<https://doi.org/10.1162/jocn.2010.21496>

Buckner, R. L., Andrews-Hanna, J. R., & Schacter, D. L. (2008). The brain's default network: Anatomy, function, and relevance to disease. *Annals of the New York Academy of Sciences*, 1124, 1–38. <https://doi.org/10.1196/annals.1440.011>

Butler, M., Retzlaff, P., & Vanderploeg, R. (1991). Neuropsychological Test Usage. *Professional Psychology: Research and Practice*, 22(6), 510–512. <https://doi.org/10.1037/0735-7028.22.6.510>

Buzsáki, G. (2009). Rhythms of the Brain. In *Rhythms of the Brain*.  
<https://doi.org/10.1093/acprof:oso/9780195301069.001.0001>

Buzsáki, G. (2019). The Brain from Inside Out. In *The Brain from Inside Out*. Oxford University Press.

Buzsáki, G., Anastassiou, C. A., & Koch, C. (2012). The origin of extracellular fields and currents—EEG, ECoG, LFP and spikes. *Nature Reviews Neuroscience*, 13(6), 407–420.  
<https://doi.org/10.1038/nrn3241>

Buzsaki, G., & Draguhn, A. (2004). Neuronal Oscillations in Cortical Networks. *Science*, 304(June), 1926–1929. <http://science.sciencemag.org/>

Cabral, J., Kringelbach, M. L., & Deco, G. (2014). Exploring the network dynamics underlying brain activity during rest. *Progress in Neurobiology*, 114, 102–131.  
<https://doi.org/10.1016/j.pneurobio.2013.12.005>



- Campbell, L. K., Scaduto, M., Sharp, W., Dufton, L., Slyke, D. Van, Whitlock, J. A., Compas, B., & Background., 1\*. (2007). A Meta-Analysis of the Neurocognitive Sequelae of Treatment for Childhood Acute Lymphocytic Leukemia. *Pediatric Blood & Cancer*, 49(5), 65–73. <https://doi.org/10.1002/pbc>
- Canolty, R. T., Edwards, E., Dalal, S. S., Soltani, M., Nagarajan, S. S., Kirsch, H. E., Berger, M. S., Barbare, N. M., & Knight, R. T. (2006). High gamma power is phase-locked to theta oscillations in human neocortex. *Science*, 313(5793), 1626–1628. <https://doi.org/10.1126/science.1128115>
- Cardin, J. A., Kumbhani, R. D., Contreras, D., & Palmer, L. A. (2010). Cellular mechanisms of temporal sensitivity in visual cortex neurons. *Journal of Neuroscience*, 30(10), 3652–3662. <https://doi.org/10.1523/JNEUROSCI.5279-09.2010>
- Chai, W. J., Abd Hamid, A. I., & Abdullah, J. M. (2018). Working memory from the psychological and neurosciences perspectives: A review. *Frontiers in Psychology*, 9(MAR), 1–16. <https://doi.org/10.3389/fpsyg.2018.00401>
- Chan, B. Y. C. Y., & Nicholson, C. (1986). Electric fields of purkinje. *New York*, 1986, 89–114.
- Chang, C., Crottaz-Herbette, S., & Menon, V. (2007). Temporal dynamics of basal ganglia response and connectivity during verbal working memory. *NeuroImage*, 34(3), 1253–1269. <https://doi.org/10.1016/j.neuroimage.2006.08.056>
- Chen, L., Zhan, Y., He, F., Zhang, S., Wu, L., Gong, H., Zhou, F., Zeng, X., & Xu, H. (2020). <p>Altered Functional Connectivity Density in Young Survivors of Acute Lymphoblastic Leukemia Using Resting-State fMRI</p>. *Cancer Management and Research*, Volume 12, 7033–7041. <https://doi.org/10.2147/cmar.s253202>
- Cheung, Y. T., & Krull, K. R. (2015). Neurocognitive outcomes in long-term survivors of childhood acute lymphoblastic leukemia treated on contemporary treatment protocols: A systematic review. *Neuroscience and Biobehavioral Reviews*, 53, 108–120. <https://doi.org/10.1016/j.neubiorev.2015.03.016>
- Cheung, Y. T., Sabin, N. D., Reddick, W. E., Bhojwani, D., Liu, W., Brinkman, T. M., Glass, J. O.,

- Hwang, S. N., Srivastava, D., Pui, C. H., Robison, L. L., Hudson, M. M., & Krull, K. R. (2016). Leukoencephalopathy and long-term neurobehavioural, neurocognitive, and brain imaging outcomes in survivors of childhood acute lymphoblastic leukaemia treated with chemotherapy: a longitudinal analysis. *The Lancet Haematology*, *3*(10), e456–e466. [https://doi.org/10.1016/S2352-3026\(16\)30110-7](https://doi.org/10.1016/S2352-3026(16)30110-7)
- Cisek, P. (1999). Beyond the computer metaphor: Behaviour as interaction. *Journal of Consciousness Studies*, *6*(11–12), 125–142.
- Cisek, P. (2019). Resynthesizing behavior through phylogenetic refinement. *Attention, Perception, and Psychophysics*, *81*(7), 2265–2287. <https://doi.org/10.3758/s13414-019-01760-1>
- Cisek, P., & Kalaska, J. F. (2010). Neural mechanisms for interacting with a world full of action choices. *Annual Review of Neuroscience*, *33*, 269–298. <https://doi.org/10.1146/annurev.neuro.051508.135409>
- Clark, D. G., Wadley, V. G., Kapur, P., DeRamus, T. P., Singletary, B., Nicholas, A. P., Blanton, P. D., Lokken, K., Deshpande, H., Marson, D., & Deutsch, G. (2014). Lexical factors and cerebral regions influencing verbal fluency performance in MCI. *Neuropsychologia*, *54*(1), 98–111. <https://doi.org/10.1016/j.neuropsychologia.2013.12.010>
- Conklin, H. M., Krull, K. R., Reddick, W. E., Pei, D., Cheng, C., & Pui, C. H. (2012). Cognitive outcomes following contemporary treatment without cranial irradiation for childhood acute lymphoblastic leukemia. *Journal of the National Cancer Institute*, *104*(18), 1386–1395. <https://doi.org/10.1093/jnci/djs344>
- Craik, F. I. M., & Lockhart, R. S. (1972). Levels of processing: A framework for memory research. *Journal of Verbal Learning and Verbal Behavior*, *11*(6), 671–684. [https://doi.org/10.1016/S0022-5371\(72\)80001-X](https://doi.org/10.1016/S0022-5371(72)80001-X)
- Crosson, B. (2008). An intention manipulation to change lateralization of word production in nonfluent aphasia: Current status. *Seminars in Speech and Language*, *29*(3), 188–200. <https://doi.org/10.1055/s-0028-1082883>
- Crosson, B., Rao, S. M., Woodley, S. J., Rosen, A. C., Bobholz, J. A., Mayer, A., Cunningham, J. M.,

- Hammeke, T. A., Fuller, S. A., Binder, J. R., Cox, R. W., & Stein, E. A. (1999). Mapping of semantic, phonological, and orthographic verbal working memory in normal adults with functional magnetic resonance imaging. *Neuropsychology, 13*(2), 171–187. <https://doi.org/10.1037/0894-4105.13.2.171>
- D.C. Delis, J.H. Kramer, E. Kaplan, B. A. O. (2000). California Verbal Learning Test – second edition. Adult version. Manual. *Psychological Corporation, San Antonio, TX.*
- Daams, M., Schuitema, I., van Dijk, B. W., van Dulmen-den Broeder, E., Veerman, A. J. P., van den Bos, C., & de Sonnevile, L. M. J. (2012). Long-term effects of cranial irradiation and intrathecal chemotherapy in treatment of childhood leukemia: a MEG study of power spectrum and correlated cognitive dysfunction. *BMC Neurology, 12*. <https://doi.org/10.1186/1471-2377-12-84>
- Davis, C., Heidler-Gary, J., Gottesman, R. F., Crinion, J., Newhart, M., Moghekar, A., Soloman, D., Rigamonti, D., Cloutman, L., & Hillis, A. E. (2010). Action versus animal naming fluency in subcortical dementia, frontal dementias, and Alzheimer’s disease. *Neurocase, 16*(3), 259–266. <https://doi.org/10.1080/13554790903456183>
- De Pasquale, F., Della Penna, S., Snyder, A. Z., Lewis, C., Mantini, D., Marzetti, L., Belardinelli, P., Ciancetta, L., Pizzella, V., Romani, G. L., & Corbetta, M. (2010). Temporal dynamics of spontaneous MEG activity in brain networks. *Proceedings of the National Academy of Sciences of the United States of America, 107*(13), 6040–6045. <https://doi.org/10.1073/pnas.0913863107>
- Desmond, J. E., Gabrieli, J. D. E., Wagner, A. D., Ginier, B. L., & Glover, G. H. (1997). Lobular patterns of cerebellar activation in verbal working-memory and finger-tapping tasks as revealed by functional MRI. *Journal of Neuroscience, 17*(24), 9675–9685. <https://doi.org/10.1523/jneurosci.17-24-09675.1997>
- Ewald, A., Aristei, S., Nolte, G., & Abdel Rahman, R. (2012). Brain oscillations and functional connectivity during overt language production. *Frontiers in Psychology, 3*(JUN), 1–12. <https://doi.org/10.3389/fpsyg.2012.00166>

- Faroqi-Shah, Y., & Milman, L. (2018). Comparison of animal, action and phonemic fluency in aphasia. *International Journal of Language and Communication Disorders*, *53*(2), 370–384. <https://doi.org/10.1111/1460-6984.12354>
- Fellah, S., Cheung, Y. T., Scoggins, M. A., Zou, P., Sabin, N. D., Pui, C. H., Robison, L. L., Hudson, M. M., Ogg, R. J., & Krull, K. R. (2019). Brain activity associated with attention deficits following chemotherapy for childhood acute lymphoblastic leukemia. *Journal of the National Cancer Institute*, *111*(2), 201–209. <https://doi.org/10.1093/jnci/djy089>
- Florin, E., & Baillet, S. (2015). The brain's resting-state activity is shaped by synchronized cross-frequency coupling of neural oscillations. *NeuroImage*, *111*, 26–35. <https://doi.org/10.1016/j.neuroimage.2015.01.054>
- Fox, M. D., & Greicius, M. (2010). Clinical applications of resting state functional connectivity. *Frontiers in Systems Neuroscience*, *4*(June). <https://doi.org/10.3389/fnsys.2010.00019>
- Fox, M. D., & Raichle, M. E. (2007). Spontaneous fluctuations in brain activity observed with functional magnetic resonance imaging. *Nature Reviews Neuroscience*, *8*(9), 700–711. <https://doi.org/10.1038/nrn2201>
- Freund, T. F., & Buzsáki, G. (1996). Interneurons of the Hippocampus. *Hippocampus*, *6*(4), 347–470. [https://doi.org/10.1002/\(sici\)1098-1063\(1996\)6:4<347::aid-hipo1>3.0.co;2-i](https://doi.org/10.1002/(sici)1098-1063(1996)6:4<347::aid-hipo1>3.0.co;2-i)
- Friedman, N. P., & Miyake, A. (2017). Unity and diversity of executive functions: Individual differences as a window on cognitive structure. *Cortex*, *86*, 186–204. <https://doi.org/10.1016/j.cortex.2016.04.023>
- Friston, K., FitzGerald, T., Rigoli, F., Schwartenbeck, P., O'Doherty, J., & Pezzulo, G. (2016). Active inference and learning. *Neuroscience and Biobehavioral Reviews*, *68*, 862–879. <https://doi.org/10.1016/j.neubiorev.2016.06.022>
- Friston, K. J., Daunizeau, J., Kilner, J., & Kiebel, S. J. (2010). Action and behavior: A free-energy formulation. *Biological Cybernetics*, *102*(3), 227–260. <https://doi.org/10.1007/s00422-010-0364-z>

- Gao, H., He, F., Lin, X., & Wu, Y. (2017). *Drosophila VAMP7 regulates Wingless intracellular trafficking. PLoS ONE, 12*(10), 1–14. <https://doi.org/10.1371/journal.pone.0186938>
- Garnero, L., Baillet, S., & Renault, B. (1998). Magnétoencéphalographie / électroencéphalographie et imagerie cérébrale fonctionnelle. *Annales de l'Institut Pasteur/Actualites, 9*(3), 215–226. [https://doi.org/10.1016/S0924-4204\(99\)80001-8](https://doi.org/10.1016/S0924-4204(99)80001-8)
- Gavaret, M., Badier, J. M., & Chauvel, P. (2008). High-resolution EEG (HR-EEG) and magnetoencephalography (MEG). *Neurochirurgie, 54*(3), 185–190. <https://doi.org/10.1016/j.neuchi.2008.02.014>
- Gibson, J. J. (1981). The ecological approach to visual perception. *Behavioral Science Boston: Houghton Mifflin, 26*(3), 308–309. <https://doi.org/https://doi.org/10.1002/bs.3830260313>
- Goldberg-Stern, H., Cohen, R., Pollak, L., Kivity, S., Eidlitz-Markus, T., Stark, B., Yaniv, I., & Shuper, A. (2011). The mystery of electroencephalography in acute lymphoblastic leukemia. *Seizure, 20*(3), 194–196. <https://doi.org/10.1016/j.seizure.2010.11.016>
- Goldman-Rakic, P. S. (1996). Regional and cellular fractionation of working memory. *Proceedings of the National Academy of Sciences of the United States of America, 93*(24), 13473–13480. <https://doi.org/10.1073/pnas.93.24.13473>
- Goodale, M. A., & Milner, A. D. (2014). Separate visual pathways for perception and action. *Research Journal of Pharmaceutical, Biological and Chemical Sciences, 5*(3), 1275–1279.
- Gordon, J. K., Young, M., & Garcia, C. (2018). Why do older adults have difficulty with semantic fluency? *Aging, Neuropsychology, and Cognition, 25*(6), 803–828. <https://doi.org/10.1080/13825585.2017.1374328>
- Gosseries, O., Demertzi, A., Noirhomme, Q., Tshibanda, J., Boly, M., Op De Beeck, M., Hustinx, R., Maquet, P., Salmon, E., Moonen, G., Luxen, A., Laureys, S., & De Tiège, X. (2008). Que mesure la neuro-imagerie fonctionnelle: IRMf, TEP & MEG? *Revue Medicale de Liege, 63*(5–6), 231–237.
- Graziano, M. S. A. (2016). Ethological Action Maps: A Paradigm Shift for the Motor Cortex. *Trends*

- in Cognitive Sciences*, 20(2), 121–132. <https://doi.org/10.1016/j.tics.2015.10.008>
- Hagoort, P., & Indefrey, P. (2014). The neurobiology of language beyond single words. *Annual Review of Neuroscience*, 37, 347–362. <https://doi.org/10.1146/annurev-neuro-071013-013847>
- Hanakawa, T., Honda, M., Okada, T., Fukuyama, H., & Shibasaki, H. (2003). Differential activity in the premotor cortex subdivisions in humans during mental calculation and verbal rehearsal tasks: A functional magnetic resonance imaging study. *Neuroscience Letters*, 347(3), 199–201. [https://doi.org/10.1016/S0304-3940\(03\)00692-X](https://doi.org/10.1016/S0304-3940(03)00692-X)
- He, B., Astolfi, L., Valdes-Sosa, P. A., Marinazzo, D., Palva, S. O., Benar, C. G., Michel, C. M., & Koenig, T. (2019). Electrophysiological Brain Connectivity: Theory and Implementation. *IEEE Transactions on Biomedical Engineering*, 66(7), 2115–2137. <https://doi.org/10.1109/TBME.2019.2913928>
- He, B. J. (2014). Scale-free brain activity: Past, present, and future. *Trends in Cognitive Sciences*, 18(9), 480–487. <https://doi.org/10.1016/j.tics.2014.04.003>
- Henry, J. D., Crawford, J. R., & Phillips, L. H. (2004). Verbal fluency performance in dementia of the Alzheimer's type: A meta-analysis. *Neuropsychologia*, 42(9), 1212–1222. <https://doi.org/10.1016/j.neuropsychologia.2004.02.001>
- Hesse, J., & Gross, T. (2014). Self-organized criticality as a fundamental property of neural systems. *Frontiers in Systems Neuroscience*, 8(September), 1–14. <https://doi.org/10.3389/fnsys.2014.00166>
- Hickok, G., & Poeppel, D. (2004). Dorsal and ventral streams: A framework for understanding aspects of the functional anatomy of language. *Cognition*, 92(1–2), 67–99. <https://doi.org/10.1016/j.cognition.2003.10.011>
- Hickok, G., & Poeppel, D. (2007). The cortical organization of speech understanding. *Nature*, 8(May), 393–402. [www.nature.com/reviews/neuro](http://www.nature.com/reviews/neuro)<https://www-nature-com.ezp-prod1.hul.harvard.edu/articles/nrn2113.pdf>

- Hipp, J. F., Hawellek, D. J., Corbetta, M., Siegel, M., & Engel, A. K. (2012). Large-scale cortical correlation structure of spontaneous oscillatory activity. *Nature Neuroscience*, *15*(6), 884–890. <https://doi.org/10.1038/nn.3101>
- Hommel, B., Chapman, C. S., Cisek, P., Neyedli, H. F., Song, J. H., & Welsh, T. N. (2019). No one knows what attention is. *Attention, Perception, and Psychophysics*, *81*(7), 2288–2303. <https://doi.org/10.3758/s13414-019-01846-w>
- Honey, G. D., Bullmore, E. T., & Sharma, T. (2000). Prolonged reaction time to a verbal working memory task predicts increased power of posterior parietal cortical activation. *NeuroImage*, *12*(5), 495–503. <https://doi.org/10.1006/nimg.2000.0624>
- Hotson, J. R., & Prince, D. A. (1980). A calcium-activated hyperpolarization follows repetitive firing in hippocampal neurons. *Journal of Neurophysiology*, *43*(2), 409–419. <https://doi.org/10.1152/jn.1980.43.2.409>
- Husserl, E. (1917). On the Phenomenology of the Consciousness of Internal Time. *Trans. J. B. Brough, Dordrecht: Kluwer*.
- Iyer, N. S., Balsamo, L. M., Bracken, M. B., & Kadan-Lottick, N. S. (2015). Chemotherapy-only treatment effects on long-term neurocognitive functioning in childhood ALL survivors: A review and meta-analysis. *Blood*, *126*(3), 346–353. <https://doi.org/10.1182/blood-2015-02-627414>
- Jacobson, S. C., Blanchard, M., Connolly, C. C., Cannon, M., & Garavan, H. (2011). An fMRI investigation of a novel analogue to the Trail-Making Test. *Brain and Cognition*, *77*(1), 60–70. <https://doi.org/10.1016/j.bandc.2011.06.001>
- Jensen, O., Gelfand, J., Kounios, J., & Lisman, J. E. (2002). Oscillations in the alpha band (9-12 Hz) increase with memory load during retention in a short-term memory task. *Cerebral Cortex*, *12*(8), 877–882. <https://doi.org/10.1093/cercor/12.8.877>
- Jensen, O., & Mazaheri, A. (2010). Shaping functional architecture by oscillatory alpha activity: Gating by inhibition. *Frontiers in Human Neuroscience*, *4*(November), 1–8. <https://doi.org/10.3389/fnhum.2010.00186>

- Jerbi, K., Vidal, J. R., Ossandon, T., Dalal, S. S., Jung, J., Hoffmann, D., Minotti, L., Bertrand, O., Kahane, P., & Lachaux, J. P. (2010). Exploring the electrophysiological correlates of the default-mode network with intracerebral EEG. *Frontiers in Systems Neuroscience*, 4(June), 1–9. <https://doi.org/10.3389/fnsys.2010.00027>
- Kaas, J. H., & Stepniewska, I. (2016). Evolution of posterior parietal cortex and parietal-frontal networks for specific actions in primates. *Journal of Comparative Neurology*, 524(3), 595–608. <https://doi.org/10.1002/cne.23838>
- Kalénine, S., Peyrin, C., Pichat, C., Segebarth, C., Bonthoux, F., & Baciú, M. (2009). The sensory-motor specificity of taxonomic and thematic conceptual relations: A behavioral and fMRI study. *NeuroImage*, 44(3), 1152–1162. <https://doi.org/10.1016/j.neuroimage.2008.09.043>
- Kesler, S. R., Meike Gugel, Pritchard-Berman, M., Lee, C., Kutner, E., Hosseini, H., Dahl, G., & Lacayo, N. (2014). Altered Resting State Functional Connectivity in Young Survivors of Acute Lymphoblastic Leukemia. *Pediatric Blood & Cancer*, 61, 1295–1299. <https://doi.org/10.1002/pbc.25022>
- Kesler, S. R., Ogg, R., Reddick, W. E., Phillips, N., Scoggins, M., Glass, J. O., Cheung, Y. T., Pui, C. H., Robison, L. L., Hudson, M. M., & Krull, K. R. (2018). Brain Network Connectivity and Executive Function in Long-Term Survivors of Childhood Acute Lymphoblastic Leukemia. *Brain Connectivity*, 8(6), 333–342. <https://doi.org/10.1089/brain.2017.0574>
- Khalsa, S. S., Adolphs, R., Cameron, O. G., Critchley, H. D., Davenport, P. W., Feinstein, J. S., Feusner, J. D., Garfinkel, S. N., Lane, R. D., Mehling, W. E., Meuret, A. E., Nemeroff, C. B., Oppenheimer, S., Petzschner, F. H., Pollatos, O., Rhudy, J. L., Schramm, L. P., Simmons, W. K., Stein, M. B., ... Zucker, N. (2018). Interoception and Mental Health: A Roadmap. *Biological Psychiatry: Cognitive Neuroscience and Neuroimaging*, 3(6), 501–513. <https://doi.org/10.1016/j.bpsc.2017.12.004>
- Kibby, M. Y., Schmitter-Edgecombe, M., & Long, C. J. (1998). Ecological validity of neuropsychological tests: focus on the California Verbal Learning Test and the Wisconsin Card Sorting Test. *Archives of Clinical Neuropsychology: The Official Journal of the National*



*Academy of Neuropsychologists, 13(6), 523–534.*

Klimesch, W., Schimke, H., & Pfurtscheller, G. (1993). Alpha frequency, cognitive load and memory performance. *Brain Topography, 5(3), 241–251.*

<https://doi.org/10.1007/BF01128991>

Klimesch, Wolfgang. (1999). EEG alpha and theta oscillations reflect cognitive and memory performance: a review and analysis. *Brain Research Reviews, 29(2-3), 169–195.*

doi:10.1016/S0165-0173(98)00056-3

[https://doi.org/10.1016/S0165-0173\(98\)00056-3](https://doi.org/10.1016/S0165-0173(98)00056-3)

Klimesch, Wolfgang. (2012). Alpha-band oscillations, attention, and controlled access to stored information. *Trends in Cognitive Sciences, 16(12), 606–617.*

<https://doi.org/10.1016/j.tics.2012.10.007>

Klimesch, Wolfgang, Sauseng, P., & Hanslmayr, S. (2007). EEG alpha oscillations: The inhibition-timing hypothesis. *Brain Research Reviews, 53(1), 63–88.*

<https://doi.org/10.1016/j.brainresrev.2006.06.003>

Koch, M. (1999). The neurobiology of startle. *Progress in Neurobiology, 59(2), 107–128.*

[https://doi.org/10.1016/S0301-0082\(98\)00098-7](https://doi.org/10.1016/S0301-0082(98)00098-7)

Kochhann, R., Holz, M. R., Beber, B. C., Chaves, M. L. F., & Fonseca, R. P. (2018). Reading and writing habits as a predictor of verbal fluency in elders. *Psychology and Neuroscience, 11(1), 39–49.*

<https://doi.org/10.1037/pne0000125>

Korinthenberg, R., & Igel, B. (1990). Prospective neurophysiological study in children treated for acute lymphoblastic leukaemia: Serial EEG during treatment and long-term follow up with evoked potentials. *European Journal of Pediatrics, 150(2), 127–131.*

<https://doi.org/10.1007/BF02072055>

Krull, K. R., Cheung, Y. T., Liu, W., Fella, S., Reddick, W. E., Brinkman, T. M., Kimberg, C., Ogg, R., Srivastava, D., Pui, C. H., Robison, L. L., & Hudson, M. M. (2016). Chemotherapy pharmacodynamics and neuroimaging and neurocognitive outcomes in long-term survivors

- of childhood acute lymphoblastic leukemia. *Journal of Clinical Oncology*, 34(22), 2644–2653. <https://doi.org/10.1200/JCO.2015.65.4574>
- L. VAINIONPAA, A.-L. S. and M. L. (1991). *Initial Electroencephalographic Findings in Children with Acute Lymphoblastic Leukaemia*. 288(March 1976), 319–342.
- Lachaux, J. P., Rodriguez, E., Martinerie, J., & Varela, F. J. (1999). Measuring phase synchrony in brain signals. *Human Brain Mapping*, 8(4), 194–208. [https://doi.org/10.1002/\(SICI\)1097-0193\(1999\)8:4<194::AID-HBM4>3.0.CO;2-C](https://doi.org/10.1002/(SICI)1097-0193(1999)8:4<194::AID-HBM4>3.0.CO;2-C)
- Lewis, S. J. G., Dove, A., Bobbins, T. W., Barker, R. A., & Owen, A. M. (2004). Striatal contributions to working memory: A functional magnetic resonance imaging study in humans. *European Journal of Neuroscience*, 19(3), 755–760. <https://doi.org/10.1111/j.1460-9568.2004.03108.x>
- Lezak, Muriel D, Howieson, D. B., Loring, D. W., Hannay, H. J., & Fischer, J. S. (2004). Neuropsychological assessment, 4th ed. In *Neuropsychological assessment, 4th ed.* Oxford University Press.
- Lezak, Muriel Deutsch. (1995). Neuropsychological assessment, 3rd ed. In *Neuropsychological assessment, 3rd ed.* Oxford University Press.
- Lichter-Konecki, U., Benninger, C., Brandeis, W. E., Matthis, P., & Scheffner, D. (1987). Changes in the eeg background activity of children with acute lymphoblastic leukemia during cytotoxic therapy. *Pediatric Hematology and Oncology*, 4(1), 77–85. <https://doi.org/10.3109/08880018709141252>
- Liljeström, M., Stevenson, C., Kujala, J., & Salmelin, R. (2015). Task- and stimulus-related cortical networks in language production: Exploring similarity of MEG- and fMRI-derived functional connectivity. *NeuroImage*, 120, 75–87. <https://doi.org/10.1016/j.neuroimage.2015.07.017>
- Liu, Z., Fukunaga, M., de Zwart, J. A., & Duyn, J. H. (2010). Large-scale spontaneous fluctuations and correlations in brain electrical activity observed with magnetoencephalography. *NeuroImage*, 51(1), 102–111. <https://doi.org/10.1016/j.neuroimage.2010.01.092>
- Llinas, R. R. (1988). *Intrinsic Electrophysiological Properties Central Nervous System Function*.

*Science*, 242, 1654–1664.

- Lobier, M., Siebenhühner, F., Palva, S., & Palva, J. M. (2014). Phase transfer entropy: A novel phase-based measure for directed connectivity in networks coupled by oscillatory interactions. *NeuroImage*, 85, 853–872. <https://doi.org/10.1016/j.neuroimage.2013.08.056>
- Luna, B., Padmanabhan, A., & O’Hearn, K. (2010). What has fMRI told us about the Development of Cognitive Control through Adolescence? *Brain and Cognition*, 72(1), 101–113. <https://doi.org/10.1016/j.bandc.2009.08.005>
- Maris, E., & Oostenveld, R. (2007). Nonparametric statistical testing of EEG- and MEG-data. *Journal of Neuroscience Methods*, 164(1), 177–190. <https://doi.org/10.1016/j.jneumeth.2007.03.024>
- Marko, M., Cimrová, B., & Riečanský, I. (2019). Neural theta oscillations support semantic memory retrieval. *Scientific Reports*, 9(1), 1–10. <https://doi.org/10.1038/s41598-019-53813-y>
- Martin, A. (2007). The Representation of Object Concepts in the Brain. *Annual Review of Psychology*, 58(1), 25–45. <https://doi.org/10.1146/annurev.psych.57.102904.190143>
- Merleau Ponty, M. (1942). *La structure du comportement* (P. press univeristaires de France (ed.); 8ieme ed.).
- Merleau Ponty, M. (1945). *Phenomenologie de la perception* (paris gallimard (ed.)).
- Mirman, D., Landrigan, J.-F., & Britt, A. E. (2017). Psychological Bulletin Taxonomic and Thematic Semantic Systems Taxonomic and Thematic Semantic Systems. *Psychological Bulletin*, 143(5), 499–520. <http://dx.doi.org/10.1037/bul0000092>
- Miyake, A., & Friedman, N. P. (2012). The nature and organization of individual differences in executive functions: Four general conclusions. *Current Directions in Psychological Science*, 21(1), 8–14. <https://doi.org/10.1177/0963721411429458>
- Miyake, A., Friedman, N. P., Emerson, M. J., Witzki, A. H., Howerter, A., & Wager, T. D. (2000). The Unity and Diversity of Executive Functions and Their Contributions to Complex “Frontal Lobe” Tasks: A Latent Variable Analysis. *Cognitive Psychology*, 41(1), 49–100.

<https://doi.org/10.1006/cogp.1999.0734>

- Moll, J., De Oliveira-Souza, R., Moll, F. T., Bramati, I. E., & Andreiuolo, P. A. (2002). The cerebral correlates of set-shifting: An fMRI study of the trail making test. *Arquivos de Neuro-Psiquiatria*, *60*(4), 900–905. <https://doi.org/10.1590/S0004-282X2002000600002>
- Mousavi, N., Nazari, M. A., Babapour, J., & Jahan, A. (2020). Electroencephalographic characteristics of word finding during phonological and semantic verbal fluency tasks. *Neuropsychopharmacology Reports*, *40*(3), 254–261. <https://doi.org/10.1002/npr2.12129>
- Narayanan, N. S., Prabhakaran, V., Bunge, S. A., Christoff, K., Fine, E. M., & Gabrieli, J. D. E. (2005). The role of the prefrontal cortex in the maintenance of verbal working memory: An event-related fMRI analysis. *Neuropsychology*, *19*(2), 223–232. <https://doi.org/10.1037/0894-4105.19.2.223>
- Newen, A. (2018). The embodied self, the pattern theory of self, and the predictive mind. *Frontiers in Psychology*, *9*(NOV), 1–14. <https://doi.org/10.3389/fpsyg.2018.02270>
- Niedermayer, E. & Lopes da Silva, F. H. (2005). *Electroencephalography: Basic Principles, Clinical Applications, And Related Fields. 5th Edn Wolters Kluwer.*
- Nigro, L. Lo, Di Cataldo, A., & Schiliro, G. (2000). Acute neurotoxicity in children with B-lineage acute lymphoblastic leukemia (B-ALL) treated with intermediate risk protocols. *Medical and Pediatric Oncology*, *35*(5), 449–455. [https://doi.org/10.1002/1096-911X\(20001101\)35:5<449::AID-MPO2>3.0.CO;2-X](https://doi.org/10.1002/1096-911X(20001101)35:5<449::AID-MPO2>3.0.CO;2-X)
- Nikouline, V. V., Linkenkaer-Hansen, K., Huttunen, J., & Ilmoniemi, R. J. (2001). Interhemispheric phase synchrony and amplitude correlation of spontaneous beta oscillations in human subjects: A magnetoencephalographic study. *NeuroReport*, *12*(11), 2487–2491. <https://doi.org/10.1097/00001756-200108080-00040>
- Nolte, G., Bai, O., Wheaton, L., Mari, Z., Vorbach, S., & Hallett, M. (2004). Identifying true brain interaction from EEG data using the imaginary part of coherency. *Clinical Neurophysiology*, *115*(10), 2292–2307. <https://doi.org/10.1016/j.clinph.2004.04.029>

- Nolte, G., Ziehe, A., Nikulin, V. V., Schlögl, A., Krämer, N., Brismar, T., & Müller, K. R. (2008). Robustly estimating the flow direction of information in complex physical systems. *Physical Review Letters*, *100*(23), 1–4. <https://doi.org/10.1103/PhysRevLett.100.234101>
- O'Regan, J. K., & Noë, A. (2001). A sensorimotor account of vision and visual consciousness. *Behavioral and Brain Sciences*, *24*(5), 939–973. <https://doi.org/10.1017/S0140525X01000115>
- Obleser, J., & Weisz, N. (2012). Suppressed alpha oscillations predict intelligibility of speech and its acoustic details. *Cerebral Cortex*, *22*(11), 2466–2477. <https://doi.org/10.1093/cercor/bhr325>
- Östberg, P., Crinelli, R. M., Danielsson, R., Wahlund, L. O., Bogdanovic, N., & Fernaeus, S. E. (2007). A temporal lobe factor in verb fluency. *Cortex*, *43*(5), 607–615. [https://doi.org/10.1016/S0010-9452\(08\)70491-X](https://doi.org/10.1016/S0010-9452(08)70491-X)
- Ouyang, G., Hildebrandt, A., Schmitz, F., & Herrmann, C. S. (2020). Decomposing alpha and 1/f brain activities reveals their differential associations with cognitive processing speed. *NeuroImage*, *205*(September 2019), 116304. <https://doi.org/10.1016/j.neuroimage.2019.116304>
- Owen, A. M., McMillan, K. M., Laird, A. R., & Bullmore, E. (2005). N-back working memory paradigm: A meta-analysis of normative functional neuroimaging studies. *Human Brain Mapping*, *25*(1), 46–59. <https://doi.org/10.1002/hbm.20131>
- Özkurt, T. E., & Schnitzler, A. (2011). A critical note on the definition of phase-amplitude cross-frequency coupling. *Journal of Neuroscience Methods*, *201*(2), 438–443. <https://doi.org/10.1016/j.jneumeth.2011.08.014>
- Pääkkö, E., Harila-Saari, A., Vanionpää, L., Himanen, S., Pyhtinen, J., & Lanning, M. (2000). White matter changes on MRI during treatment in children with acute lymphoblastic leukemia: Correlation with neuropsychological findings. *Medical and Pediatric Oncology*, *35*(5), 456–461. [https://doi.org/10.1002/1096-911X\(20001101\)35:5<456::AID-MPO3>3.0.CO;2-1](https://doi.org/10.1002/1096-911X(20001101)35:5<456::AID-MPO3>3.0.CO;2-1)
- Palva, J. M., & Palva, S. (2012). Infra-slow fluctuations in electrophysiological recordings, blood-

- oxygenation-level-dependent signals, and psychophysical time series. *NeuroImage*, 62(4), 2201–2211. <https://doi.org/10.1016/j.neuroimage.2012.02.060>
- Palva, S., & Palva, J. M. (2007). New vistas for  $\alpha$ -frequency band oscillations. *Trends in Neurosciences*, 30(4), 150–158. <https://doi.org/10.1016/j.tins.2007.02.001>
- Paulesu, E., Frith, C. D., & Frackowiak, R. S. J. (1993). The neural correlates of the verbal component of working memory. *Nature*, 362(6418), 342–345. <https://doi.org/10.1038/362342a0>
- Pennington, B. F., & Ozonoff, S. (1996). Executive functions and developmental psychopathology. *Journal of Child Psychology and Psychiatry and Allied Disciplines*, 37(1), 51–87. <https://doi.org/10.1111/j.1469-7610.1996.tb01380.x>
- Per Bak, Chao Tang, and K. W. (1987). Self-Organized Criticality: An Explanation of 1/f Noise. *Physical Review Letters*, 59(4), 191–206. <https://doi.org/10.1111/j.1536-7150.1981.tb01388.x>
- Petrides, M., Alivisatos, B., Meyer, E., & Evans, A. C. (1993). Functional activation of the human frontal cortex during the performance of verbal working memory tasks. *Proceedings of the National Academy of Sciences of the United States of America*, 90(3), 878–882. <https://doi.org/10.1073/pnas.90.3.878>
- Piaget, J. (1937). *La construction du reel chez l'enfant* (delachaux et niestlé neuchatel et paris (ed.)).
- Piatt, A. L., Fields, J. A., Paolo, A. M., Koller, W. C., & Tröster, A. I. (1999). Lexical, semantic, and action verbal fluency in Parkinson's disease with and without dementia. *Journal of Clinical and Experimental Neuropsychology*, 21(4), 435–443. <https://doi.org/10.1076/jcen.21.4.435.885>
- Poskanzer, K. E., & Yuste, R. (2011). Astrocytic regulation of cortical UP states. *Proceedings of the National Academy of Sciences of the United States of America*, 108(45), 18453–18458. <https://doi.org/10.1073/pnas.1112378108>

- Price, C. J. (2012). A review and synthesis of the first 20 years of PET and fMRI studies of heard speech, spoken language and reading. *NeuroImage*, 62(2), 816–847. <https://doi.org/10.1016/j.neuroimage.2012.04.062>
- Pulvermüller, F., Hauk, O., Nikulin, V. V., & Ilmoniemi, R. J. (2005). Functional links between motor and language systems. *European Journal of Neuroscience*, 21(3), 793–797. <https://doi.org/10.1111/j.1460-9568.2005.03900.x>
- Rabin, L. A., Barr, W. B., & Burton, L. A. (2005). *Assessment practices of clinical neuropsychologists in the United States and Canada : A survey of INS , NAN , and APA Division 40 members & .* 20, 33–65. <https://doi.org/10.1016/j.acn.2004.02.005>
- Raichle, M. E., MacLeod, A. M., Snyder, A. Z., Powers, W. J., Gusnard, D. A., & Shulman, G. L. (2001). A default mode of brain function. *Proceedings of the National Academy of Sciences of the United States of America*, 98(2), 676–682. <https://doi.org/10.1073/pnas.98.2.676>
- Ravizza, S. M., & Carter, C. S. (2008). Shifting set about task switching: Behavioral and neural evidence for distinct forms of cognitive flexibility. *Neuropsychologia*, 46(12), 2924–2935. <https://doi.org/10.1016/j.neuropsychologia.2008.06.006>
- Reinhart, R. M. G., & Nguyen, J. A. (2019). Working memory revived in older adults by synchronizing rhythmic brain circuits. *Nature Neuroscience*, 22(5), 820–827. <https://doi.org/10.1038/s41593-019-0371-x>
- Riedner, B. A., Hulse, B. K., Murphy, M. J., Ferrarelli, F., & Tononi, G. (2011). Temporal dynamics of cortical sources underlying spontaneous and peripherally evoked slow waves. *Progress in Brain Research*, 193, 201–218. <https://doi.org/10.1016/B978-0-444-53839-0.00013-2>
- Robinson, K. E., Livesay, K. L., Campbell, L. K., Scaduto, M., Cannistraci, C. J., Anderson, A. W., Whitlock, J. A., & Compas, B. E. (2010). Working Memory in Survivors of Childhood Acute Lymphocytic Leukemia: Functional Neuroimaging Analyses. *Pediatric Blood & Cancer*, 54, 585–598. <https://doi.org/10.1002/pbc.22362>
- Rommers, J., Dickson, D. S., Norton, J. J. S., Wlotko, E. W., & Federmeier, K. D. (2017). Alpha and

theta band dynamics related to sentential constraint and word expectancy. *Language, Cognition and Neuroscience*, 32(5), 576–589. <https://doi.org/10.1080/23273798.2016.1183799>

Salthouse, T. A. (2011). What cognitive abilities are involved in trail-making performance? *Intelligence*, 39(4), 222–232. <https://doi.org/10.1016/j.intell.2011.03.001>

Sanjuán, A., Bustamante, J. C., Forn, C., Ventura-Campos, N., Barrós-Loscertales, A., Martínez, J. C., Villanueva, V., & Ávila, C. (2010). Comparison of two fMRI tasks for the evaluation of the expressive language function. *Neuroradiology*, 52(5), 407–415. <https://doi.org/10.1007/s00234-010-0667-8>

Scanziani, M., & Häusser, M. (2009). Electrophysiology in the age of light. *Nature*, 461(7266), 930–939. <https://doi.org/10.1038/nature08540>

Schaefer, A., Kong, R., Gordon, E. M., Laumann, T. O., Zuo, X.-N., Holmes, A. J., Eickhoff, S. B., & Yeo, B. T. T. (2018). Local-Global Parcellation of the Human Cerebral Cortex from Intrinsic Functional Connectivity MRI. *Cerebral Cortex*, 28(9), 3095–3114. <https://doi.org/10.1093/cercor/bhx179>

Schear, J. M., & Craft, R. B. (1989). Examination of the concurrent validity of the California verbal learning test. *Clinical Neuropsychologist*, 3(2), 162–168. <https://doi.org/10.1080/13854048908403289>

Scheeringa, R., Petersson, K. M., Oostenveld, R., Norris, D. G., Hagoort, P., & Bastiaansen, M. C. M. (2009). Trial-by-trial coupling between EEG and BOLD identifies networks related to alpha and theta EEG power increases during working memory maintenance. *NeuroImage*, 44(3), 1224–1238. <https://doi.org/10.1016/j.neuroimage.2008.08.041>

Schwartz, M. F., Kimberg, D. Y., Walker, G. M., Brecher, A., Faseyitan, O. K., Dell, G. S., Mirman, D., & Coslett, H. B. (2011). Neuroanatomical dissociation for taxonomic and thematic knowledge in the human brain. *Proceedings of the National Academy of Sciences of the United States of America*, 108(20), 8520–8524. <https://doi.org/10.1073/pnas.1014935108>

Sellers, A. H., & Nadler, J. D. (1993). A Survey of Current Neuropsychological Assessment



- Procedures Used for Different Age Groups. *Psychotherapy in Private Practice*, 11(3), 47–57.  
[https://doi.org/10.1300/J294v11n03\\_10](https://doi.org/10.1300/J294v11n03_10)
- Shao, Z., Janse, E., Visser, K., & Meyer, A. S. (2014). What do verbal fluency tasks measure? Predictors of verbal fluency performance in older adults. *Frontiers in Psychology*, 5(JUL), 1–10. <https://doi.org/10.3389/fpsyg.2014.00772>
- Smith, E. E., & Jonides, J. (1999). *Frontal Lobes*. 283(MARCH), 1657–1662.
- Stam, C. J., Nolte, G., & Daffertshofer, A. (2007). Phase lag index: Assessment of functional connectivity from multi channel EEG and MEG with diminished bias from common sources. *Human Brain Mapping*, 28(11), 1178–1193. <https://doi.org/10.1002/hbm.20346>
- Stenroos, M., & Nummenmaa, A. (2016). Incorporating and compensating cerebrospinal fluid in surface-based forward models of magneto- And electroencephalography. *PLoS ONE*, 11(7), 1–23. <https://doi.org/10.1371/journal.pone.0159595>
- Stokholm, J., Jørgensen, K., & Vogel, A. (2013). Performances on five verbal fluency tests in a healthy, elderly Danish sample. *Aging, Neuropsychology, and Cognition*, 20(1), 22–33. <https://doi.org/10.1080/13825585.2012.656576>
- Thürling, M., Hautzel, H., Küper, M., Stefanescu, M. R., Maderwald, S., Ladd, M. E., & Timmann, D. (2012). Involvement of the cerebellar cortex and nuclei in verbal and visuospatial working memory: A 7T fMRI study. *NeuroImage*, 62(3), 1537–1550. <https://doi.org/10.1016/j.neuroimage.2012.05.037>
- Tombaugh, T. N. (2004). Trail Making Test A and B: Normative data stratified by age and education. *Archives of Clinical Neuropsychology*, 19(2), 203–214. [https://doi.org/10.1016/S0887-6177\(03\)00039-8](https://doi.org/10.1016/S0887-6177(03)00039-8)
- Tort, A. B. L., Komorowski, R., Eichenbaum, H., & Kopell, N. (2010). Measuring phase-amplitude coupling between neuronal oscillations of different frequencies. *Journal of Neurophysiology*, 104(2), 1195–1210. <https://doi.org/10.1152/jn.00106.2010>
- Tremblay, P., & Dick, A. S. (2016). Broca and Wernicke are dead, or moving past the classic model

- of language neurobiology. *Brain and Language*, 162, 60–71.  
<https://doi.org/10.1016/j.bandl.2016.08.004>
- Tucker, J., Prior, P. F., Green, C. R., Ede, G. M. V., Stevenson, J. F., Gawler, J., Jamal, G. A., Charlesworth, M., Thakkar, C. M., Patel, P., & Lister, T. A. (1989). Minimal neuropsychological sequelae following prophylactic treatment of the central nervous system in adult leukaemia and lymphoma. *British Journal of Cancer*, 60(5), 775–780.  
<https://doi.org/10.1038/bjc.1989.358>
- Tuladhar, A. M., Ter Huurne, N., Schoffelen, J. M., Maris, E., Oostenveld, R., & Jensen, O. (2007). Parieto-occipital sources account for the increase in alpha activity with working memory load. *Human Brain Mapping*, 28(8), 785–792. <https://doi.org/10.1002/hbm.20306>
- Tulving, E. (1972). Episodic and semantic memory. In *Organization of memory*. (pp. xiii, 423–xiii, 423). Academic Press.
- Ueberall, M. A., Skirl, G., Straßburg, H. M., Wenzel, D., Hertzberg, H., Langer, T., Meier, W., Berger-Jones, K., Huk, W. J., Korinthenberg, R., & Beck, J. D. (1997). Neurophysiological findings in long-term survivors of acute lymphoblastic leukaemia in childhood treated with the BFM protocol 81 SR-A/B. *European Journal of Pediatrics*, 156(9), 727–733.  
<https://doi.org/10.1007/s004310050700>
- van Diessen, E., Numan, T., van Dellen, E., van der Kooij, A. W., Boersma, M., Hofman, D., van Lutterveld, R., van Dijk, B. W., van Straaten, E. C. W., Hillebrand, A., & Stam, C. J. (2015). Opportunities and methodological challenges in EEG and MEG resting state functional brain network research. *Clinical Neurophysiology*, 126(8), 1468–1481.  
<https://doi.org/10.1016/j.clinph.2014.11.018>
- Varela, F. J., Thompson, E., & Rosch, E. (1991). *The embodied mind: Cognitive science and human experience*. Cambridge, Mass: MIT Press. (M. M. P. Cambridge (ed.)).
- Varjadic, A., Mantini, D., Demeyere, N., & Gillebert, C. R. (2018). Neural signatures of Trail Making Test performance: Evidence from lesion-mapping and neuroimaging studies. *Neuropsychologia*, 115(June 2017), 78–87.

<https://doi.org/10.1016/j.neuropsychologia.2018.03.031>

- Veltman, D. J., Rombouts, S. A. R. B., & Dolan, R. J. (2003). Maintenance versus manipulation in verbal working memory revisited: An fMRI study. *NeuroImage*, *18*(2), 247–256. [https://doi.org/10.1016/S1053-8119\(02\)00049-6](https://doi.org/10.1016/S1053-8119(02)00049-6)
- Vigneau, M., Beaucousin, V., Hervé, P. Y., Duffau, H., Crivello, F., Houdé, O., Mazoyer, B., & Tzourio-Mazoyer, N. (2006). Meta-analyzing left hemisphere language areas: Phonology, semantics, and sentence processing. *NeuroImage*, *30*(4), 1414–1432. <https://doi.org/10.1016/j.neuroimage.2005.11.002>
- Vijayanathan, V., Gulinello, M., Ali, N., & Cole, P. D. (2011). Persistent cognitive deficits, induced by intrathecal methotrexate, are associated with elevated CSF concentrations of excitotoxic glutamate analogs and can be reversed by an NMDA antagonist. *Behavioural Brain Research*, *225*(2), 491–497. <https://doi.org/10.1016/j.bbr.2011.08.006>
- Vinck, M., Oostenveld, R., Van Wingerden, M., Battaglia, F., & Pennartz, C. M. A. (2011). An improved index of phase-synchronization for electrophysiological data in the presence of volume-conduction, noise and sample-size bias. *NeuroImage*, *55*(4), 1548–1565. <https://doi.org/10.1016/j.neuroimage.2011.01.055>
- Vorwerk, J., Cho, J. H., Rampp, S., Hamer, H., Knösche, T. R., & Wolters, C. H. (2014). A guideline for head volume conductor modeling in EEG and MEG. *NeuroImage*, *100*, 590–607. <https://doi.org/10.1016/j.neuroimage.2014.06.040>
- Voytek, B., Kramer, M. A., Case, J., Lepage, K. Q., Tempesta, Z. R., Knight, R. T., & Gazzaley, A. (2015). Age-related changes in 1/f neural electrophysiological noise. *Journal of Neuroscience*, *35*(38), 13257–13265. <https://doi.org/10.1523/JNEUROSCI.2332-14.2015>
- Vrba, J., & Robinson, S. E. (2001). Signal processing in magnetoencephalography. *Methods*, *25*(2), 249–271. <https://doi.org/10.1006/meth.2001.1238>
- Wagner, S., Sebastian, A., Lieb, K., Tüscher, O., & Tadić, A. (2014). A coordinate-based ALE functional MRI meta-analysis of brain activation during verbal fluency tasks in healthy control subjects. *BMC Neuroscience*, *15*. <https://doi.org/10.1186/1471-2202-15-19>

- Wong, R. K. S., Prince, D. A., & Basbaum, A. I. (1979). Intradendritic recordings from hippocampal neurons. *Proceedings of the National Academy of Sciences of the United States of America*, 76(2), 986–990. <https://doi.org/10.1073/pnas.76.2.986>
- Zakzanis, K. K., Mraz, R., & Graham, S. J. (2005). An fMRI study of the Trail Making Test. *Neuropsychologia*, 43(13), 1878–1886. <https://doi.org/10.1016/j.neuropsychologia.2005.03.013>
- Ziemke, T. (2016). The body of knowledge: On the role of the living body in grounding embodied cognition. *BioSystems*, 148, 4–11. <https://doi.org/10.1016/j.biosystems.2016.08.005>
- Zou, D., Wen, F., Zeng, H., Mai, H., Yuan, X., Wang, L., Li, Y., Liu, L., Liu, S., & Liu, G. (2019). Improving brain function of pediatric acute lymphoblastic leukemia patients after induction chemotherapy, a pilot self-contrast study by fractional amplitude of low-frequency fluctuation. *Journal of Clinical Neuroscience*, 66, 149–155. <https://doi.org/10.1016/j.jocn.2019.04.033>
- Zou, P., Mulhern, R. K., Butler, R. W., Li, C. S., Langston, J. W., & Ogg, R. J. (2005). BOLD responses to visual stimulation in survivors of childhood cancer. *NeuroImage*, 24(1), 61–69. <https://doi.org/10.1016/j.neuroimage.2004.08.030>